Titre: Title:	Linéarisation des amplificateurs de puissance micro ondes utilisant une technique de prédistorsion numérique adaptative
Auteur: Author:	Ernesto Gerardo Jeckeln
Date:	2004
Type:	Mémoire ou thèse / Dissertation or Thesis
Référence: Citation:	Jeckeln, E. G. (2004). Linéarisation des amplificateurs de puissance micro ondes utilisant une technique de prédistorsion numérique adaptative [Ph.D. thesis, École Polytechnique de Montréal]. PolyPublie. https://publications.polymtl.ca/7441/

UNIVERSITÉ DE MONTRÉAL

LINÉARISATION DES AMPLIFICATEURS DE PUISSANCE MICRO ONDES UTILISANT UNE TECHNIQUE DE PRÉDISTORSION NUMÉRIQUE ADAPTATIVE

ERNESTO G. JECKELN

DÉPARTEMENT DE GÉNIE ÉLECTRIQUE

ÉCOLE POLYTECHNIQUE DE MONTRÉAL

THÈSE PRÉSENTÉ EN VUE DE L'OBTENTION

DU DIPLÔME DE PHILOSOPHIAE DOCTOR (Ph.D)

(GÉNIE ÉLECTRIQUE)

AVRIL 2004

Your file Votre référence
ISBN: 0-612-98178-9
Our file Notre référence
ISBN: 0-612-98178-9

UNIVERSITÉ DE MONTRÉAL

ÉCOLE POLYTECHNIQUE DE MONTRÉAL

Cette thèse intitulée:

LINÉARISATION DES AMPLIFICATEURS DE PUISSANCE MICRO ONDES UTILISANT UNE TECHNIQUE DE PRÉDISTORSION NUMÉRIQUE ADAPTATIVE

Présenté par: JECKELN Ernesto G.
En vue de l'obtention du diplôme de: Philosophie Doctor
a été dûment accepté par le jury d'examen constitué de:

M. LAURIN, Jean-Jacques, Ph.D., président

M. GANNOUCHI, Fadhel M, Ph.D., membre et directeur de recherche

M. SAWAN, Mohamed, Ph.D., membre et co-directeur de recherche

M. SAVARIA, Yvon, Ph.D., membre

M. POITAU, Gwenael, Ph.D., membre externe

DÉDICACE

À mon épouse Rosi

À mes enfants Géraldine et Sophie

À mes parents Hipolito et Nelly

À mes frères Enrique et Beby

REMERCIEMENTS

Je remercie le Professeur Fadhel M. Ghannouchi pour avoir accepté la responsabilité de directeur de thèse, pour la confiance totale qu'il m'a accordée ainsi que pour les rôles clefs qu'il a tenusdans ce travail de recherche: Initiateur du projet et conseiller durant les 5 années passées dans son équipe.

Je remercie le Professeur Mohamad A Sawan, co-directeur de thèse, pour l'intérêt qu'il a montré face à mon travail ainsi que pour l'éclairage personnel qu'il a apporté grâce à sa compétence dans son domaine scientifique.

Je remercie également le Professeur Jean-Jacques Laurin, président du jury, le Professeur Yvon Savaria, membre du jury et le Professeur Gwenael Poitau, membre externe du jury, d'avoir accepté de participer au jury de thèse.

J'exprime tous mes remerciements à l'ensemble des membres du PolyGRAMES pour leur sympathie, et en particulier au personnel administratif et technique dont l'aide quotidienne me fut précieuse.

Une immense reconnaissance à ma tendre Rosi pour son soutien pendant les moments les plus difficiles durant ces années d'études et une éternelle gratitude à mes enfants Géraldine et Sophie.

RÉSUMÉ

Les amplificateurs de puissance sont généralement contraints d'opérer dans la région non linéaire, et ce, dans le but d'optimiser l'efficacité énergétique ou d'obtenir le maximum de puissance à la sortie. Ces conditions ont pour effets de générer des distorsions qui dégradent le comportement du système et la qualité du signal à amplifier. La réduction de ces distorsions pousse les concepteurs à s'intéresser et à développer des techniques de linéarisation capables de maintenir le rendement en puissance tout en conservant une bonne linéarité.

Pour répondre à ces exigences, plusieurs techniques de linéarisation ont été proposées. Les progrès technologiques des processeurs destinés aux traitements des signaux numériques et leurs applications dans le domaine des télécommunications a conduit à leur utilisation dans plusieurs techniques de linéarisation. Ces dispositifs, pouvant atteindre une fréquence d'horloge de l'ordre des micro-ondes, ils suscitent l'intérêt des concepteurs pour permettre l'exécution des algorithmes de compensation des distorsions en temps réel. À cet égard l'application des techniques de linéarisation comme la méthode de prédistorsion numérique adaptative présente un grand intérêt pour la recherche actuelle.

Le but de cette thèse est de présenter deux méthodes appliquées à la technique de prédistorsion numérique adaptative pour la linéarisation des amplificateurs de puissance

micro-ondes. L'objectif principal du projet était d'implémenter ces méthodes algorithmiques dans le but d'optimiser la performance, d'un point de vue de la linéarité et de l'efficacité énergétique, de deux amplificateurs de puissance opérant en classe AB pour une puissance moyenne de 30 et 44 dBm et à une fréquence centrale de 1.78 et 1.96 GHz respectivement.

ABSTRACT

The current trend in developing highly linear multi-carrier microwave transmitter with high power efficiency, suitable for wireless communication, pressures power amplifier designers to focus on more sophisticated circuit topologies (class AB, F, Doherty and switching mode family) combined with efficient distortion compensation such as Digital Predistortion, Envelope Elimination and Restoration, LINC, etc.

Digital Predistortion is one of the most promising techniques that can recuperate linearity without worsening the efficiency of a given optimal PA. It has demonstrated the capability in reducing the spectral spreading and how adaptive correction can be achieved using high-speed arithmetic. However, its performance is greatly affected in the adaptation transition time by critical conditions such as starting point of optimization, stability and convergence rate. To address the aforementioned shortcomings this theses proposes efficient algorithms suitable for two different digital predistortion technique structures. The new methods develop an instantaneous characterization of the PA behaviors, which remove the need for complex convergence algorithms in the adaptation update step. In addition, the methods propose new look-up tables' configurations for predistortion purpose using polar representation. The first linearizer is implemented using a DSP environment to linearize an efficient 1 W class AB PA at 1,78 GHz. The second linearizer is implemented under open loop condition, supported by software-instruments connectivity, for a 20 W Class AB PA operating at 1.96 GHz.

TABLE DES MATIÈRES

LISTE DES FIGURES

LISTE DES SIGLES ET DES ABRÉVIATIONS

A/D	Analog to Digital Converter
ACPR	Adjacent Channel Power Ratio
ACP	Adjacent Channel Power
AM	Modulation d'amplitude (Amplitude Modulation).
AM-AM	Amplitude Modulation to Amplitude Modulation
AM-PM	Amplitude Modulation to Phase Modulation
ADS	Advance Design System
BER	Bit Error Rate
BW	Signal Bandwidth
BPSK	Binary-Phase Shift Keying
CDMA	Code Division Multiple Access
CDMA2000	Code Division Multiple Access 2000
CCDF	Complementary Cumulative Distribution Function
CF	Crest Factor
C/I	Carrier to Intermodulation
CGS	Code Generation System
D/A	Digital to Analog Converter
DSP	Digital Signal Processing
EVM	Error Vector Magnitude
FPGA	Field Programmable Gate Array

FET	Transistor à effet de champ (Field Effect Transistor).
FSK	Modulation numérique de fréquence (Frequency Shift Keying).
IF	Signal à une fréquence intermédiaire (Intermediate Frequency).
IBW	Integration Bandwidth
LO	Signal de l'oscillateur local (Local Oscillator).
NBW	Normalization Bandwidth
NRZ	Non Return to Zero
PA	Power Amplifier
PD	Predistorter
OBO	Output-Back-Off
RF	Signal à une fréquence radio
RTM	Real Time Modeling
RBW	Resolution Bandwidth
RMS	Root-Mean-Square
16-QAM	16 Quadrature Amplitude Modulation
SPW	Signal Processing WorkSystem
W-CDMA	Wideband Code Division Multiple Access

LISTE DES ANNEXES

CHAPITRE I

Introduction

La conception des amplificateurs de puissance RF/micro-ondes, qui sont utilisés dans les systèmes de radiocommunications mobiles, nous oblige de relever aujourd'hui un défi complexe en terme d'efficacité énergétique. La détermination du point de fonctionnement optimal de ces dispositifs, du point de vue de la puissance moyenne, constitue un des principaux dilemmes dans la conception des émetteurs numériques. En effet, leur comportement non-linéaire exige souvent un compromis entre la qualité de modulation (EVM), le rapport de puissance pour les canaux adjacents (ACPR) et l'efficacité énergétique, notée $\eta(\%)$ [1-4].

Dans le but de répondre à de tels compromis, nous avons essentiellement orienté notre recherche vers l'implémentation d'une nouvelle méthode algorithmique qui s'appuie sur la technique de ***predistortion numérique adaptative,*** technique applicable aux amplificateurs de puissance micro-ondes. La synthèse et l'implémentation originale de deux techniques de linéarisation développées dans ce travail ont permis d'atteindre nos objectifs. Ce chapitre d'introduction présente les principales motivations et justifications liées au travail rapporté dans cette thèse. Ensuite suivra une description de la méthodologie utilisée, d'une liste de contributions originales et de l'organisation de la thèse.

La première partie de cette introduction peut se ramener à quelques termes qui ne sont pas encore définis. Ces termes sont définis dans l'annexe III.

1.1 Motivation

Afin de bien cerner les contributions apportées de ce travail de thèse, nous allons d'abord situer le sujet dans le contexte des systèmes de communication sans fils. Ainsi, cela nous permettra de mettre en évidence la nécessité de techniques de linéarisation comme la méthode de ***predistortion numérique adaptative***. Ce travail se situe dans le cadre des recherches menées par le Département de génie électrique de l'École Polytechnique de Montréal et s'inscrit dans les développements du *Centre de recherche avancée en micro-ondes et en électronique spatiale (POLY-GRAMES)*, du programme Synergie (Groupe AMPLI) et de la collaboration avec la compagnie AmplX, Inc.

1.1.1 Tendances et difficultés des systèmes de communication sans fils

La capacité de véhiculer divers télé-services, à travers un même canal de transmission, a stimulé l'environnement des télécommunications vers l'utilisation de la voie numérique. Ainsi, cette nouvelle orientation a conduit à l'élaboration de systèmes de radiocommunications mobiles numériques permettant leur insertion harmonieuse dans les réseaux intégrés. On peut citer à titre d'exemple la formidable évolution des systèmes cellulaires pour la radiotéléphonie personnelle sans fils, qui a permis un véritable avancement dans le domaine des télécommunications numériques. De plus, ces systèmes nécessitent de disposer de débits de plus en plus importants. De cette façon, les fournisseurs seront capables de fournir une grande gamme de services incluant l'accès à l'Internet mobile, aux terminaux portables multimédia et permettant les transferts de données.

En contrepartie, l'accroissement formidable de la demande liée aux services radio mobiles a conduit à la saturation du domaine spectral alloué à ces services. Or, Cette tendance a exhorté les industriels et les chercheurs du domaine à concentrer leurs efforts sur l'optimisation de *l'efficacité spectrale.* C'est ainsi que des **techniques d'accès multiples** et des **techniques de modulation,** plus performantes en matière de capacité d'information par unité spectrale (bits par seconde par Hertz), furent utilisées.

En ce qui concerne les systèmes d'accès multiples, le système CDMA, (Code Division

Multiple Access) actuellement en utilisation en Amérique du Nord, et ses dérivés cdma2000 et W-CDMA définis pour la troisième génération, répondent aux exigences en terme *d'efficacité spectrale*. Ils permettent une utilisation efficace des bandes de fréquences disponibles avec un traitement de l'information entièrement numérique. Le système CDMA a commencé à prendre place dans les systèmes radio-mobiles de deuxième génération et il est devenu prépondérant dans la définition de la norme de troisième génération [2,5].

Pour ce qui est des systèmes de modulation, la modulation analogique, caractéristique des mobiles de première génération, a été remplacée par la modulation numérique. Cela a été rendu possible grâce à l'évolution technologique des circuits numériques et des microprocesseurs de plus en plus rapides. Les modulations numériques, tels que le π/4DQPSK, QPSK ou encore le M-aires QAM ont permis une amélioration considérable de *l'efficacité spectrale* à travers le codage en bande de base. De plus, la qualité du signal a été accrue grâce à une meilleure immunité au bruit [6].

Bien qu'il existe de nombreuses modulations numériques, elles n'ont pas le même niveau de performance lors de leur application dans les radiocommunications mobiles. Plusieurs critères de sélection permettent de les dissocier, comme la puissance d'émission, les évanouissements, l'occupation spectrale, la sensibilité aux non-linéarités et la simplicité de réalisation. Dans ce contexte, les normes cdma2000 et W-CDMA supplantent la modulation QPSK, car elle sont plus robustes pour les applications radio-

mobiles. Ces systèmes, numérisés à cent pour-cent, représentent la troisième génération des radio-mobiles qui permettent leur insertion dans les réseaux intégrés. Cependant, des complications majeures au niveau technique placent les industriels face à plusieurs défis pour ce qui est de l'implémentation et l'optimisation des systèmes [2].

Le principal inconvénient de ces systèmes réside dans leur sensibilité aux non-linéarités. En effet, la forme d'onde générée à la sortie de ces systèmes exige que l'étape d'amplification soit ultra-linéaire, ceci est dû à une très forte variation de l'amplitude de l'enveloppe. Cette variation, qui est caractérisée par le rapport entre un pic de puissance instantanée et la puissance moyenne du signal, joue un rôle important dans le comportement des amplificateurs de puissance. Les niveaux de puissance instantanée élevés relatif à la puissance d'opération amènent les amplificateurs à la zone de saturation, provoquant une compression et, finalement, un écrêtage et une distorsion qui interfèrent avec le signal principal. Un tel comportement oblige les amplificateurs à opérer dans une région éloignée de la région de saturation, là ou l'efficacité énergétique est faible [2,5].

1.1.2 Prédistorsion numérique

En vue d'optimiser *l'efficacité énergétique* d'un système d'amplification et de répondre aux exigences sévères imposées des normes telles que CDMA IS-95, IS-97 ou encore cdma2000, l'application des techniques de linéarisation comme la méthode de

prédistorsion numérique adaptative présente un grand intérêt pour la recherche actuelle [7-11]. Ces techniques sont les seules qui peuvent permettre la conception de systèmes d'amplifications ultra-linéaire présentant une *efficacité énergétique* optimale. De plus, la structure de contrôle adaptatif par la partie logicielle et le traitement de signal (en bande de base) entièrement numérique rendent ces techniques applicables pour différentes formes d'ondes tout en respectant différentes normes en vigueur. Aujourd'hui, les progrès technologiques dans le domaine des processeurs de traitement numérique de signaux "DSP", permettent d'accélérer l'exécution d'algorithmes complexes avec une fréquence d'horloge de l'ordre des micro-ondes. Ceci incite les chercheurs à concentrer leurs efforts sur l'évolution des techniques de linéarisation basées sur la migration d'une grande partie du traitement de signal analogique vers le domaine numérique. Il est donc à souligner que l'incorporation des circuits "DSP" dans la conception de systèmes d'amplifications ultra-linéaire devient de plus en plus capitale.

Pour résumer, la tendance pour la conception des systèmes d'amplifications ultra-linéaire, appliquée aux radiocommunications mobiles de nouvelle génération, a des objectifs importants qui peuvent s'exprimer de la façon suivante:

a) rendre linéaire un amplificateur de puissance à haute performance en termes d' d'efficacité énergétique (Classe AB, classe F, Doherty, etc.) plutôt que d' utiliser un amplificateur linéaire en classe A avec une faible efficacité énergétique,

b) le développement des techniques de linéarisation en utilisant des circuits "DSP" et "FPGA", permettant ainsi aux techniques de répondre aux différentes normes contrôlées par programmation.

1.2 Objectif principal du projet

Le but de cette thèse est de présenter deux méthodes appliquées à la "technique de prédistorsion numérique adaptative pour la linéarisation des amplificateurs de puissance micro-ondes". L'objectif principal du projet était d'implémenter ces méthodes algorithmiques dans le but d'optimiser les performances, d'un point de vue de la linéarité et de l'efficacité énergétique, de deux amplificateurs de puissance opérant en classe AB pour une puissance moyenne de 30 et 44 dBm et à une fréquence centrale de 1.78 et 1.96 GHz respectivement.

Les travaux de recherche ont été réalisés en deux parties. La première partie consistait à développer et à implémenter la technique pour des systèmes de communications cellulaires à bande étroite, c'est à dire 30 KHz. L'application de la méthode s'adresse aux ingénieurs concepteurs ayant accès à l'environnement en bande de base des systèmes de communications cellulaires. La deuxième partie consistait à adapter la technique, avec une structure différente, pour être utilisable par des ingénieurs n'ayant pas accès à l'environnement en bande de base. De plus, nous devions respecter les 1.25 MHz imposés parla norme du système CDMA IS-97 [5].

1.3 Méthodologie

Les travaux décrits dans cette thèse ont été réalisés en utilisant trois approches: a) une analyse mathématique et statistique, b) des simulations et co-simulation DSP/RF et c) des méthodes expérimentales. Le logiciel Matlab a permis à l'auteur d'effectuer des calculs mathématiques, des analyses et la représentation graphique des données [12]. Les simulations et la compilation des codes ont été effectuées en utilisant les logiciels de traitement de signaux SPW et CGS, qui ont permis l'optimisation et l'exécution des codes dans un environnement numérique[13]. La première partie expérimentale a été réalisée à l'aide d'une carte de développement de la compagnie Spectrum LSI. La carte de développement inclut un microprocesseur TMS320C40 de la compagnie Texas Instrument, un générateur d'horloge, un bloc de mémoire SRAM et des convertisseurs A/D et D/A. La co-simulation du système DSP/RF a été effectuée en utilisant le logiciel ADS, qui permet de simuler intégralement les parties DSP et RF et d'étudier leur interaction [14]. La deuxième partie expérimentale a été réalisée à l'aide d'une interface, entre un ordinateur, le logiciel ADS et les instruments de tests et de mesures.

1.4 Point saillants et sommaire des contributions originales

Les méthodes proposées incluent de nouveaux algorithmes très performants, pouvant être exécutés en temps réel par des circuits de traitement de signaux. Les algorithmes exécutent une caractérisation complexe instantanée de la non-linéarité, ce qui déterminera ainsi la fonction de prédistorsion qui est corrélée à la fonction de transfert de l'amplificateur. Ces deux fonctions non-linéaires cascadées permettront une amplification linéaire. Ceci aura comme conséquence de faire opérer l'amplificateur de puissance dans des conditions énergétiques optimales. Essentiellement, le signal résultant de la modulation numérique est conduit à travers une non-linéarité virtuelle qui est complémentaire à celle de l'amplificateur de puissance. Cette non-linéarité complémentaire est réalisée en utilisant une table de correspondance formée de valeurs discrètes et en faisant appel à une interpolation de type linéaire ou "spline" cubique.

La technique prend en considération une action adaptative de la fonction de prédistorsion, ce qui permet de compenser la variation des caractéristiques non linéaires AM-AM et AM-PM de l'amplificateur de puissance. L'adaptabilité est contrôlée à travers la surveillance, d'une part, du niveau de distorsion contenu dans le signal de sortie et en réalisant, d'autre part, une mise à jour de la table de correspondance.

Le travail décrit dans cette thèse apporte des contributions originales en ce qui concerne la caractérisation et la compensation des non-linéarités. En outre, des contributions sont

apportées au niveau des systèmes aux techniques de linéarisation des amplificateurs de puissance utilisés pour les systèmes de deuxième et troisième génération des communications mobiles sans fils. Une liste détaillée des contributions originales est donnée ci-dessous.

- Processus de caractérisation instantanée du comportement non linéaire de l'amplificateur.
- Processus de caractérisation instantanée du comportement non linéaire de l'amplificateur basé sur l'utilisation des récepteurs numériques.
- Processus de détermination de la fonction de prédistorsion.
- L'élimination complète des algorithmes itératifs.
- La configuration de la table de correspondance et le type d'interpolation utilisé pour générer, d'une part, la fonction de transfert de prédistorsion et d'autre part, pour générer la fonction du gain complexe de prédistorsion.
- Le processus de poursuite en temps réel du niveau de distorsion à la sortie de l'amplificateur basé sur l'utilisation des récepteurs numériques.
- La surveillance simultanée des niveaux de puissance de distorsion pour différents intervalles de fréquences, selon la norme stipulée, servant à contrôler l'action adaptative de la prédistorsion.

1.5 Organisation de la thèse

Cette thèse est présentée selon les normes et procédures concernant les thèses par articles intégrés et elle regroupe les sections suivantes:

- Après l'introduction, ayant pour objet une présentation générale sur l'évolution des systèmes de radiocommunications mobiles, les problématiques, les effets des non-linéarité et le but de la linéarisation, le chapitre II aura comme objectif une revue critique de la littérature pour situer l'état des recherches et développements sur le sujet au démarrage du projet. Une introduction de la technique de prédistorsion est présentée en décrivant les concepts les plus importants comme l'adaptabilité et la caractérisation instantanée de la non linéarité des amplificateurs de puissance.
- Le chapitre III a pour principal objet d'introduire les chapitres IV et V rédigés sous forme d'article scientifique selon les normes et procédures concernant les thèses par articles intégrés. La mise en situation des articles est présentée avec la définition de chaque technique, leurs points saillants, leur contexte historique et les aspects méthodologiques concernant la validation des algorithmes.
- Le chapitre IV présente l'article traitant la technique pour des applications à bande étroite, c'est à dire 30 KHz, et ayant accès à l'environnement en bande de base des systèmes de communications cellulaires.
- Le chapitre V présente l'article traitant la technique pour des applications imposées par la norme IS-97 et n'ayant pas accès à l'environnement en bande de base des

systèmes de communications cellulaires.

- Le chapitre VI présente une synthèse qui fera ressortir les concepts importants tels que: la forme d'onde, la modélisation, la caractérisation instantanée, l'action de l'adaptabilité et l'utilisation de la table de correspondance. Une conclusion clôture ce rapport en introduisant les orientations futures. Une bibliographie regroupant les articles et ouvrages cités suit la conclusion.

1.6 Publications

Ce qui suit est une liste de publications produites par l'auteur sur des sujets concernant la thèse. Des copies des publications sont intégrées dans les annexes I et II.

- E. G. Jeckeln, F. M. Ghannouchi and M. Sawan, `` Non Iterative Adaptive Digital Predistortion Technique for Power Amplifiers linearization ``, **US Patent No: 6,072,364**.

- E. G. Jeckeln, F. M. Ghannouchi, M. Sawan and F. Beauregard "Adaptive Baseband/Rf Predistorter for Power Amplifiers through Instantaneous AM-AM and AM-PM Characterization Using Digital Receivers ", **(US Patent No: US20020191710 and CA Patent No CA2349916)**.

- E G. Jeckeln, F. M. Ghannouchi and M. Sawan "*A New Adaptive Predistortion Technique Using Software-Defined Radio and DSP Technologies Suitable for Base Station 3G Power Amplifiers*", IEEE Transactions on Microwave Theory and Techniques (to be published, 2004)

- E G. Jeckeln, F. M. Ghannouchi and M. Sawan "Efficient Baseband/RF Feedforward Linearizer through a Mirror Power Amplifier Using Software-Defined Radio and Quadrature Digital Up-Conversion", IEEE MTT-S 2001 International Microwave Symposium, Phoenix, May 20-25, 2001.

- E. G. Jeckeln, F. M. Ghannouchi, M. Sawan and F. Beauregard "Adaptive Baseband/RF Predistorter for Power Amplifiers through Instantaneous AM-AM and AM-PM Characterization Using Digital Receivers" IEEE MTT-S International Microwave Symposium, Boston, June 11-16, 2000, pp. 489-492.

- E. G. Jeckeln, F. M. Ghannouchi, M. Sawan and F. Beauregard "Amplifier's Predistortion -based Linearizers for Forward-channel Link Broadband Applications" ICECS'2K, December 17, 2000, pp. 719-722

- E. G. Jeckeln, F. M. Ghannouchi and M. Sawan, ``An L Band Adaptive Digital Predistorter for Power Amplifiers Using Direct I-Q Modem``, IEEE MTT-S International Microwave Symposium, Baltimore, June 7-12, 1998, pp. 719-722.

- E. G. Jeckeln, F. M. Ghannouchi and M. Sawan, ``Linearization of Microwave Emitters using an Adaptive Digital Predistorter``, 27TH EUROPEN MICROWAVE-97, September 8-12, 1997.

- F. M. Ghannouchi, G. Zhao and E. G. Jeckeln, ``Linearization Techniques of SSPAs : State of the Art and Prospective for Future Communication Transceivers``, invited paper, *Asia Pacific Microwave Conference* ***APMA'96,*** Decembre 17-20, 1996.

CHAPITRE II

Techniques de linéarisation numériques

2.1 Introduction

Le présent chapitre a pour principal objet de passer en revue les techniques de linéarisation numériques des amplificateurs de puissance. Les publications consultées ont permis d'estimer l'état actuel des recherches dans ce domaine, d'établir les différents axes de développement et le point de départ de ce projet. Cette revue critique nous permettra, d'une part, de discerner les avantages et les inconvénients de chacune de ces techniques, et d'autre part, de positionner notre contribution en matière de linéarisation par prédistorsion qui est proposée dans cette thèse.

Tout d'abord, nous allons introduire certains concepts tels que les effets des non-linéarités, la modélisation polynomiale sans effet mémoire et la compensation des distorsions. Ces concepts permettront au lecteur de se familiariser avec le sujet principal traité dans cette thèse. Plus particulièrement, nous mettons l'accent sur la forme d'onde généré par un émetteur numérique. La fonction de distribution cumulée complémentaire (CCDF) est présentée et le point de compression de 1 dB (CP_{1dB}) et le point d'interception du troisième ordre, IP_3, sont également définis. Dans un deuxième temps, les techniques de linéarisation numériques sont abordées. Nous commençons par présenter la technique de linéarisation analogique par post-compensation. Le concept de la prédistorsion est introduit à travers la description de la méthode de rétroaction cartésienne et de la technique de prédistorsion numérique adaptative.

2.2 Forme d'onde générée par un émetteur numérique

2.2.1 Filtre de mise en forme, facteur de retombée α

Nous allons maintenant décrire de façon succincte les différents éléments qui constituent une chaîne de transmission, en partant de la source du message vers le modulateur. Ainsi, nous serons en mesure d'identifier les paramètres qui affectent le rapport du pic instantanée de puissance sur la puissance moyenne du signal caractérisé par la fonction de distribution cumulée complémentaire (CCDF)

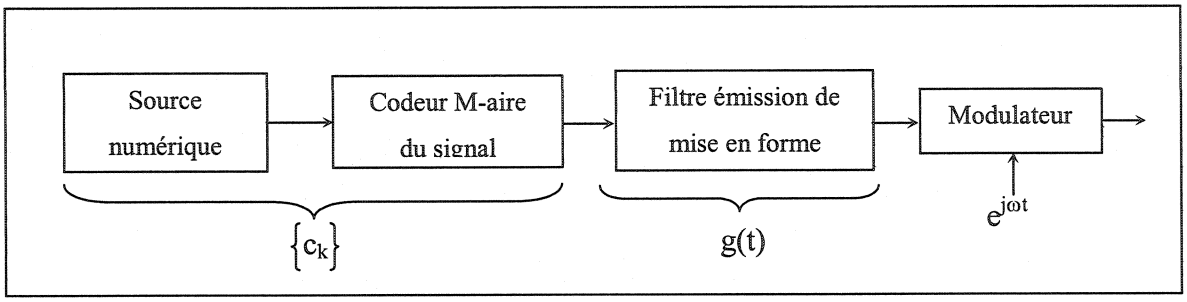

Figure 2.1 Schéma global d'un émetteur pour une transmission numérique

La Figure 2.1 représente un modèle simple d'émetteur pour une transmission numérique. A l'aide d'un convertisseur analogique-numérique et d'un codeur de source, la source numérique génère des symboles M-aire prenant leurs valeurs dans un alphabet à M éléments [6]. Ces symboles sont représentés par la séquence $\{c_k\}$. Le codage M-aires de signal ou codage en bande de base, transforme le message numérique en un signal électrique représenté par l'équation suivante:

$$c(t) = \sum_{k=-\infty}^{\infty} c_k g(t - kT), \tag{2.1}$$

Où à chaque instant T, la fonction $g(t)$ modélise la mise en forme de chaque impulsion, de valeur $\{c_k\}$, à la sortie du codeur. Ceci signifie qu'on utilise le filtrage d'émission, en principe facultatif, pour contrôler la largeur de bande du signal modulé par une mise en forme de l'impulsion produite par le codeur. Pour mieux visualiser la représentation

mathématique d'une transmission numérique, on peut écrire l'équation (2.1) de la façon suivante :

$$c(t) = \sum_{k=-\infty}^{\infty} c_k \delta(t - kT) \otimes g(t), \tag{2.2}$$

Où $\delta(t)$ est l'impulsion de Dirac, le symbole «$\otimes$» représente l'opération de convolution et $g(t)$ représente la réponse impulsionnelle du filtre de mise en forme.

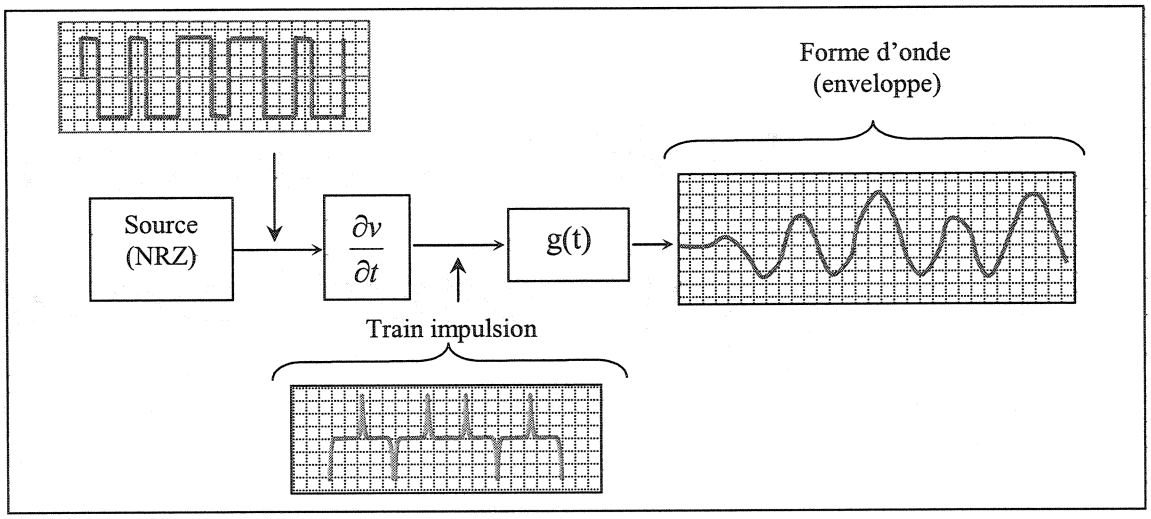

Figure 2.2- Illustration de l'échantillonnage et de la mise en forme du code NRZ

La figure 2.2 montre une représentation graphique de l'échantillonnage et de la mise en forme du code NRZ, (non-retour à zéro). On voit que le train d'impulsion est dérivée de la séquence $\{c_k\}$. Sa convolution avec $g(t)$ donne l'allure du signal généré par chaque impulsion [6]. Le filtrage à la réception dans le récepteur est typiquement adapté au filtrage d'émission et la convolution de ces deux filtres, représentée par l'équation

(2.3), est telle que l'interférence intersymbole (ISI) est nulle au moment de l'échantillonnage.

$$f(t) = g(t) \otimes g(-t) \tag{2.3}$$

Un exemple d'un tel filtre est un filtre en cosinus surélevé, qui peut être représenté dans le domaine temporel par la forme :

$$f(t) = \frac{\sin(\pi\, t/T)}{\pi\, t/T} \frac{\cos(\pi\, \alpha\, t/T)}{1 - 4\alpha^2 t^2 / T^2} \tag{2.4}$$

ou α, compris entre 0 et 1, est le facteur d'arrondi ou de retombée (roll off). Ce facteur joue un rôle important sur le contrôle de la largeur de bande du signal et il aura un impact directe sur la forme d'onde du signal en ce qui concerne le rapport de la puissance crête sur la puissance moyenne [6,15].

2.2.2 Modulation à multi -niveaux

Pour visualiser la compression de l'information et la génération de la forme d'onde prenons une modulation à multi-niveaux. Dans un cas comme celui-ci, le signal en bande de base a une représentation complexe. En effet, il comprend deux composantes I et Q ou I est la partie réelle et Q la partie imaginaire. Un tel modulateur I/Q accorde n'importe quel paramètre, amplitude, fréquence ou phase à moduler simultanément.

Cette manipulation simultanée des paramètres du signal permet à chaque symbole transmis de représenter plus d'un bit des données. En effet, l'optimisation de la largeur de bande du signal va dépendre du taux de symbole qui représente le rapport du débit binaire au nombre de bits transmis par chaque symbole [15].

$$\text{taux de symbole} = \frac{\text{débit binaire}}{\text{nombre de bits par symbole}} \tag{2.5}$$

Ce qui revient à dire que si le nombre de bits par symbole augmente, on aura une augmentation du débit binaire. Par contre, le fait d'optimiser le nombre de bits par symbole entraîne une augmentation du facteur de crête pour la forme d'onde. Autrement dit, si on augmente le débit binaire par Hz, l'écart de la variation de l'enveloppe devient plus significatif. La Figure 2.3 illustre la génération d'une forme d'onde résultant d'une modulation vectorielle. Le modulateur génère un signal dont le spectre est centré autour d'une fréquence RF ou à une fréquence plus élevée [6,15,16].

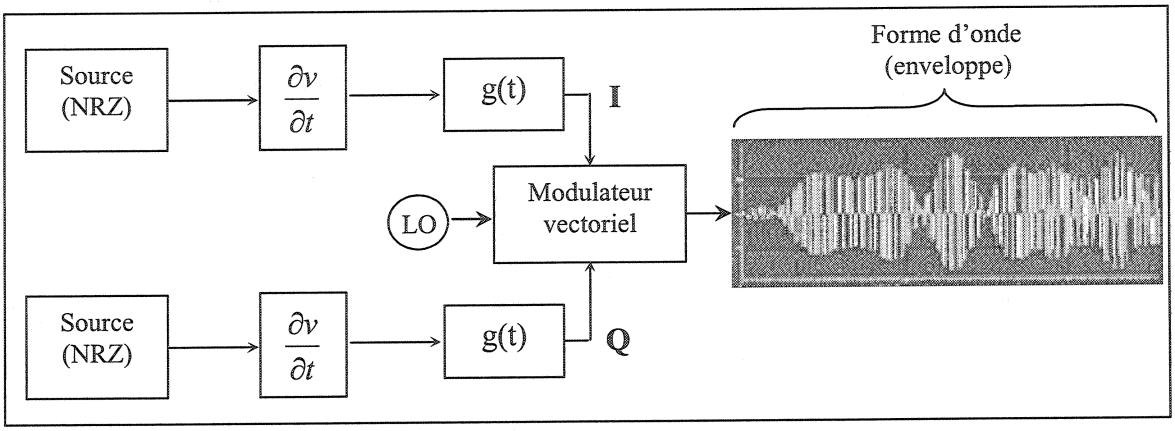

Figure 2.3 Génération d'une forme d'onde résultant d'une modulation vectorielle.

La Figure 2.4 montre la fonction CCDF d'une forme d'onde CDMA et d'une modulation multi-étages 16-QAM pour plusieurs valeurs numériques du facteur de retombée α [17,18].

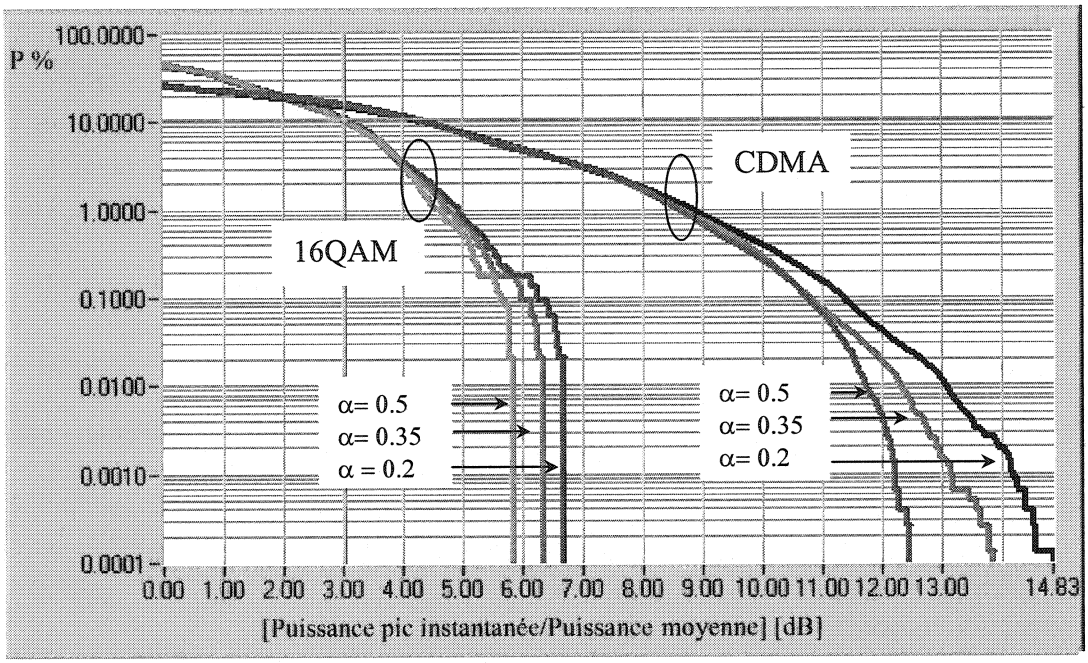

Figure 2.4 - Fonction CCDF des formes d'ondes résultant d'un système CDMA et d'une modulation 16QAM [17]

Il est à noter que les formes d'ondes générées par ces systèmes présentent une grande variation de l'amplitude de l'enveloppe. Les courbes reportées sur la figure 2.4 montrent que les niveaux de puissance instantanée relatifs à la puissance d'opération ont un écart de 6 à 14 dB selon le type de signal utilisé. Ces variations instantanées amènent les amplificateurs à opérer dans leur zone de saturation, provoquant une compression et, finalement, un écrêtage et une distorsion qui dégradent le signal amplifié. Un tel comportement amène les amplificateurs à opérer dans une région éloignée de la zone de saturation, mais présentant une efficacité énergétique faible.

2.3 Les effets des non-linéarités

En dépit des efforts des ingénieurs concepteurs des systèmes de communication, chaque dispositif physique présente, dans une certaine mesure, un comportement non linéaire. Ce qui signifie que le signal de sortie présentera une distorsion par rapport au signal d'entrée. La non-linéarité crée des effets indésirables qui doivent être éliminés par des moyens secondaires tels que le filtrage ou certains types de compensation. Dans le cas contraire, ces effets doivent respecter les normes en vigueur.

Un des effets indésirables qu'on retrouve communément dans la non-linéarité des systèmes de transmission est la génération des harmoniques et des produits d'intermodulation, qui causent des interférences avec le signal désiré. Les produits d'intermodulation résultent des combinaisons fréquentielles (sommes et différences) entre les fréquences des fondamentales et de leurs harmoniques. Si le signal d'entrée est composé seulement d'une seule porteuse de fréquence f_c, alors la sortie sera composée de la fréquence fondamentale plus ses harmoniques $2f_c, 3f_c ...etc..$ Les produits d'intermodulation apparaîtront lorsque le signal d'entrée se compose, soit de deux porteuses ou plus, espacées de quelques MHz, ou bien lorsque la porteuse est modulée.

Les produits d'intermodulation sont classés selon la bande fréquentielle à l'intérieur de laquelle ils sont générés. Les produits d'intermodulation dit *"dans la bande"* sont générés par les composants du signal de modulation et apparaissent dans toute la largeur

de bande de la modulation. Ces produits affectent la qualité de l'information transmise. Les produits d'intermodulation dit *"hors bande"* sont générés en dehors du lobe principal du signal modulant et ils sont répartis dans le spectre selon l'ordre de non-linéarité. Généralement, ils se manifestent sous la forme d'émissions indésirables qui affectent les canaux adjacents. De plus, ils sont beaucoup plus perturbant que les harmoniques, car ils sont regroupés autour de la fondamentale et des harmoniques avec un niveau de puissance comparable à celui des harmoniques. Les harmoniques sont considérés comme un cas particulier des produits d'intermodulation [3].

2.3.1 Modélisation polynomiale sans mémoire. Fonction de transfert

Pour modéliser les effets des non-linéarités, considérons un dispositif d'amplification. C'est à dire, un amplificateur de puissance qui a un faible comportement non-linéaire et présentant une saturation aux extrémités positive et négative de l'amplitude. Le signal de sortie v_0 du dispositif est caractérisé par sa fonction de transfert qui peut s'exprimer sous la forme d'un développement polynomial :

$$v_o = \sum_{n=1}^{\infty} G_n v_i^n \tag{2.6}$$

ou G_n représente les coefficients complexe de la série. En théorie, il existe une infinité de termes dans la fonction de transfert, qui permettent de générer des produits

d'intermodulation et des harmoniques qui s'étendent à l'infini. Cependant, dans la pratique, les facteurs de gain, G_n, deviennent si faibles qu'à partir d'un certain ordre $n = k$ il est inutile de considérer les termes additionnels au-delà de la valeur k [3,4].

2.3.2 Harmoniques

A titre d'exemple, considérons une tension d'entrée sinusoïdale donnée par :

$$v_i = V\cos(2\pi ft) \tag{2.7}$$

Si la liaison est linéaire, alors la sortie est une reproduction fidèle de l'entrée affectée seulement par le coefficient d'amplification ou gain, G_1. Ceci s'exprime sous la forme d'une approximation linéaire pour un fonctionnement petit signal. Dans ce cas, aucune nouvelle composante fréquentielle n'est générée et la sortie est alors représentée par le premier terme de la série de l'équation (2.6) :

$$v_o = G_1 V\cos(2\pi ft) \tag{2.8}$$

Par la suite, nous limiterons la fonction de transfert à trois termes, car les termes d'ordre $n \geq 4$ sont généralement négligeables. En reprenant l'expression (2.6) avec une représentation d'ordre $n = 3$ et avec une tension d'entrée sinusoïdale exprimée par l'équation (2.7) on obtient :

$$v_o(t) = \tfrac{1}{2}G_2V^2 + (G_1V + \tfrac{3}{4}G_3V^3)\cos(2\pi f_1 t) + \\ + \tfrac{1}{2}G_2V^2\cos[2\pi(2f_1)t] + \tfrac{1}{4}G_3V^3\cos[2\pi(3f_1)t] \tag{2.9}$$

On observe que la fonction de transfert du troisième ordre se compose d'un terme DC, de deux termes qui sont fonction de la fondamentale et de deux termes relatifs à la première et la deuxième harmonique. Autrement dit, l'énergie supposée être contenue dans la fondamentale à la sortie de l'amplificateur est, en fait, répartie dans ces cinq termes. Ceci est due à la compression de gain exercée par la fonction de transfert sur la fondamentale. Ce phénomène est observé dans le domaine de puissance en regardant la puissance en dBm dissipée par les deux termes de la fondamentale à travers une charge R. En prenant le deuxième terme de l'expression (2.9) on obtient :

$$P_o(f_1)_{[dBm]} = 10\log[1000(G_1V + \tfrac{3}{4}G_3V^3)^2/\sqrt{2}R] \\ = 20\log(G_1V + \tfrac{3}{4}G_3V^3) + 10\log(1000/\sqrt{2}R) \tag{2.10}$$

Lorsque le signal d'entrée augmente, le signal de sortie augmente linéairement. Pour un certain niveau de signal d'entrée on observe que la puissance de la fondamentale présente un comportement de compression. Cette zone est définie par le point de compression de 1 dB (CP_{1dB}) où la puissance de sortie est de 1 dB au-dessous de la puissance de sortie du gain linéaire, Figure 2.5. Ce comportement exige que dans le modèle de la fonction de transfert, représenté par l'équation (2.9), G_3 soit de signe contraire à G_1. Ce qui aura pour effet d'incurver la courbe qui caractérise le rapport de

puissance de la fondamentale. De plus, on observe dans l'équation (2.9) que la deuxième et la troisième harmoniques ont des pentes, en échelle logarithmique, deux et trois fois plus importantes que la partie linéaire « $G_1 V$ ». Lors de l'augmentation du signal d'entrée, la contribution de la puissance présente dans les harmoniques est plus importante à la sortie. On observe par la suite que la fondamentale atteint une valeur maximale définie par le point ou zone de saturation.

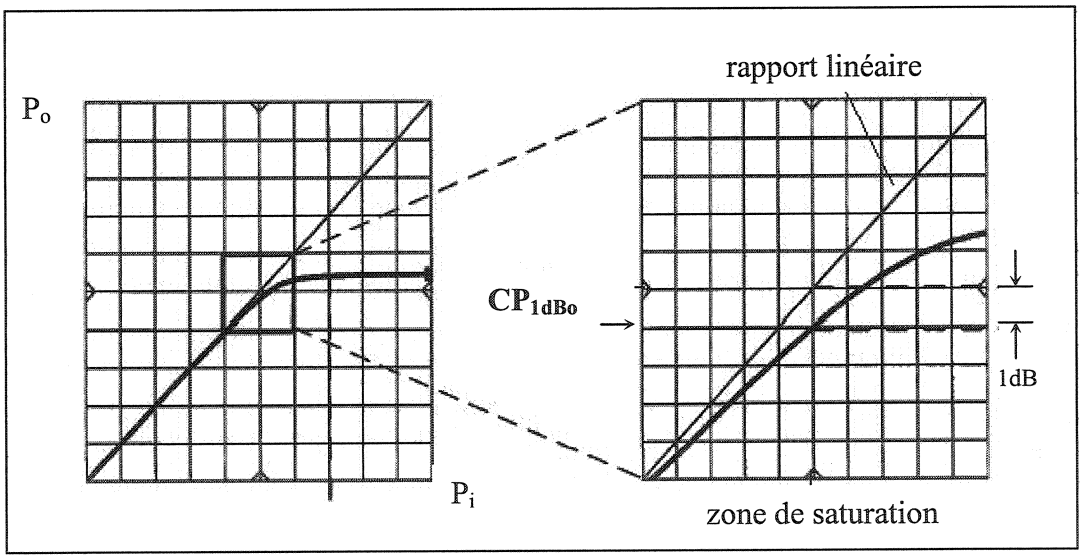

Figure 2.5 Zone de saturation et point de compression de 1 dB (CP_{1dB})

2.3.3 Intermodulations

Considérons maintenant le cas où le signal d'entrée est formé de deux sinusoïdes de fréquences légèrement différentes f_1 et f_2 :

$$v_i = V\cos(2\pi f_1 t) + V\cos(2\pi f_2 t) \tag{2.11}$$

Du point de vue de la génération des harmoniques, la réponse fréquentielle sera toujours conforme à la relation (2.9) pour chacune des composantes fondamentales. En effet, quatre termes seront générés pour la composante de fréquence f_1 et quatre termes pour la composante de fréquence f_2. De plus, la non-linéarité révèle une action de mixage, entre les composantes fondamentales et leurs harmoniques, qui génère des produits d'intermodulation. Ce mixage ajoute au signal de sortie des termes qui apparaissent par combinaisons fréquentielles (sommes et différences) entre les fréquences des fondamentales et des harmoniques [3]. Donc, on peut exprimer le signal de sortie en ajoutant six termes de plus issus des produits d'intermodulation, et ce, aux huit termes générés par les composantes de fréquence f_1 et f_2 selon l'équation (2.9). De façon intuitive, et sans entrer dans les détails du développement mathématique, on obtient :

$$\begin{aligned} v_o(t) = {} & \tfrac{1}{2}G_2V^2 + (G_1V + \tfrac{9}{4}G_3V^3)\cos(2\pi f_1 t) + \tfrac{1}{2}G_2V^2\cos[2\pi(2f_1)t] + \tfrac{1}{4}G_3V^3\cos[2\pi(3f_1)t] \\ & + \tfrac{1}{2}G_2V^2 + (G_1V + \tfrac{9}{4}G_3V^3)\cos(2\pi f_2 t) + \tfrac{1}{2}G_2V^2\cos[2\pi(2f_2)t] + \tfrac{1}{4}G_3V^3\cos[2\pi(3f_2)t] \\ & + \; G_2V^2\{\cos[2\pi(f_2 - f_1)t] + \cos[2\pi(f_1 + f_2)t]\} \\ & + \tfrac{3}{4}G_3V^3\{\cos[2\pi(2f_2 - f_1)t] + \cos[2\pi(2f_1 - f_2)t]\} \\ & + \tfrac{3}{4}G_3V^3\{\cos[2\pi(2f_2 + f_1)t] + \cos[2\pi(2f_1 + f_2)t]\} \end{aligned} \tag{2.12}$$

La puissance dissipée à la fondamentale à travers une charge R est donnée par l'expression suivante :

$$\begin{aligned} P_o(f_1)_{[dBm]} &= 10\log[1000(G_1V + \tfrac{9}{4}G_3V^3)^2 / \sqrt{2}R] \\ &= 20\log(G_1V + \tfrac{9}{4}G_3V^3) + 10\log(1000/\sqrt{2}R) \end{aligned} \tag{2.13}$$

En comparant les expressions (2.10) et (2.13) on peut observer que le facteur de multiplication de G_3V^3 dans les expressions (2.13) est trois fois plus grand que celui contenu dans l'expression (2.10). Ceci a une influence sur la courbure de la zone de saturation de la fondamentale, qui s'incurve alors pour atteindre des valeurs plus basses que la puissance de sortie explicitée par l'expression (2.10). Un tel effet est important à souligner car il caractérise le comportement de la non-linéarité selon la forme d'onde amplifiée. Autrement dit, aucune caractéristique de rapport de puissance (AM-AM) ne représente, en forme générale, le comportement non-linéaire d'un amplificateur de puissance. Ceci peut se résumer de la façon suivante :

L'allure de la courbe qui caractérise le rapport de puissance moyenne d'un amplificateur de puissance (AM-AM) est fonction de la forme d'onde du signal amplifié.

2.3.4 Distribution fréquentielle

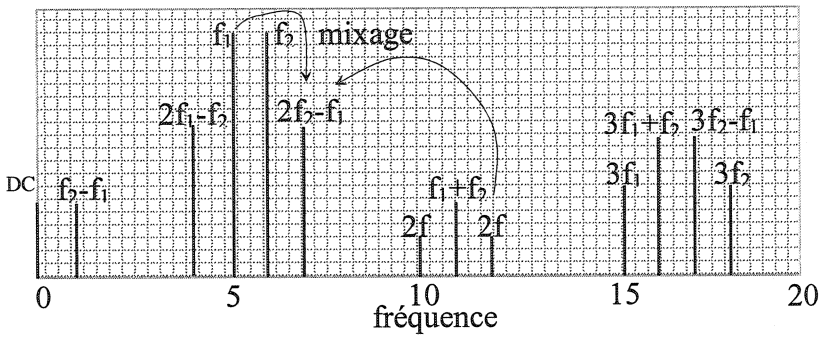

Figure 2.6 - Distribution fréquentielle

Sur la Figure 2.6, on peut visualiser la distribution fréquentielle de l'expression (2.12). On observe clairement que les produits d'intermodulation tendent à être regroupés autour de la fondamentale et des harmoniques. En ajoutant une composante de plus au signal d'entrée, le nombre de termes devient presque trois fois plus grand. Dans le cas de dix composantes en l'entrée et en considérant une fonction de transfert limitée au $5^{ème}$ ordre, le nombre de termes peut atteindre environ dix-huit mille. Dans le cas d'une porteuse modulée résultante d'une forme d'onde CDMA de 1,25 MHz de largeur de bande, le calcul du nombre de produits d'intermodulation générés sera fonction de la résolution du filtre de mesure (RBW) ou de la transformation de Fourier rapide. Par exemple, avec une résolution de 50 Hz on obtient 25,000 composantes pour la fondamentale. Ceci donne un nombre élevé de produits d'intermodulation, qui sont distribués dans le domaine fréquentiel selon l'ordre de non-linéarité considéré. La Figure 2.7 illustre le cas d'une non-linéarité du cinquième ordre, on observe, d'une part, les produits

d'intermodulation *"dans la bande"* qui affectent la qualité de l'information transmise, et d'autre part, les produits d'intermodulation *"hors bande"* qui affectent les canaux adjacents [4]. Une façon de prédire approximativement l'énergie répartie en fréquence est d'utiliser le point d'interception IP_3. Ce dernier est défini dans la section suivante.

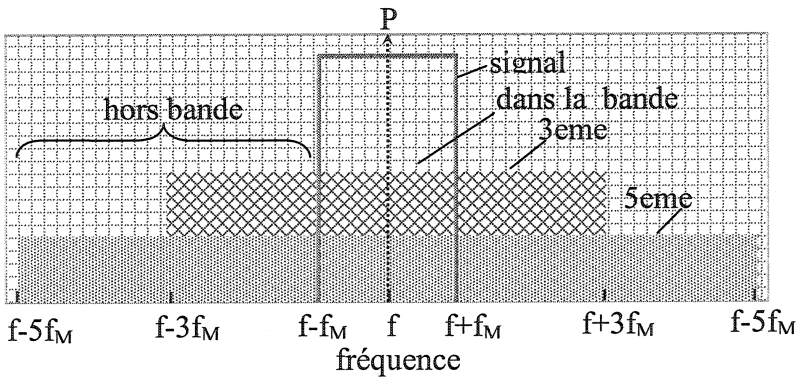

Figure 2.7 - Produits d'intermodulation *dans la bande* et *hors bande*

2.3.5 Point d'interception IP_3

On observe dans l'expression (2.12) que la réponse fréquentielle (ou spectrale) des termes en $(2f_2 - f_1)$ et $(2f_1 - f_2)$ est une pente, en échelle logarithmique, trois fois plus grande que celles des composantes fondamentales. Ceci revient à dire que pour chaque dB de variation de la puissance des composantes fondamentales à la sortie, les niveaux de la puissance des produits du troisième ordre changeront de 3 dB. Cela conduit à un point d'interception IP_3, donné par le rapport linéaire de puissance des composantes fondamentales et de la puissance des composantes d'intermodulation du troisième ordre (voir Figure 2.8)

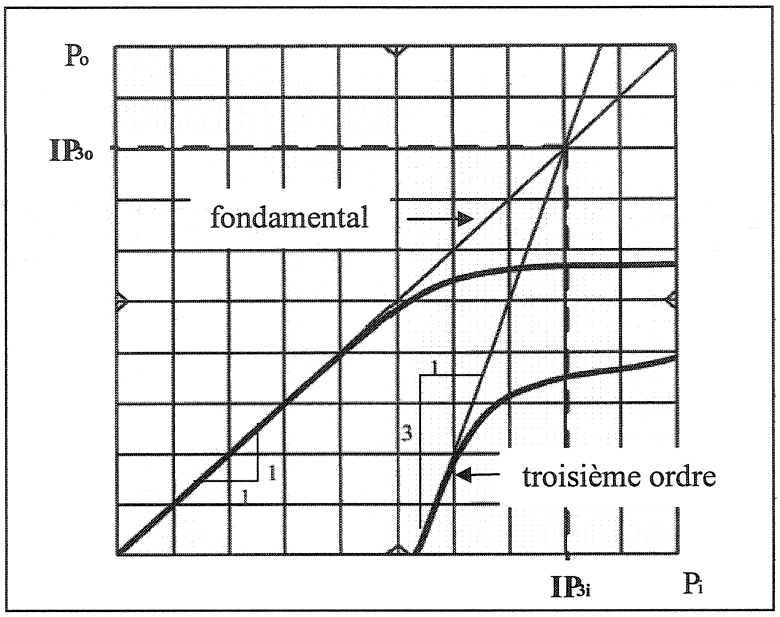

Figure 2.8 Point d'interception IP_3 donné par le rapport linéaire de puissance des composantes fondamentales et de la puissance des composantes d'intermodulation du troisième ordre

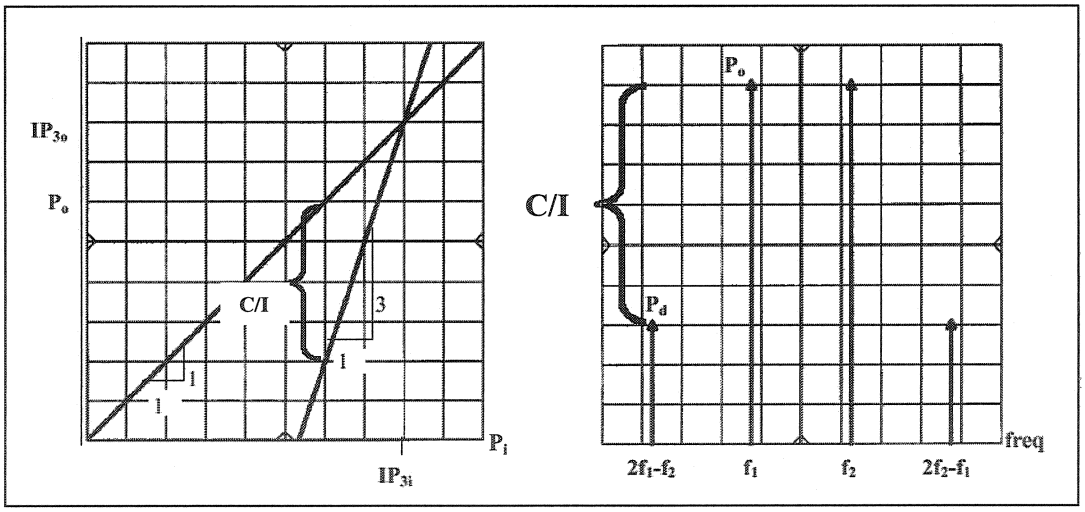

Figure 2.9 Point d'interception IP_3 et le rapport porteuse-intermodulation C/I

La Figure 2.9 illustre le rapport linéaire d'une composante fondamentale P_o et d'une composante du troisième ordre P_d par rapport à la puissance d'entrée P_i. On remarque

également sur la figure le spectre de fréquence donnée pour un niveau fixé de la puissance d'entrée. On observe clairement que le rapport porteuse-intermodulation C/I diminue lorsque P_i augmente.

A partir du graphique de la Figure 2.9, on peut voir que le point d'interception IP_3 permet une estimation rapide du niveau de puissance de la distorsion du troisième ordre en fonction du niveau de puissance de la sortie à la fondamentale. En se basant sur des relations géométriques on obtient :

$$IP_{3o[dBm]} = P_o + \frac{C/I}{2} \tag{2.14}$$

ou

$$C/I = P_o - P_d \tag{2.15}$$

La substitution de l'équation (2.15) dans l'équation (2.14) permet d'extraire le point d'interception du troisième ordre à la sortie.

$$IP_{3o[dBm]} = P_o + \frac{P_o - P_d}{2} \tag{2.16}$$

On obtient alors la puissance de distorsion en fonction de différents niveaux de puissance de la composante fondamentale :

$$P_d = 3P_0 - 2IP_3 \tag{2.17}$$

2.4 Compensation des distorsions. Réciprocité

Dans tout ce qui précède, on a supposé que la distorsion est générée par une fonction de transfert non-linéaire comme illustré sur la figure 2.10 (a). Si on examine en détails l'équation (2.9) qui se réduit ici par commodité :

$$v_o(t) = \tfrac{1}{2} G_2 V^2 + (G_1 V + \tfrac{3}{4} G_3 V^3)\cos(2\pi f_1 t) + \\ + \tfrac{1}{2} G_2 V^2 \cos[2\pi(2f_1)t] + \tfrac{1}{4} G_3 V^3 \cos[2\pi(3f_1)t] \tag{2.18}$$

on peut supposer que la tension de sortie $v_o(t)$, qui représente l'onde sinusoïdale qui présente des distorsions explicitées dans l'expression (2.7), est une forme d'onde résultant de l'addition de cinq sources indépendantes à travers un dispositif linéaire de sommation, figure 2.10 (b). Basé sur cette hypothèse, on peut affirmer que la distorsion et les harmoniques ont une relation de réciprocité [19]. Ce qui peut être résumé de la façon suivante :

> *«Si une onde sinusoïdale est distordue par une non-linéarité quelconque, alors des harmoniques du sinus sont générées. Réciproquement, si des harmoniques sont ajoutées à une onde sinusoïdale, alors l'onde résultante est distordue»*

Ceci peut être généralisé pour n'importe quelle forme d'onde contenant des harmoniques et des intermodulations.

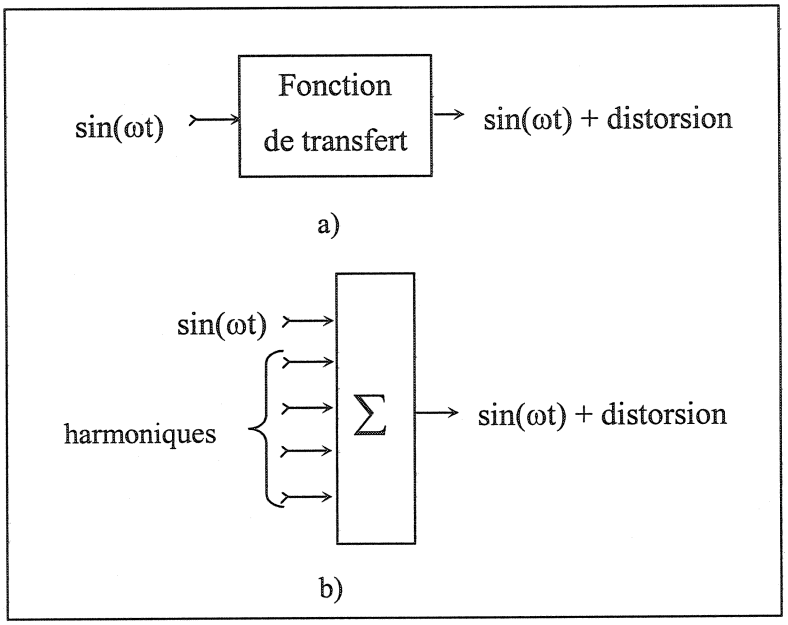

Figure 2.10 - Illustration de la réciprocité

Par la suite, on peut modéliser un générateur de distorsion à l'aide d'un estimateur de cohérence, tel qu'ajouté au signal de sortie v_o ou d'entrée v_i , il permettra de compenser la distorsion générée par la fonction de transfert. Autrement dit, les termes générés par le générateur de distorsion sont corrélés en amplitude et phase aux termes de distorsion générés par la fonction de transfert dans le but d'optimiser leur annulation. Sur la Figure 2.11 on peut visualiser les deux méthodes conventionnelles de compensation; on définit la méthode de «pré-compensation» (connue sous le nom de prédistorsion) quand la distorsion est ajoutée à l'entrée de la fonction de transfert. De plus, on définit la méthode de « post-compensation » lorsque la distorsion est superposée à la sortie de la

fonction de transfert. C'est à partir de ces concepts que se basent toutes les techniques de linéarisation des amplificateurs de puissance. La façon de générer et d'injecter la distorsion sur le signal utile est propre à chaque technique. De tels concepts sont explicités dans la section suivante.

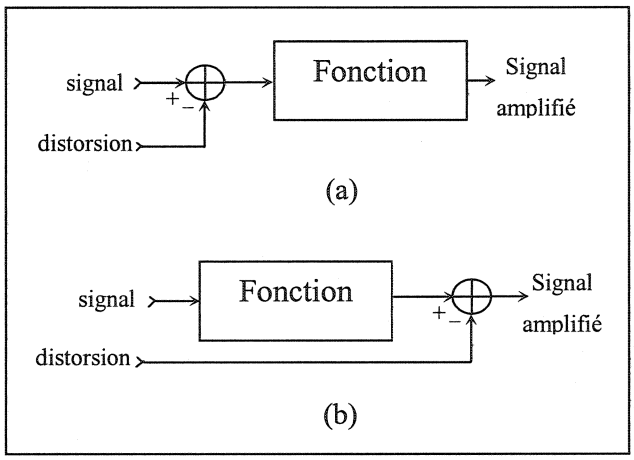

Figure 2.11 Méthodes conventionnelles de compensation
a) pré-compensation; b) post-compensation

2.5 Techniques de linéarisation

Nous avons mentionné, dans le chapitre précédant, que les amplificateurs de puissance sont généralement contraints d'opérer dans la région non linéaire, et ce, dans le but d'optimiser l'efficacité énergétique ou d'obtenir le maximum de puissance à la sortie. Ces conditions ont pour effet de générer des distorsions qui dégradent le comportement du système et la qualité du signal à amplifier. La réduction de ces distorsions pousse les concepteurs à s'intéresser et à développer des techniques de linéarisation capables de maintenir le rendement en puissance tout en conservant une bonne linéarité [4,20]. Pour répondre à ces exigences, plusieurs techniques de linéarisation ont été proposées et selon leurs caractéristiques elles peuvent être classées en trois groupes appelés: rétroaction, prédistorsion et post-compensation.

Le but de cette section est de présenter une revue critique de ces techniques. Étant donné la tendance par laquelle le traitement analogique du signal évolue vers le domaine numérique et vers le contrôle par logiciel, l'accent sera mis sur des concepts importants appliqués aux systèmes numériques. Les techniques par rétroaction et par prédistorsion seront présentées sous la forme numérique. Nonobstant, une brève présentation de la technique de post-compensation analogique est faite.

2.5.1 Techniques de linéarisation numériques

Les progrès technologiques des processeurs destinés aux traitements des signaux numériques et leurs applications dans le domaine des télécommunications a conduit à leur utilisation dans plusieurs techniques de linéarisation. Ces dispositifs, pouvant atteindre une fréquence d'horloge de l'ordre des micro-ondes, ils suscitent l'intérêt des concepteurs pour permettre l'exécution des algorithmes de compensation des distorsions en temps réel.

À cet égard, la description des techniques de linéarisation peut se faire à partir d'une structure généralisée composée d'une partie analogique et d'une partie numérique (circuit DSP) où sont exécutés les différents algorithmes qui caractérisent chaque technique. La figure 2.12 montre la structure généralisée d'un système intégré DSP/ RF.

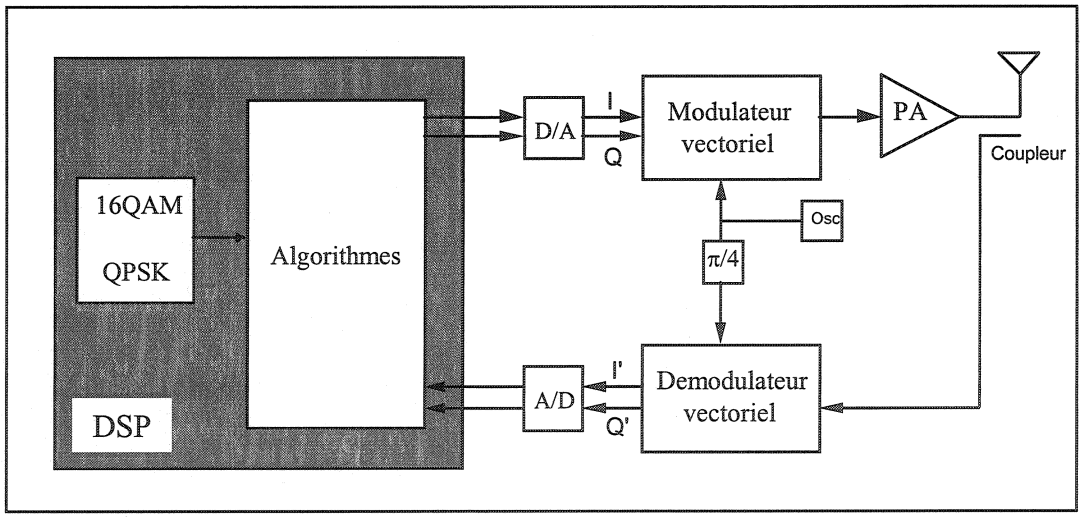

Figure 2.12 - Structure généralisée de la technique de linéarisation numérique

2.5.1.1 Rétroaction cartésienne

Comme son nom l'indique, le système est en effet basé sur le comportement dynamique d'une boucle de rétroaction cartésienne, voir figure 2.13 [21,22]. Le signal de rétroaction est démodulé de façon synchrone pour récupérer l'enveloppe complexe en bande de base représentée par les composantes I'/Q'. Celles-ci sont comparées de façon dynamique avec les composantes du signal en bande de base I/Q généré par le codeur [23,24]. La fonction erreur f_e résultante de la comparaison est conduite à travers un modulateur vectoriel et amplifiée par l'amplificateur de puissance.

Conformément à la structure de la technique, elle peut être conçue de façon numérique et analogique [4,20]. Cette technique, qui présente une bonne suppression des bandes latérales, est plus performante que certaines méthodes car la poursuite des variations de l'enveloppe s'exécute en temps réel. Pour obtenir le maximum de performance, il faut une bonne égalité en terme de gain et un alignement orthogonal sur les composantes en quadrature dans l'étage du modulateur et du démodulateur vectoriel. De plus, il est important que le gain de la boucle soit d'amplitude suffisante pour effectuer une correction continue de la non-linéarité et que la boucle de rétroaction soit la plus précise possible, afin de produire la fonction erreur et de répondre à la correction optimale.

Un point critique des systèmes de rétroaction est d'assurer la stabilité de la boucle lorsqu'on recherche une bande passante en boucle fermée relativement large. L'amplificateur de puissance génère une variation significative de la phase en fonction de l'amplitude et de la fréquence. De plus, le signal de la boucle est retardé par son passage à travers l'amplificateur, le coupleur et le démodulateur vectoriel. Donc une

rétroaction positive risque de se produire et d'induire un comportement instable.

D'un point de vue fonctionnel, la technique de rétroaction est considérée comme une technique de prédistorsion avec une correction continue de la fonction de prédistorsion. Ce qui signifie que l'adaptabilité de la fonction de prédistorsion est exécutée de manière continue par une comparaison en temps réel des signaux d'entrée et de sortie. Cette définition nous aide à visualiser clairement l'action discontinue de la mise à jour de la fonction de prédistorsion pour la technique de prédistorsion adaptative. Cette technique sera présentée dans la section suivante.

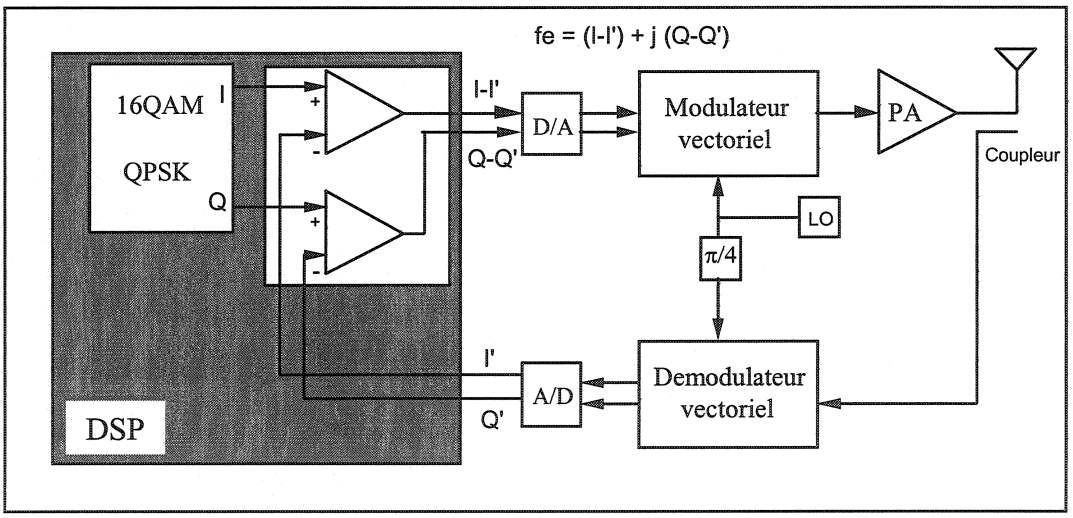

Figure 2.13 - Schéma bloc du système linéarisé par rétroaction cartésienne

2.5.1.1.1 Les points saillants de la technique

En résumé, le contrôle de la linéarité est limité par : la stabilité de la boucle, la précision du circuit de la boucle de rétroaction et le niveau de non-linéarité de l'amplificateur de puissance. Les inégalités en gain et le désalignement orthogonal introduit par le

modulateur vectoriel dans les composantes I,Q du signal modifient la fonction erreur, donc il faut avoir un gain suffisant de la boucle pour répondre à une telle correction. D'autre part, la stabilité de la boucle, qui est fonction de la réponse en phase de l'amplificateur de puissance, limite le gain donc la correction.

Les avantages et les inconvénients de la technique sont:

- Avantages
  1. Temps de convergence nul avec une correction continue.
  2. Permet d'être conçue de façon numérique et analogique.
  3. Simplicité
- Inconvénients
  1. La linéarité et la largeur de bande sont fortement dépendante du délai dans la boucle de rétroaction.
  2. La stabilité critique de la boucle.
  3. Le filtrage de mise en forme doit être conçu après l'amplificateur de puissance.

2.5.1.2 Prédistorsion

La façon la plus simple de compenser la distorsion produite par une non-linéarité quelconque est d'appliquer une non-linéarité complémentaire. Ce concept est utilisé par la plus ancienne technique de linéarisation appelée "prédistorsion"[25]. Dans cette technique, un élément ayant un comportement non linéaire et servant de générateur de distorsion complémentaire est placé avant le dispositif non linéaire qui doit être corrigé. Ces deux fonctions non-linéaires cascadées permettront d'améliorer la linéarité globale. Dans le cas des amplificateurs de puissance, une telle action de compensation permet de les faire opérer dans des conditions énergétiques optimales.

Cette technique à été utilisée pendant des années dans des systèmes de communication grâce à la simplicité de sa conception. Cependant, avec les phénomènes de dérive, de vieillissement, etc., la technique offre des performances qui se dégradent et il devient nécessaire d'inclure du traitement numérique adaptatif pour réajuste rapide net afin de compenser ces types de variations. Aujourd'hui, la conception entièrement numérique de cette technique devient de plus en plus un sujet de grand intérêt [7]. En effet, elles permettent, à elles seules, la conception de systèmes d'amplification ultra-linéaires présentant une *efficacité énergétique* optimale. De plus, la structure de contrôle par programmes et le traitement de signal entièrement numérique rend ces techniques applicables pour différentes formes d'onde, et elles répondent aux exigences imposées par les normes actuelles [26,27].

2.5.1.2.1 L'action discontinue de l'adaptabilité

Nous avons mentionné dans la section 2.4.1 que le comportement adaptatif de la technique de rétroaction peut être considéré comme une technique de prédistorsion adaptative présentant une correction en temps réel de la fonction de prédistorsion. Cette caractéristique met en évidence la capacité de la technique à poursuivre les variations des paramètres non linéaires avec une bonne suppression des bandes latérales. Nonobstant, l'atteinte de tels niveaux de performance est limitée par la largeur de bande du signal traité.

Pour surmonter ce problème, la technique de predistorsion adaptative offre une action discontinue de l'adaptabilité [7,8]. Étant donné que les phénomènes de dérive génèrent des variations lentes de la non-linéarité en comparaison avec la variation du signal, la correction de la fonction de prédistorsion est obtenue de façon discontinue. Celle-ci est contrôlée à travers la prise en considération du niveau de distorsion contenu dans le signal. Plus clairement, si la distorsion dépasse un niveau préfixé, l'adaptation est déclenchée et un réajustement de la fonction de prédistorsion est exécuté avec un temps de convergence qui dépend des algorithmes utilisés [7,8, 28]. Une fois la correction de la fonction de prédistorsion effectuée, l'adaptabilité est interrompue et le processus de la linéarisation continue.

Cette particularité permet à la linéarisation de se faire de façon indépendante de

l'adaptabilité. Ceci permet de surmonter le problème de l'instabilité dont souffre la technique de rétroaction cartésienne.

2.5.1.2.2 La méthode de la table de correspondance

L'élément ayant une caractéristique non linéaire et qui fait office de générateur de prédistorsion, peut prendre la forme d'une table de correspondance [29], voir la figure 2.14. Cette dernière possède un certain nombre d'entrées composées de valeurs discrètes couvrant ainsi la plage de variation de l'amplitude du signal. À l'aide d'une interpolation linéaire où avec un "spline" cubique, elle peut fournir, pour n'importe quelle valeur du signal d'entrée, une valeur équivalente prédistorsionnée à la sortie.

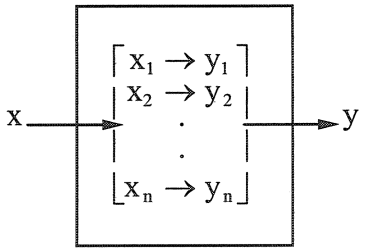

Figure 2.14 Table de correspondance

2.5.1.3 Prédistorsion complexe (table à deux dimensions)

Une des techniques de prédistorsion numérique les plus prometteuses fut inventée par Nagata [7]. Cette technique est basée sur une table de correspondance à deux

dimensions, qui permet une correction complexe de la distorsion sans être dépendante du type de modulation utilisée ou de l'ordre de non-linéarité. Cette technique a montré de bonnes performances, mais elle présente tout de même certains inconvénients auxquels il faut faire face.

2.5.1.3.1 Description générale

Supposons que l'enveloppe complexe $S = I + jQ$ est une série d'impulsions qui résulte d'une modulation linéaire, voir la figure 2.4, et S_i l'échantillon complexe $"i"$ du signal quantifié avec 2^n niveaux de quantification (n= nombre de bits par échantillon). La valeur complexe $S_i = I_i + jQ_i$ agit sur la table complexe où sont stockées toutes les valeurs discrètes de la prédistorsion D. Chaque somme complexe $S_i + D_I$ affiche l'échantillon complexe $"i"$ avec prédistorsion et la série $S + D$ représente la série d'impulsions avec prédistorsion qui traversera le bloc de conversion D/A, générant ainsi le signal analogique $S(t) + D(t)$. Ensuite, ce signal sera conduit à travers un modulateur vectoriel et sera amplifié par l'amplificateur de puissance. Étant donné que la distorsion $D(t)$ est déterminée en fonction d'une non-linéarité complémentaire à celle de l'amplificateur de puissance, la distorsion générée par celui-ci sera annulée par $D(t)$ en donnant comme résultat une amplification linéaire. Le signal d'entrée de l'amplificateur est exprimé par:

$$A(t) = \left[S(t) + D(t)\right] e^{j\omega t} \tag{2.19}$$

Et le signal de sortie de l'amplificateur sera donné par:

$$Z(t) = F\left[S(t) + D(t)\right] e^{j\omega t} \tag{2.20}$$

où $F\left[S(t) + D(t)\right]$ représente le gain complexe non linéaire de l'amplificateur. Afin d'obtenir une amplification linéaire du signal $S(t)$ avec l'annulation de la distorsion, la sortie sera donnée par:

$$Z'(t) = KS(t) e^{j\omega t} \tag{2.21}$$

où K est le gain de l'amplificateur en régime linéaire. En comparant les équations (2.20) et (2.21) et pour obtenir une annulation complète de la distorsion, $D(t)$ dois prendre des valeurs telles que la condition suivante soit satisfaite pour toutes les valeurs définies de $S(t)$:

$$KS(t) e^{j\omega t} = F\left[S(t) + D(t)\right] e^{j\omega t} \tag{2.22}$$

Si la condition d'égalité de l'équation (2.22) n'est pas satisfaite, $D(t)$ est recalculé de façon itérative à partir d'une mise à jour de la table de correspondance. Ce processus est

réalisé en prélevant un échantillon du signal de sortie de l'amplificateur, figure 2.15. Puis, le signal est démodulé de façon synchrone pour obtenir le signal de rétroaction en bande de base $P(t) = I' + Q'$. Ce signal est traité dans le convertisseur A/D pour obtenir une série d'impulsions P. Chaque échantillon complexe P_i de P est comparé avec l'échantillon complexe S_i de S qui lui correspond. Le résultat obtenu est une erreur E_i, qui compense le changement des valeurs D_i de la table de correspondance, et ce, jusqu'à satisfaire la condition (2.22). Une fois que les valeurs de la table sont recalculées et mises à jour, la boucle s'ouvre et le système se comporte comme un contrôle à boucle ouverte. Le processus donne une stabilité inconditionnelle du système.

L'erreur $E_i = S_i - P_i$ est minimisée de façon itérative à travers le calcul de $(D_i)_n$ selon l'équation suivante:

$$(D_i)_n = (D_i)_{n-1} + \alpha E_j \tag{2.23}$$

où $(D_i)_n$ est la valeur suivante de prédistorsion, $(D_i)_{n-1}$ la valeur initiale ou précédente de prédistorsion et α le coefficient d'amplification. Le nombre d'itérations *"n"* dépend de l'ordre de distorsion et de la relation Porteuse/Intermodulation (C/I) requise à la sortie.

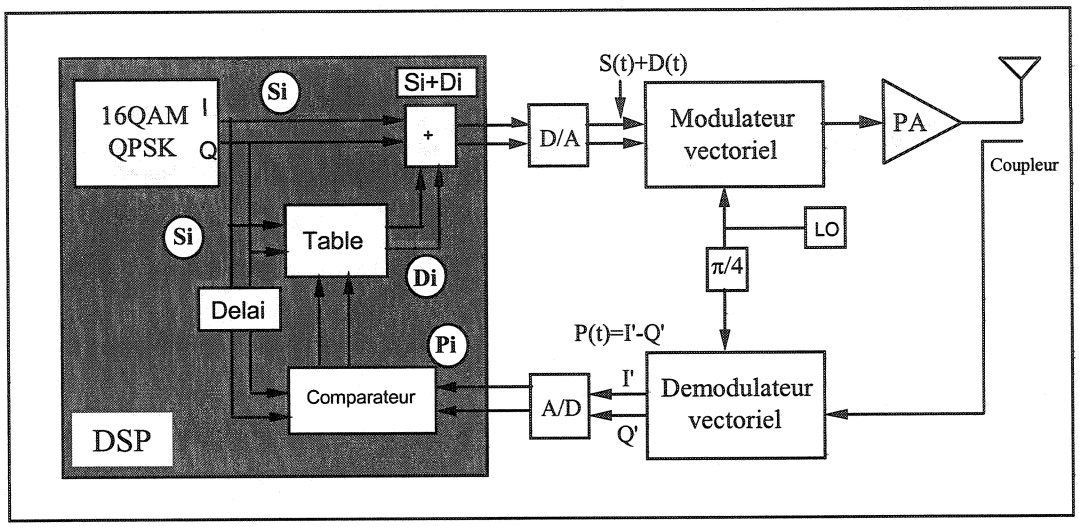

Figure 2.15 Schéma bloc du système linéarisé par prédistorsion avec une table à deux dimensions

2.5.1.3.2 Temps de convergence

Le temps de convergence pour l'ensemble des valeurs D_i vers les valeurs optimales dépend des variations des paramètres non linéaires en fonction de la température, du vieillissement et du changement de la fréquence de la porteuse. Dans les deux premiers cas les variations sont très lentes, donc le système est capable de suivre ces variations sans produire de dégradation dans le domaine spectral. Dans le troisième cas, c'est à dire lors de brusques variations de la non linéarité, l'asservissement a besoin de mettre à jour une grande partie des valeurs D_i de la table de correspondance. Ce qui demande, selon la condition, un temps de traitement d'environ 10 secondes avec une forte dégradation du spectre.

2.5.1.3.3 Les points saillants de la technique

La technique offre d'excellentes performances: une bonne efficacité, une bonne adaptabilité et un bon rapport C/I = -60 dBc. La technique s'apparente à un système de contrôle en boucle ouverte où la prédistorsion est effectué à partir d'une table de correspondance à deux dimensions. Les avantages et les inconvénients de la technique sont:

- Avantages
    1. Le processus de linéarisation est fait de façon indépendante de la mise à jour des valeurs contenues dans la table de correspondance.
    2. Compatible avec tout type de modulation et tout ordre de non linéarité.
    3. Le filtrage de mise en forme peut être conçu avant l'étape de prédistorsion.
- Inconvénients
    1. Temps de convergence assez long.
    2. Espace mémoire nécessaire important.

2.5.1.4 Prédistorsion complexe (table à une seule dimension)

Se basant sur la technique précédente, Caver [8], a proposé une nouvelle technique basée sur une table à une seule dimension pour minimiser le temps de convergence et la quantité de mémoire requise. Cette technique offre l'avantage d'afficher un temps de convergence très réduit (4 msec contre 10 sec.) De plus, le gain d'espace mémoire

permet d'allouer des segments de mémoire rendus disponibles pour différentes fréquences de la porteuse.

2.5.1.4.1 Description générale

La figure 2.16 montre le schéma théorique de la technique. L'amplificateur de puissance est modélisé comme un dispositif non linéaire sans mémoire au moyen d'une fonction de gain complexe $G(x_d)$ et d'un argument réel x_d [30]. Cette fonction lie les enveloppes complexes du signal d'entrée $V_d(t)$ et de sortie $V_a(t)$ de la façon suivante:

$$V_a(t) = G(x_d)V_d \tag{2.24}$$

où $x_d = |V_d|^2$ représente la puissance instantanée. Le gain complexe $G(x_d)$ est donnée par :

$$G(x_d) = G_x(x_d) + jG_y(x_d) \tag{2.25}$$

Il est à noter que $G(x_d)$ dépend seulement de la puissance instantanée d'entrée $|V_d|^2$, c'est-à-dire que le gain complexe est fonction de la variation de l'amplitude et non de la variation de la phase du signal d'entrée. $G(x_d)$ représente le gain complexe, qui, une fois multiplié par le signal d'entrée référencé au signal de sortie, permet de caractériser les courbes instantanées d'amplitude AM/AM et de phase AM/PM. Ces courbes représentent le comportement instantané de l'amplificateur de puissance.

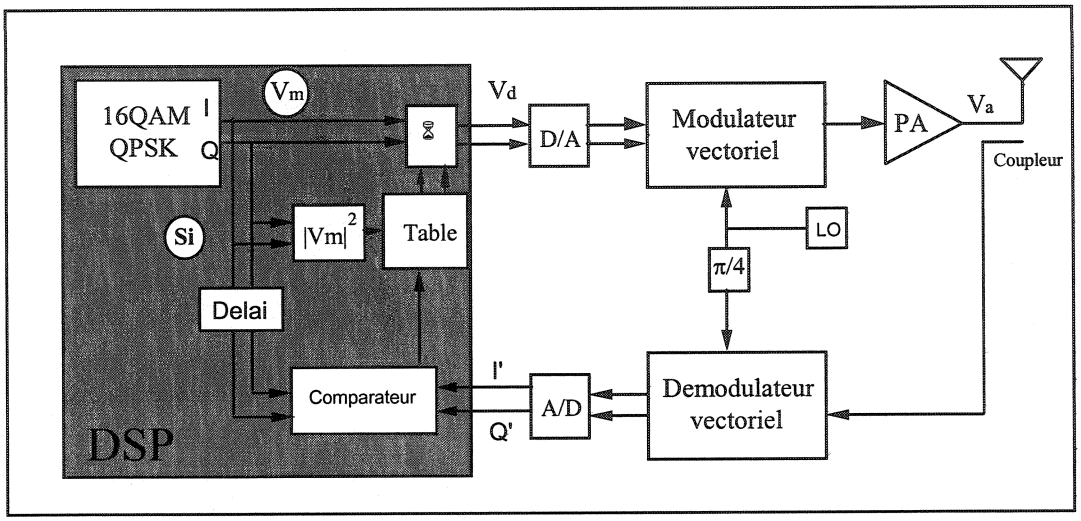

Figure 2.16 Schéma bloc du système linéarisé par prédistorsion avec une table à une seule dimension.

De la même façon, la fonction de gain de prédistorsion est formulée comme une fonction de gain $F(x_m)$ où les enveloppes complexes du signal d'entrée $V_m(t)$ et de sortie $V_d(t)$ sont liées par la relation suivante:

$$V_d = V_m F(x_m) \tag{2.26}$$

où $x_m = |V_m|^2$ représente la puissance instantanée. Le gain complexe $F(x_m)$ est donnée par :

$$F(x_m) = F_x(x_m) + jF_y(x_m) \tag{2.27}$$

En combinant les équations (2.24) et (2.26) et en utilisant la condition linéaire d'amplification $V_a(t) = KV_m(t)$, on obtient:

$$V_m F(x_m) G\left\{x_m \left[F(x_m)\right]^2\right\} = V_m K \tag{2.28}$$

Ce qui donne:

$$F(x_m) G\left\{x_m \left[F(x_m)\right]^2\right\} = K \tag{2.29}$$

L'équation (2.29) représente la condition de compensation idéale de la distorsion à travers la non linéarité complémentaire de la fonction $F(x_m)$. Le facteur K est un gain de valeur constante, qui permettra d'obtenir toutes les valeurs optimales de $F(x_m)$ en fonction des valeurs de la puissance instantanée qui sont inclues dans la plage de variation de x_m.

Il est à noter que le gain complexe $F(x_m)$,qui est représenté par une fonction complexe dépendante de la variable réelle x_m, peut être représenté à partir d'une table de correspondance à une seule dimension. Ce qui représente un net avantage pour cette technique par rapport à la technique précédente qui utilise, quant à elle, une table à deux dimensions (I/Q). Cette différence permet de réduire la quantité de mémoire nécessaire, et par conséquent, de réduire des temps de convergence. Par exemple, pour obtenir de bonnes performances, cette technique nécessite seulement 64 entrées pour la table de correspondance contre 1 million d'entrées pour le cas précédent. Cette réduction du nombre d'entrées permet ainsi l'implémentation de tables de correspondance pour la représentation de $F(x_m)$ pour différentes fréquences de la porteuse.

2.5.1.4.2 Calcul de la fonction de transfert de prédistorsion $F(x_m)$

Dans le but de résoudre l'équation (2.29) par le biais d'une estimation adaptative de chaque valeur de $F(x_m)$, la technique utilise comme méthode numérique de calcul la méthode dite par la sécante, qui est définie par la relation:

$$F(k+1) = \frac{F_i(k-1)\ e(F_i(k)) - F_i(k)\ e(F_i(k-1))}{e(F_i(k)) - e(F_i(k-1))}\ , \qquad (2.30)$$

où $F_i(k)$ est la $k^{ième}$ itération de l'entrée "i" dans la table de correspondance et où la fonction erreur *"e"* est donnée par:

$$e(F) = V_a(F) - KV_m. \qquad (2.31)$$

Comme nous l'avons mentionné précédemment, le nombre d'itérations pour le calcul dépend du niveau de distorsion de l'amplificateur et de la relation C/I requise à la sortie. La technique a été expérimentée avec 64 entrées et pour une valeur de dix itérations pour chaque entrée. Un temps de convergence de 4 ms a été obtenu pour chacune des mises à jour de la table de correspondance.

Une fois que la table est mise à jour avec les coefficients de distorsion qui correspondent à chaque entrée, la boucle s'ouvre et le système se présente comme un contrôle en boucle

ouverte. Ceci signifie que la linéarisation est faite de façon indépendante de l'adaptabilité des coefficients de la table de correspondance, ce qui rend le système inconditionnellement stable.

2.5.1.4.3 Les points saillants de la technique

La technique offre un temps de convergence réduit pour des variations lentes. De plus, le temps de convergence, dépendant du changement de fréquence d'opération, est réduit grâce à la possibilité d'allouer des tables de correspondance pour différentes fréquences de la porteuse. Les avantages et les inconvénients de la technique sont:

- Avantages
  1. Le processus de linéarisation est fait indépendamment de la mise à jour de la table de correspondance.
  2. La technique accepte n'importe quel ordre de non-linéarité.
  3. Le filtrage de mise en forme peut être conçu avant l'étape de prédistorsion.
  4. Le temps de convergence est faible.
  5. La quantité de mémoire requise est minimale.
- Inconvénients
  1. Le coût de compilation (mise en opération) est très élevé
  2. Les problèmes de divergence.

2.5.1.5 Post-compensation

Caractérisée par sa conception uniquement analogique, la linéarisation par post-compensation [31,32] s'avère être plus performante en termes de largeur de bande. Basée sur le fait que la compensation de la distorsion est réalisée à la sortie de l'amplificateur de puissance, son architecture ne permet pas de conception numérique. Des échantillons du signal d'entrée et de sortie de l'amplificateur de puissance sont égalisés en amplitude et mis en opposition de phase pour être finalement combinés. La sommation des ces deux signaux donne le signal de distorsion isolé qui est amplifié et combiné avec le signal de sortie de l'amplificateur de puissance. Pour une compensation optimale, la distorsion isolée et la distorsion contenue dans le signal de sortie doivent être en parfaite opposition de phase et d'amplitude égale.

La technique offre une excellente réduction des produits d'intermodulation avec une stabilité inconditionnelle, qui est due à son architecture en boucle ouverte. Malgré la faible efficacité énergétique, compte tenu de sa largeur de bande importante, cette technique est largement et exclusivement utilisée dans les stations de base des systèmes cellulaires.

Il est à souligner que les phénomènes de dérive qui sont fonctions de la température, du vieillissement, de la variation du point d'opération, etc., sont contrôlés en bande de base avec des algorithmes exécutés par un circuit de traitement numérique de signaux [18].

2.6 Conclusion

Nous avons présenté dans ce chapitre les concepts de base d'une part, de la génération d'une forme d'onde, et d'autre part de la distorsion issue de la non-linéarité et de la compensation de cette distorsion. Leurs définitions, leurs relations et leurs influences ont été présentés de façon didactique dans le but de développer une meilleure compréhension des techniques de linéarisation.

En premier lieu, nous avons évoqué les paramètres qui sont susceptibles d'affecter les propriétés de la forme d'onde, comme le taux de symbole ou encore le facteur de retombée α. La caractérisation de la variation de l'enveloppe, à travers la fonction CCDF, a été illustrée pour des signaux typiques et l'impact de cette variation sur le comportement des amplificateurs de puissance a été mentionnée. Puis nous avons mis en évidence les effets de la non-linéarité, en identifiant la distorsion *"dans la bande"* qui affecte la qualité de l'information transmise, et la distorsion *"hors bande"* qui affecte les canaux adjacents. De plus, à partir d'une analyse intuitive, nous avons identifié la dépendance de la réponse AM-AM en fonction de la forme d'onde du signal à amplifié.

En ce qui concerne la compensation de la distorsion, nous avons défini les concepts de pré-compensation et de post-compensation en se basant sur la propriété de réciprocité de la distorsion. Ces concepts ont constitué les fondements permettant d'introduire les

techniques de linéarisation et de dégager les mécanismes des techniques de prédistorsion avec comme point de départ la technique de rétroaction cartésienne.

Les chapitres suivants traitent du développement théorique et de l'implémentation des nouveaux algorithmes proposés dans cette thèse. Ces algorithmes permettent de concrétiser deux nouvelles techniques de prédistorsion avec l'introduction d'un modèle (fonction de transfert dans le domaine temporel) basé sur les principaux concepts décrits dans ce chapitre. L'objectif principal est de réduire l'espace mémoire nécessaire aux différents calculs numériques, et d'autre part, de diminuer la complexité du système tout en supprimant l'instabilité des processus itératifs.

CHAPITRE III

Présentation des articles intégrés dans la thèse

Le présent chapitre a pour principal objectif d'introduire les chapitres IV et V. En effet, ces derniers sont rédigés sous la forme d'articles scientifiques selon les critères et normes requis pour la rédaction des thèses par articles intégrés. La mise en situation des articles est présentée avec la définition de chaque technique, leurs points saillants, leur contexte historique et les aspects méthodologiques concernant la validation des algorithmes.

3.1 Présentation: article I, chapitre IV

L'article présenté dans le chapitre IV vise les résultats de travaux de recherche réalisés

dans le cadre du projet AMPLI et il représente le texte d'origine rédigé en anglais, qui a servi comme base d'une demande de brevet déposée au bureau des brevets américain. La technique faisant l'objet de telle divulgation est protégée par le brevet américain No. US6072364, émis en juin 2000, une copie est intégrée dans l'annexe I.1. Également, l'article a été soumis pour publication dans la revue "IEEE Transaction on Vehicular Technology" et représente une version augmentée d'un article qui a été présenté et publié dans le congrès international de micro-ondes à Baltimore "IEEE-IMS1998 International Microwave Symposium", ce dernier est intégré dans l'annexe II.1.

3.1.1 Mise en situation

3.1.1.1 Définition et points saillants de la technique

Le travail décrit dans ce chapitre consiste essentiellement à une implémentation d'une nouvelle méthode algorithmique dédiée à la technique de ***prédistorsion numérique adaptative*** applicable pour les amplificateurs de puissance micro-ondes. Il est connu que les algorithmes itératifs complexes, utilisée dans ces techniques en vue de déterminer une nonlinéarité complémentaire à celle de l'amplificateur de puissance, sont soumis à un temps de convergence qui en limite la performance. La contribution originale de la nouvelle méthode algorithmique consiste en une détermination, dans le domaine du temps, d'une fonction de prédistorsion en utilisant des données fournies par une modélisation en temps réel des caractéristiques non linéaires des amplificateurs de puissance. Les points saillants sont l'élimination des algorithmes itératifs, la modélisation en temps réel des caractéristiques non linéaires de l'amplificateur de

puissance, la configuration de la table de correspondance et le type d'interpolation utilisé. Les champs d'applications possibles sont l'utilisation de cette technique pour la conception d'émetteurs de haute performance pour les systèmes de communications par satellite et systèmes cellulaires de deuxième et troisième génération qui nécessitent des émetteurs ultra linéaires. Particulièrement, l'application de la méthode s'adresse aux concepteurs ayant accès à l'environnement de bande de base d'un système de communications cellulaires à bande étroite, 30 kHz.

3.1.1.2 Contexte historique

Différentes approches, visant une réduction du temps de convergence ont été proposées pour la réalisation de la technique de prédistorsion numérique adaptative. Parmi ces approches, nous mentionnons la technique qui utilise une table de correspondance à deux dimensions avec un algorithme de convergence linéaire et temps de convergence assez long, 10 sec. [7] et la technique qui utilise une table de correspondance à une dimension avec un algorithme de convergence par la méthode de la sécante ``Secant Method`` avec un temps de convergence de 4 ms [8].

3.1.1.3 Comportement de la technique

La technique propose une solution pour l'élimination des algorithmes de convergence. Elle utilise une modélisation en temps réel des caractéristiques non linéaires des amplificateurs de puissance, avec un temps de caractérisation d'environ 10 symboles. Ceci représente un temps de 0,3 ms pour un débit de symboles de 30 kHz. L'information

fournie par ce processus permet la détermination de la fonction de prédistorsion par l'interpolation inverse de la fonction qui modélise le comportement de l'amplificateur de puissance pendant son fonctionnement. Les données obtenues forment une table de correspondance où la nonlinéarité complémentaire est déduite en faisant appel à une interpolation de type linéaire ou cubique. Les algorithmes sont exécutés par un processeur de traitement du signal (DSP) dans la transmission en bande de base.

3.1.1.4 Validation des algorithmes

La technique a été implémentée et validée expérimentalement, pour un amplificateur de puissance typique de la classe AB de 30-dBm, en utilisant une carte de développement de la compagnie Spectrum LSI. La carte de développement inclut un microprocesseur TMS320C40 de la compagnie Texas Instrument, d'un générateur d'horloge, un bloc de mémoire SRAM et des convertisseurs A/D et D/A.

3.2 Présentation: article II, chapitre V

L'article présenté dans le chapitre V vise les résultats de la deuxième partie des travaux de recherche réalisés par l'auteur a l'École Polytechnique de Montréal et avec le support financier de la compagnie Amplix, Inc. L'article représente le texte d'origine rédigé en anglais, qui a servi comme base des demandes de brevet déposées aux bureaux des brevets canadien et américain. Les demandes de brevet ont été rendues publiques le 8 décembre 2002 sous le No CA2349916 et le No US20020191710 respectivement, une

copie est intégrée dans l'annexe I.2. Également, l'article a été soumis et accepté pour publication dans la revue "IEEE Transactions on Microwave Theory and Techniques" et représente une version augmentée d'un article qui a été présenté et publié dans le congrès international de micro-ondes à Boston "IMS-2001 International Microwave Symposium", ce dernier est intégré dans l'annexe II.2.

3.2.1 Mise en situation

3.2.1.1 Définition de la technique

Le travail décrit dans ce chapitre consiste essentiellement à une implémentation d'une nouvelle technique de ***predistorsion dynamique adaptative*** applicable pour les amplificateurs de puissance micro-ondes. Cette deuxième partie a consisté à adapter la technique présentée dans le chapitre IV, avec une structure différente, pour être appliquée par des concepteurs n'ayant pas accès à l'environnement de bande de base d'un systèmes de communications cellulaires. De plus, pour atteindre 1.25 MHz de largeur de bande selon la norme du système CDMA IS-97. La contribution originale propose une nouvelle méthode algorithmique pour l'implémentation de la technique dans un environnement numérique basé sur l'utilisation des récepteurs numériques. Cette technique permet avec grande précision : i) une caractérisation instantanée du comportement non linéaire de l'amplificateur, ii) une poursuite en temps réel du niveau de distorsion à la sortie de l'amplificateur et iii) un ajustement dynamique de la compensation de distorsion. On remarque l'avantage de cette méthode dans l'action de la prédistorsion, générée en bande de base, qui est appliquée directement à travers une

modulation dans le domaine RF. Les champs d'applications possibles sont l'utilisation de cette technique pour la conception d'émetteurs de haute performance pour les systèmes de communications cellulaires de deuxième et troisième génération qui nécessitent des émetteurs ultra linéaires.

3.2.1.2 Points saillants

Les points saillants sont la haute sélectivité des intervalles de fréquence dans le domaine spectral, la surveillance simultanée des niveaux de puissance de distorsion dans différents intervalles de fréquences selon la norme stipulée, la performance du processus de calcul des niveaux de puissance, soit dans le domaine des fréquences ou dans le domaine temporel et la configuration de la table de correspondance pour générer la fonction du gain complexe de la fonction de prédistorsion.

3.2.1.3 Contexte historique

Deux approches ont été proposées, par le même auteur, basés sur des algorithmes itératifs après une minimisation de puissance et avec un processus de mesure scalaire entièrement analogique [28-36]. Un troisième approche a été présenté dans la référence [37] en utilisant la même structure présentée en [28]. Les inconvénients sont la convergence lente vers le minimum et la sensibilité au bruit de mesure.

3.2.1.4 Comportement de la technique

La contribution de la technique répond à des attentes comme la sélectivité des bandes de

fréquences, la haute sensibilité dans la mesure de niveau de distorsion et la rapidité de l'action adaptative. La contribution propose une haute sélectivité donnée par un processus de translation et décimation entièrement numérique, qui rend le système flexible à la sélection de tout signal dans le domaine RF pour le placer de façon directe dans la bande de base avec une très haute précision. L'application de ce processus aux signal d'entré et de sortie de l'amplificateur de puissance permet l'exécution de la caractérisation instantanée à travers la comparaison des formes d'ondes sélectionnées. La haute sensibilité qui caractérise la technique est une conséquence directe de la haute sélectivité et des algorithmes de calcul implanté dans un environnement numérique. Ces algorithmes permettent la surveillance simultanée des niveaux de puissance de la distorsion dans différents intervalles de fréquences servant à contrôler l'action adaptative de la prédistorsion. En plus, le contrôle des valeurs de référence (niveaux de puissance de la distorsion) donne la flexibilité à la méthode pour s'adapter à différentes conditions selon la norme stipulée.

3.2.1.5 Validation des algorithmes

La technique a été validée au niveau simulation a boucle fermée et au niveau expérimental en boucle ouverte, pour un amplificateur de puissance typique de la classe AB de 44-dBm, en utilisant le logiciel ADS de la compagnie Agilent Technologies et grâce à des instruments ROHDE&SCHWARZ. La caractérisation instantanée a été validée au niveau expérimental en utilisant les instruments « Peak Power Analyzer » et « Microwave Transition Analyzer » de la compagnie Agilent Technologies.

CHAPITRE IV

Experimental Implementation and validation of an Adaptive Digital Predistortion Technique

Experimental Implementation and validation of an Adaptive Digital Predistortion Technique

Ernesto G. Jeckeln, *Member, IEEE,* Fadhel M. Ghannouchi, *Senior Member, IEEE* and, Mohamad A. Sawan, *Fellow, IEEE*

Abstract

This paper presents an experimental implementation of an adaptive digital predistortion technique in the area of power amplifier linearization. The technique is validated through an L band experimental implementation using a direct I-Q modem and driven by spectrally efficient 16-QAM signals. The linearizer, which is implemented in digital signal processor (DSP) environment, accomplishes the extraction of the PA nonlinear behavior in real time and correlates a numerical quasi-perfect cancellation function for predistortion purposes. Experimental results demonstrate that the spectral regrowth is reduced by 20 dB, driving the PA at 6 dB output back off (OBO) referenced to the single carrier saturation point.

4.2 Introduction

Linearization techniques become a useful way to compensate the distortion effects and spectral spreading caused by the non-linearities of a power-efficient amplifier on spectrally efficient standard signals. In addition, linearization techniques through digital predistortion allow achieving both power efficiency and spectral efficiency while signal degradation is compensated. Thus, while spectrally efficient standard signals that have high envelope variation, are adopted to maximize the spectral efficiency, a linearized class AB power amplifier (PA) operating close to saturation (non-linear region) is needed to achieve both high power efficiency and high output power emission.

Various linearization methods have been reported and many different ways can be used to segment this topic. In general, all these techniques are, by any measure, derived from three main types named: i) Feed-forward [31], ii) Feedback [21-23] and iii) Predistortion [25]. The last technique, that has historically been the most common method in analog implementation, now can be well suited to digital implementation using digital signal processor (DSP) environment. Today, the high clock speeds in DSPs, which are entering the microwave frequency bands, offer the possibility to migrate most of the analog signal processing to the digital domain. The benefits of fast computational engine from this technology in several applications motivate the designers to focus toward the DSP/RF integration. In this way, predistortion became one of the most robust linearization techniques that can be suited within this environment and dedicated to improve efficiency. In addition, for greater accuracy and flexibility, digital predistortion

is a promising technique that could replace the feed-forward correction, which is the most common multi-carrier amplifier technology available today. Important experimental results of this technique have been reported [7-11] demonstrating the capability in reducing the spectral spreading and how adaptive correction for drift, aging and temperature variation can be achieved. All algorithms of these previous works are based on iterative procedures [7,28], where the adaptation is exposed to critical conditions such as starting point of optimization, stability and convergence rate. In this sense, this paper proposes efficient algorithms suitable for adaptive digital predistortion. The new method develops an instantaneous characterization of the PA behaviors, which removes the need for complex convergence algorithms in the adaptation update step. In addition, the method proposes a new look-up tables configuration using polar representation and where the tables are accessed in pipeline form [11,33,34]. The technique is implemented using a DSP environment where the algorithms are performed to linearize an efficient class AB power amplifier.

The remaining of this paper presents a brief description of the system, the PA modeling and the ideal operating conditions for the predistorter (PD) in section II. Section III presents the linearizer algorithms, where the concept of the instantaneous characterization and the look-up tables configuration are developed and discussed. The implementation and the results are shown in section IV and the conclusions are presented in section V.

4.3 The Adaptive Digital Predistorter

4.3.1 General description

Figure 4.1 shows a simplified block diagram of the adaptive predistortion linearizer where, in addition to the digital domain, a dual DA/AD converters, a quadrature modulator (QM) and demodulator, a coupler and a microwave power amplifier form the analog domain to complete the entire system. In the digital domain, the spectrally efficient 16-QAM-modulation schema is used by a source to produce a 16-QAM modulated signal to be transmitted. It is within the scope of the present technique to use another type of digitally modulated signal. After the signal is picked up by the pulse-shaping filter, the signal is passed through the predistorting block, which introduce a corrective signal to cancel out the non-linear gain of the PA. The predistorter uses two one-dimensional lookup tables where the real time modeling block (RTM) stores a set of data resulting from the extraction of the non-linear behaviors. This process is accomplished by sampling the input $V_d e^{j\varphi_d}$ and the output $V_f e^{j\varphi_f}$ equivalent lowpass complex envelope signals of the PA. An important feature that the system considers is the adaptability dedicated to drift correction. In this process, the system uses a feedback path through which the linearizer is notified of these changes. Mean error criterion between the desired and the distorted feedback signals is performed and the result is compared with a defined threshold. After each adaptation and during normal data transmission, the feedback loop is opened until new significant drifts have occurred and new data has to be entered in the look-up tables. The feedback path's delay is estimated

by performing cross correlation between the input signal of the PA and the delayed feedback signal, then, the sample of the input signal is delayed through a delay block.

4.3.2 Memoryless Nonlinear Model and Inverse Function

Class AB power amplifier operating close to saturation (non-linear region) can achieve both high power efficiency and high output power emission with an acceptable gain. The PA is considered saturated when the output level no longer increases when the input power level increases. Near this region, the input/output relationship becomes nonlinear and, therefore, the output is a distorted version of the input when digital modulation with fluctuating envelope is amplified. In addition, the distortion from the cross over point must be considered. These effects are identified within the modulated signal as additional amplitude and phase modulations that may degrade the Bit-Error-Rate (BER) performance of modulation schemes.

For modeling purpose of the no-linearity, several nonlinear analyses have been reported and one of the most useful methods is the narrow-band quadrature model proposed by Kaye [30]. In this method, it is assumed that the nonlinearity is independent of frequency because the nonlinear device is considered wideband in comparison with the bandwidth of the input signal (small part of an octave in frequency, centered around some angular frequency ω_0). The reader is referred to [26] and [30] for detailed discussion. It means that the device can be modeled as memoryless through an

instantaneous complex transfer function having a complex independent variable. Such input-output relationship can be written as:

$$v_f(t) = T[v_d(t)], \tag{4.1}$$

where $v_d(t)$ and $v_f(t)$ represent the input complex baseband signal and the output lowpass equivalent complex envelopes of the emitter respectively. These signals are expressed in polar form by

$$v_d(t) = V_d(t)e^{j\varphi_d(t)}. \tag{4.2}$$

$$v_f(t) = V_f(t)e^{j\varphi_f(t)}. \tag{4.3}$$

Then, the complex transfer function is given by:

$$T[v_d(t)] = \left|T[v_d(t)]\right| e^{j\Phi[v_d(t)]}. \tag{4.4}$$

where $\left|T[v_d(t)]\right|$ represents the output envelope voltage, and $\Phi[v_d(t)]$ represents the phase shift mapped by the transfer function. In this representation $T[\bullet]$ behaves as an operator by which any given input $v_d(t)$ is mapped into a unique output $v_f(t)$. A more mathematical definition of this rule in order to determine the inverse function is that the complex transfer function $T[v_d(t)]$ must be analytic on all $v_d(t)$ values. Then, it is always possible to find a complex function $v_d(t) = P[v_f(t)]$ that satisfies

$v_f(t) = T\{P[v_f(t)]\}$ and which is unique in that no other function has this property. Then, $P[v_f(t)]$ becomes the inverse function of the $T[v_d(t)]$ and can be used as a complex predistortion transfer function given by:

$$P[v_f(t)] = \left|P[v_f(t)]\right| e^{j\alpha[v_f(t)]}. \tag{4.5}$$

Note that $T[v_d(t)]$ and $P[v_f(t)]$ are complex-valued functions of complex variables. Exploiting the rotational invariance of the amplifier no-linearity, both the output envelope voltage and the phase shift will be dependent on the input envelope variation $V_d(t)$, [8,30]. In this case, the non-linear behavior of both PA and PD will be represented by a complex transfer function having a real independent variable. They are expressed by:

$$\begin{aligned} T[V_d(t)] &= G[V_d(t)]e^{j\Phi[V_d(t)]} \\ P[V_f(t)] &= D[V_f(t)]e^{j\alpha[V_f(t)]} \end{aligned} \tag{4.6}$$

where $G[V_d(t)]$ and $\Phi[V_d(t)]$ represent a pair of memoryless nonlinear functions named AM-AM transfer characteristics and AM-PM conversion factor respectability, $D[V_f(t)]$ represents the inverse function of the AM-AM, and $\alpha[V_f(t)]$ the complementary function of the AM-PM. In this case, the input-output relationship of the PA model can be written as:

$$v_f(t) = G[V_d(t)]e^{j\{\varphi_d(t)+\Phi[V_d(t)]\}} \tag{4.7}$$

Figure 4.2 shows the block diagram illustrating the model algorithm using polar representation with parallel access.

4.3.3 Ideal Predistortion condition

In order to determine the ideal predistortion condition let consider the complex baseband signal to be transmitted across the system shown in Fig.4.1:

$$v_m(t) = V_m(t)e^{j\theta_m(t)}. \tag{4.8}$$

Using the model defined in the previous section, the resulting predistorted signal is given by:

$$v_d(t) = D[V_m(t)]e^{j\{\theta_m(t)+\alpha[V_m(t)]\}} \tag{4.9}$$

Since the signals under consideration are narrowband signals centered at some frequency ω_0, the amplifier input bandpass signal may be expressed in complex envelope notation as

$$s(t) = \mathrm{Re}[D[V_m(t)]e^{j[\omega_0 t+\theta_m(t)+\alpha[V_m(t)]}]. \tag{4.10}$$

Then, the PA output bandpass signal can be represented by:

$$z(t) = \mathrm{Re}\{G[D[V_m(t)]]e^{j\{\omega_0 t+\theta_m(t)+\alpha[V_m(t)]+\Phi[D[V_m(t)]]\}}\}. \tag{4.11}$$

From equation (4.8) and (4.11) and denoting $V_d(t) = D[V_m(t)]$ we can see that the conditions that must be satisfied to properly correct the AM-AM and AM-PM distortions are:

$$G[V_d(t)] = \beta V_m(t) \tag{4.12}$$

$$\Phi[V_d(t)] + \alpha[V_m(t)] = 0 \tag{4.13}$$

where β is the expected constant gain of the system and $V_m(t)$ represent the envelope variation of the input signal to be transmitted. Assuming that such conditions is satisfied, the amplified bandpass signal $z_c(t)$ will be given by:

$$z_c(t) = \mathrm{Re}\{\beta V_m(t) e^{j[\omega_0 t + \theta_m(t)]}\}. \tag{4.14}$$

4.4. Linearizer Algorithms

This section introduces a brief overview of the signal representation in the signal space diagram. It will allow developing the instantaneous characterization algorithm. In addition, the configuration of the look-up tables including curve fitting will be presented.

4.4.1 Equivalent lowpass signal

The complex envelope method [6,13], which uses the concept of equivalent lowpass signals and systems, has been used to analyze and characterize the behavior of the amplifier system. It is advantageous to model the microwave system at baseband because it simplifies the analysis. In this process, the representation of bandpass signals is given in terms of equivalent lowpass waveforms under the condition that their bandwidths are much smaller than the carrier frequency [6]. In this case, from the modulated carrier signal that is represented by

$$s(t) = \mathrm{Re}[V_m(t)e^{j[\omega_0 t+\theta_m(t)]}], \tag{4.15}$$

the equivalent lowpass signal $v_m(t)$ can be derived straightforward and is given by

$$v_m(t) = V_m(t)e^{j\theta_m(t)}. \tag{4.16}$$

This is an equivalent polar representation of the waveforms that may be viewed as combined amplitude and phase modulation. In other words, the signal waveforms represent the mapping of successive groups of binary information into a corresponding set of discrete amplitudes and phases. The mapping may be represented by the following equation:

$$v_m(t) = V_m e^{j\theta_m} u(t), \qquad m = 1,2,3....M \tag{4.17}$$

where $\{V_m, \theta_m, m = 1,2,3,\ldots, M\}$ represent the M finite deterministic energies (symbols) in the signal-space diagram and $u(t)$ is the waveform impulse response of the pulse shaping filter that is selected to control the spectral characteristics of the transmitted signal. The transmitted equivalent lowpass complex signal can be written as:

$$S(t) = \sum_{n=1}^{\infty} V_n e^{j\theta_n} u(t - nT), \tag{4.18}$$

where $\{V_n, \theta_n\}$ represents the sequence of transmitted symbols that change at the signaling intervals nT, n = *1,2,3,...,* and T is the symbol period. It mean that every T seconds, the basic waveform $u(t)$ is multiplied by one of M complex value. A convenient way of rewriting *S(t)* is in the form:

$$S(t) = \sum_{n=1}^{\infty} V_n e^{j\theta_n} \delta(t - nT) * u(t), \tag{4.19}$$

where $\delta(t)$ is the Dirac delta function and the symbol * indicates the convolution operation.

4.4.2 Instantaneous characterization

The waveforms expressed by the equations (4.18) and (4.19), exhibit different levels of instantaneous signal amplitudes representing widely varying envelopes that drive the PA into its non-linear region. Under this condition, it is understood that the complex envelope $V_f e^{j\varphi_f}$ from the output of the PA brings the information of non-linearity as shown in figure 4.1. This information can be discriminated when this complex envelope is referenced to the complex envelop $V_d e^{j\varphi_d}$ from the input of the PA. It means that the instantaneous characterization of the PA behaviors (i.e., AM-AM and AM-PM curves) can be performed following both complex envelopes variation during a real work condition. Notice that the delay between them must be compensated. At this point, it is important to take into consideration the required sampling frequency to capture the *nth* order intermodulation products of the distorted signals. Following the Nyquist criterion, the required sampling frequency for a signal of bandwidth BW is given by:

$$f' = n \cdot BW . \tag{4.20}$$

It means that over-sampling the signals will allow to estimate the locus of both band-limited signals $v_d(t)$ and $v_f(t)$ in the signal-space diagram and to obtain information of the non-linearity in the transition time between signal states as shown in figure 4.3. In order to simplify the mathematical representation of the equation (4.19), we can express

the discrete signal through the impulse sampling representation considering the sample-data *S(n)* as a number occurring at a specific instant of time.

$$S(n) = \sum_{i=1}^{\infty} V_i e^{j\varphi_i} \gamma(n - iT'), \tag{4.21}$$

where $\gamma(n\text{-}iT')$ represents the impulse sampling at the signaling intervals iT' (i = 1,2,3,...), T' is the sampling period and $\{V_i, \phi_i\}$ are the discrete amplitudes and phases of the signal trajectory in the signal-space diagram. Using the equation (4.21) and assuming that the delay between $v_d(t)$ and $v_f(t)$ is compensated, both signals can be expressed by:

$$v_d(n) = \sum_{i=1}^{\infty} V_{di} e^{j\varphi_{di}} \gamma(n - iT'), \tag{4.22}$$

$$v_f(n) = \sum_{i=1}^{\infty} V_{fi} e^{j\varphi_{fi}} \gamma(n - iT'), \tag{4.23}$$

Then, a number q of successive complex values from both signals are sampled and sorted as an ascending list of values, which use as index the input signal's amplitude V_d. These values must be spread out to cover the overall range of the input envelope levels and must satisfy

$$0 \le V_{d0} < V_{d1} < V_{d2} < \cdots\cdots < V_{dq}. \tag{4.24}$$

The finite length sequences of complex samples are represented as:

$$\dot{V}_d(n) = \sum_{l=1}^{q} V_{dl} e^{j\varphi_{dl}} \gamma(n-l), \tag{4.25}$$

$$\dot{V}_f(n) = \sum_{l=1}^{q} 1/k V_{fl} e^{j\varphi_{fl}} \gamma(n-l), \tag{4.26}$$

where k is the gain of the feedback loop of the equivalent baseband system and, $\{V_{dl}, \varphi_{dl}\}$ and $\{V_{fl}, \varphi_{fl}\}$ are the discrete amplitudes and phases of both signal trajectories in the signal-space diagram. For this purpose the value of T' is unimportant. From equations (4.25) and (4.26), the samples of phase distortion can be obtained as

$$\phi(n) = \sum_{l=1}^{q} (\varphi_{fl} - \varphi_{dl}) \gamma(n-l). \tag{4.27}$$

Then, the sets of data points given by:

$$A\{(V_{d1}, 1/k V_{f1}), (V_{d2}, 1/k V_{f2}), \ldots, (V_{dq}, 1/k V_{fq})\} \tag{4.28}$$

$$B\{(V_{d1}, \phi_1), (V_{d2}, \phi_2), \ldots, (V_{dq}, \phi_q)\} \tag{4.29}$$

are used to determine, by interpolation, both the relative envelope transfer functions $g[V_d(t)]$ and the envelope dependent phase shift $\Phi[V_d(t)]$ which are expressed as:

$$1/k V_f(t) = g[V_d(t)], \tag{4.30}$$

$$\phi(t) = \Phi[V_d(t)]. \tag{4.31}$$

Notice that both functions are time function, which are performed when the input signal drive the interpolation algorithm using the sets of data points *{A, B}*. Then, the non-linear behavior of the PA is represented by the equivalent complex envelope transfer function as follows:

$$T_d(t) = G[V_d(t)]e^{j\Phi[V_d(t)]}, \tag{4.32}$$

where $G[V_d(t)]$ is obtained from the relative envelope transfer functions $g[V_d(t)]$.

In order to estimate the delay through the feedback loop, the input signal sequence of the PA and the feedback signal sequence, which is the delayed and distorted version of the input, are cross-correlated. In practice, it is possible to access only a finite segment of these sequences. Let N be the longer of these segments, m the delay variable and L the delay between signals, the correlation sequence z(m) can be written as :

$$z(m) = \frac{1}{N}\sum_{n=0}^{N-1} x(k)y^*(k+m). \tag{4.33}$$

Then, the sequence z(m) is expected to reach a maximum for m=L.

4.4.3 Predistortion and Look-up Tables Configuration

Based on the conditions (4.12) and (4.13) that must be satisfied to ideally correct the AM-AM and AM-PM distortion, the optimal compensation made by predistortion can be achieved when the predistorter envelope transfer function is given by:

$$V_d(t) = g^{-1}[1/K V_f(t)], \tag{4.34}$$

and the compensation phase characteristic is given by:

$$\alpha[V_m(t)] = -\Phi[V_d(t)]. \tag{4.35}$$

Under these conditions, and using the sets of data points *{A, B}* from equations (4.28) and (4.29), the updating of the lookup tables is made in the form that there are correspondence between input and output values of the tables as illustrated by (4.36). The input amplitude $V_m(t)$ and the predistorted output amplitude $V_d(t)$ are used to point to the look-up tables address. These tables implement a mapping from the input to the output, according to the number of sampled pairs, using linear or cubic spline interpolation. Notice that the sample values V_{fq} are normalized relative to the small-signal gain k of the feedback loop of the equivalent baseband system.

$$V_m(t) \rightarrow 1/k \begin{bmatrix} V_{f1} \\ V_{f2} \\ \cdot \\ V_{fq} \end{bmatrix} \rightarrow \begin{bmatrix} V_{d1} \\ V_{d2} \\ \cdot \\ V_{dq} \end{bmatrix} \rightarrow V_d(t) \qquad V_d(t) \rightarrow \begin{bmatrix} V_{d1} \\ V_{d2} \\ \cdot \\ V_{dq} \end{bmatrix} \rightarrow \begin{bmatrix} \alpha_1 \\ \alpha_2 \\ \cdot \\ \alpha_q \end{bmatrix} \rightarrow \alpha \tag{4.36}$$

Figure 4.4 shows the configuration of the predistorter to obtain the predistorted signal. In this case, a polar representation was chosen to configure the look-up tables and these

can be accessed in cascade form where the first and the second table generate the amplitude predistortion and phase predistortion respectively.

4.4.4 Interpolation and curve fitting

As we have mentioned before, the look up tables must implement a mapping from the input to the output in order to generate the predistorted signal. Therefore, for a good accuracy, this mapping must be performed using an effective approximation between entry. In our case, when a set of data point such as $(V_{f1}, V_{d1}), \ldots, (V_{fq}, V_{dq})$ are known and the abscissas $\{V_{fk}\}$ are distinct, different methods can be used to determine a function that relates these variables [35]. One possibility is to construct a polynomial with coefficients that can be calculated such that the curve passes through the data points. For a successful result, the set of points must be known with a high degree of accuracy, which constrains the use of this approach. Another possibility is the use of curve fitting methods, like least-squares polynomial optimization techniques, that offer a good accuracy when the set of data points are produced through an experimental set up. This method is frequently unsatisfactory, because a polynomial of degree N can have $N-1$ local extreme and it may exhibit large oscillations when data points do not lie on a polynomial curve. A good solution for this problem is to use interpolation by spline functions. In this method, the curve denoted by a polynomial is formed by a set of lower-degree polynomials and the interpolation is performed between the successive data points. Linear, quadratic and cubic spline interpolation may be used and can be

extended to higher-degree polynomial with more additional computation. Cubic spline shows a good performance and is the most tempting when a smooth curve is required. Drawback of spline interpolation is the variation at the edge points. Figure 4.5 and figure 4.6 show 23 processed samples from the instantaneous characterization, which fit the AM-AM and AM-PM characteristics of the PA and the predistortion functions that have been interpolated according to equations (4.30) and (4.31). Note that the AM-AM characteristic of the PA has been normalized relative to the small-signal gain.

4.5 Implementation and Results

4.5.1 Prototype

The entire system has been built as shown in figure 4.7. The system boards is a LSI card, running on a PC, including a TMS320C40/50 MHz device and a module with 16 bit/60-200 KHz dual DA/AD converters. The power amplifier is a 1 W class AB driven at 1,780 GHz. The 16-QAM-modulation method is used as the signal source with a baud rate of 6 kHz. The pulse-shaping filter is a raised cosine having a roll off (α) of 0.35, which gives a crest factor of 6.8 dB. The over sampled rate was 10 samples per symbol. Careful attention has been paid to reduce the local oscillator carrier feed-through from the QM, [10]. This impairment was reduced by using a cancellation loop, which includes an attenuator and phase shifter in parallel with the QM.

4.5.2 Results

To evaluate the predistorter performance, the PA was driven near saturation with 0.1 dB peak back-off (the radio of the saturation output power and peak output power) [8]. From the experimental results, as shown in figure 4.8, it is demonstrated that the spectral regrowth may be reduced in excess of 20 dB. A further reduction can be achieved by improving the compensation of the feedback loop impairments (carrier leak, gain and phase imbalance, etc.,). Note that the degradation on spectral magnitude from these impairment limits the out of band spectral reduction obtained from the linearizer.

4.5.3 Advantage

This technique uses the benefits that any mathematics function is easy to be performed by software and therefore, significant improvements can be obtained using inverse nonlinearities from the instantaneous characterization algorithm. Due to its operating principle, the proposed linearizer performs adaptation without the need of complex convergence algorithms and can supply correction for any order of nonlinearity and any modulation format.

4.5.4 Limitation

The precision of the instantaneous characterization algorithm to accomplishes the extraction of the non-linear behaviors have a critical dependence of the feedback loop impairments. The distortion, due to imperfection from other components are added to the signal limiting the accuracy of the characterization. In addition, a limitation in

bandwidth is imposed to the system. In fact, the processor performs its task in real time where data are presented to the system by the external environment and whether the processor is ready or not. Therefore, if the algorithm cannot process data in real time because of time consuming, it may lose input data resulting a failure in the system.

4.6 Conclusion

In this paper, an experimental validation of a new method dedicated to adaptive digital predistorter with the instantaneous characterization of the non-linear behaviors was presented. The instantaneous characterization algorithm has demonstrated to be a powerful tool to extract the PA non-linear behaviors during normal data transmission. Its purpose is to supply the knowledge of the nonlinearity to the predistorter where the predistorted signal is performed using one-dimensional lookup table technique. Furthermore, it eliminates the need for complex convergence algorithms in the adaptation update step. Experimental results demonstrate that the spectral regrowth is reduced by of 20 dB, driving the PA at 6 dB output back off referenced to the single carrier saturation point. The predistorter can be self-corrected for any drift in the operating points and also, any order of nonlinearity and any modulation format can be supported. Finally, although the implementation presented here was limited in bandwidth, the improvement of the processing speed of the same algorithms using high clock speeds will allow handling higher bandwidth signals.

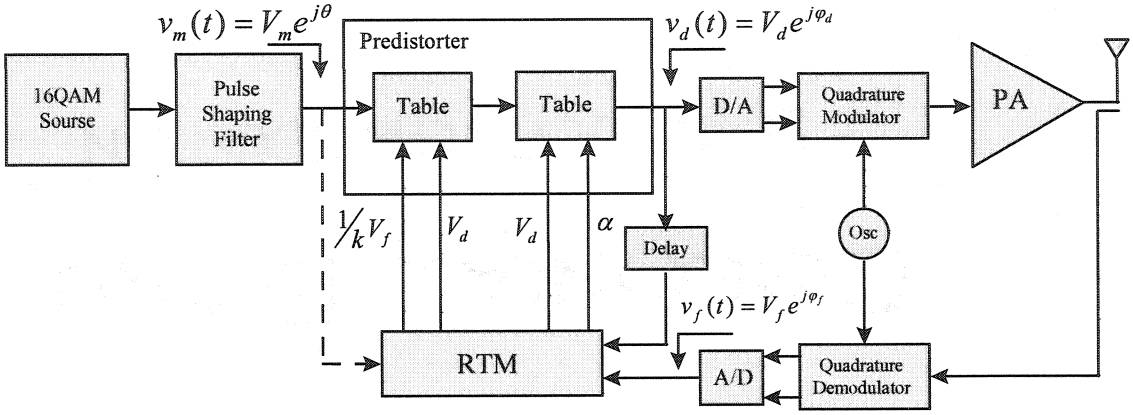

Figure 4.1. General block diagram of the linearizer.

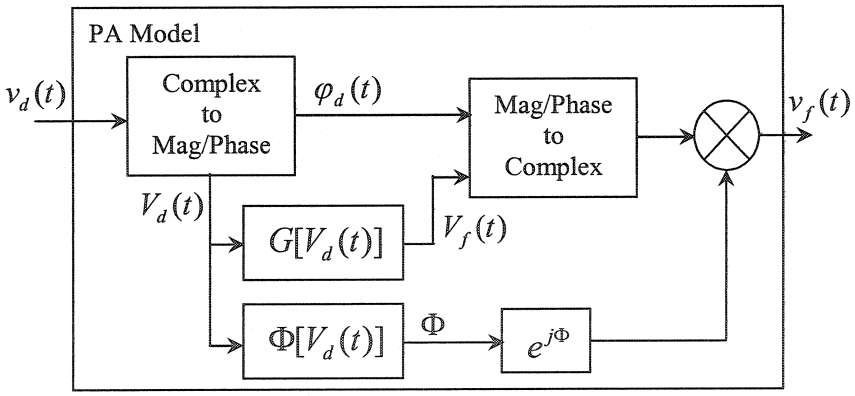

Figure 4. 2. Block diagram of the PA model algorithm using polar representation with parallel access.

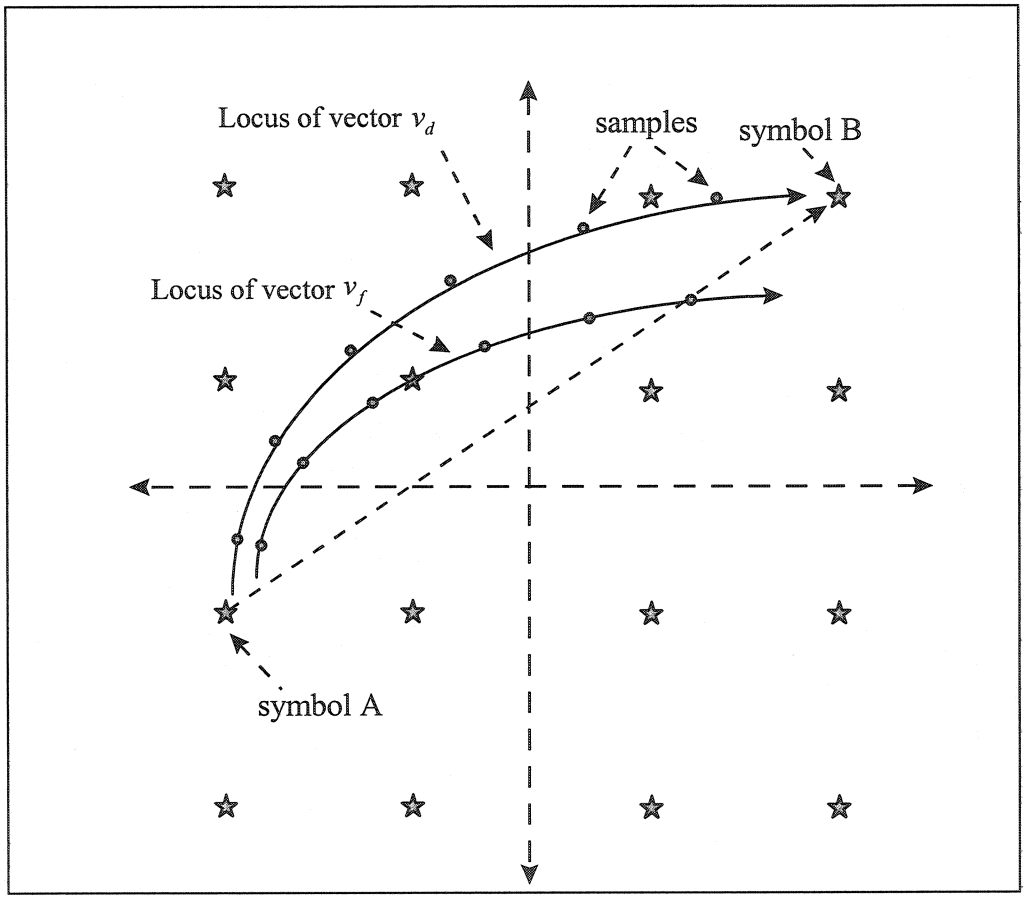

Figure 4.3 Signal state diagram of 16-QAM. Distortion estimation procedure showing the signal trajectory from symbol A to symbol B of $v_d(t)$ and $v_f(t)$

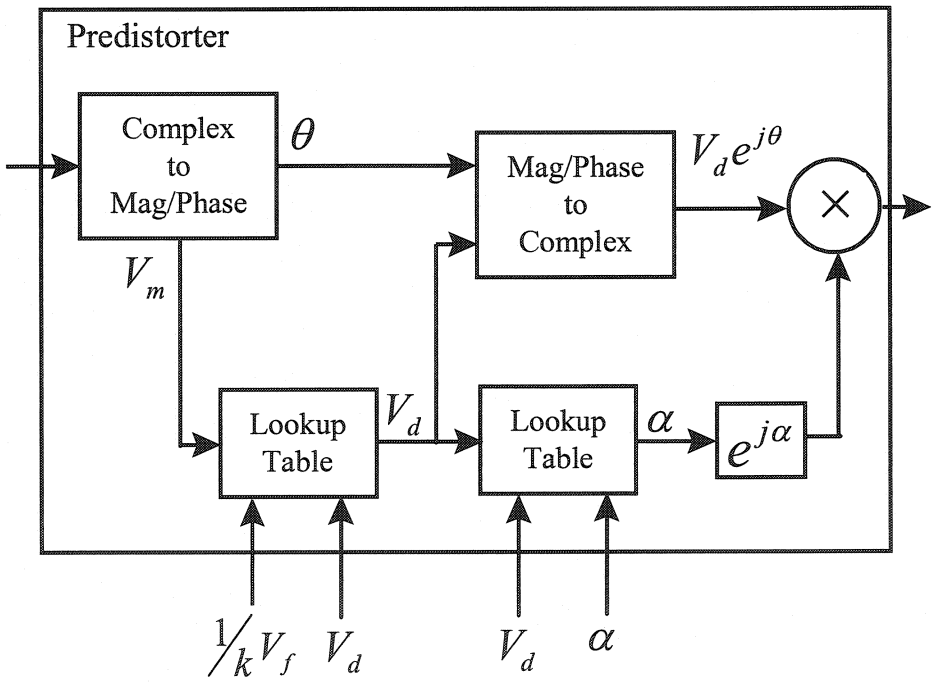

Figure 4.4. Lookup tables configuration using polar representation with pipeline access.

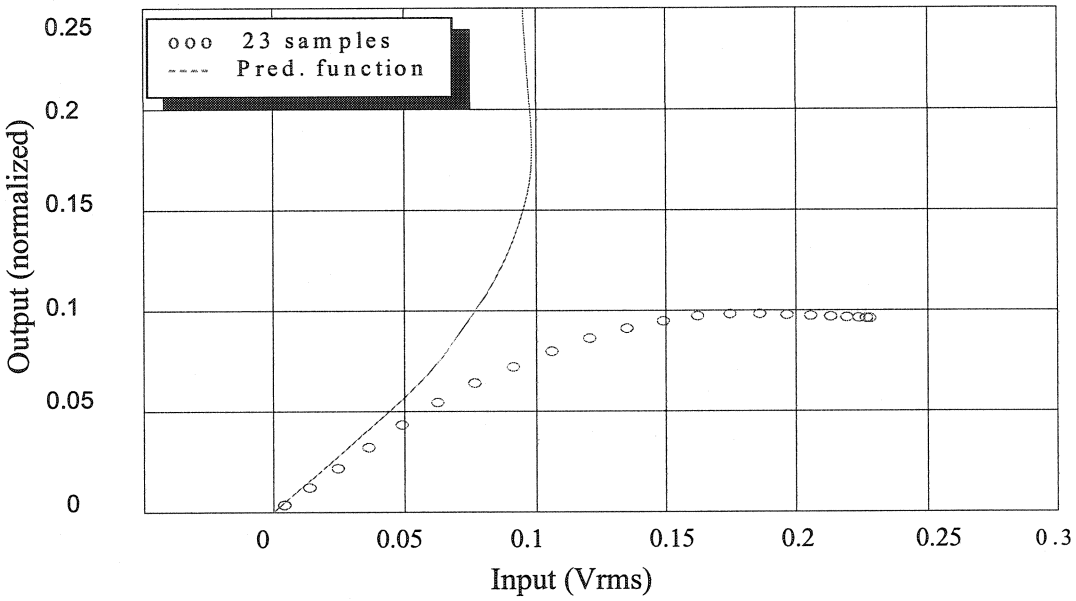

Figure 4.5 Samples set from the instantaneous characterization fitting the AM-AM characteristics of the PA and the predistortion function. Output sample values are normalized relative to the small-signal gain k of the feedback loop of the equivalent baseband system

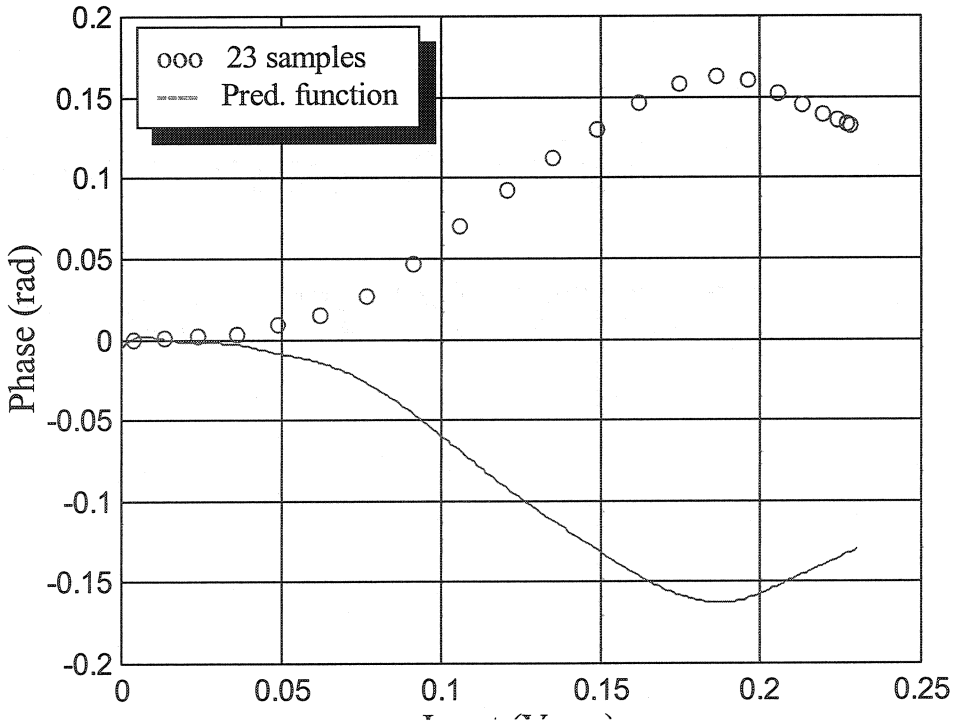

Figure 4.6 Samples set from the instantaneous characterization fitting the AM-PM characteristics of the PA and the predistortion function

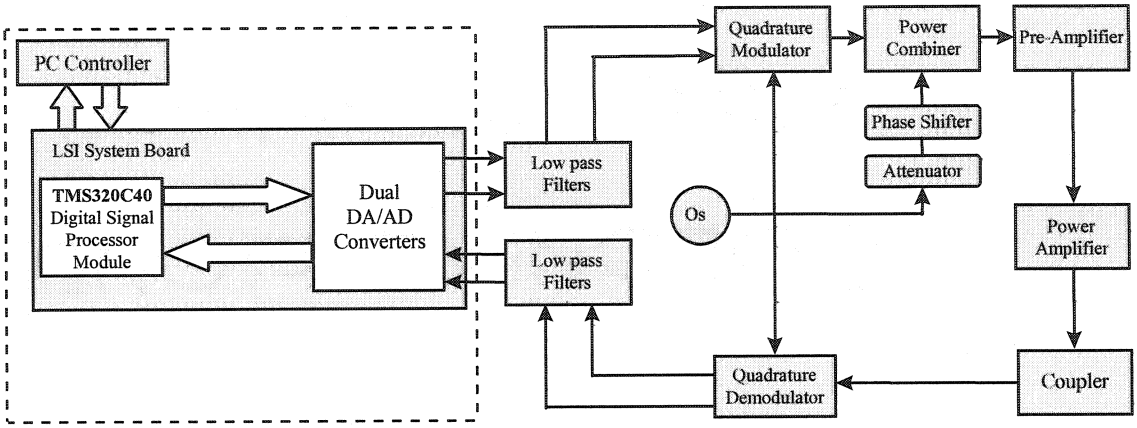

Figure 4.7 Simplified block diagram of the hardware.

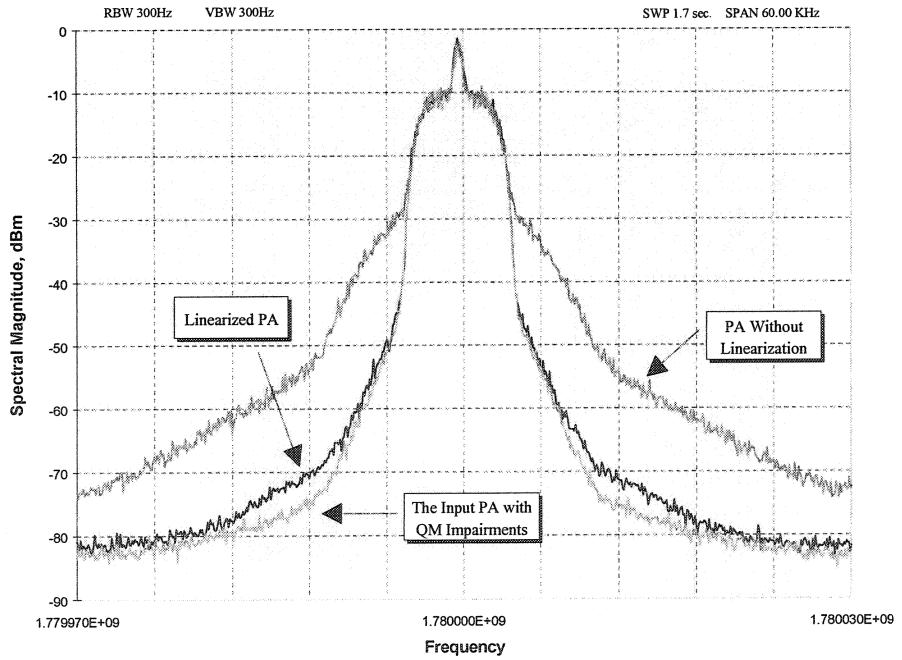

Figure 4.8. Power spectrum showing the effect of the linearization and the QM impairment.

CHAPITRE V

A New Adaptive Predistortion Technique Using Software-Defined Radio and DSP Technologies Suitable for Base Station 3G Power Amplifiers

A New Adaptive Predistortion Technique Using Software-Defined Radio and DSP Technologies Suitable for Base Station 3G Power Amplifiers

Ernesto G. Jeckeln, *Member, IEEE,* Fadhel M. Ghannouchi, *Senior Member, IEEE* and, Mohamad A. Sawan, *Fellow, IEEE*

Abstract

We present in this paper an advanced adaptive baseband/RF predistorter that integrates the concept of the software-defined radio technology into the power amplifier (PA) linearization area. The linearizer performs an instantaneous characterization of the PA, using two digital receivers, in order to supply its instantaneous AM-AM and AM-PM curves. Then, it determines an inverse function that represents the best fit to the reciprocal of the PA behavior. CDMA and 3G standard signals applying different stress level on the PA are used to evaluate the performance of the linearizer. The system is validated using DSP/RF co-simulation for a typical 44-dBm Class AB power amplifier. To estimate the performance of the linearizer under realistic condition, experimental results have been carried out in open loop condition, supported by a software-instruments connectivity, for a 20 W Class AB power amplifier operating at 1.96 GHz. Results for different cases of standards signals reveal a significant reduction, in the order of 5 dB, in effective output power back off (OBO).

5.2 Introduction

While the third generation (3G) of mobile radio standards is being defined, the demand for developing ultra-linear microwave transmitters, supporting high crest factor signals is greater than ever. The demanding adjacent channel power ratio (ACPR) requirements of these new systems, i.e., W-CDMA or CDMA2000, present a critical issue for transmitter designers if both ultra-linearity and high power efficiency must be met. In fact, the degradation of linearity becomes significant as the PA operates close to saturation where both high power efficiency and high output power emission are achieved. Therefore, for different stimulus levels driving the amplifiers and for a given ACPR specifications, the trade-offs between power efficiency and linearity impose an operating point with poor power efficiency. In this case, linearization techniques become the only possible way to recuperate the linearity and to allow optimal trade-offs.

Various linearization methods have been reported and are derived, by any measure, from three main types named: i) Feed-forward, ii) Feedback and iii) Predistortion. Referring to the last one, the predistortion technique has historically been the most common method in analog implementation. Now, this technique is well suited for digital implementation by integrating a DSP chip to handle high-speed arithmetic. Hence, important experimental results have been presented [7-11] demonstrating the capability in reducing the spectral spreading and how adaptive correction for drift, aging and temperature variation can be achieved using DSP circuits.

Although the above-mentioned technique is powerful due to its digital operating principles, it presents certain inflexibility in the sense that it is suitable only when the baseband signal is acceded directly before the up-conversion. In most cases, linearizer designers have no access to baseband signal; hence, they found themselves confined to use traditional RF analog predistortion techniques. In this case, it is more difficult to meet severe ACPR for a high crest factor's signal specifications while operating not in far back-off regions.

The RF-based predistorter proposed in [28] offer an interesting alternative. It includes a complex gain tuning circuit that controls the amplitude and phase of the RF signal. The baseband environment is confined to optimize two nonlinear work functions by monitoring the ACP-minimization measured by a power detector. Drawbacks of this method are its slow convergence toward the minimum and its sensitivity to the measurement noise, especially near minimum. The average power measurements are inherently noisy with noise level relatively high. Therefore, low-level measurement capability is limited and long dwell times are required at each step to reduce the variance of the measurement. In addition, because of its broadband nature, it cannot be used to measure the average power of one specific channel. The input filter needs an extremely sharp roll off and severe out of band rejection.

We present in this paper an advanced adaptive baseband/RF predistorter, which integrate the concept of digital receiver technology into the linearization techniques. By taking

advantage of this technology to digitally translate signals from IF to baseband with very high accuracy, the linearizer performs the instantaneous characterization of the nonlinearity to determine a correlated predistortion function. The distortion is generated in baseband by addressing the extracted predistortion function and then, it is embedded into the RF signal by dynamically adjusting the amplitude and the phase of the carrier. The linearization system is evaluated by applying different stress level of CDMA standard signals and computing the ACPR between in-band and out-of-channel power spectral densities at specified offset channels. Notice that for all ACPR specifications of these standard signals, the requirements for *EVM* (%) levels are considerate acceptable. The channel power measurement is performed by transforming a number of data point from the time domain to frequency domain using FFT and then calculate the channel power. In addition, the paper presents a helpful analysis of a soft limiter response representing the highest theoretical performance that a predistortion-based linearizer can achieve. The entire system is RF/DSP co-simulated using Advance Design System (ADS) software for a typical 44-dBm Class AB Power Amplifier [14]. Experimental results have been obtained in open loop condition for a 20 W Class AB power amplifier operating at 1.96 GHz. Results from different cases of standards signals reveal a significant reduction, in the order of 5 dB, in effective OBO.

The remainder of this paper is organized as follows. Section 5.3 presents a general description of the linearizer structure and treats in detail the principal mechanism in term of algorithms. In addition, expressions are derived to determine the ACPR and to predict

the noise floor level of the system. Section 5.4 describes the stimulus condition characterized statically by the CCDF function. The clipping effect and soft limiter performances are discussed, and supporting calculations are given to evaluate the ACPR. Section 5.5 presents the simulation and measurement results and Section 5.6 highlights the important points treated in the paper.

5.3 Description of the Linearizer

5.3.1 General Description

The proposed technique is based on a new concept supported by the emergent digital receiver technology. This technique uses an envelope detector to provide the envelope variation that is digitized to index a lookup table implemented in the distorting generator block, as shown in figure 5.1. Following the RF signal path, after the delay line, an IQ modulator is used as a complex gain adjuster that controls the amplitude and phase of the RF input signal. Then, the RF signal is picked up from the input and the output of the PA and translated down to within an alias-free sampling range from DC up to 35 MHz. Right after the translator stages, one for each branch, the signals are converted by 12-bit A/D converters into digital samples at the high rate of 70 MHz. Then, two digital receivers perform high-speed complex down conversion, filtering, and decimation, all done in digital domain. It is understood that, the complex envelope from the output of the PA in branch "B" brings the information of non-linearity when it is driven further into nonlinear operation mode. This non-linearity information can be discriminated

when this complex envelope is referenced to the complex envelop from the input of the PA in branch "A". It means that the instantaneous characterization (i.e., AM-AM and AM-PM curves) can be performed following both complex envelopes variation during real time operating condition [11,34,38]. It allows to determine the predistortion function and to control the adaptation update step whenever it is necessary to update the distorting generator.

5.3.2 Instantaneous Characterization Algorithms

In terms of algorithms, the translation and filtering process are the two majors signals processing operations performed by the digital receiver blocks. First, a single-sideband complex translation is accomplished by mixing the real signal with the complex output of a digital quadrature local oscillator (LO), as shown in figure 5.2. Then, a decimation filter conditions the complex baseband signal by fixing an appropriate value of the decimation parameter M. It controls the reduction of the cutoff frequency f_{cutoff} and the sampling rate f_s as follows:

$$f_{cutoff} = f_s/2M\,, \tag{5.1}$$

$$f' = f_s/M\,. \tag{5.2}$$

It means that, by tuning the digital LO frequency and the M value, any signal can be selected digitally from the IF domain and put into the baseband domain for further processing. Based on this principle, the linearizer performs both the instantaneous

characterization to extract the band-pass complex envelope from the input and output of the PA, and the monitoring of the ACPR in order to control the adaptation step. In the first task, the two receivers output data that represent the equivalent complex envelopes are routed through the instantaneous characterization block to determine the PA nonlinear behavior. For this purpose, it is important to consider the required sample frequency to capture the *nth* order intermod products of both signals. Following the Nyquist criterion, the required sampling frequency for a signal of RF bandwidth BW is given by:

$$f' = n \cdot BW . \tag{5.3}$$

Note that the sampling rate for the real signal is twice that of the complex signal. Using the equation (5.2) and fixing the sampling frequency f_s, the decimator parameter M can be calculated by:

$$M = \frac{f_s}{n \cdot BW}. \tag{5.4}$$

In order to characterize the PA through its input and output signal, we assume that the PA input bandpass signal is given by:

$$v_i(t) = \mathrm{Re}\{\rho(t) e^{j\{\omega_c t + \theta(t)\}}\}, \tag{5.5}$$

where ω_c is the midband angular frequency, $\rho(t)$ is the amplitude variation and $\theta(t)$ is the phase variation. Then, the PA output bandpass signal can be represented by

$$v_{out}(t) = \mathrm{Re}\{g[\rho(t)]e^{j\{\omega_c t + \phi[\rho(t)]+\theta(t)\}}\}, \tag{5.6}$$

where $g[\rho(t)]$ and $\phi[\rho(t)]$ are two memoryless nonlinear functions that represent the instantaneous AM-AM and AM-PM curves [27]. Notice that these functions are characterized in terms of the input and output bandpass complex envelopes, without including all harmonics effect. In addition, it is understood that both bandpass complex envelopes are oversampled at the rate of f'. Then, the optimal compensator is correlated straightforward as follows:

$$\rho_d(t) = g^{-1}[\rho(t)], \tag{5.7}$$

$$\alpha(t) = -\phi\{g^{-1}[\rho(t)]\}. \tag{5.8}$$

where, the complex envelope gain function of the predistorter can be written as:

$$G_{PD}[\rho(t)] = \frac{\rho_d(t)}{\rho(t)} e^{j\alpha(t)}. \tag{5.9}$$

The time domain functions of equations 5.7 and 5.8, characterize the amplitude

predistortion transfer g^{-1} and the phase predistortion conversion ϕ in function of the input amplitude variation $\rho(t)$ and the distorted amplitude variation $\rho_d(t)$ respectively. They are implemented in the distorting generator block through a mapping process using look-up tables' technique as shown in figure 5.3. The mapping process is performed from the input to the output using linear interpolation and according to the number of complex sampled pairs acquired from the instantaneous characterization block. Notice that the tables are configured in polar representation and they are accessed in cascade form at a sampling rate f' adequate to generate the highest order distortion of interest [27]. The complex converter block accomplishes the reconstruction of the complex distortion gain and converts it into the Cartesian I/Q waveform.

In order to control the adaptation step, the system use ACPR as figure of merit. Thus, taking advantage of the decimation process to perform a dramatic reduction in the signal bandwidth, the ACPR is monitored in different range of frequency by processing simultaneous real time FFT spectra. This is accomplished by tuning both the LO frequency and the M value of each digital receiver as shown in figure 5.4. A comparator C starts the adaptation step when the measured ACPR overflow the reference value R (refer to section 5.4.3). Notice that the system needs one digital receiver for each offset channel to be monitored in real time.

In all cases, the signals are captured in time domain and converted to the frequency domain by applying FFT algorithm. In this process, the control of trade-off between leakage and loss of frequency resolution is performed by windowing a finite number of signal samples $x(n)$ plus noise by the window function $w(n)$ as follows

$$x_{sw}(n) = [x(n) + \gamma(n)]w(n) \qquad 0 \le n \le L-1 \tag{5.10}$$

Then,

$$\begin{aligned} x_w(n) &= x(n)w(n). \qquad 0 \le n \le L-1 \\ \gamma_w(n) &= \gamma(n)w(n) \end{aligned} \tag{5.11}$$

Here, $x(n)$ is the signal sequence, $\gamma(n)$ is a white noise process, L is the window length that represents the number of captured signal samples, $x_w(n)$ is the windowed sequence, and $\gamma_w(n)$ is the windowed noise sequence. The real time FFT spectra is governed by the required sample rate f' in each channel and the required frequency resolution Δf that are related by the number of sample points N as:

$$N = \frac{f'}{\Delta f} \tag{5.12}$$

In other words, N is the FFT length and it is used to control the density of equally spaced frequency-sampling points represented by

$$f_k = \frac{k}{N}, \qquad 0 \le k \le N-1 \tag{5.13}$$

where k is an integer. Thus, the frequency domain of (5.10) is determined via the following expressions using FFT algorithms:

$$\begin{aligned} X_w(k) &= \sum_0^{L-1} x_w(n)\, e^{-j\frac{2\pi}{N}kn} \qquad 0 \le k \le N-1, \\ \Gamma_w(k) &= \sum_0^{L-1} \gamma_w(n)\, e^{-j\frac{2\pi}{N}kn} \qquad 0 \le k \le N-1. \end{aligned} \tag{5.14}$$

Then, the total power in a specified channel is computed by:

$$P_{channel}(dBm) = 10\log\left[\left(\frac{NBW}{BW_{Noise}}\right)\left(\frac{C}{N}\right)\sum_{k=0}^{N-1}|X(k)|^2\right] \tag{5.15}$$

where C is a factor that considers the 1 mW reference power and the impedance condition, NBW is the normalization bandwidth (refer to Section 5.4.3) and BW_{noise} is the equivalent noise bandwidth of the resolution bandwidth (RBW) filter, which is the 3 dB measurement bandwidth. The ACPR is performed between in-band and out-of-band power spectral densities at specified offset channels as follow:

$$ACPR(dB) = P_{offset}(dB) - P_{mean}(dB) \tag{5.16}$$

In terms of the dynamic performance, the dynamic range (DR) is established using full-scale voltage V_{FS} and a subsequent examination of the noise floor. To describe the noise floor the signal to noise ratio SNR is evaluated considering the quantization noise and how the window function $w(n)$ impacts on such evaluation. The window function affects the SNR because of the measured value at the FFT bin includes noise from the whole bandwidth of the window function's kernel. Therefore, it is necessary to compare the amount by which the window function attenuates the signal with the amount of noise the window function collects. Following the development in [36], and considering the magnitude spectrum of the $w(n)$ fairly flat, and the record length reasonably large, then the k^{th} frequency bin, where k is the integer nearest to $N(NBW / f^{'})$ will contain the signal components. Then the SNR can be approximated as:

$$SNR \cong \frac{N}{\sigma^2 BW_{noise}} \tag{5.17}$$

where BW_{noise} is governed by the window function $w(n)$, and σ^2 is the mean-square quantization noise power of n-bits resolution represented by:

$$\sigma^2 = \frac{V_{FS}^2}{(2^n - 1)^2 12} \tag{5.18}$$

Assuming a sinusoid with a peak-to-peak value of 2 and considering the magnitude-

squared spectrum normalized by the fundamental, the noise floor level can be represented by the (5.17) and it is given in decibels by:

$$F_N \cong 10\log\left(\frac{3N}{BW_{noise}}\right) + 6.02n \ \ dB \tag{5.19}$$

Notice that this expression predicts the noise floor level of the system in terms of the equivalent noise bandwidth that depends of the window function $w(n)$, the record length N, and the number of bits n. If the noise floor level is substantially higher than the expected value from (5.19), then other adaptive noise source (thermal noise) and distortion source are dominant [36].

5.4 Evaluation Condition

5.4.1 Stimulus conditions

For evaluation purpose, the system is exposed under different stimulus conditions that allow it to be characterized in term of distortion. CDMA, W-CDMA, and CDMA2000 standard signals are implemented under simulation to apply different stress level characterized by their complementary cumulative distribution functions (CCDF).

As known, these standards signal exhibit different levels of the instantaneous signal amplitudes representing widely varying envelopes that drive the system following a

random property. Usually, a set of these level values are referenced to the root-mean-square (RMS) value of the signal giving a set of peak voltage-to-RMS voltage ratio values that allows characterizing a time waveform into the statistical domain. This capability is represented by the CCDF function and it becomes a common tool to represent the stress degree that a stimulating signal can places on a nonlinear system. In this function, the ratio values are also referred as peak power-to-average power ratio and the highest ratio value, called crest factor (CF), give a measure of the dynamic range of the signal. In figure 5.5, we can see the CCDF curves showing the statistical property of each standard signal built in simulation. In all cases, the simulator generates around 800,000 signal samples that allow attaining the 0.0001% probability value with high stability.

In the case of the CDMA signal, the statistical property reveals a peak-to-average ratio of 10.29 dB for a 0.1% of probability and the CF is 13.28 dB. This signal is implemented using a typical Walsh-code channels configuration, i.e., pilot, sync, paging, 8, 16, 24, 40, 48 and 56, and it is among the most stressful signal that satisfies the nine channel requirements of IS-97. For the W-CDMA signal, two different channel configurations including 11 and 15 code channels are implemented; the chip rate is 3.84 MHz and the shaping filter is a root cosine with a roll-off of 0.22 and using Hanning as window function. In the case of the cdma2000, the simulation is performed using a direct spread (DS) as air interface with a single 3.75 MHz-wide carrier and with a

spreading rate of 3.6864 Mcps. The filter is three times wider than the CDMA case and the window function is a Hanning type. Under these simulation conditions, a comparison of the statistical properties represented by the CCDFs in figure 5.5 reveals that for a given probability, i.e. 0.1%, each signal presents different peak factor. Therefore, each signal will drive the nonlinear PA further into saturation having a different impact in terms of distortion. It point out the effect that as the curves move farther to the right, the peak-to-average value becomes higher, which makes the signals more stressful. Consequently, for an acceptable amount of distortion according to the spectrum emission mask, as the signal become more stressful the PA will be conditioned to operate in higher back off with the corresponding worsening of the power efficiency. This kind of evaluation allows characterizing the PA in term of distortion and efficiency and predicting the system performance under different operating conditions.

5.4.2 Clipping effect and Soft Limiter

It is well known that a Class AB power amplifier presents different type of distortion sources and not all of them can be compensated by predistortion. While distortion from the nonlinearities near both the crossover point and the saturation point can be compensated by fitting numerically a correlative predistortion function, distortion from clipping effect escapes from the cancellation capability of the predistortion technique. This limitation represents an important drawback of this technique.

In order to evaluate this kind of limitation and to predict the highest theoretical performance that can be reached by the predistortion-based linearizer, the performance of a soft limiter is analyzed for all stimulus condition. As known, in an ideal limiter, the phase conversion is constant over the range of the input signal and the output voltage follows exactly the input voltage up to a certain value. Above this value, the output voltage remains constant when the input voltage is further increased. Under this condition, it is evident that as the probability of instantaneous clipped peak values increase distortion from clipping effect will increase. Consequently, this phenomenon wills places a rigorous limitation in the PA operating point with a direct impact in the power efficiency. Again, we point out that signals having high crest factor will impose an operating point beyond a region of poor power efficiency. Backing-off the operating point will prevent that the distortion masked by the clipping effect overflow the standard requirement. Notice that the characteristic of an ideal limiter represents a perfect linearized power amplifier. Therefore, its performance places an important reference to the degree of improvement given by a predistortion linearizer.

5.4.3 ACPR

For analysis purpose, the ACPR is evaluated for different operating point by computing the ratio between the in-band and the out-of-band power spectral densities at specified offset channels. In the case of the CDMA standard signal, the ACPR is evaluated in three pairs of offset channels that are normalized to the same bandwidths of *30 kHz* at

the offset frequencies of *±885 kHz, ±1.256 MHz,* and *±2.75 MHz*. The normalization factor NF is calculated by logging the ratio between the normalization bandwidth NBW and the specified bandwidth BW, as follow:

$$NF(dB) = 10\log(\frac{NBW}{BW}) \tag{5.20}$$

By applying (5.20) to the J-STD-008 standard requirements [5] where the relative and absolutes power emissions limitation must be at least: $-45dBc/30kHz$ for the first channel, and lower than $-13\,dBm/12.5\,kHz$ and $-13dBm/1\,MHz$ for the second and third channel respectively, the NF values become: -16.2 dB, 3.8 dB, and -15.2 dB. The normalized limit values of the standard requirement become $-28.8\,dB/30\,kHz$, $-9.2\,dBm/30\,kHz$ and $-28.2\,dBm/30\,kHz$, and the relative limit values of the power spectral densities for the three offset channel are given by:

$$R_1(dB) = 28.8\,dB \tag{5.21}$$

$$R_2(dB) = 28.8\,dB + \Delta\,dB \tag{5.22}$$

$$R_3(db) = 47.8\,dB + \Delta\,dB \tag{5.23}$$

where Δ is given by:

$$\Delta = \begin{cases} P_{PA}\,(dBm) - 35.8dBm & for\ P_{PA} \geq 35.8\,dBm \\ 0 & elsewhere \end{cases} \tag{5.24}$$

In figure 5.6 we can see a graphical representation of requirement for a typical *44 dBm* PA. After normalization the mean power become *27.8 dBm/30 kHz,* Δ take the value *8.2 dB* and the relative limit values are R_1= *28.8 dB,* R_2=*37 dB* and R_3=*56 dB*. Notice that the dBc unit is used when the total power contained in the mean channel is given as reference.

In the case of cdma2000 with DS as air interface, we assume the similar methodology that is applied in the CDMA case [2]. The frequency centers of the offset channel are *2.65 MHz, 3.75 MHz,* and *5.94 MHz*. For W-CDMA standard, the ACPR is evaluated over *3.84 MHz* bandwidth at the offset frequency of *5 MHz* and the limited emission power is considerate at *–55 dBc*. For all cases, the spectrum analysis is accomplished by converting the time domain signal to frequency domain using Hanning window with $BW_{noise} = 1.5$, and FFT length of 1074 points for CDMA and cdma2000, and 8192 points for W-CDMA. The integration bandwidth (IBW) method is used to calculate both mean channel power and offset channel power and it is performed by applying (5.15) [1]. In addition, the simulator computes an average power for each specified integration channel bandwidth and over a specified number of data acquisitions $avr = 16$.

5.4.4 General consideration

The entire system is RF/DSP co-simulated using the ADS software for a typical 44-dBm Class AB Power Amplifier [14]. Temperature noise, quantization noise, and impairment from other components such as amplitude and phase imbalance of I/Q modulator have been taken into consideration to realistically model the system [38]. The A/D and D/A converters are simulated having 12-bits and 14 bits resolution respectively at the high rate of 70 MHz. The dynamic range of the characterization system (branches "A" and "B") are the minimum DR between one that is limited by the carrier to intermodulation levels governed by the third order intercept point of the path, and one that is limited by the carrier to noise ratio governed by the F_N and the LO phase noise. Here, the key objective is to establish a desired DR and SNR. Therefore, the parameters of the filters, mixers, and gain stages have been tuned to optimize the performance of the characterization system. To maintain the same performance in terms of OBO, the characterization system was recalibrated for each operating point. In all cases, the noise floor levels of the input standard signals, i.e., 61 dB, 62 dB, and 71 dB for CDMA, cdma2000, and W-CDMA respectively, have been higher than the expected F_N of the characterization system. Therefore, they have been considered dominant. The digital receivers are considered both narrowband and wideband distinguished by the programmable range of decimation factors. For the instantaneous characterization the decimation factor is tuned depending on the standard signal bandwidth and on the highest order of intermod to be considered. It ranges from 2 to 64 providing output

bandwidths from 1 MHz to 35 MHz. In the case of narrowband condition, it ranges from 64 to 65,536 delivering output bandwidths from 1 kHz to 1 MHz

To estimate the performance of the linearizer under realistic condition, experimental results have been carried out in open loop condition for a 20 W Class AB power amplifier operating at 1.96 GHz. Based on a high connectivity between measurement equipments and simulation tools, the AM-AM and AM-PM transfer characteristics were measured by instantaneous characterization using a Microwave Transition Analyzer, a two-channel peak power analyzer, and the ADS software [37]. In addition, a conventional measurement using a network analyzer was performed for a reference purpose. Data from these measurements were introduced into the simulator to determine, by simulation, the inverse function that represents the best fit to the reciprocal of the PA behavior. Then, a long string of predistorted samples of the W-CDMA standard signal was generated and downloaded into an arbitrary waveform generator with the purpose to synthesize and supply a realistic predistorted signal to the PA.

5.5 Results And Discussions

Simulations are performed applying the set of stimulus mentioned in section 5.4.1 on the ideal limiter, on the PA, and on the PA including the linearizer. Each simulation is repeated for different operating points to allow characterizing the performance in terms

of distortion. The OBO referenced to Single Carrier (SC) saturation, the peak power-to-average power characterized by the CCDF, and the ACPR are chosen as important factors to analyze the performance for the three cases. Figure 5.7 and figure 5.10 detail the simulated results of ACPR versus OBO corresponding for the offset bands above the mean signal frequency and the Table I summarize the relevant OBO comparisons. In all cases, the horizontal lines indicate the system specifications for ACPR where the minimum acceptable OBO are illustrated. For replication purpose, it is important to consider the conditions and parameters values established in Section 5.5.

Figure 5.7 shows the effect of the CDMA signal on the ACPR of the ideal limiter. In the three plots, corresponding to the three offset channels, we can see that the minimum acceptable OBO are 6 dB at 885 kHz, 7.4 dB at 1.25 MHz and 9.4 dB at 2.75 MHz. According to the specifications, the results reveal that the ideal limiter cannot be operated with an OBO lower than 9.4 dB. In Figure 4.8, the ideal limiter is simulated under the stimulus of cdma2000 signal, in this case, the minimum acceptable OBO are 5.25 dB at 2.65MHz, 6.8 dB at 3.75 MHz and 9.4 dB at 5.94 MHz. Like CDMA signal case, the third offset channel limits the operating point at least 9.4 dB of OBO. By comparing both OBO performances, we can notice that although the CDMA signal is shown to be most stressful than the cdma2000 signal (see figure 5.5), which is justified in the first and the second offset channels, both case show the same minimum acceptable OBO. From this analysis, the clipping effect seems to be dominant on both first and second channel and with a slight effect on the third channel. It is foreseeable because the

AM-PM conversion factor, that has a significant effect in generating higher order of intermodulation, is considered constant over the range of the input signal. This is the case for an ideal limiter. In addition, in both cases the third offset channel governs the minimum acceptable OBO.

Now, considering the situation of the PA under the stimulus of the CDMA standard signal in figure 5.9, it is clear that more OBO is necessary to pass the spectrum emission mask. This is because now the spectral leakage includes both the clipping effect and the continuous nonlinearity effect of the PA. In this case, the standard requirement limits the PA operating point at least 8.2 dB at 885 kHz, 9.9 dB at 1.25 MHz, and 14.15 dB at 2.75 MHz. Again we can see that the third offset channel governs the minimum acceptable OBO. Therefore, the PA cannot be operated with an OBO smaller than 14.15 dB. As expected, we can see by comparing results from figure 5.7 and figure 5.9 that the PA needs 4.75 dB more in OBO than the minimum theoretical value given by the ideal limiter. Notice that, it is the maximum amount in OBO reduction that theoretically could be achieved by predistortion. With linearization effects, the plots in figure 5.10 show a minimum OBO of 7 dB at 885 kHz, 7.95 dB at 1.25 MHz and 10.5 dB at 2.75 MHz prevailing the value of 10.5 dB as the minimum acceptable OBO according to the spectrum emission mask. This result shows that the predistortion action from the linearizer diminish the OBO by 3.6 dB, which represents 1 dB less than the maximum reduction in OBO that could be achieved theoretically. Notice that this difference is absorbed by the impairments from other components considered in the simulation.

Examination of the plots in the region of 16 dB OBO at 2.75MHz offset, figure 5.9 and figure 5.10, revels a reduced out of band spectral floor in comparison to the reference signal. This is attributed to the thermal noise and distortion from LO carrier feedthough, gain imbalance and phase imbalance of the I/Q modulator. Clearly, these impairments define a fundamental limit on the performance of the linearizer.

The last set of simulation is performed for the same PA under W-CDMA standard signal including 11 channels as was described in Section 5.4.1. Figure 5.11 shows the ACPR performance of the PA with and without linearization and including the ACPR plot of the ideal limiter. The plots reveal a reduction of 4.8 dB resulting a minimum acceptable OBO of 10.6 dB.

Finally, experimental results under open loop condition are shown in figure 5.12. The measurements of the ACPR were performed using the same waveform of the W-CDMA standard signal. In addition, the ACPR performances from the simulation of the ideal limiter are included by aims of comparison. We can observe that the PA must be operated at least 17 dB OBO to meet the standard requirement, 1 dB more than the simulation result. With linearization effects, the minimum acceptable OBO become about 13 dB allowing moving the operating point 4 dB toward saturation region and giving an ACPR improvement of 5 dB. Notice that the lowest theoretical OBO performed by the ideal limiter is reached at 10 dB and still an improvement of 3 dB more in OBO reduction can be theoretically achieved. This difference shows the

limitation of the linearizer operating under open loop condition. Unfortunately, the signals that arise from the PA are non-stationary and therefore, some adaptation action must be considered. Clearly, the linearizer operating under close loop condition has enough headroom to reduce further the OBO by tracking the time-varying behavior of the PA. These results help us to predict the performance for the whole system with a minimum acceptable OBO of around 11 dB and with a predictable improvement of 6 dB in OBO reduction.

In summary, the improvement in OBO reduction is significant in the sense that in all cases the output power can be at least doubled with a resulting increase in power efficiency. It means that for the same linear output power, the OBO reduction allows the reduction of the absolute power rating of the PA. On the other hand, although the improvement in OBO reduction is significant, around 5 dB, the operating point still lay within the region of low efficiency forced by the clipping effect. Notice that the highest theoretical performance reached by a soft limiter fall around 9 dB OBO depending purely on the peak power-to-average power ratio of the signal. This is an important drawback of all techniques based in the predistortion method and become more sensitive when the predistortion method is applied under high crest factor's signal condition. A prolific area for investigation should be crest factor reduction of the standard signals, and the development of a technique for 3G applications that could compensate the clipping effect while keeping a high power efficiency of the whole system.

5.6 Conclusion

An adaptive baseband/RF predistorter based on the emerging technology of digital receivers was presented. The linearizer develops the algorithm of two digital receivers to execute an instantaneous characterization of the AM-AM and AM-PM nonlinearities. The digital receivers allow a direct I/Q demodulation in digital form from RF to baseband. Consequently, the disturbing effects of gain and phase imbalances of a RF analogue quadrature demodulator are completely avoided by directly processing the data with very high accuracy using analytical expressions. The system can monitor the ACPR by processing simultaneous real time FFT spectra in different range of frequencies; it is accomplished by the advantage of the decimation process to perform a dramatic reduction in the signal bandwidth. RF/DSP co-simulation and experimental results have been carried out for evaluation purposes under different signal conditions. Results reveal a significant reduction, in the order of 5 dB, in effective output power back off for the linearized power amplifier. Finally, the fact that the system can support different standard signals by tuning the values of LO, M and R by software, this technique provide an attractive design suitable for mass production.

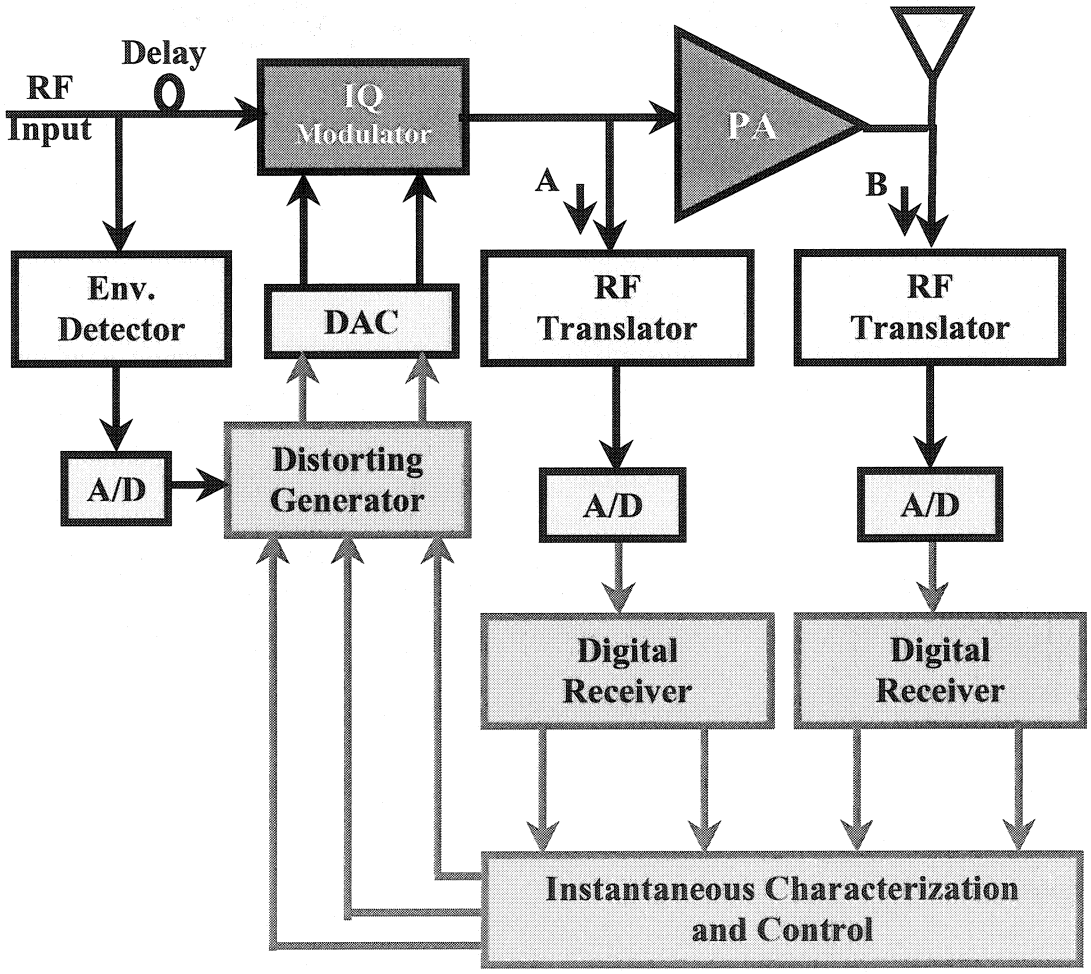

Figure 5.1 General block diagram of the linearizer.

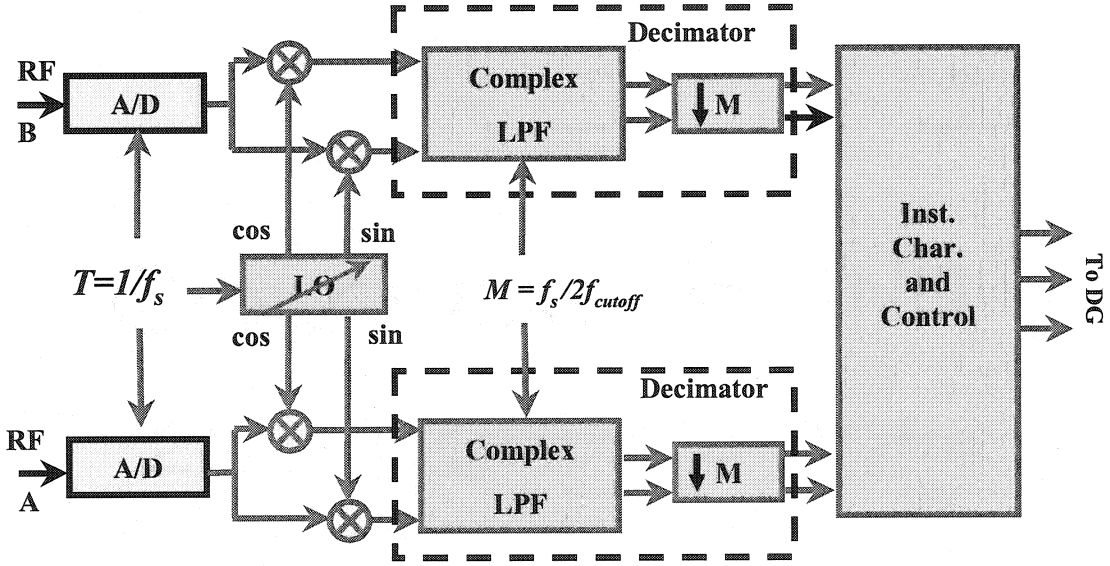

Figure 5.2 Block diagram of the digital receiver algorithms showing the translation and decimation process.

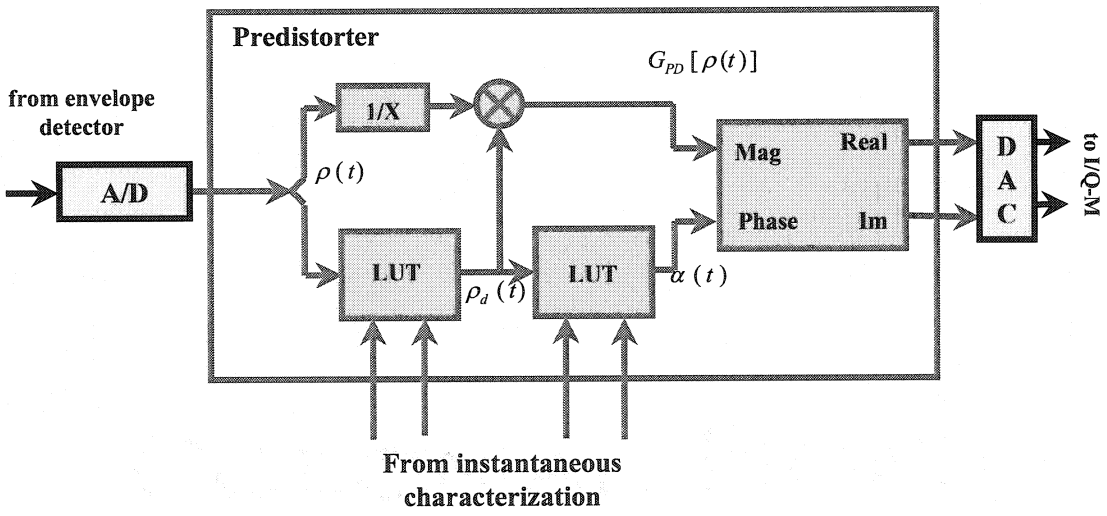

Figure 5.3 Look up tables' configuration using polar representation in cascade form.

..

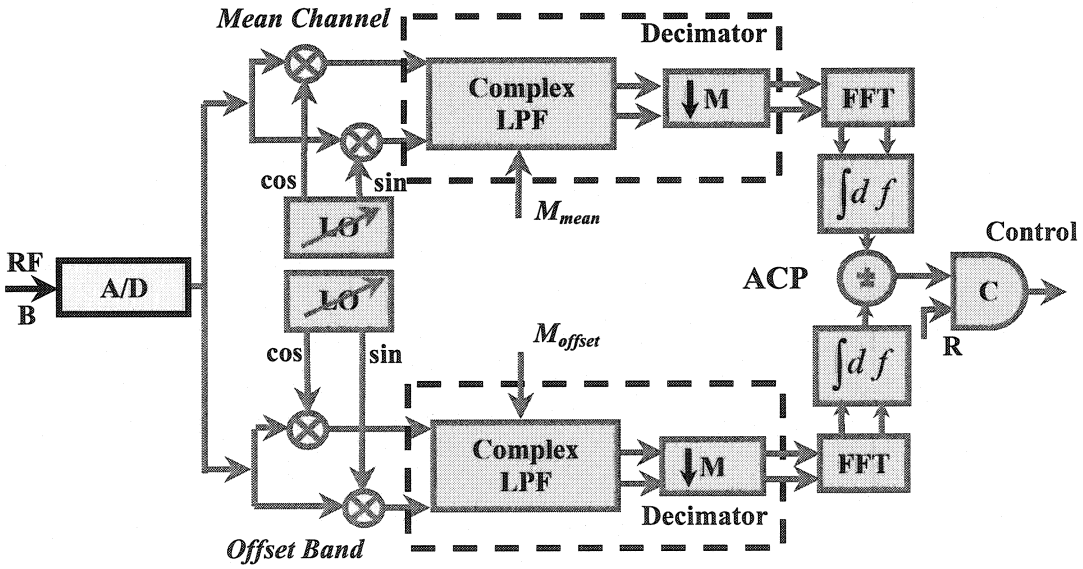

Figure 5.4 Graphical representation of the algorithm to process the ACPR for the PA output signal.

..

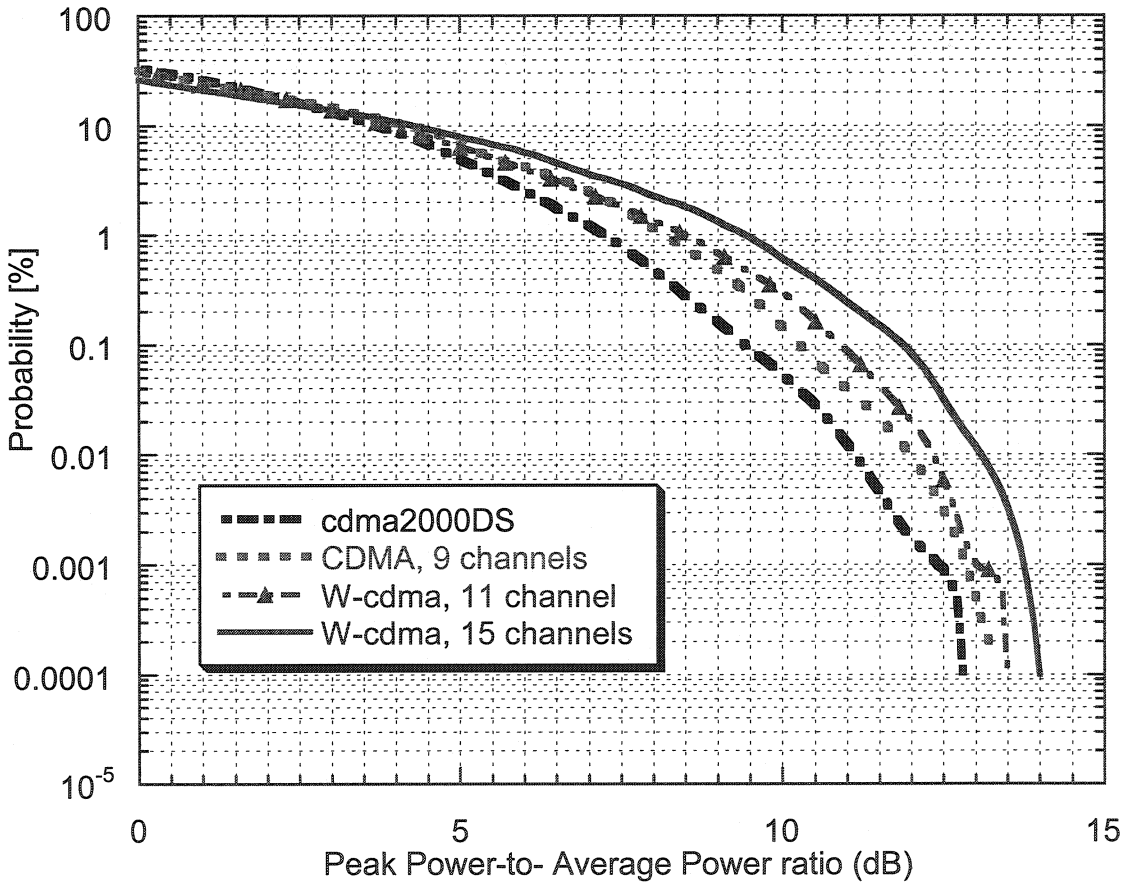

Figure 5.5 The CCDF plots of different CDMA standard signals

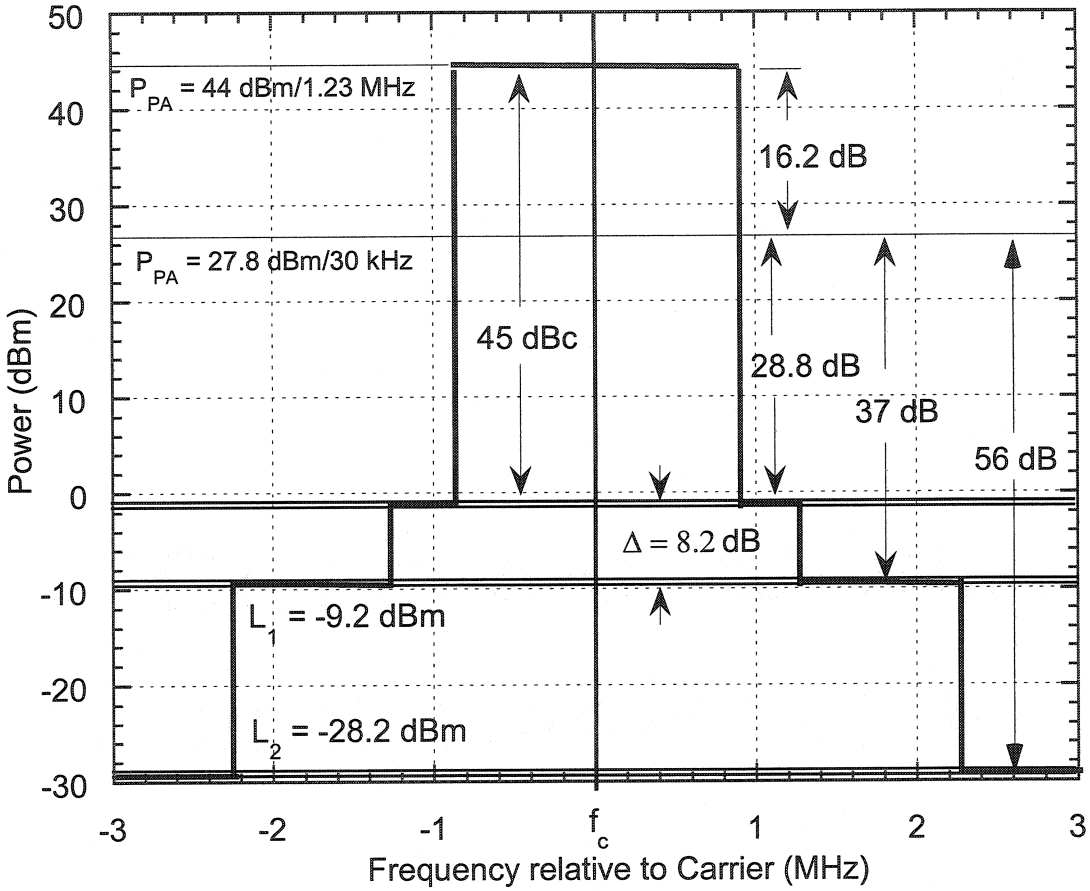

Figure 5.6 Graphical representation of 30 kHz normalized CDMA standard requirement for 44 dBm PA.

Table I

OBO [dB] Performance Comparison

Channel	PA		LPA		LIMITER	
	CDMA	W-CDMA	CDMA	W-CDMA	CDMA	Cdma2000
1st	8.2	15.4	7	10.6	6	5.25
2nd	9.9	x	7.95	x	7.4	6.8
3rd	14.1	x	10.5	x	9.4	9.4

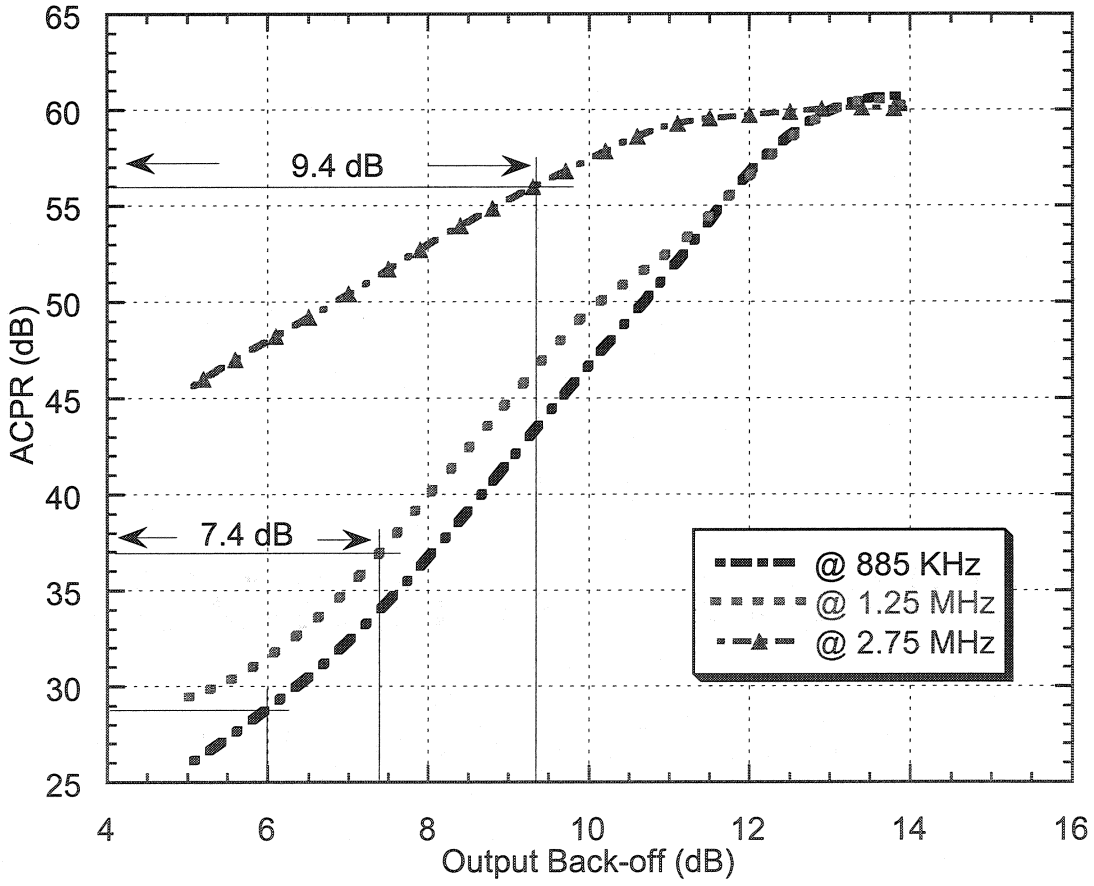

Figure 5.7 Simulation of ACPR vs. OBO of the ideal limiter under the stimulus of nine channels CDMA standard signal.

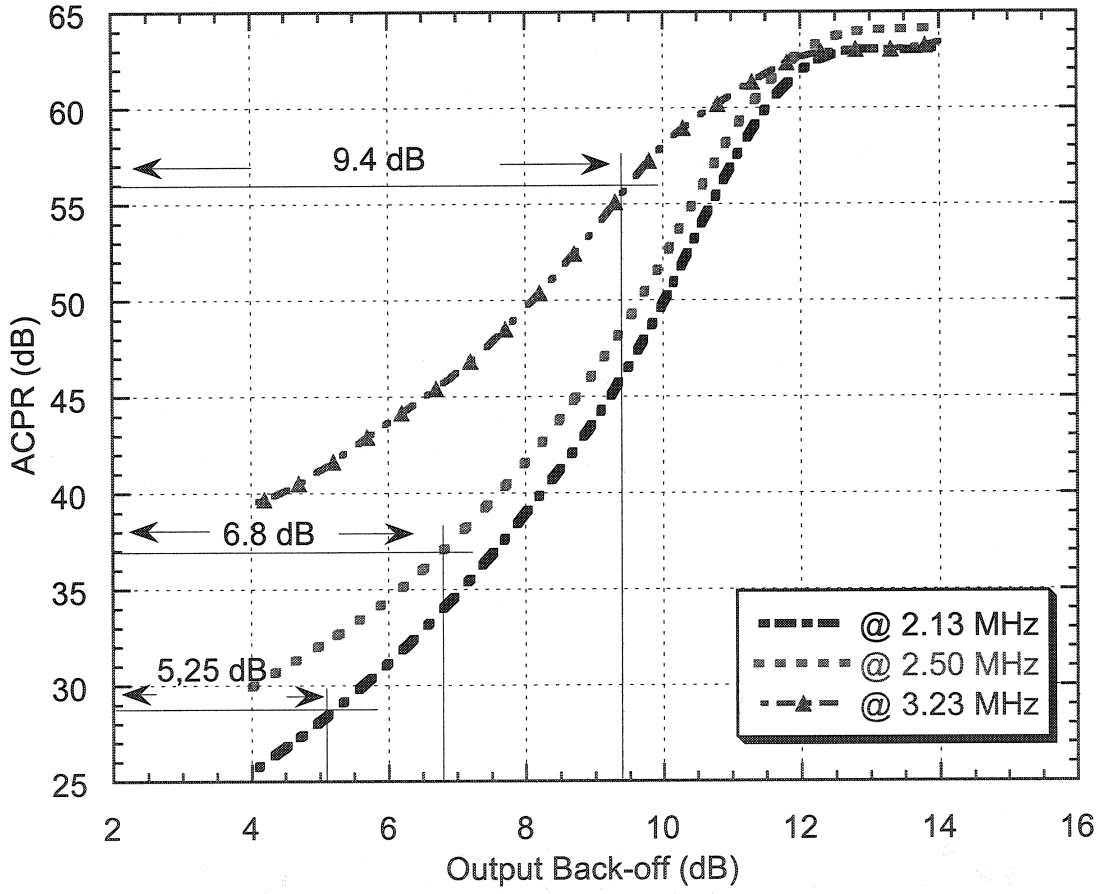

Figure 5.8 Simulation of ACPR vs. OBO of the ideal limiter under the stimulus of cdma2000 DS signal.

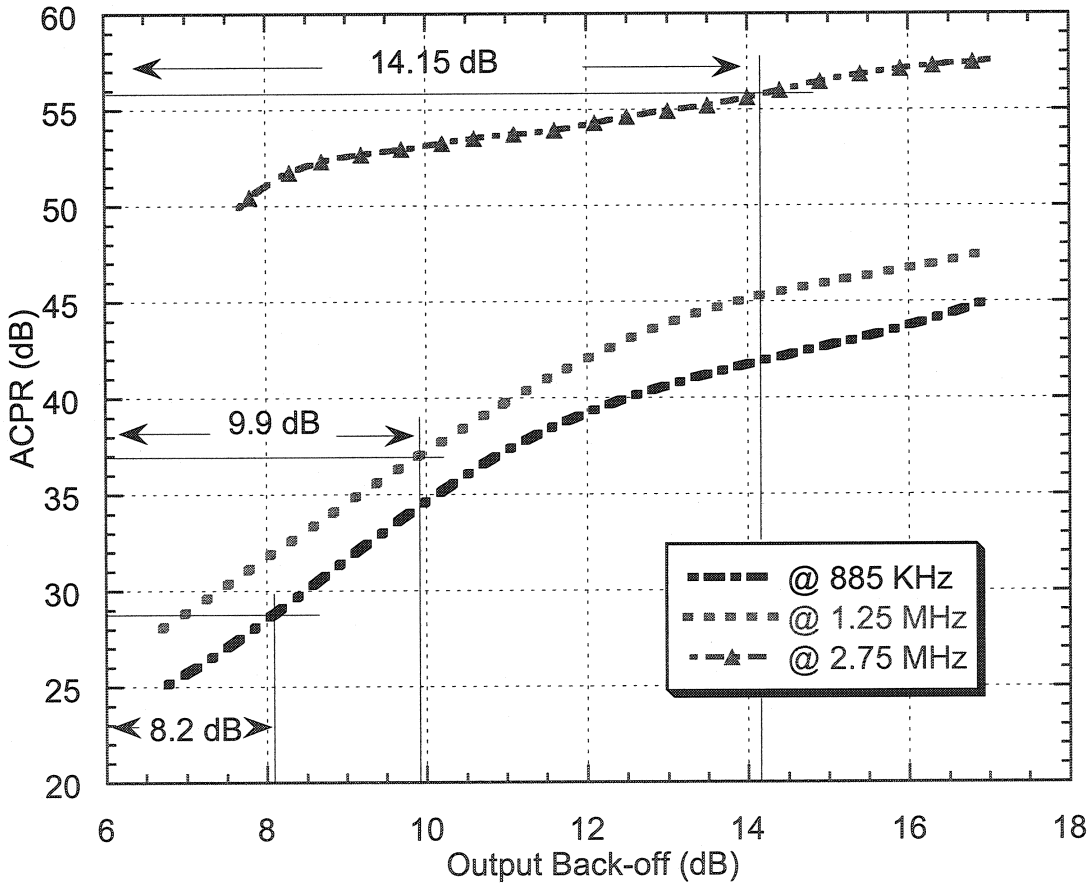

Figure 5.9 Simulation of ACPR vs. OBO of a 44 dBm PA under the stimulus of nine channels CDMA standard signal.

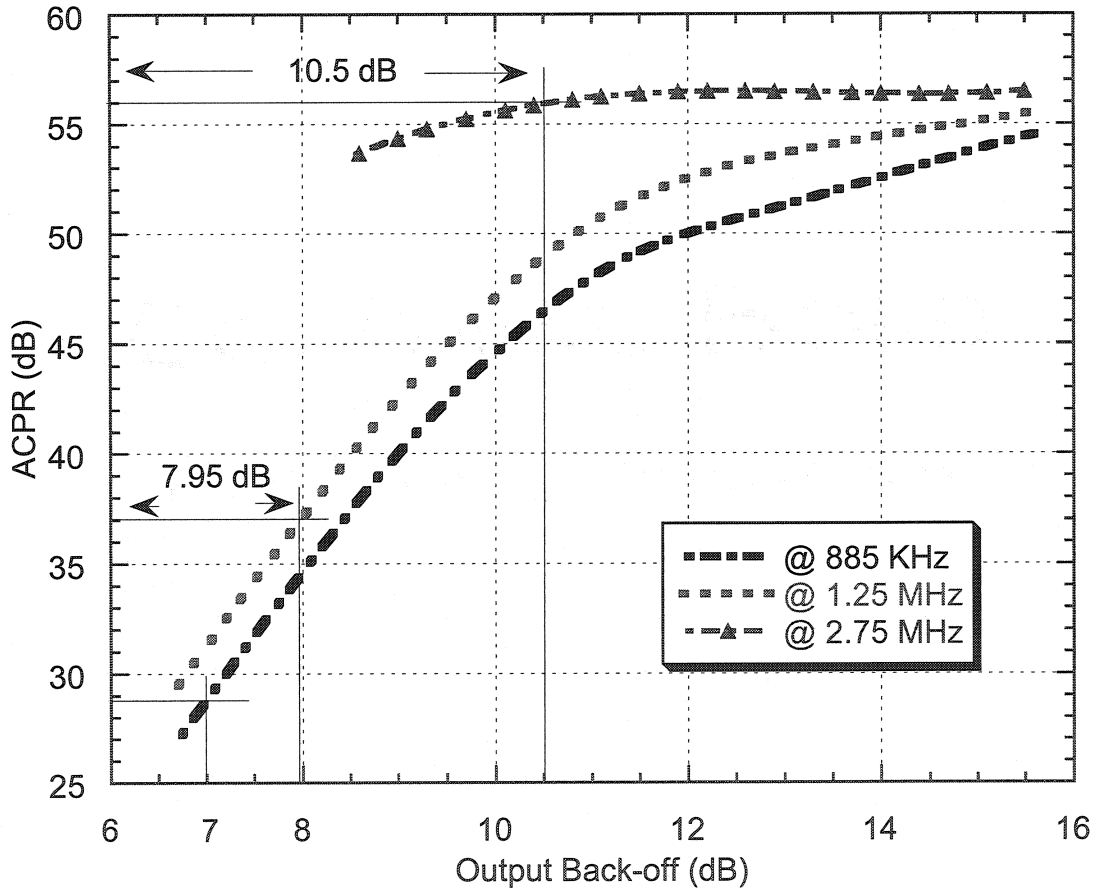

Figure 5.10 Simulation of ACPR vs. OBO of a linearized 44 dBm PA under the stimulus of nine channels CDMA standard signal.

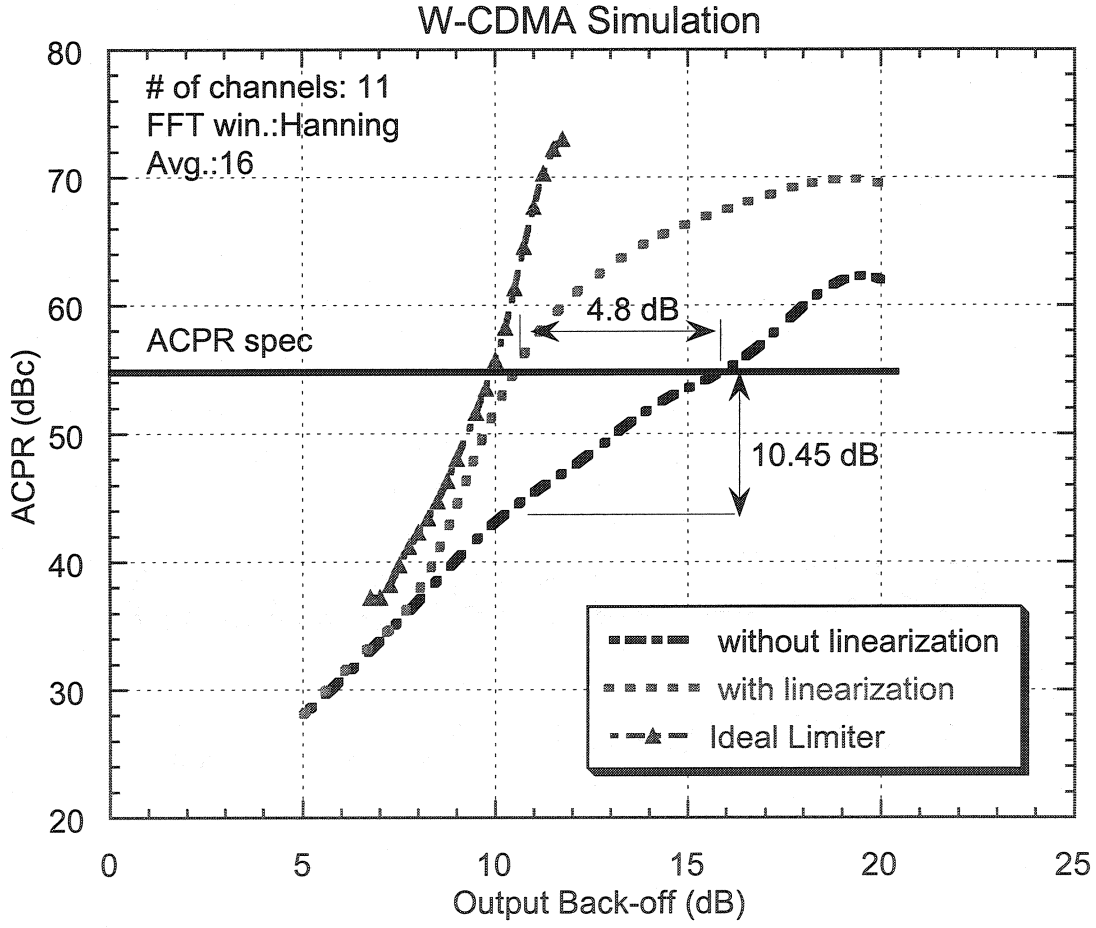

Figure 5.11 Simulation of ACPR vs. OBO of both ideal limiter and a 40 dBm PA under the stimulus of W-CDMA standard signal. The plot reveals an OBO reduction of 4.8 dB under the linearization effect.

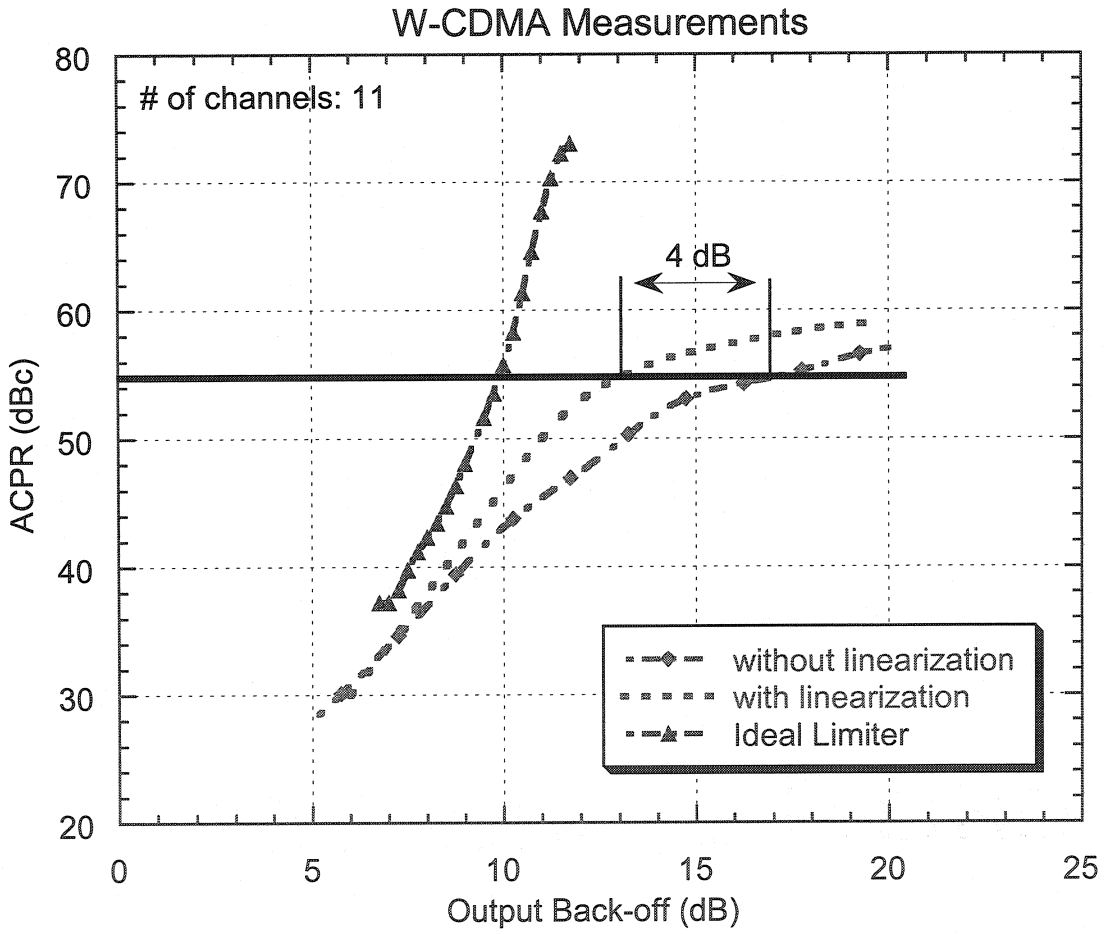

Figure 5.12 Measurements of ACPR vs OBO of both ideal limiter and a 40 dBm PA under the stimulus of W-CDMA standard signal. The plot reveals an OBO reduction of 4 dB under the linearization effect.

CHAPITRE VI

Synthèse

6.1 Généralités

Les systèmes d'accès multiple, l'application des circuits de traitement numérique*, les amplificateurs de puissance RF à haute performance et l'ensemble des techniques de linéarisation sont devenus des éléments clefs dans le domaine des télécommunications mobiles. L'intégration de ces sous-systèmes a lancé un défi au secteur industriel dans la conception de systèmes complexes, capables de répondre à des critères en termes *d'efficacité spectrale* et *d'efficacité énergétique*.

---

* Circuits DSP et FPGA

Dans ce contexte, le projet faisant l'objet de cette thèse est lié à l'optimisation de la performance des amplificateurs de puissance RF. Ce travail apporte des contributions qui découlent de l'implémentation originale de deux techniques de linéarisation. Ces techniques s'appuient sur des méthodes algorithmiques pouvant être exécutées dans un environnement numérique et en générant la prédistorsion soit en bande de base soit en RF. Les éléments clefs que nous avons traités dans ce travail sont résumés dans les points suivants:

6.2 Forme d'onde

Au cours de cette thèse, nous avons souligne la problématique associée à la variation de l'amplitude de la forme d'onde et l'impacte de telle variation sur le point de fonctionnement des amplificateurs. L'écart de cette variation est apparu comme le problème principal pour les concepteurs d'amplificateurs de haute performance. À cet égard, nous avons identifié les paramètres qui affectent le rapport de la puissance pic instantanée à la puissance moyenne du signal. Par exemple, le fait d'optimiser la valeur du facteur d'arrondi α et le débit binaire par Hz rende l'écart de la variation de l'enveloppe à des valeurs plus significatif. Ceci a été illustré statistiquement à travers la fonction CCDF révélant un écart de 6 a 14 dB selon le type de signal caractérisé. Rappelons que ces valeurs instantanées occasionnant une compression et un écrêtage sur

le signal amplifié dû à l'effet de compression et au maximum physique expérimenté par les amplificateurs de puissance.

Après notre étude, nous avons mentionné que, si bien la distorsion par compression peut être annulée à travers l'action de prédistorsion, ce n'est pas le cas de la distorsion par écrêtage. Dans ce contexte, nous avons analysé un certain nombre de scénarios reliés à la distorsion par écrêtage à l'aide d'un limiteur idéel. Ceci nous a permis d'estimer le point de fonctionnement optimal d'un amplificateur et de prédire, dans de conditions idéelles, sa performance selon le type de signal amplifié. En effet, la forme d'onde générée à la sortie d'un système CDMA, gouvernée par la norme IS-97, exige que le limiteur idéel opère avec un minimum OBO de 9.4 dB. Dans le cas des systèmes cdma2000 et W-CDMA les résultats illustrent un minimum OBO de 9.4 et 10 dB respectivement. Il est important de souligné que ces valeurs représentent les points de fonctionnement optimaux pour une étape d'amplification avec une prédistorsion idéel. Ces valeurs limites servent de référence pour évaluer la performance des techniques de prédistorsion.

6.3 Modélisation

Concernant la modélisation du comportement non-linéaire des amplificateurs, nous avons développé notre approche basée sur le modèle en quadrature à bande étroite proposé par Kaye. Dans cette méthode, nous supposons que la non-linéarité est indépendante de la fréquence. Ceci est à condition que le dispositif non-linéaire soit

bande large en comparaison de la largeur de bande du signal d'entrée. Autrement dit, le dispositif à modéliser est considéré sans mémoire. Le modèle est représenté mathématiquement à travers une fonction de transfert temporel complexe $T[v_d(t)]$ ayant une variable complexe dépendante du temps. Ensuite, basé sur la définition des fonctions analytiques dans le plan complexe, nous avons établi par définition l'inverse de la fonction de transfert. Ceci nous permet de déterminer la fonction de transfert $P[v_f(t)]$ que modélise le comportement de la prédistorsion corrélée à une correction optimale de la non-linéarité. En effet, la détermination de la fonction de prédistorsion à travers une interpolation inverse propose une alternative qui permet l'élimination des temps de convergence des algorithmes itératifs.

À propos du modèle, il offre une structure ouverte permettant de modéliser des comportements selon l'information fournie par la caractérisation instantanée. Dans notre case, nous avons considéré les amplificateurs à bande étroite sans mémoire. De plus nous avons exploité l'invariance rotationel de l'amplificateur. Autrement dit, nous avons considéré la distorsion générée par la variation de l'amplitude et no par la variation de la phase. En effet, la variable complexe de la fonction de transfert a été réduite à une variable réelle, ce qui permet l'implémentation de la table de correspondance a une dimension.

6.4 La caractérisation instantanée

L'un des objectifs de nos travaux de recherche était d'éliminer l'instabilité des processus itératifs. Le succès d'atteindre tel objectif a été fortement lié à la caractérisation instantanée de la non-linéarité. Sa capacité à représenter le comportement non-linéaire en temps réel permet une manipulation directe de l'information pour la détermination de la fonction de predistorsion. Un point critique à citer est la limitation de sa précision fortement dépendante de la performance des dispositifs analogiques.

Après notre analyse dans le chapitre III, nous avons souligné que pour tirer le maximum des performances de la caractérisation, il faut une bonne égalité de gain et de centrage orthogonal sur les composantes en quadrature dans l'étage du démodulateur vectoriel. Les inégalités en gain et l'excentrage orthogonale introduit par le démodulateur vectoriel génèrent un excentrage dans les composantes I, Q limitant la précision de la caractérisation. Pour surmonter cette limitation, nous avons proposé dans le chapitre IV une nouvelle méthode algorithmique basée sur l'utilisation des récepteurs numériques. Nous avons décrit les différents éléments qui constituent une chaîne de récepteurs numériques et nous avons mis l'accent sur le processus de décimation et sur la fréquence d'échantillonnage liée à la largeur de bande à caractériser.

En effet, la contribution de ces algorithmes propose une haute sélectivité donnée par un processus de translation et décimation entièrement numérique. Ceci rend le système flexible à la sélection de tout signal dans le domaine RF et le placer de façon directe dans la bande de base avec très haute précision.

6.5 Mise à jour des tables de correspondance

Dans le but de mieux comprendre le comportement adaptatif dans la technique de prédistorsion et développer un asservissement capable de suivre des changements dus aux phénomènes de dérive, nous avons introduit le concept de l'action discontinue de l'adaptabilité. Notre point de départ a été base sur l'hypothèse que le comportement adaptatif de la technique de rétroaction est considéré comme un mécanisme ou la fonction de prédistorsion est automatiquement mise à jour de façon continue. Plus précisément, chaque valeur instantanée de la fonction de prédistorsion est le résultat d'une comparaison en temps réel des valeurs instantanées de deux signaux. Puis, nous avons basé notre développement sur le fait que les phénomènes de dérive génèrent des variations lentes de la non-linéarité en comparaison avec la variation du signal. Il faut préciser que c'est cette différence de vitesse qui permet l'implémentation de la mise à jour de la fonction de predistorsion de façon discontinue. Donc, c'est en se basant sur ce phénomène que la technique de prédistorsion incorpore une action discontinue de l'adaptabilité.

Du point de vu fonctionnel, le développement de tel mécanisme dans nos techniques est accompli, d'une part, avec l'implémentation d'une table de correspondance formée des données obtenues du processus de la modélisation, et d'autre part, avec une mise à jour

des tables de correspondances contrôlée à travers la prise en considération du niveau de distorsion contenu dans le signal. Plus clairement, si la distorsion dépasse un niveau préfixé, l'adaptabilité est déclenchée et un réajustement de la fonction de prédistorsion est exécuté. Une fois la correction de la fonction de prédistorsion est effectuée, l'adaptabilité est interrompue et le processus de la linéarisation continue à boucle ouverte.

Les mesures et les calculs des niveaux de puissance de distorsion sont exécutés avec une haute sensibilité grâce aux algorithmes des récepteurs numériques. Ces algorithmes permettent la surveillance simultanée de ces niveaux de puissance dans différents intervalles de fréquences. De plus, l'ajustement des valeurs de référence (niveaux de puissance de la distorsion) donne la flexibilité à la méthode à s'adapter à différentes conditions servant à contrôler l'action adaptative selon la norme stipulée. Dans le cas de la norme J-STD-008 nous avons normalisé les valeurs limites des canaux adjacents relatifs à une largeur de bande de 30 kHz.

CHAPITRE VII

Conclusion

7.1 Sommaire des contributions de la thèse

La synthèse et l'implémentation des techniques de linéarisation développées dans ce travail constituent l'aboutissement de cette recherche. Nous avons présenté des développements théoriques et l'implémentation des nouveaux algorithmes liés à la technique de prédistorsion numérique. Ces algorithmes permettent de concrétiser deux nouvelles techniques de prédistorsion avec l'introduction d'un modèle dans le domaine temporel basé sur la caractérisation instantanée.

La contribution originale de la première technique consiste en une détermination, dans le domaine temporel, d'une fonction de prédistorsion utilisant des données fournies par une

modélisation en temps réel des caractéristiques non linéaires des amplificateurs de puissance. Les points saillants sont l'élimination complète des algorithmes itératifs, la modélisation en temps réel des caractéristiques non linéaires de l'amplificateur de puissance, la configuration de la table de correspondance et le type d'interpolation utilisé. Les champs d'applications possibles sont l'utilisation de cette technique pour la conception d'émetteurs de haute performance pour les systèmes de communications par satellite et systèmes cellulaires de deuxième et troisième génération, qui nécessitent des émetteurs ultra linéaires. Plus particulièrement, l'application de la méthode s'adresse aux ingénieurs concepteurs ayant accès au signal en bande de base d'un système de communication.

La deuxième technique représente une version adaptée de la technique précédente, avec une structure différente, pour être appliquée par des ingénieurs concepteurs n'ayant pas accès au signal en bande de base. La contribution originale consiste en une nouvelle méthode algorithmique basée sur l'utilisation des récepteurs numériques. Elle permet une caractérisation instantanée du comportement non linéaire de l'amplificateur avec grande précision, une poursuite en temps réel du niveau de distorsion à la sortie de l'amplificateur et un ajustement dynamique de la compensation de distorsion. On remarque l'avantage de cette méthode dans l'action de la prédistorsion, générée en bande de base, qui est appliquée directement à travers une modulation dans le domaine RF. Les champs d'applications possibles sont l'utilisation de cette technique pour la conception d'émetteurs de haute performance pour les systèmes de communications

cellulaires de deuxième et troisième génération. Les points saillants sont tout d'abord la haute sélectivité des intervalles de fréquence dans le domaine spectral et la surveillance simultanée des niveaux de puissance de distorsion dans différents intervalles de fréquences selon la norme stipulée. Aussi, la haute performance du processus de calcul des niveaux de puissance, dans le domaine fréquentiel ou dans le domaine temporel et la configuration de la table de correspondance pour générer la fonction du gain complexe de la fonction de prédistorsion.

7.2 Orientations futures

L'élaboration des algorithmes développés dans cette recherche procure une ouverture vers plusieurs développements intéressants. En effet, à l'opposé d'un système fermé, la structure de ces techniques basées sur la caractérisation instantanée se présente comme un système ouvert pouvant améliorer sa versatilité pour s'insérer dans d'autres applications. A cette ouverture algorithmique correspond des potentialités de recherches prometteuses telles que la manifestation de l'effet mémoire des amplificateurs de puissance opérant dans une plus grande largeur de bande et la variation de la puissance de sortie par rapport à la largeur de bande [39-44]. Ces dépendances fréquentielles pourraient être compensées par le biais d'une action corrective d'un filtre linéaire d'égalisation fréquentielle comme c'est le cas pour les modèles de Wiener ou Hammerstein [44-46] ou encore le développement de filtres non-linéaire tels que les filtres de Volterra et de NARMA [47-49].

BIBLIOGRAPHIE

[1] M. Slovick."Measuring ACPR in CDMA Amplifier", Microwave Journal, December 1998.

[2] Performing cdma2000 Measurements Today, Application Note 1325, HEWLETT PACKARD.

[3] Stephen A. Mass, Nonlinear Microwave Circuits, Artech House, 1998.

[4] Steve C. Cripps, RF Power Amplifiers for Wireless Communication, Artech House, Boston London, March 1999.

[5] Personal Station-Base Station Compatibility Requirements for 1.8 to 2.0 GHz CDMA Personal Communication Systems, ANSI.

[6] J.G.Proakis, "Digital Communications", McGraw Hill, 1983.

[7] Y. Nagata, "Linear Amplification Technique for Digital Mobil Communications", in Proc. IEEE Veh. Technol. Conf., San Francisco, CA, 1989, pp. 159-164.

[8] J. Cavers, "Amplifier Linearization Using a Digital Predistorter with Fast Adaptation and Low Memory Requirement", IEEE Transactions on Vehicular Technology, vol. 39, no 4, pp 374-382, November 1990.

[9] M. Faulkner, T. Mattsson and W. Yates, "Adaptive Linearization Using Predistortion" in Proc. 40th IEEE Veh. Technol. Conf. 1990. pp. 35-40.

[10] A. S. Wright and Willem G. Durtled, "Experimental Performance of an Adaptive Digital Linearized Power Amplifiers", IEEE Transactions on Vehicular Technology, vol. 41, no 4, pp 395-400, November 1992.

[11] E.G. Jeckeln, F.M. Ghannouchi and Mohamad Sawan, " An L Band Adaptive Digital Predistorter for Power Amplifiers Using Direct I-Q Modem ", IEEE MTT-S 1998 International Microwave Symposium, Baltimore, MD, June 1998, pp. 719-722.

[12] MATLAB manual, The MatWork, Inc.

[13] Signal Processing WorkSystem (SPW) and Code Generation System, Alta Groupe of Cadence Design System.

[14] Agilent Eesof-Advance Design System (ADS).

[15] K. Feher, "Wireless Digital Communications: Modulation & Spread Spectrum Applications", Prentice Hall PTR,1995.

[16] K. Feher, "Digital Communications - Microwave Applications: Microwave Applications", Noble Publishing Corporation,1997.

[17] ROHDE&SCHWARZ, Winiqsim Simulator Manual.

[18] ROHDE&SCHWARZ, AMIQ/SMIQ Generator Manual.

[19] J. L. Smith, "Intermodulation Prediction and Control", Interfernce Control Technologies, Inc., 1993.

[20] P. B. Kenington, "High Linearity RF Amplifier Design", Artech House Publishers, 2000.

[21] Blumlein, A., and H. Clark, U.K. Patent 425,553, Amplifier Using Negative Feedback loop, 1993.

[22] C. C. Hsieh and E. Strid. "A S-band high power feedback amplifier", IEEE MTT-S International Microwave Symposium, San Diego, CA, June 21-23, 1977, pp. 182-184.

[23] A. Bateman, D. M. Haines and R. J. Wilkinson, "Direct Conversion Linear Transceiver design", IEE 5th International Conference on Mobile Radio and Personal Communication, War wick, UK, December 1989, pp. 53-56.

[24] A. Bateman and D. M. Haines, "Direct Conversion Transceiver Design for Compac Low-Cost Portable Mobile Radio Terminals", 39th IEEE Vehicular. Technology. Conference, San Francisco, May 1-3, 1989, Vol. 1, pp. 57-62.

[25] N. Imai, T. Nojima and T. Murase, "Novel Linearizer Using Balanced Circulators and Its Application to Multilevel Digital Radio Systems", IEEE Transactions on Microwave Theory and Techniques, vol. 37, no 8, pp. 1237-1243, August 1989.

[26] A. A. Saleh, "Frequency independent and frequency dependent nonlinear models of TWT amplifiers", IEEE Trans. Commun., vol. COM-29, no. 11, pp. 1715-1720, Nov. 1981.

[27] E. G. Jeckeln, F. M. Ghannouchi and M. Sawan, ``Adaptive Digital Predistortion for Power Amplifiers with real time modeling of memoryless complex gain``, U.S. Patent 6,072,364, June 6, 2000.

[28] S. P. Stapleton and F. C. Costescu, "An Adaptive Predistorter for a Power Amplifier Based on Adjacent Channel Emissions", IEEE Transactions on Vehicular Technology, vol. 41, no 1, pp 49-56, February 1992.

[29] Girard H. and Feher, K. "A New Baseband Linearizer for more Efficient Utilization of Earth Station Amplifier Used for QPSK Transmission " IEEE J. Select Areas Communication., Vol. SAC-1, no. 1, 1983.

[30] A. Kaye, D. George, and M. Eric, " Analysis and Compensation of Bandpass Nonlinearities for Communications", IEEE Transactions on Comm., pp. 965-972, October 1972.

[31] R. Meyer, R. Eschenbach and W. Edgerley, Jr." A Wide-Band Feedforward Amplifier", IEEE J of Solid-State Circuits, vol.sc-9, no. 6, pp. 442-428, December 1974.

[32] Zhao, G., and Kouki, A. V. "Digital Implementations of Adaptive Feedforward Amplifier Linearization Techniques", IEEE 1996 International Microwave Symposium, San Francisco, CA, June 1996.

[33] E. G. Jeckeln, F. M. Ghannouchi and M. Sawan, ``Adaptive Digital Predistortion for Power Amplifiers with real time modeling of memoryless complex gain``, U.S. Patent 6,072,364, June 6, 2000

[34] E.G. Jeckeln, F.M. Ghannouchi and Mohamad Sawan, "Adaptive Digital Predistorter for Power Amplifiers with Real Time Modeling of Memoryless Complex Gains", IEEE MTT-S 1996 International Microwave Symposium, San Francisco, CA, June 1996.

[35] J. H. Mathews, "Numerical Methods", for Computer Science, Engineering, and Mathematics, McGraw Hill, 1989.

[36] C. Y. Jenq "Digital Spectra of Nonuniformly Sampled Signal: Theory and Applications - Measuring Clock/Aperture Jitter of an A/D System", IEEE Trans. Instrumentation and Measurement, Vol. 39. No.6, Dec. 1990, pp. 969-971.

[37] HP/Agilent 70820A Microwave Transition Analyzer, dc to 40 GHz.

[38] E. G. Jeckeln, F. M. Ghannouchi and M. Sawan, ``Linearization of Microwave Emitters using an Adaptive Digital Predistorter``, 27TH EUROPEN MICROWAVE-97, September 8-12, 1997.

[39] W. Bosch, and G. Gatti, "Measurement and simulation of memory effects in predistortion linearizers," IEEE Trans. Microwave Theory and Tech, vol. 37, no. 12, pp. 1885 -1890, Dec. 1989.

[40] J. Staudinger, "The importance of Sub-harmonic Frequency Terminations In Modeling Spectral Regrowyh From CW Am-Am & Am&Pm Derived Non-Linearities", IEEE Wireless Communication Conference, 1997.

[41] J. F. Sevic, K. L. Burger, M. B. Steer, "A Novel Envelope-Termination Load-Pull Method for ACPR Optimization of RF/Microwave Power Amplifier", 1998 IEEE MTT-S, Digest, pp 723-726.

[42] M. Eron, E. G. Jeckeln, "Measurement of Accurate, Wideband Characterization and Optimization of High Power LDMOS Amplifier Memory Properties" IEEE MTT-s Digest, 2003.

[43] Vuolevi, J., Manninen, J., Rahkonen, T., "Canceling the memory effects in RF power amplifiers," International Symposium on Circuits and Systems, vol. 1, pp. 50-60, 6-9 May 2001.

[44] E. G. Jeckeln, Huei-Yuan Shih; E. Martony, M. Eron, "Method for modeling amplitude and bandwidth dependent distortion in nonlinear RF devices", IEEE MTT-S International Microwave Symposium, Philadelphie, 8-13 June 2003, vol.3, pp. 1733-1736.

[45] N. Wiener, Nonlinear Problems in Random Theory, The Technology Press of MIT and John Wiley and Sons, 1958.

[46] Antoine Rabany, Long Nguyen and Dave Rice, "Memory Effect Reduction for LDMOS Bias Circuits", Microwave Journal, pp. 124-130, Feb 2003.

[47] S. Chen and S. A. Billings, ''Representations of non–linear systems: the NARMAX model,'' *Int. J. Control*, Vol. 49, No. 3, pp. 1013–1032, 1989.

[48] J.S. Kenney, W. Woo, L. Ding, R. Raich, and G.T. Zhou, "The impact of memory effects on predistortion linearization of RF power amplifiers," 8th Intl. Symposium on Microwave and Optical Technolog, pp. 189-193, Montreal, Quebec, Canada, June 2001.

[49] Boumaiza, S.; Ghannouchi, F.M.; "Thermal memory effects modeling and compensation in RF power amplifiers and predistortion linearizers", IEEE Transactions on Microwave Theory and Techniques, Vol. 51 , Issue: 12 , Dec. 2003, Pages:2427 - 2433

ANNEXE I

BREVETS

ANNEXE I.1:

US Patent No: 6,072,364

Non Iterative Adaptive Digital Predistortion Technique for Power Amplifiers Linearization

US006072364A

United States Patent [19]

Jeckeln et al.

[11] Patent Number: 6,072,364

[45] Date of Patent: Jun. 6, 2000

144

[54] **ADAPTIVE DIGITAL PREDISTORTION FOR POWER AMPLIFIERS WITH REAL TIME MODELING OF MEMORYLESS COMPLEX GAINS**

[75] Inventors: **Ernesto G. Jeckeln**; **Fadhel M. Ghannouchi**, both of Montreal; **Mohamad A. Sawan**, Laval, all of Canada

[73] Assignee: **Amplix**, Montreal, Canada

[21] Appl. No.: **08/877,479**

[22] Filed: **Jun. 17, 1997**

[51] **Int. Cl.**[7] **H03F 1/26**

[52] **U.S. Cl.** **330/149**; 332/103

[58] **Field of Search** 330/149; 332/103, 332/107, 123, 159, 160; 375/297; 455/63, 126

[56] **References Cited**

U.S. PATENT DOCUMENTS

4,291,277	9/1981	Davis et al.	330/149
4,700,151	10/1987	Nagata	332/18
4,985,688	1/1991	Nagata	332/123
5,049,832	9/1991	Cavers	330/149
5,113,414	5/1992	Karam et al.	375/60
5,119,040	6/1992	Long et al.	330/149
5,148,448	9/1992	Karam et al.	375/60
5,237,288	8/1993	Cleveland	330/107
5,262,734	11/1993	Dent et al.	330/52
5,396,190	3/1995	Murata	330/149
5,404,378	4/1995	Kimura	375/296
5,420,536	5/1995	Faulkner et al.	330/149
5,491,457	2/1996	Feher	332/103
5,524,285	6/1996	Wray et al.	455/126
5,524,286	6/1996	Chiesa et al.	455/126
5,568,088	10/1996	Dent et al.	330/151
5,598,436	1/1997	Brajal et al.	375/297
5,650,758	7/1997	Xu et al.	330/149
5,699,383	12/1997	Ichiyoshi	375/297

OTHER PUBLICATIONS

E.G. Jeckeln, F.M. Ghannouchi and M. Sawan, "Adaptive Digital Predistorter for Power Amplifiers with Real Time Modeling of Memoryless Complex Gain", IEEE MTT–S International Microwave Symposium, San Francisco, Jun. 1996.

E.G. Jeckeln, F.M. Ghannouchi and M. Sawan, "Adaptive Digital Predistorter for Power Amplifiers with Real Time Modeling of Memoryless Complex Gain", IEEE Transaction on Microwave Theory and Thechniques (submitted, Mar. 29, 1996).

J.G. Proakis, "Digital Communications", McGraw Hill, 1983.

J.H. Mathews, "Numerical Methods", for Computer Science, Engineering, and Mathematics, McGraw Hill, 1989.

"Adaptive Linearization of Power Amplifiers in Digital Radio Systems" Saleh et al., The Bell System Technical Journal, vol. 62, No. 4, Apr. 1983 pp. 1019–1033.

(List continued on next page.)

Primary Examiner—Robert Pascal
Assistant Examiner—Khanh Van Nguyen
Attorney, Agent, or Firm—Griffin, Butler, Whisenhunt & Szipl, LLP

[57] **ABSTRACT**

In an adaptive method and device for predistorting a signal to be transmitted, supplied by a signal source to an input of a power amplifier having a output for delivering an amplified output signal, the following steps are conducted: predistorting the signal to be transmitted by means of cascaded predistortion amplitude and phase look-up tables interposed between the signal source and the input of the power amplifier, producing a first feedback signal in response to the predistorted signal, producing a second feedback signal in response to the amplified output signal from the power amplifier, delaying the first feedback signal for eliminating any time lag between the first and second feedback signals, and real time modeling the predistortion amplitude and phase look-up tables in response to the first and second feedback signals in order to update these two tables. The position of the delay circuit (delaying step), that permits the use of the real time modeling procedure, eliminates the convergence time and the requirement for any iterative algorithms.

18 Claims, 4 Drawing Sheets

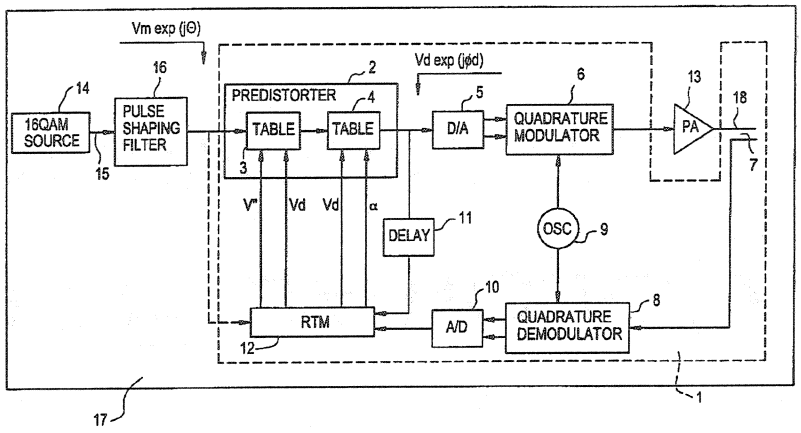

145

OTHER PUBLICATIONS

"A New Baseband Linearizer for More Efficient Utilization of Earth Station Amplifiers Used for QPSK Transmissions" Girard et al., IEEE J. on Selec. Areas in Comm. vol. Sac–1, No. 1, Jan. 1983, pp. 46–56.

"Adaptation Behavior of a Feedforward Amplifier Linearizer" J.K.Cavers, IEEE Trans. on Vehicular Technology, vol. 44, No.1. Feb. 1995, pp. 31–40.

"A Wide–Band Feedforward Amplifier" Meyer et al., IEEE Journal of Solid–State Circuits vol. SC–9, No. 6, Dec. 1974, pp. 422–428.

"Direct Conversion Transceiver Design for Compact Low–Cost Portable Mobile Radio Terminals" Bateman et al., Center for Communications Research, U. of Bristol, pp. 57–62, 1989.

"Novel Linearizer Using Balanced Circulators aand Its Application to Multilevel Digital Radio Systems" Imai et al., IEEE Trans. on Micro. Theory and Tech. vol. 37, No. 8, Aug. 1989 pp. 1237–1243.

"An assessment of the Performance of Linearisation schemes in the Australian Mobilesat System by simulation" T.A.Wilkinson, 6th Int'l Conf. on Mobile Radio and Personal Comm. UK 1991, pp. 74–76.

"Linear Amplification Technique for Digital Mobile Communications" Y.Nagata, Comm. Res. Lab. C&C Systems Res. Labs. 1989, pp. 159–164.

"Amplifier Linearization Using a Digital Predisorter with Fast Adaptation and Low Memory Requirements" J.K. Cavers, IEEE Trans. on Vehic.Tech. vol. 39, No. 4, Nov. 1990, pp. 374–382.

"Adaptive Linearisation Using Pre–Distortion" Faulkner et al. CH2846–4/90/0000–0035 1990 IEEE, pp. 35–39.

"Analysis and Compensation of Bandpass Nonlinearities for Communications" Kaye et al., IEEE Trans. on Communications, Oct. 1972, pp. 965–972.

"Signal Processing WorkSystem" Communications Library Reference, Alta Group of Cadence Design Systems, Inc, Mar. 1995, pp. i–iii, pp. iv–xiv.

FIG.1

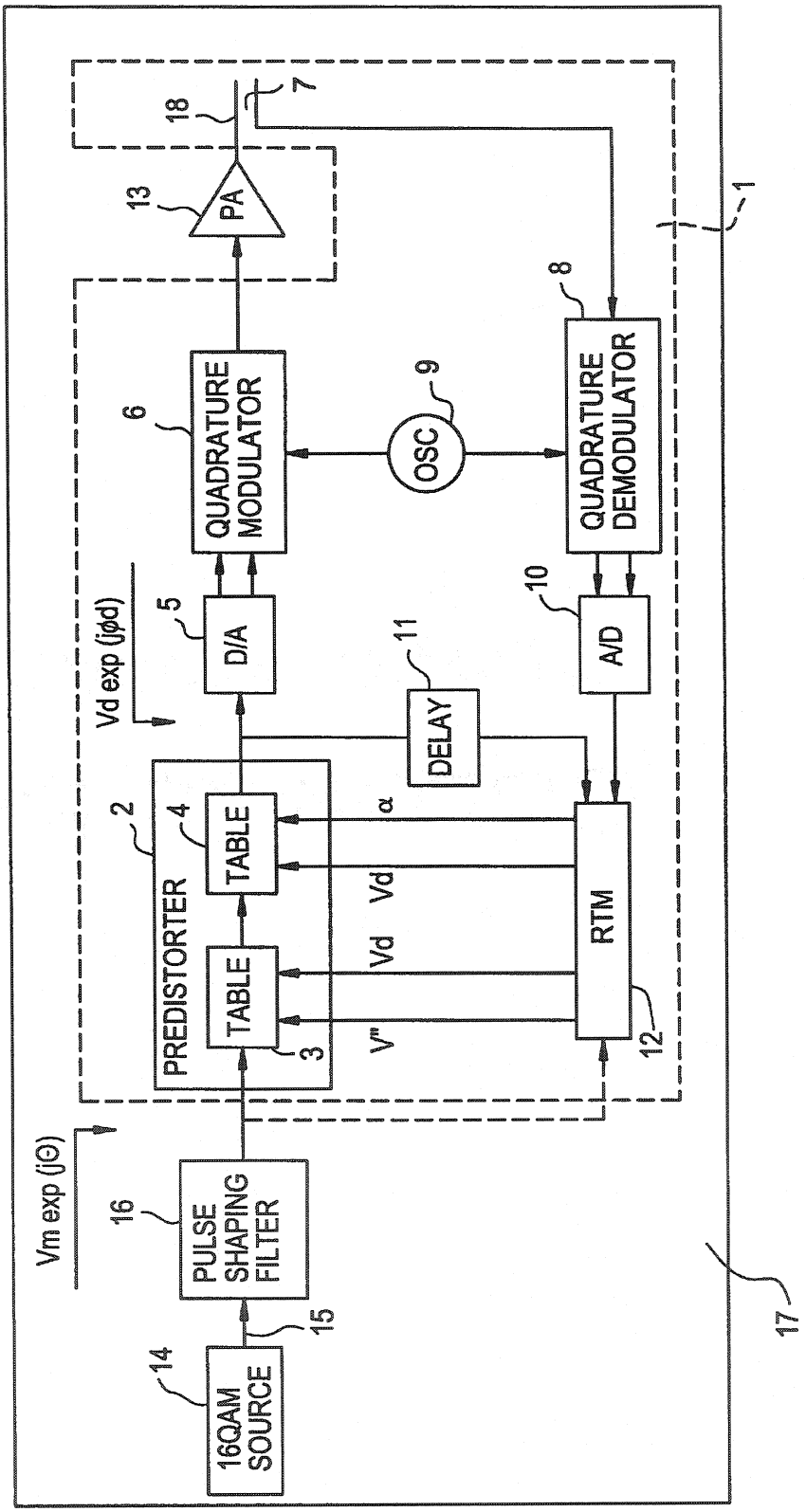
1
2
PREDISTORTER
3
TABLE
4
TABLE
5
D/A
6
QUADRATURE MODULATOR
7
8
QUADRATURE DEMODULATOR
9
OSC
10
A/D
11
DELAY
12
RTM
13
PA
14
16QAM SOURCE
15
16
PULSE SHAPING FILTER
17
18
Vm exp (jΘ)
Vd exp (jφd)
α
Vd
Vd
V''

147

FIG.2a

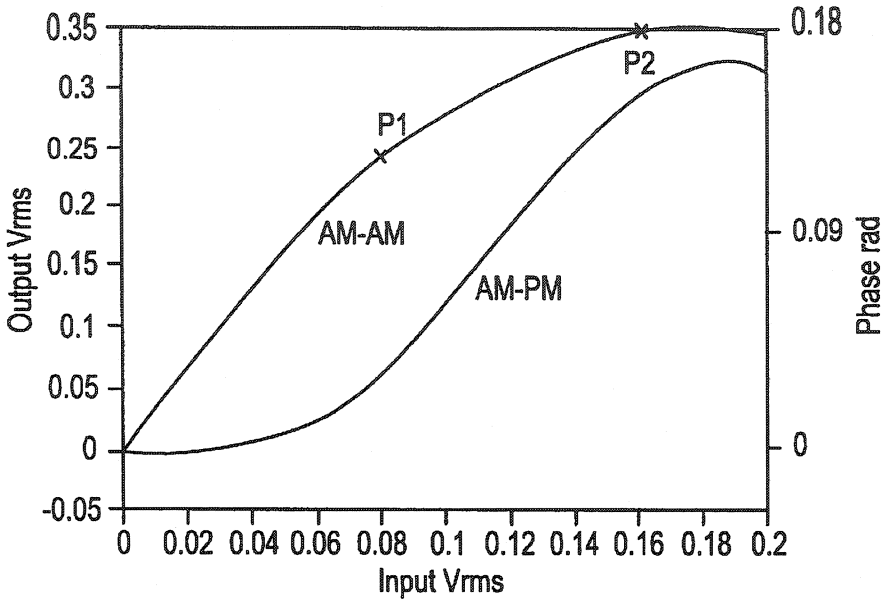

FIG.2b

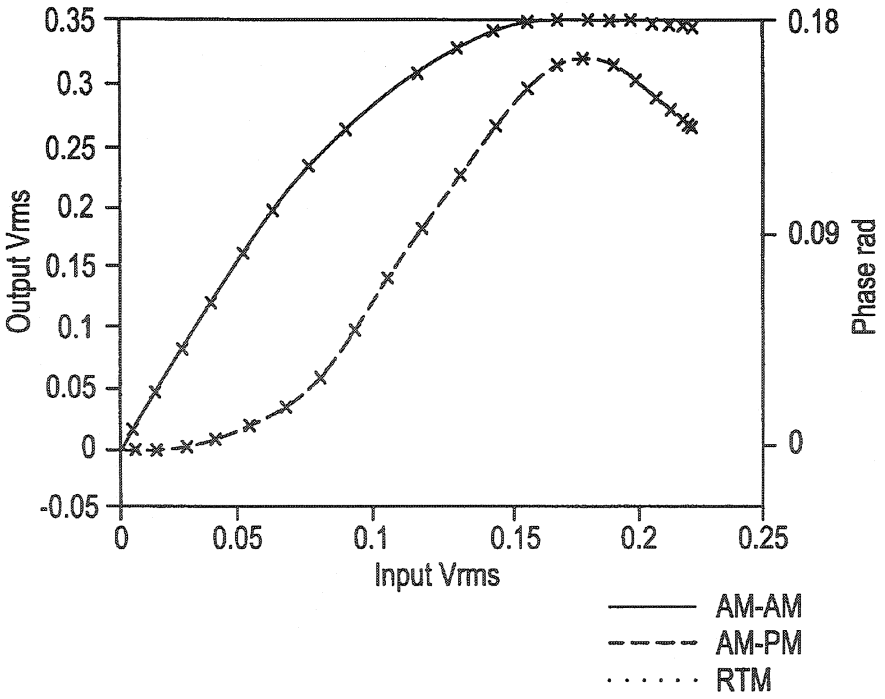

148

FIG.3a

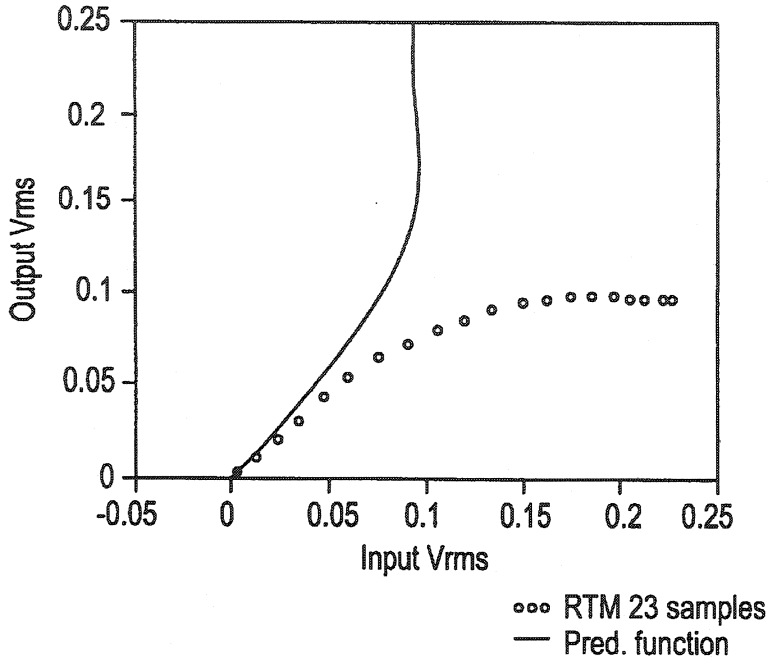

FIG.3b

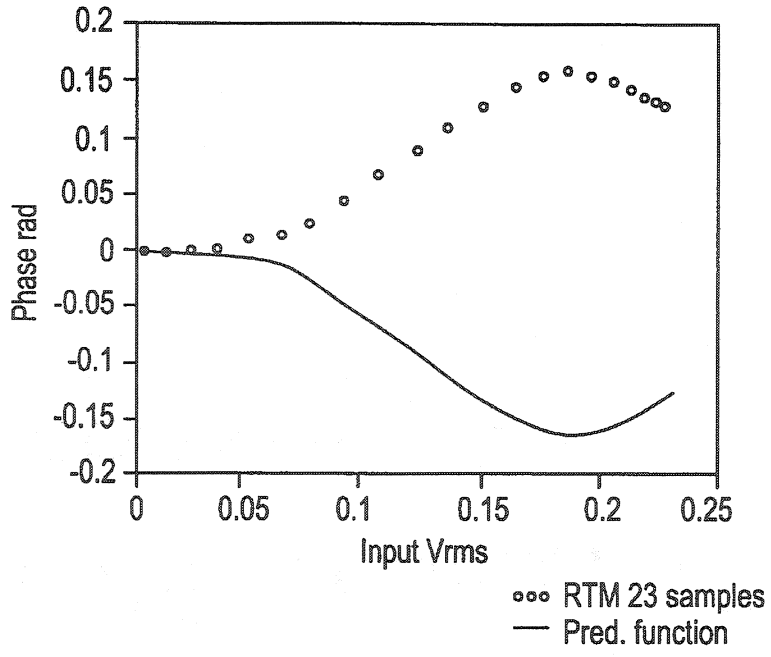

FIG.4

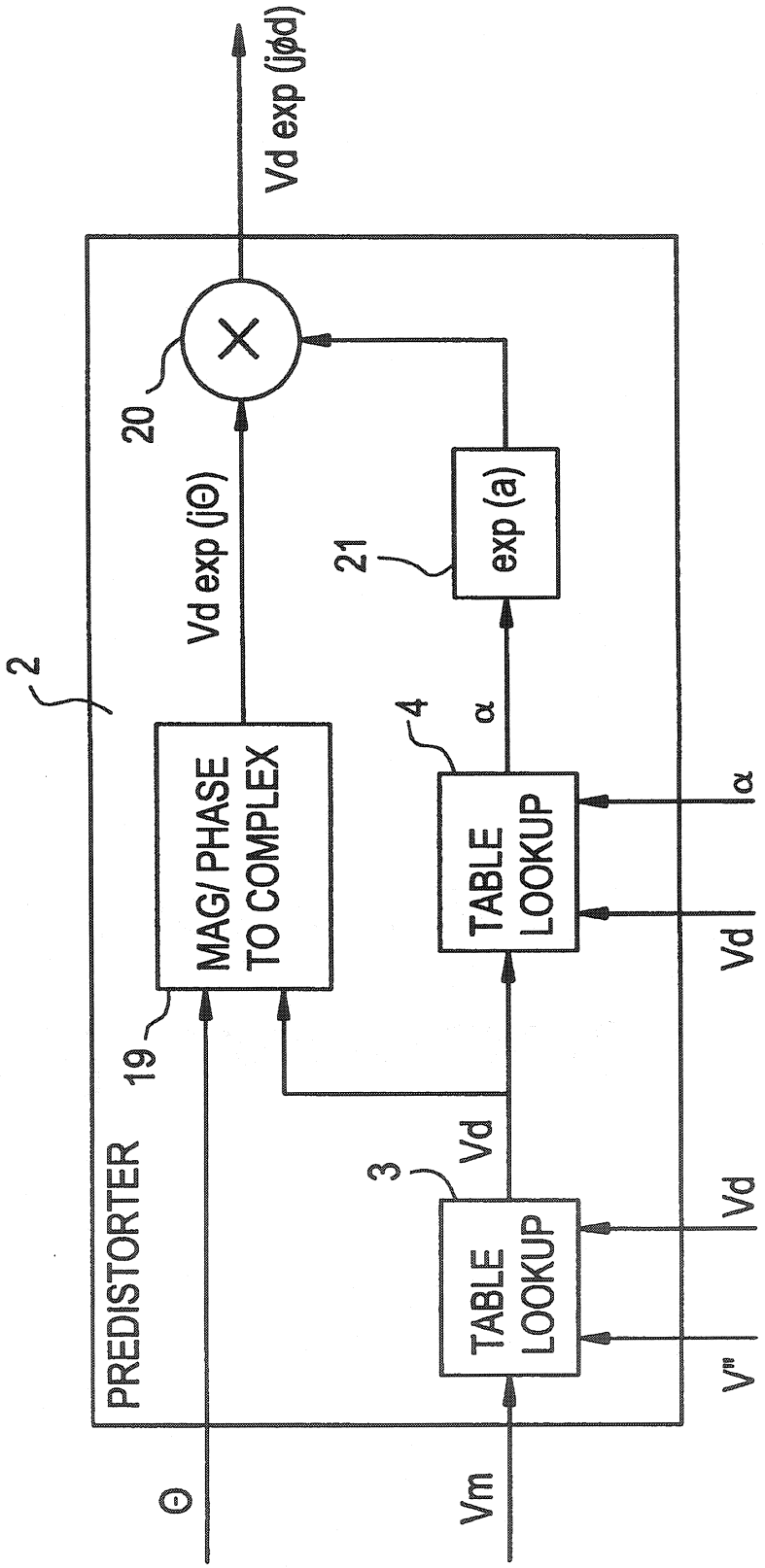
Vd exp (jφd)
20
Vd exp (jΘ)
21
exp (a)
2
4
α
MAG/ PHASE TO COMPLEX
TABLE LOOKUP
α
Vd
19
PREDISTORTER
3
Vd
TABLE LOOKUP
Vd
V'''
Θ
Vm

ADAPTIVE DIGITAL PREDISTORTION FOR POWER AMPLIFIERS WITH REAL TIME MODELING OF MEMORYLESS COMPLEX GAINS

BACKGROUND OF THE INVENTION

1. Field of the Invention

The present invention relates to an adaptive predistortion method and device for power amplifiers dedicated in particular but not exclusively to spectrally efficient microwave mobile communication equipments.

2. Brief Description of the Prior Art

With the increasing demand on the RF and microwave spectrum, caused by the proliferation of wireless communications and satellite networks, more spectrally efficient modulation techniques will have to be developed. Linear modulation methods, like M-ary QAM, meet this requirement with high units of bits per second per Hertz. But since it has a high envelope variation, their performance is strongly dependent on the linearity of the transmission system. In addition, modern wireless radio systems like mobile cellular and emerging Personal Communication Systems (PCS) require a high power efficiency to extend the battery life of the portables. To maximize the power added efficiency and the power output, the power amplifier is often operated near saturation where the input/output power characteristics become nonlinear. Unfortunately, if linear modulation with fluctuating envelope is used in conjunction with a highly efficient nonlinear amplification, distortion and spectral spreading into adjacent channels will occur. In order to reduce these undesired effects and meet the desired power and spectral efficiency, linearization techniques have been introduced.

A variety of linearization methods have been reported and many different ways can be used to segment this topic. Factors such as average transmitter power, operating bandwidth, power efficiency, adaptability and complexity are significant considerations in design compromises that can be used to categorize the different techniques. In general, all these techniques are, by any measure, derived from three main types named:

i) Feed-forward (R. Meyer, R. Eschenbach and W. Edgerley, Jr. "A wide-Band Feedforward Amplifier", IEEE J. of Solid-State Circuits, vol. sc-9, no. 6, pp. 442–428, December 1974), which includes an open loop configuration, can handle a multicarrier signal but can not easily be controlled against the effects of drift. Moreover, their low power efficiency make it suitable in base station only. A good analysis of adaptation behavior has been presented in J. Cavers, "Adaptation Behavior of a Feedforward Amplifier Linearizer", IEEE Transactions on Vehicular Technology, vol. 44, no. 1, pp. 31–40, February 1995;

ii) Feedback (A. Bateman & D. Haines, "Direct Conversion Transceiver Design for Compact Low-Cost Portable Mobile Radio Terminals" IEEE Conf. pp. 57–58, 1989), which presents an excellent reduction of out-of-band emissions, is relatively easy to implement. However, stability requirement limits its bandwidth because of its critical dependence on the loop delay; and

iii) Predistortion (N. Imai, T. Nojima and T. Murase, "Novel Linearizer Using Balanced Circulators and Its Application to Multilevel Digital Radio Systems", IEEE Transactions on Microwave Theory and Techniques, vol. 37, no. 8, pp. 1237–1243, August 1989), this technique has historically been the most common method in analog implementation. This method uses a nonlinear element which precedes the device to be compensated, its gain-expansion characteristic cancels the gain compression of the amplifier. Like feed-forward, it has an open loop configuration and therefore is very sensitive to drifts.

In recent years, the technology progress of Digital Signal Processors (DSP) has been one of the motive of the imminent course toward digital modulation techniques. Actually, the digital signal can be processed in such a way that greater bandwidth efficiency and voice quality can be obtained. In addition various applications such as generation of accurate gain and phase matching in two quadrature modulating signals, real-time compensation for channel impairments and the benefits of fast computational machines have motivated the use of these processors in several methods of linearization. These techniques are called Digital Linearization Techniques.

One of the features of the digital techniques is the control against the effects of drift. It is well known, that the power amplifier characteristic are quite sensitive to temperature variation and some unbalance in the linearization process can be occurred. In order to overcome this problem and avoid the effect of device power supply precision and drifts produced by switching between channels, adaptability is needed. In this way, an adaptive digital predistorter is the most promising technique that can be applied to narrow band Personal Communication Service using a DSP. The first successful work was presented by Y. Nagata, "Linear Amplification Technique for Digital Mobile Communications", in Proc. IEEE Veh. Technol. Conf. Sans Francisco, Calif., pp. 159–164, 1989 using a two-dimensional Look-Up Table (LUT) technique with adaptive digital feedback at baseband and pulse shaping filter prior to predistortion. This technique has shown the advantage that any order of nonlinearity and any modulation format can be supported. Followed later by J. Cavers, "Amplifier Linearization Using a Digital Predistorter with Fast Adaptation and Low Memory Requirement", IEEE Transactions on Vehicular Technology, vol. 39, no. 4, pp. 374–382, November 1990 and M. Faulkner, T. Mattsson and W. Yates, "Adaptive Linearization Using Predistortion", in Proc. 40th IEEE Veh. Technol. Conf. pp. 35–40, 1990, several drawbacks were eliminated using a one-dimensional table. This has made possible that less memory is needed and therefore, the convergence time has been reduced. These previous techniques were based on iterative algorithms.

An interesting idea was proposed by T. Wilkinson, "An Assessment of the Performance of Linearization Schemes in the Australian Mobilsat System by Simulation", IEE 6th Int. Conf. on Mobile Radio, London, pp. 74–76, 1991 using two look-up tables, one for the amplitude and the second for the phase. Each LUT includes one hundred entries covering the range of input levels and linear interpolation is used to determine values between entries. This later technique does not consider any adaptability dedicated to drift correction.

OBJECTS OF THE INVENTION

An object of the present invention is therefore to eliminate the above described drawbacks of the prior art, in particular to eliminate the convergence time and the need for iterative algorithms.

SUMMARY OF THE INVENTION

More specifically, in accordance with the present invention, there is provided an adaptive method for predis-

torting a signal to be transmitted, supplied by a signal source to an input of a power amplifier having an output for delivering an amplified output signal. This method comprises the steps of predistorting the signal to be transmitted by means of predistortion amplitude and phase look-up table means interposed between the signal source and the input of the power amplifier, producing a first feedback signal in response to the predistorted signal, producing a second feedback signal in response to the amplified output signal from the power amplifier, delaying at least one of the first and second feedback signals for eliminating any time lag between these first and second feedback signals, and updating the predistortion amplitude and phase look-up table means in response to the first and second feedback signals.

Preferably, the delaying step comprises delaying the first feedback signal in order to eliminate any time lag between the first and second feedback signals, the updating step comprises real time modeling the predistortion amplitude and phase look-up table means in response to the first and second feedback signals, the real time modeling comprises using a linear or third-order cubic spline interpolation, and the predistorting step comprises predistorting the signal to be transmitted by means of cascaded one-dimensional predistortion amplitude and phase look-up tables.

Also in accordance with the present invention, there is provided an adaptive device for predistorting a signal to be transmitted, supplied by a signal source to an input of a power amplifier having an output for delivering an amplified output signal. The device comprises predistorter means comprising predistortion amplitude and phase look-up table means interposed between the signal source and the input of the power amplifier for amplitude and phase predistorting the signal to be transmitted, means for producing a first feedback signal in response to the predistorted signal from the predistorter means, means for producing a second feedback signal in response to the amplified output signal from the power amplifier, delay means for eliminating any time lag between the first and second feedback signals, and means for updating the predistortion amplitude and phase look-up table means in response to the first and second feedback signals.

Advantageously, the updating means comprises means for real time modeling the predistortion amplitude and phase look-up table means in response to the first and second feedback signals, the predistortion amplitude and phase look-up table means comprises, in cascade, a one-dimensional predistortion amplitude look-up table and a one-dimensional predistortion phase look-up table, and the delay means comprises means for delaying the first feedback signal in order to eliminate any time lag between the first and second feedback signals.

In accordance with a preferred embodiment:

- the signal to be transmitted is a digital signal;
- the predistortion amplitude and phase look-up table means are digital predistortion amplitude and phase look-up table means for producing a digital predistorted signal;
- the adaptive signal predistorting device comprises a digital-to-analog converter for converting the digital predistorted signal into an analog predistorted signal and a quadrature modulator for converting the analog predistorted signal into a microwave signal supplied to the input of the power amplifier; and
- the means for producing a second feedback signal comprises a microwave coupler for supplying a portion of the amplified output signal of the power amplifier to a quadrature demodulator producing, in response to this portion of the amplified output signal of the power amplifier, a demodulated analog signal and an analog-to-digital converter for converting the demodulated analog signal into the second feedback signal, in digital form.

According to another preferred embodiment of the invention, the signal to be transmitted comprises an amplitude component and a phase component, and the predistorter means comprises:

- the one-dimensional predistortion amplitude look-up table for producing a predistorted amplitude in response to the amplitude component of the signal to be transmitted;
- the one-dimensional predistortion phase look-up table for producing a predistorted phase in response to the predistorted amplitude; and
- means for combining the phase component of the signal to be transmitted, the predistorted amplitude and the predistorted phase into the predistorted signal at the output of the predistorter means.

Thanks to the position of the delay circuit, the convergence time and the requirement for any iterative algorithms are eliminated through real time modeling and by using a linear or third-order cubic spline interpolation.

The objects, advantages and other features of the present invention will become more apparent upon reading of the following non restrictive description of a preferred embodiment thereof, given by way of example only with reference to the accompanying drawings.

BRIEF DESCRIPTION OF THE DRAWINGS

In the appended drawings:

FIG. **1** is a block diagram of an adaptive digital predistorting device in accordance with the present invention, comprising a predistorter;

FIG. **2***a* is a graph showing the AM-AM and AM-PM characteristics of a microwave power amplifier of class AB;

FIG. **2***b* is a graph comparing the AM-AM and AM-PM characteristics of a microwave power amplifier of class AB obtained by measurements and Real Time Modeling (RTM);

FIG. **3***a* is a graph showing an interpolated amplitude predistortion function and 23 amplitude samples obtained by Real Time Modeling;

FIG. **3***b* is a graph showing an interpolated phase predistortion function and 23 phase samples obtained by Real Time Modeling; and

FIG. **4** is a block diagram of the predistorter of the adaptive digital predistorting device of FIG. **1**.

DETAILED DESCRIPTION OF THE PREFERRED EMBODIMENT

Referring to FIG. **1** of the appended drawings, a preferred embodiment of the adaptive digital predistorting device according to the invention is presented. This adaptive digital predistorting device is generally identified by the reference **1**.

As shown in FIG. **1**, the amplifier system **17** includes an adaptive digital predistorting device **1** comprising: a predistorter **2** including a one-dimensional predistortion amplitude look-up table **3** and a one-dimensional predistortion phase look-up table **4**; a digital-to-analog (D/A) converter **5**; a quadrature modulator **6**; a microwave coupler **7**; a quadrature demodulator **8**; an oscillator **9**; an analog-to-digital

(A/D) converter **10**; a delay circuit **11**; and a Real Time Modeling (RTM) circuit **12**.

The amplifier system **17** further comprises a microwave power amplifier **13** to amplify the microwave signal from the quadrature modulator **6**.

In the illustrated example, the spectrally efficient 16-QAM modulation method is used by a source **14** to produce a 16-QAM modulated signal **15** to be transmitted. Of course, it is within the scope of the present invention to use another type of source. Signal **15** is passed through a pulse shaping circuit **16** ensure Free-Symbol-Interference (FSI).

A microwave power amplifier used in mobile communication, such as power amplifier **13** of FIG. **1**, must operate close to saturation to achieve both high power efficiency and high transmitted power. The microwave power amplifier **13** is said to be saturated when its output power level no longer increases in response to an increase of its input power level. Close to the saturation region, the input/output characteristic of the microwave power amplifier **13** becomes nonlinear and, therefore, amplitude and phase distortion are generated when digital modulation with fluctuating envelope is used. These effects are identified within the modulated signal as additional amplitude and phase modulations that may degrade the Bit-Error-Rate (BER) performance of the modulation scheme. In addition, a time invariant microwave power amplifier can be classified as having either zero memory or non zero memory. If the microwave amplifier **13** is wideband in comparison to the input signal, it is considered as having zero memory and its input-output characteristic can be given by the following relation:

$$y(t)=T[x(t)] \tag{1}$$

where y(t) is the output signal of the microwave power amplifier, x(t) is the input signal of the same amplifier, and T is the memoryless complex gain of that microwave power amplifier.

In this way, a memoryless nonlinearity of the microwave power amplifier **13** can be considered because of the narrowband of the baseband signal relative to the bandwidth of the power amplifier **13**. Then, the memoryless complex gain T is expressed as a function of the amplitude only, hence the possibility to use a one-dimensional look-up table during the predistortion procedure; this means that the nonlinearity of the power amplifier **13** is independent of the frequency and phase of the microwave signal. Therefore, the memoryless complex gain T is modeled through the amplitude transfer characteristic AM-AM of the power amplifier **13** and the AM-PM conversion factor of the same amplifier as shown in FIG. **2***a*. Let the input signal of the microwave power amplifier **13** be:

$$S(t)=V_m(t)\cos[\omega_c t+\theta(t)] \tag{2}$$

where $V_m(t)$ is a time-dependent amplitude, ω_c is the angular frequency of the input signal, t is a time variable, and $\theta(t)$ is a time-dependent phase shift of the input signal.

The output signal may then be expressed as follows:

$$Z(t)=G[V_m(t)]\cos\{\omega_c t+\theta(t)+\phi[V_m(t)]\} \tag{3}$$

where:

$G[V_m(t)]$ is the AM-AM amplitude transfer characteristic of the power amplifier **13**; and

$\phi[V_m(t)]$ is the AM-PM conversion factor of the power amplifier **13**.

Then, the memoryless complex gain of the power amplifier **13** is given by the following relation:

$$T_m(t)=G[V_m(t)]e^{j\phi[V_m(t)]} \tag{4}$$

Now, considering the complex gain of the predistorter **2** in a sub-system whose output is the input signal of the microwave power amplifier **13**, the resulting predistorted signal can be written as follows:

$$S_p(t)=V_d(t)\cos\{\omega_c t+\theta(t)+\alpha[V_d(t)]\} \tag{5}$$

where $V_d(t)$ and $\alpha[V_d(t)]$ are the predistorted amplitude and phase respectively.

Then, the output signal of the power amplifier **13** will be:

$$Z_p(t)=G[V_d(t)]\cos\{\omega_c t+\theta(t)+\alpha[V_d(t)]+\phi[V_d(t)]\} \tag{6}$$

From equations (2) and (6), one can see that the conditions that must be satisfied to properly correct the AM and PM distortions are:

$$G[V_d(t)]=KV_m(t) \tag{7}$$

$$\phi[V_d(t)]+\alpha[V_d(t)]=0 \tag{8}$$

where K is the expected constant gain of the power amplifier **13** and $V_m(t)$ is the amplitude modulation of the input signal to be amplified, i.e. supplied to the power amplifier **13**.

A) Equivalent Low Pass Signal

The complex envelope method as described by Signal Processing WorkSystem (SPW), Alta Group of Cadence Design System, Inc., 1996, using the concepts of equivalent lowpass signals and systems, has been used to analyse and simulate the amplifier system **17**. More specifically, the representation of bandpass signals and systems can be given in terms of equivalent lowpass waveforms under the condition that their bandwidths are much smaller than the carrier frequency (J. G. Proakis, "Digital Communications", McGraw Hill, 1983). In this case, the equivalent lowpass signal must be derived from their modulated passband counterparts. The modulated carrier signal x(t) can be written as:

$$x(t)=Re[V(t)e^{j[2\pi f_c t+\phi(t)]}]=Re[V(t)e^{j\phi(t)}e^{j2\pi f_c t}] \tag{9}$$

where V(t) is the amplitude modulation, $\phi(t)$ is the phase modulation, f_c is the carrier frequency, and Re[•] denotes the real part of the quantity in brackets. The complex envelope of the bandpass signal or the equivalent lowpass complex signal $S_b(t)$ is given by:

$$s_b(t)=V(t)e^{j\phi(t)} \tag{10}$$

This is an equivalent polar representation where V(t) is the amplitude modulation and $\phi(t)$ is the phase modulation of the baseband signal. The advantage to model the microwave signal and the linearized power amplifier **13** at baseband is that it simplifies the analysis and reduces dramatically the number of iterations during simulation when the amplifier system **17** is analysed.

In this manner, equation (10) can be treated as an equivalent lowpass signal. Then, in order to map the information into a corresponding set of discrete amplitudes and phases, the signal waveforms may be represented as:

$$x_{bm}(t)=V_m e^{j\phi_m}u(t)m=1,2,3,\ldots,M \tag{11}$$

where $\{V_m,\phi_m,m=1,2,3,\ldots,M\}$ represent the M possible symbols in the signal-space diagram and u(t) is the waveform impulse response of the pulse shaping filter **16**. The

term u(t) is selected to control the spectral characteristics of the transmitted signal. In general, the equivalent lowpass complex signal that must be transmitted over the power amplifier **13** can be written in time domain as:

$$S(t)=\sum_{n=1}^{\infty} V_n e^{j\phi_n} u(t-nT) \tag{12}$$

where $\{V_n,\phi_n\}$ represents the sequence of transmitted information symbols that change at the signalling intervals nT, n=1,2,3, . . . , and T is the symbol period.

B) Real Time Modeling (RTM)

In order to capture and eliminate the higher intermodulation levels generated by the power amplifier **13**, equation (12) must be oversampled according to the bandwidth to be compensated. To simplify the analysis, we can model a discrete signal through the impulse sampling representation considering the sample-data as a number occurring at a specific instant of time. In this case, the discrete signal may be represented as a sequence of impulse functions of the form:

$$S(n)=\sum_{i=1}^{\infty} V_i e^{j\phi_i}\gamma(n-iT') \tag{13}$$

where y(n−iT') represents the impulse sampling at the signalling intervals iT' (i=1,2,3, . . . ,), T' is the sampling period and $\{V_i, \phi_i\}$ are the discrete amplitudes and phases of the signal trajectory in the signal-space diagram.

In this manner, using the equation (13), the equivalent lowpass of the amplifier input signal $V_d e^{j\Phi_d}$ and the feedback signal $(1/K)V'e^{j\Phi'}$ (FIG. **1**), are oversampled to provide a number of data samples. These pairs of complex samples correspond to an ascending list of values of the amplitude of the input signal. These values must be spread out to cover the overall range of the input envelope levels and must satisfy:

$$0\leqq V_{d0}<V_{d1}<V_{d2}<\ldots<V_{dq} \tag{14}$$

Then, the sequences of complex samples can be written as:

$$\sum_{l=1}^{q} V_{dl} e^{j\phi_{dl}}\gamma(n-lT') \tag{15}$$

$$\sum_{l=1}^{q} V_l'' e^{j\phi_l'}\gamma(n-lT') \tag{16}$$

where q is the number of samples and V"=(1/K)V'.

From (15) and (16), the samples of phase distortion can be obtained as:

$$\sum_{l=1}^{q}\phi_l=\sum_{l=1}^{q}\phi_l'-\phi_{dl} \tag{17}$$

Then, the set of data points $(V_{d1}, V_1")$, $(V_{d2}, V_2")$, . . . ,$(V_{dq}, V_q")$ and (V_{d1}, ϕ_1), (V_{d2}, ϕ_2), . . . (V_{dq}, ϕ_q) are used to perform interpolations. These interpolations permit to determine both the relative envelope transfer functions $g[V_d(t)]$ and the envelope dependent phase shift $\phi[V_d(t)]$ which are expressed as:

$$V''(t)=g[V_d(t)] \tag{18}$$

$$\phi=\phi[V_d(t)] \tag{19}$$

Then, the memoryless complex gain of the power amplifier **13** can be expressed as an equivalent complex envelope transfer function as follows:

$$T_d(t)=G[V_d(t)]e^{j\Phi[V_d(t)]} \tag{20}$$

where $G[V_d(t)]$ is obtained from the normalized $g[V_d(t)]$.

FIG. **2***b* shows a comparison between the measured AM-AM and AM-PM characteristics and the Real Time Modeling (RTM) results of a class AB power amplifier **13**. To this end, 23 complex samples of Real Time Modeling were used to interpolate the Memoryless Complex Gains (MCG) function. Of course, the present invention is usable with other classes of amplifiers.

C) Predistortion

Based on the above equations (7) and (8) that must be satisfied to ideally correct the AM and PM distortion, the optimal compensation made by predistortion can be achieved when the compensation envelope transfer function is given by:

$$V_d(t)=g^{-1}[V''(t)] \tag{21}$$

and the compensation phase characteristic is given by:

$$\alpha[V_d(t)]=-\phi[V_d(t)] \tag{22}$$

Under these conditions, the set of data points of amplitudes $(V_{d1}, V_1")$ from (15) and (16) are interchanged as $(V_1", V_{d1})$ and the set of data points of phase distortion are put in opposition according to (22). Then, the updating of the one-dimensional amplitude and phase look-up tables **3** and **4** is made in a form in which there is correspondence between input and output values of the look-up tables as illustrated by the following relation (23). It is important to note that the input amplitude $V_m(t)$ and the predistorted input amplitude $V_d(t)$ are used to point to an address of the look-up tables **3** and **4**, respectively. These look-up tables **3** and **4** implement a mapping from the input to the output, according to the number of sampled pairs, using linear or cubic spline interpolation. If cubic spline interpolation is used, only a small number of sampled pairs are needed.

$$V_m(t)\rightarrow\begin{bmatrix}V_1\\V_2\\\vdots\\V_q\end{bmatrix}\rightarrow\begin{bmatrix}V_{d1}\\V_{d2}\\\vdots\\V_{dq}\end{bmatrix}\rightarrow V_d(t) \tag{23}$$

$$V_d(t)\rightarrow\begin{bmatrix}V_{d1}\\V_{d2}\\\vdots\\V_{dq}\end{bmatrix}\rightarrow\begin{bmatrix}\alpha_1\\\alpha_2\\\vdots\\\alpha_q\end{bmatrix}\rightarrow\alpha$$

Referring to FIGS. **1** and **4**, the 16-QAM modulated signal from the pulse shaping filter **16** is supplied to the predistorter **2**. FIG. **4** is a schematic block diagram showing a possible configuration of the predistorter **2** to obtain the predistorted power amplifier input signal. In the case of FIG. **2**, a polar representation was chosen to configure the one-dimensional predistortion amplitude and phase look-up tables **3** and **4** and these can be accessed in cascade form where the first and the second tables generate the predistorted amplitude and phase respectively.

As shown in FIG. **4**, the 16-QAM modulated signal from the pulse shaping circuit **16** has a phase component θ and an amplitude component $V_m(t)$. The phase component θ is supplied to a magnitude/phase-to-complex converter **19**.

The amplitude component $V_m(t)$ is supplied to the one-dimensional predistortion amplitude look-up table **3** which then outputs the predistorted amplitude $V_d(t)$.

The predistorted amplitude $V_d(t)$ is supplied to the converter **19** along with the phase component θ to produce the signal $V_d(t)e^{j\theta}$. The predistorted amplitude $V_d(t)$ is also supplied as input signal of the one-dimensional predistortion phase look-up table **4** to produce the predistorted phase α. The predistorted phase α is supplied to one input of a multiplier **20** through a phase-to-complex converter **21**. The other input of the multiplier **20** is supplied with the signal $V_d(t)e^{j\theta}$ to produce the predistorted input signal $V_d(t)e^{j\Phi d}$ (FIG. **1**).

The predistorted input signal $V_d(t)e^{j\Phi d}$ is digital-to-analog converted by the D/A converter **5** and the digital-to-analog converted signal $V_d(t)e^{j\Phi d}$ is processed through the quadrature modulator **6**, supplied by the oscillator **9**, to produce a microwave signal supplied to the input of the microwave power amplifier **13**. An amplified microwave signal is supplied on the output **18** of the microwave power amplifier **13**.

To enable the RTM circuit **12** of FIG. **1** to update the one-dimensional predistortion amplitude and phase look-up tables **3** and **4**:

- the signal at the output of the pulse shaping filter **16** is supplied to the RTM circuit **12**;
- a small portion of the predistorted input signal $V_d(t)e^{j\Phi d}$ at the output of the predistorter **2** is supplied to the RTM circuit **12** through a delay circuit as a first feedback signal; and
- a small portion of the microwave amplified signal at the output **18** of the microwave power amplifier **13** is supplied by the microwave coupler **7** to the quadrature demodulator **8**, also supplied with the oscillator **9**. The A/D converter **17** analog-to-digital converts the output of the quadrature demodulator **8** to produce a version of the predistorted input signal $V_d(t)e^{j\Phi d}$ corresponding to the output of the microwave power amplifier **13** supplied to the RTM circuit **12** as a second feedback signal.

To eliminate any time lag between the first and second feedback signals, the delay circuit **11** is provided to retard the predistorted input signal $V_d(t)e^{j\Phi d}$. In order to estimate the delay to be compensated for by circuit **11**, the following relation (24) is used:

$$z(m) = \frac{1}{N}\sum_{n=0}^{N-1} x(k)y^*(k+m) \qquad (24)$$

In relation (24) x(k), the input signal sequence of the power amplifier (corresponding to the predistorted input signal $V_d(t)e^{j\Phi d}$), and y(k), the feedback signal sequence (corresponding to the output of the power amplifier), are correlated to determine the delay to be compensated for by circuit **11**. In fact, y(k) is the delayed and distorted version of the input x(k). In practice, it is possible to access only a finite segment of these sequences. If N is the longer of these segments, m the delay variable and L the delay between signals, the correlation sequence z(m) can be written as in relation (24). Then the sequence z(m) is expected to reach a maximum for m=L. Because of the memoryless condition of all components in the feedback loop (D/A converter **6**, quadrature modulator **6**, power amplifier **13**, coupler **7**, quadrature demodulator **8** and A/D converter **10**), this provides an accurate measurement of the delay time.

Due to the position of the delay circuit **11**, the requirement for any iterative algorithms is eliminated through Real Time Modeling (RTM circuit **12**) and by using a linear or third-order cubic spline interpolation.

Real Time Modeling is then conducted as described hereinabove by circuit **12** to update the above described values V", V_d, and α of the one-dimensional predistortion amplitude and phase look-up tables **3** and **4**.

FIGS. **3***a* and **3***b* show both the 23 samples from Real Time Modeling which represent the AM-AM and AM-PM characteristics of the power amplifier **13** and the predistortion functions that have been interpolated according to the above relation (21). Note that the AM-AM characteristic of the power amplifier **13** has been normalized relative to the small-signal gain.

D) Interpolation and Curve Fitting

When a set of data point such as $(x^1, y_1), \ldots, (x_n, y_n)$ are known and the abscissas $\{x_k\}$are distinct, several methods can be used to determine a function y=f(x) that relates these variables (J. H. Mathews, "Numerical Methods", for Computer Science, Engineering, and Mathematics, McGraw Hill, 1989]. One possibility is to construct a polynomial with coefficients that can be calculated such that the curve passes through the data points. For a successful result, the set of points must be known with a high degree of accuracy which limits the use of this approach. Curve fitting methods, like least-squares polynomial optimization techniques, offer a good accuracy when the set of data points are produced through an experimental set up. However, this case is frequently unsatisfactory, because a polynomial of degree N can have N−1 local extrema and it may exhibit large oscillations when data points do not lie on a polynomial curve. A solution for this problem is to use interpolation by spline functions. In the present method, the curve denoted by S(x) is formed by a set of lower-degree polynomials $\{S_k(x)\}$ and interpolation is performed between the successive data points. Linear, quadratic and cubic spline interpolation may be used and can be extended to higher-degree polynomial with more additional computation.

In the case of linear spline and according to purpose which is the interpolation of the predistorsion function, a large number of data-points is needed to obtain a good compensation of the distortion. In quadratic spline, the curvature at the even node (X_{2k}, Y_{2k}) changes abruptly and this can cause an undesired distortion. Cubic splines show a good performance and is the most tempting when a smooth curve is required. In addition, only a small number of data-points is needed for a good compensation of distortion. It is known that the drawback of spline interpolation is that control at the edge point is difficult.

To conclude, the RTM algorithm has demonstrated to be a powerful tool for sounding and modeling the memoryless complex gains of a microwave power amplifier during normal data transmission. In particular, the RTM algorithm eliminates the need for complex convergence algorithms in the adaptation update step. Also, any order of nonlinearity and any modulation format can be supported by this technique.

Although the present invention has been described hereinabove by way of a preferred embodiment thereof, this embodiment can be modified at will, within the scope of the appended claims, without departing from the spirit and nature of the subject invention.

What is claimed is:

1. An adaptive method for predistorting a signal to be transmitted, supplied by a signal source to an input of a power amplifier having an output for delivering an amplified output signal, comprising the steps of:

predistorting the signal to be transmitted by means of predistortion amplitude and phase look-up table means interposed between the signal source and the input of the power amplifier;

producing a first feedback signal in response to the predistorted signal;

producing a second feedback signal in response to the amplified output signal from the power amplifier;

delaying at least one of the first and second feedback signals for eliminating any time lag between said first and second feedback signals;

modeling the power amplifier in response to the first and second feedback signals; and

updating the predistortion amplitude and phase look-up table means in response to said modeling of the power amplifier.

2. An adaptive signal predistorting method as recited in claim **1**, wherein the power amplifier has a memoryless complex gain, and wherein said modeling step comprises real time modeling the memoryless complex gain of the power amplifier in response to the first and second feedback signals.

3. An adaptive signal predistorting method as recited in claim **2**, wherein said real time modeling of the memoryless complex gain of the power amplifier comprises using spline interpolation selected from the group consisting of linear spline interpolation, quadratic spline interpolation and cubic spline interpolation.

4. An adaptive signal predistorting method as recited in claim **3**, in which said cubic spline interpolation is selected from the group consisting of linear cubic spline interpolation and third-order cubic spline interpolation.

5. An adaptive signal predistorting method as recited in claim **1**, wherein the predistorting stop comprises predistorting the signal to be transmitted by means of cascaded one-dimensional predistortion amplitude and phase look-up tables.

6. An adaptive signal predistorting method as recited in claim **1**, wherein said delaying step comprises delaying the first feedback signal in order to eliminate any time lag between the first and second feedback signals.

7. An adaptive signal predistorting method as recited in claim **1**, wherein the predistortion amplitude and phase look-up table means comprises an input for receiving said signal supplied by the signal source and an output for delivering the predistorted signal, and wherein said predistorting step comprises implementing through said predistortion amplitude and phase look-up table means a mapping from the source signal receiving input to the predistorted signal delivering output using spline interpolation selected from the group consisting of linear spline interpolation, quadratic spline interpolation and cubic spline interpolation.

8. An adaptive signal predistorting method as recited in claim **5**, wherein the cascaded one-dimensional predistortion amplitude and phase look-up tables comprise an input for receiving said signal supplied by the signal source and an output for delivering the predistorted signal, and wherein said predistorting step comprises implementing through said cascaded one-dimensional predistortion amplitude and phase look-up tables a mapping from the source signal receiving input to the predistorted signal delivering output using spline interpolation selected from the group consisting of linear spline interpolation, quadratic spline interpolation and cubic spline interpolation.

9. An adaptive device for predistorting a signal to be transmitted, supplied by a signal source to an input of a power amplifier having an output for delivering an amplified output signal, comprising:

predistorter means comprising predistortion amplitude and phase look-up table means interposed between the signal source and the input of the power amplifier for amplitude and phase predistorting the signal to be transmitted;

means for producing a first feedback signal in response to the predistorted signal from the predistorter means;

means for producing a second feedback signal in response to the amplified output signal from the power amplifier;

delay means for eliminating any time lag between the first and second feedback signals;

means for modeling the power amplifier in response to the first and second feedback signals; and

means for updating the predistortion amplitude and phase look-up table means in response to said modeling of the power amplifier.

10. An adaptive signal predistorting device as recited in claim **9**, wherein the power amplifier has a memoryless complex gain, and wherein said modeling means comprises means for real time modeling the memoryless complex gain of the power amplifier in response to the first and second feedback signals.

11. An adaptive signal predistorting device as recited in claim **9**, wherein the predistortion amplitude and phase look-up table means comprises one-dimensional predistortion amplitude and phase look-up table means.

12. An adaptive signal predistorting device as recited in claim **9**, in which the predistortion amplitude and phase look-up table means comprises, in cascade, a one-dimensional predistortion amplitude look-up table and a one-dimensional predistortion phase look-up table.

13. An adaptive signal predistorting device as recited in claim **9**, wherein said delay means comprises means for delaying the first feedback signal in order to eliminate any time lag between the first and second feedback signals.

14. An adaptive signal predistorting device as recited in claim **9**, wherein:

the signal to be transmitted is a digital signal;

the predistortion amplitude and phase look-up table means are digital predistortion amplitude and phase look-up table means for producing a digital predistorted signal;

said adaptive signal predistorting device comprises a digital-to-analog converter for converting the digital predistorted signal into an analog predistorted signal and a quadrature modulator for converting the analog predistorted signal into a microwave signal supplied to the input of the power amplifier;

said means for producing a second feedback signal comprises a microwave coupler for supplying a portion of the amplified output signal of the power amplifier to a quadrature demodulator producing, in response to said portion of the amplified output signal of the power amplifier, a demodulated analog signal and an analog-to-digital converter for converting the demodulated analog signal into said second feedback signal, in digital form.

15. An adaptive signal predistorting device as recited in claim **14**, wherein the power amplifier has a memoryless complex gain, and wherein said modeling means comprises means for real time modeling the the memoryless complex gain of the power amplifier in response to the first and second feedback signals.

16. An adaptive signal predistorting device as recited in claim **9**, wherein the predistorter means comprises an input for receiving said signal supplied by the signal source and an output for delivering the predistorted signal, and wherein said predistortion amplitude and phase look-up table means

comprises a look-up table arrangement for implementing a mapping from the source signal receiving input to the predistorted signal delivering output using spline interpolation selected from the group consisting of linear spline interpolation, quadratic spline interpolation and cubic spline interpolation.

17. An adaptive signal predistorting method as recited in claim **12**, wherein the predistorter means comprises an input for receiving said signal supplied by the signal source and an output for delivering the predistorted signal, and wherein the cascaded one-dimensional predistortion amplitude and phase look-up tables comprises means for implementing a mapping from the source signal receiving input to the predistorted signal delivering output using spline interpolation selected from the group consisting of linear spline interpolation, quadratic spline interpolation and cubic spline interpolation.

18. An adaptive device for predistorting a signal to be transmitted, supplied by a signal source to an input of a power amplifier having an output for delivering an amplified output signal, comprising:

predistorter means comprising predistortion amplitude and phase look-up table means interposed between the signal source and the input of the power amplifier for amplitude and phase predistorting the signal to be transmitted;

means for producing a first feedback signal in response to the predistorted signal from the predistorter means;

means for producing a second feedback signal in response to the amplified output signal from the power amplifier;

delay means for eliminating any time lag between the first and second feedback signals; and

means for updating the predistortion amplitude and phase look-up table means in response to the first and second feedback signals;

wherein the predistortion amplitude and phase look-up table means comprises, in cascade, a one-dimensional predistortion amplitude look-up table and a one-dimensional predistortion phase look-up table;

wherein said signal to be transmitted comprises an amplitude component and a phase component; and

wherein said predistorter means comprises:

said one-dimensional predistortion amplitude look-up table for producing a predistorted amplitude in response to the amplitude component of the signal to be transmitted;

said one-dimensional predistortion phase look-up table for producing a predistorted phase in response to the predistorted amplitude; and

means for combining the phase component of the signal to be transmitted, the predistorted amplitude and the predistorted phase into said predistorted signal.

* * * * *

ANNEXE I.2:

US Patent Application US20020191710

Adaptive Baseband/Rf Predistorter for Power Amplifiers through Instantaneous AM-AM and AM-PM Characterization Using Digital Receivers

US 20020191710A1

(19) United States

(12) Patent Application Publication (10) Pub. No.: US 2002/0191710 A1

Jeckeln et al. (43) Pub. Date: Dec. 19, 2002

158

(54) ADAPTIVE PREDISTORTION DEVICE AND METHOD USING DIGITAL RECEIVER

(76) Inventors: **Ernesto G. Jeckeln**, Montreal (CA); **Fadhel M. Ghannouchi**, Montreal (CA); **Mohamad Sawan**, Laval (CA); **Francois Beauregard**, La Prairie (CA)

Correspondence Address:
WELLS ST. JOHN ROBERTS GREGORY & MATKIN P.S.
601 W. FIRST AVENUE
SUITE 1300
SPOKANE, WA 99201-3828 (US)

(21) Appl. No.: **09/877,608**

(22) Filed: **Jun. 8, 2001**

Publication Classification

(51) **Int. Cl.**[7] **H04K 1/02**

(52) **U.S. Cl.** **375/296**

(57) **ABSTRACT**

An advanced adaptive basedband/RF predistorting device, which advantageously uses the concept of digital receiver technology into power amplifier (PA) linearization area. The predistorting device performs an instantaneous characterization of the PA using two digital receivers to supply its AM-AM and AM-PM transfer functions.

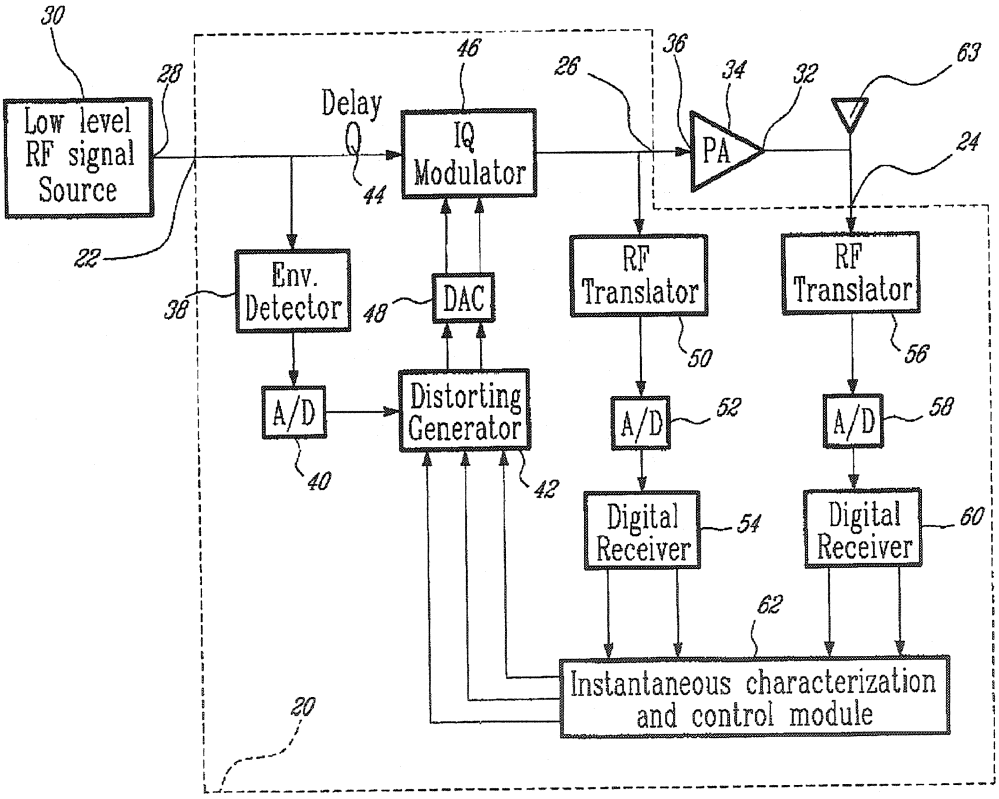

159

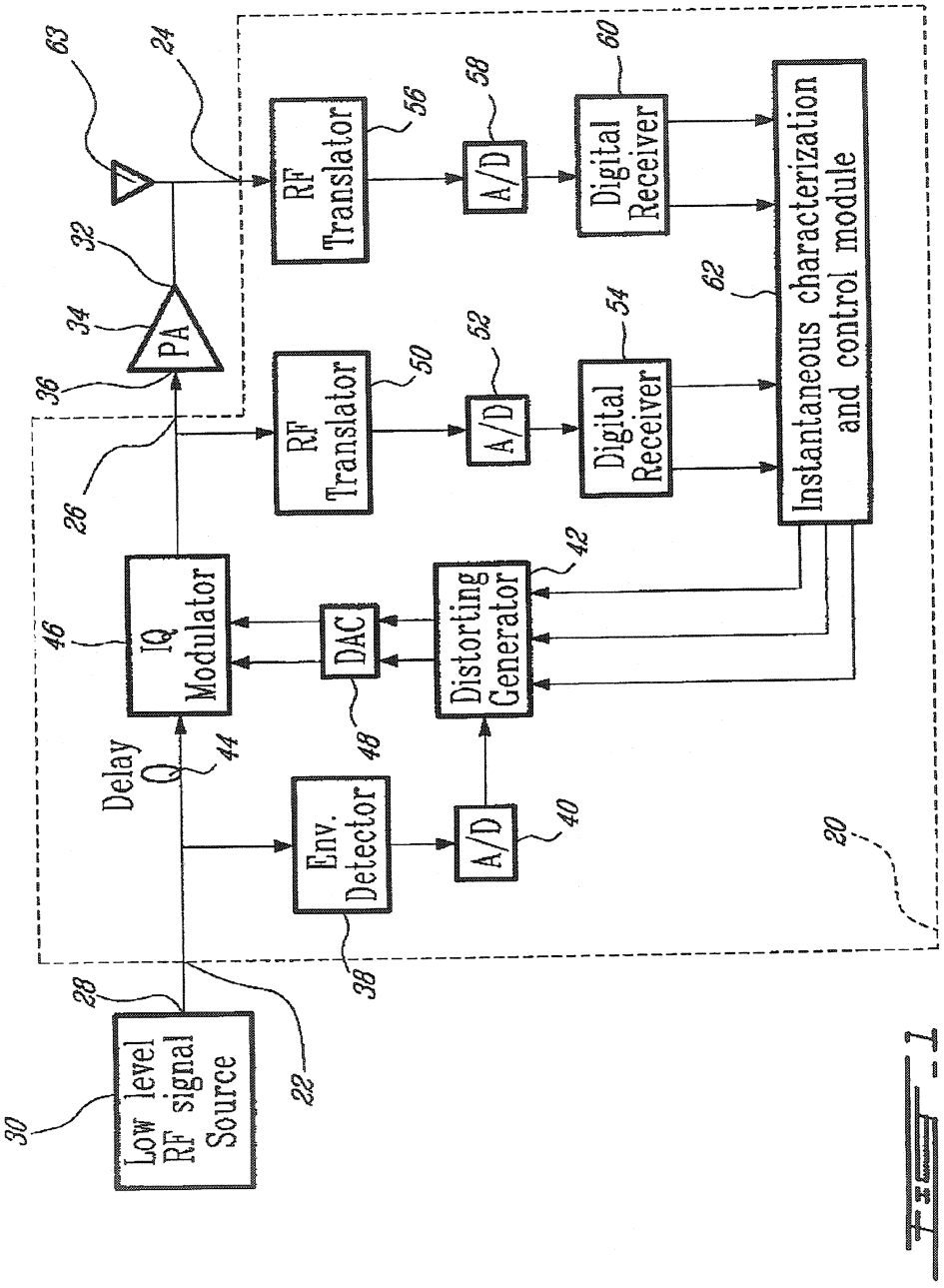

FIG - 1

160

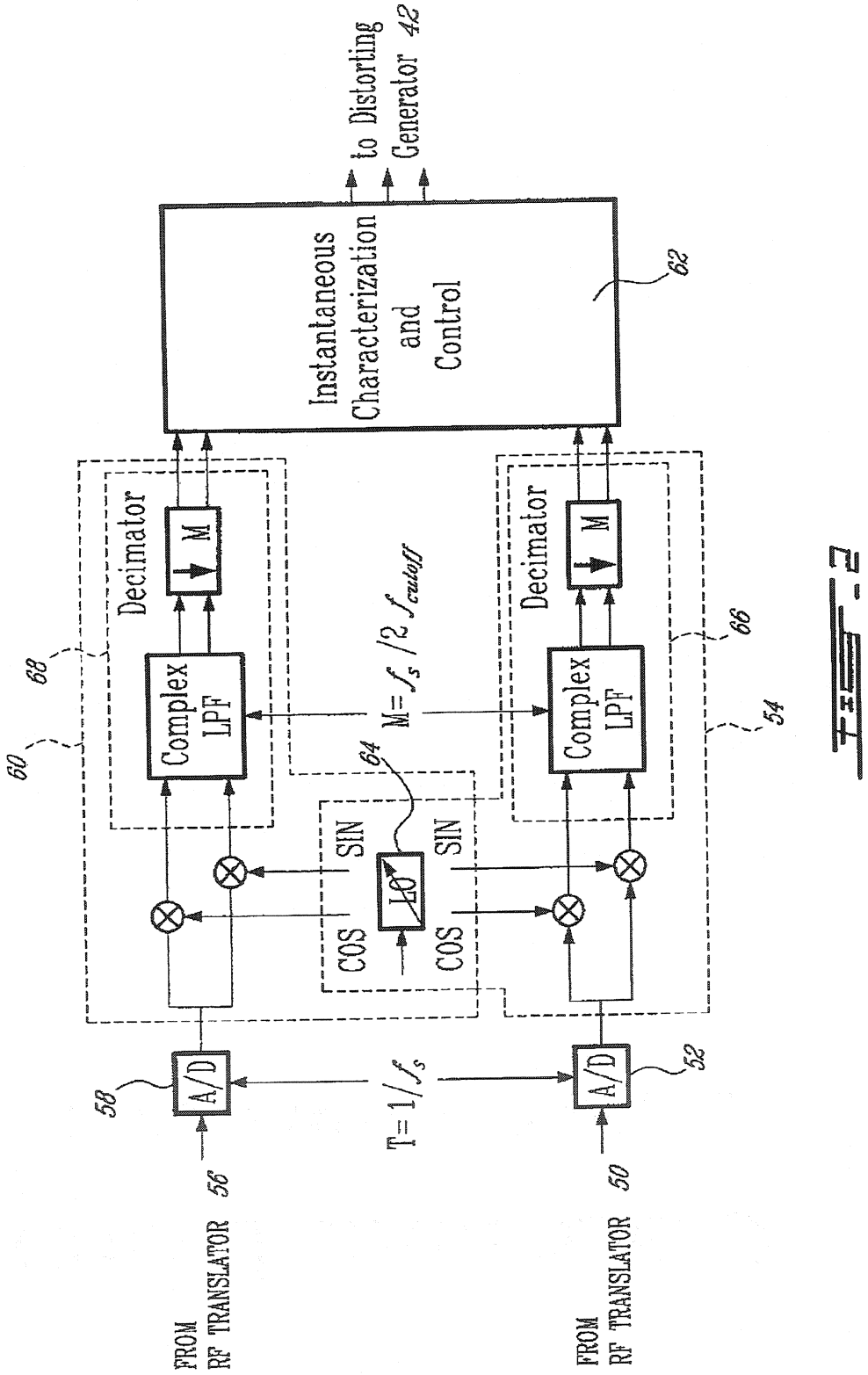

FIG - 2

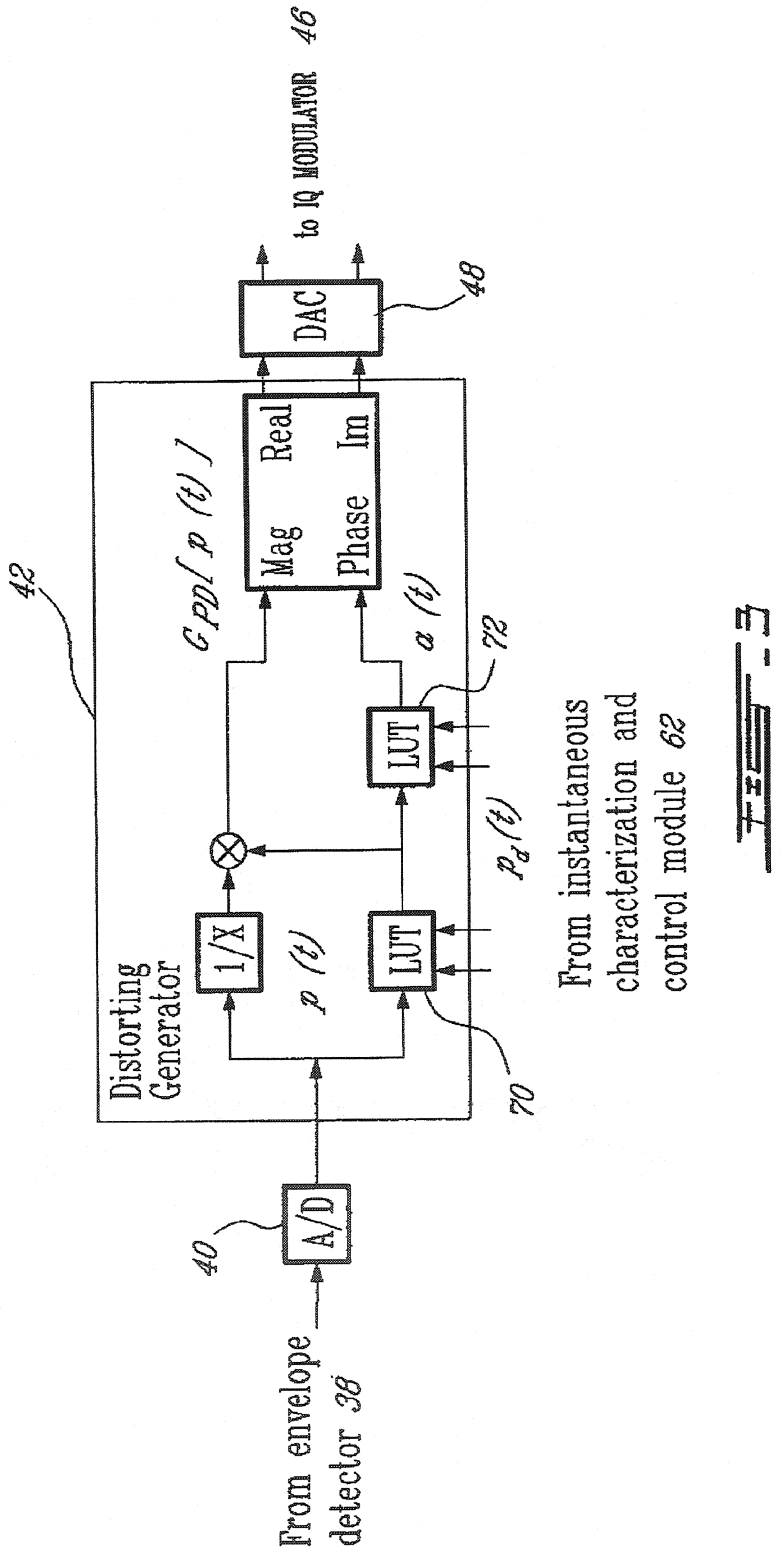

Fig. 3

162

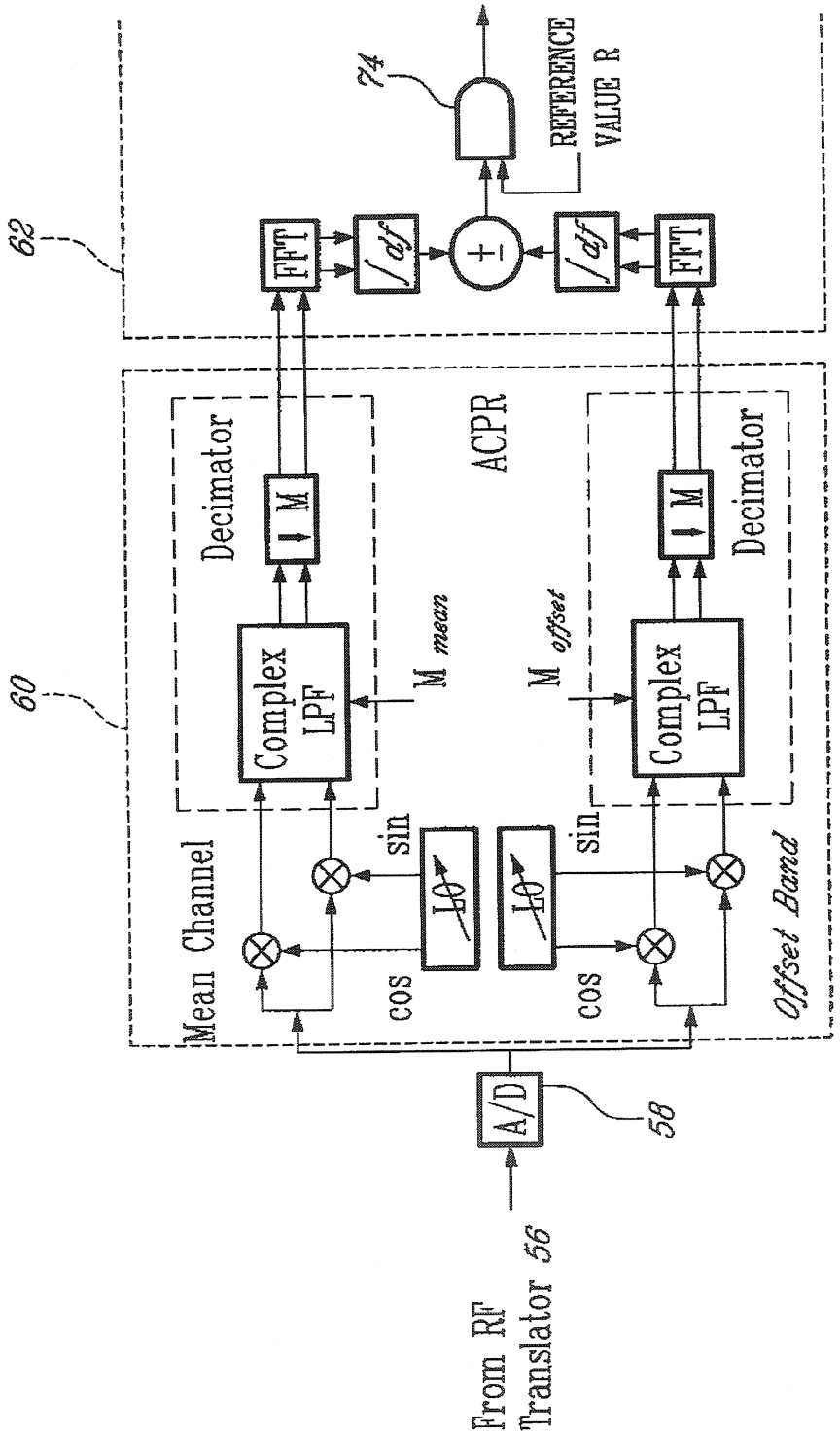

Fig. 4A

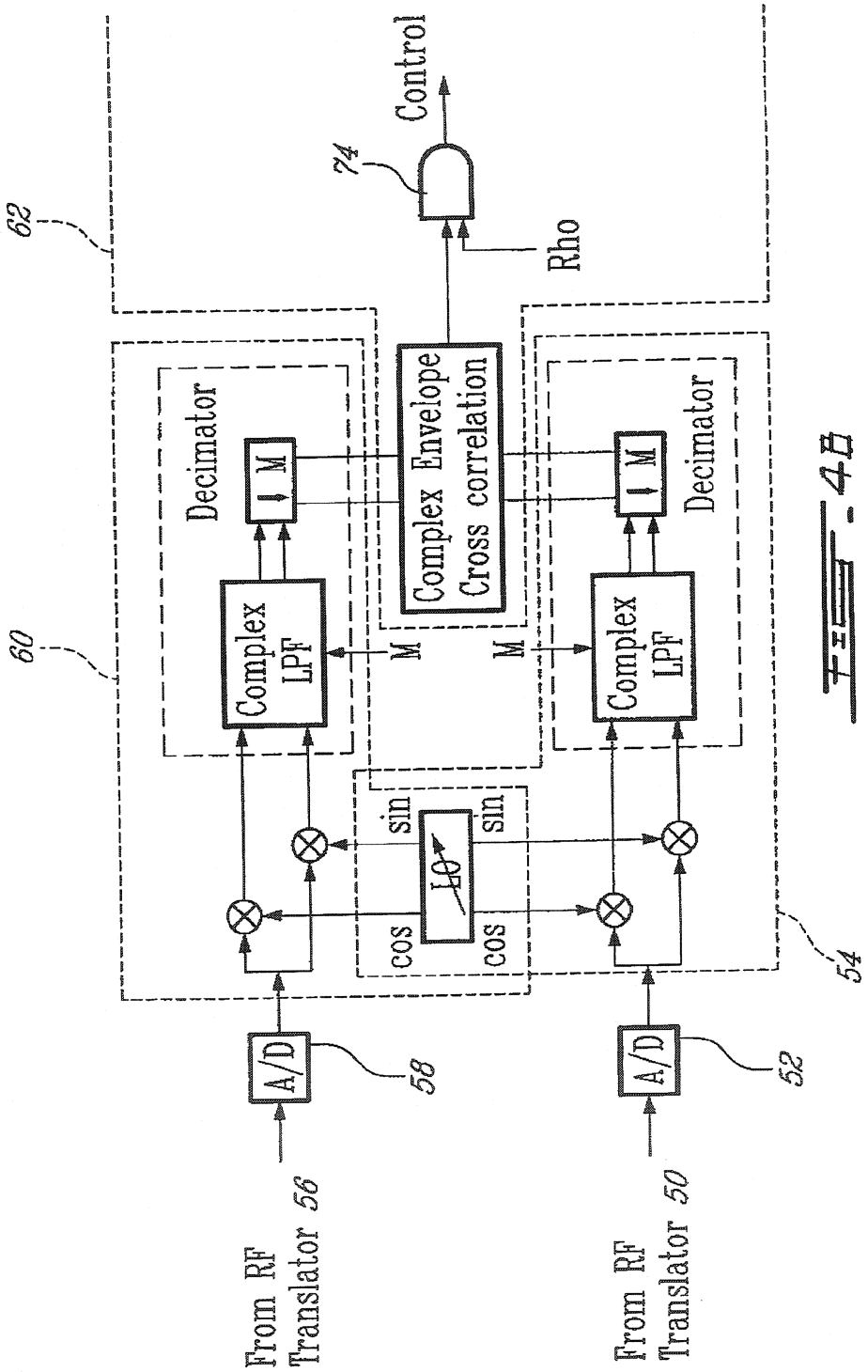
62
74
Control
Rho
Complex Envelope Cross correlation
60
Decimator
I M
Complex LPF
M
M
Complex LPF
I M
Decimator
sin
sin
LO
cos
cos
54
A/D
58
A/D
52
From RF Translator 56
From RF Translator 50

Fig. 4B

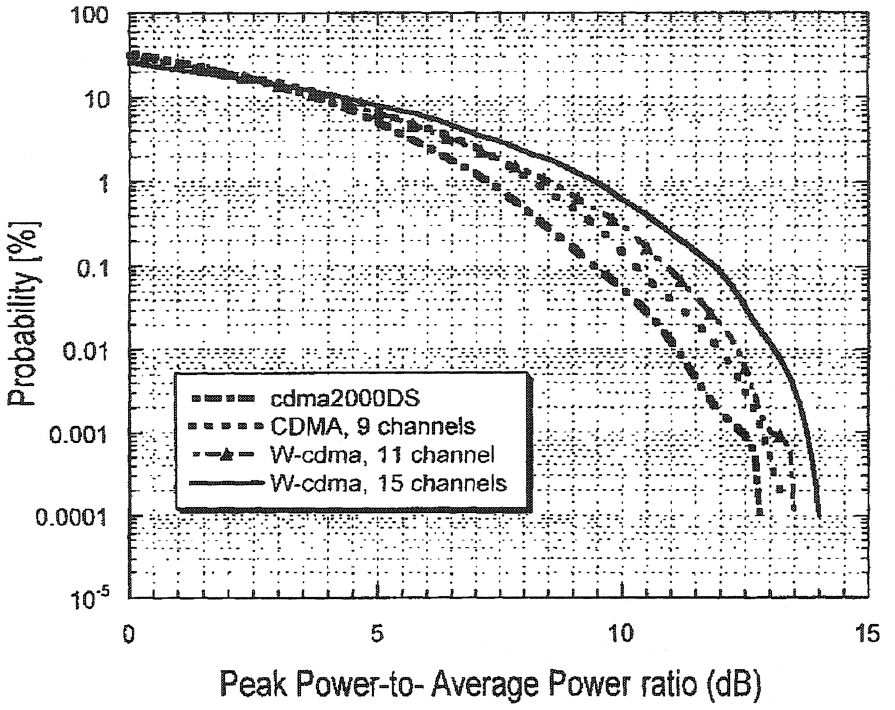

Fig_5

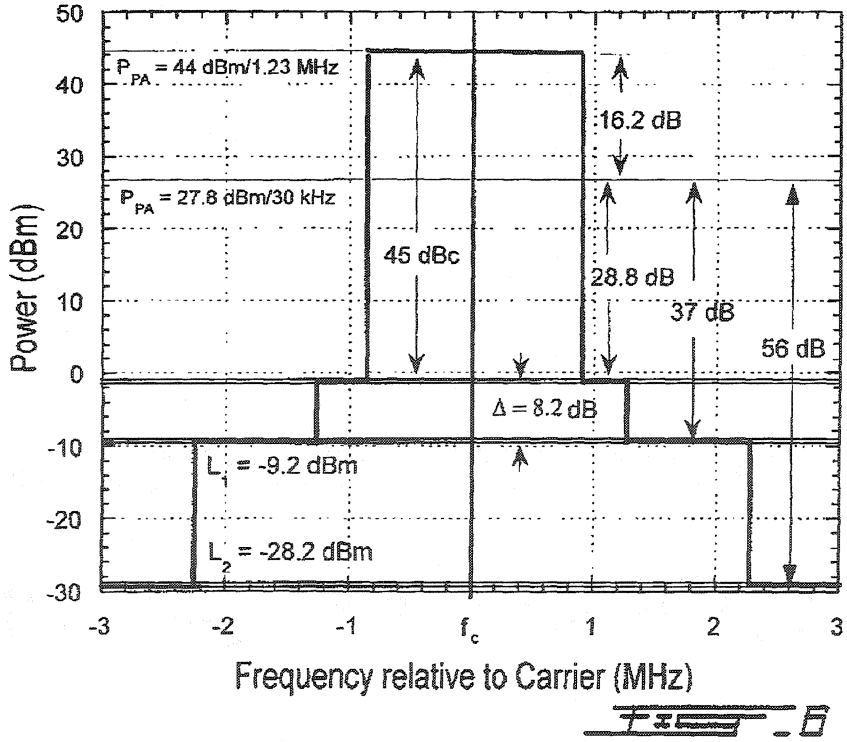

Fig_6

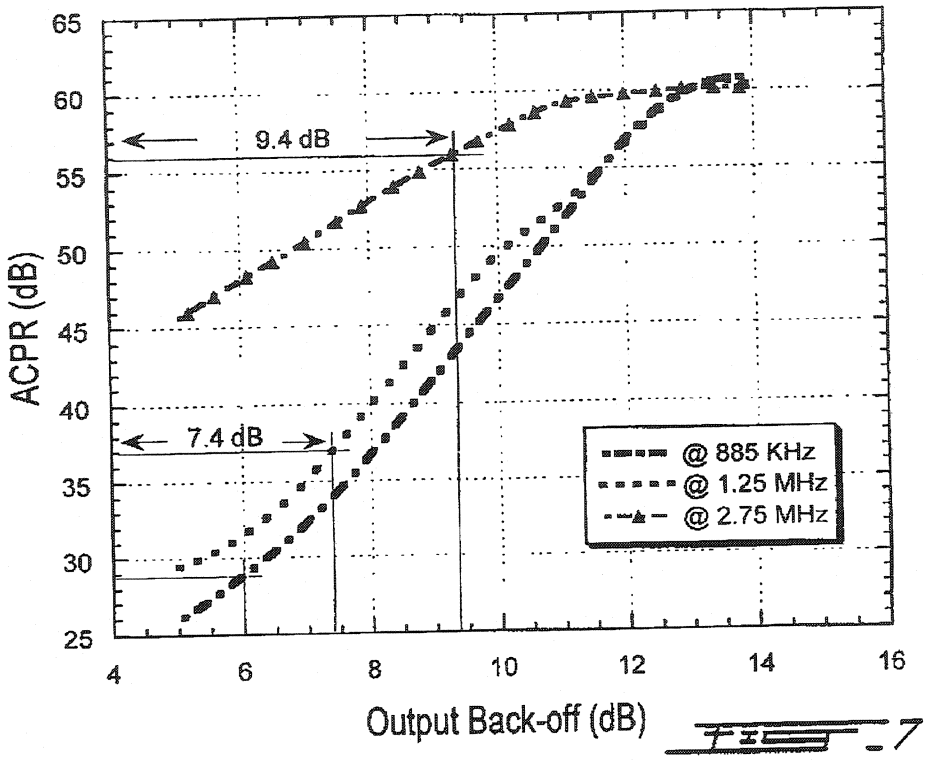

FIG. 7

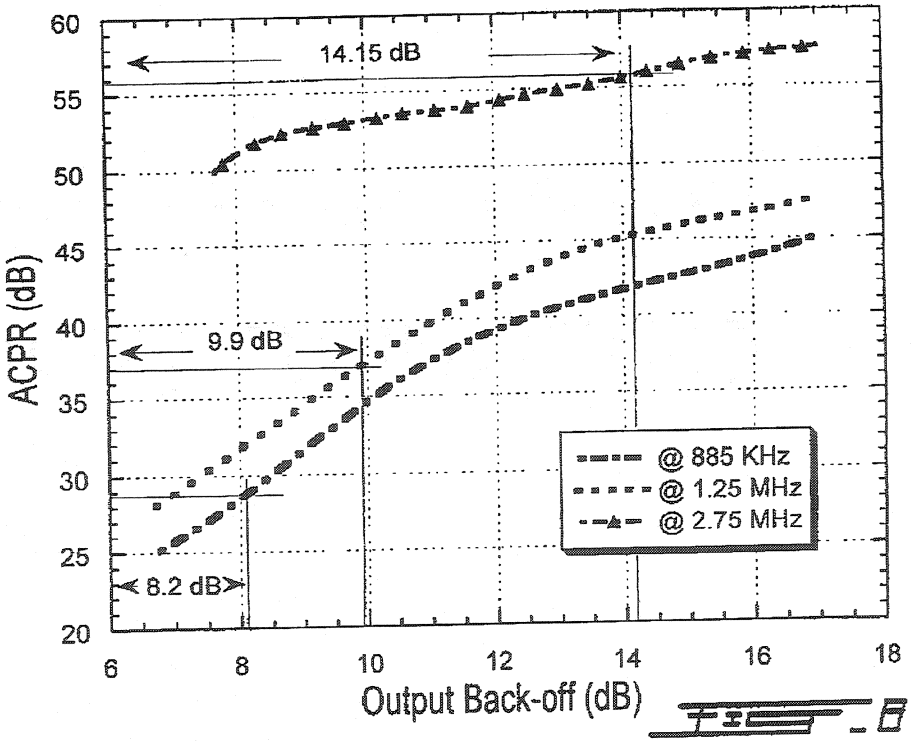

FIG. 8

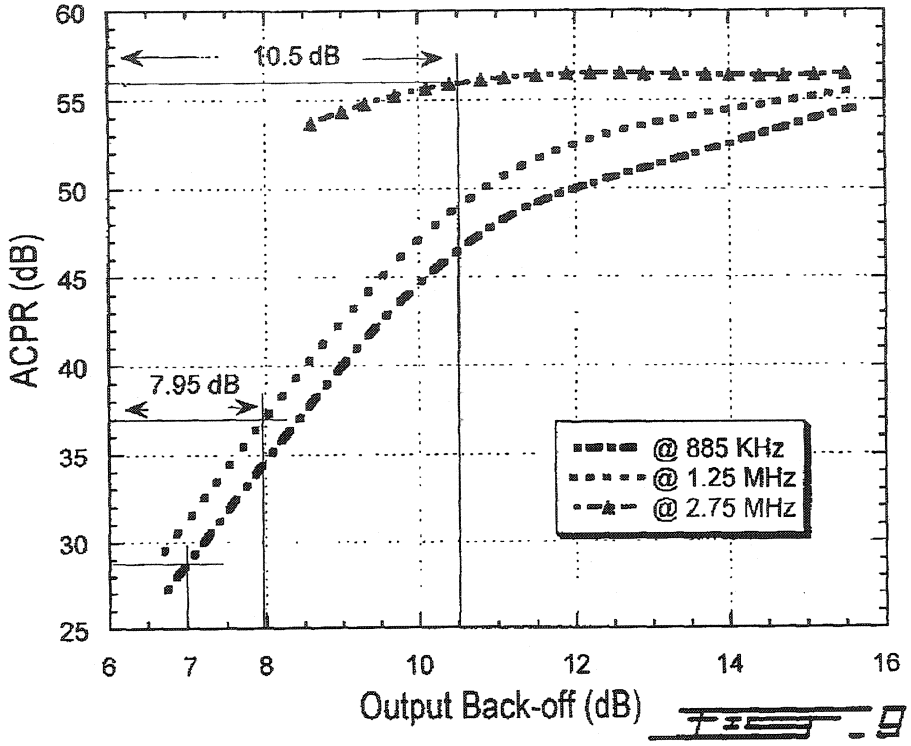

FIG. 9

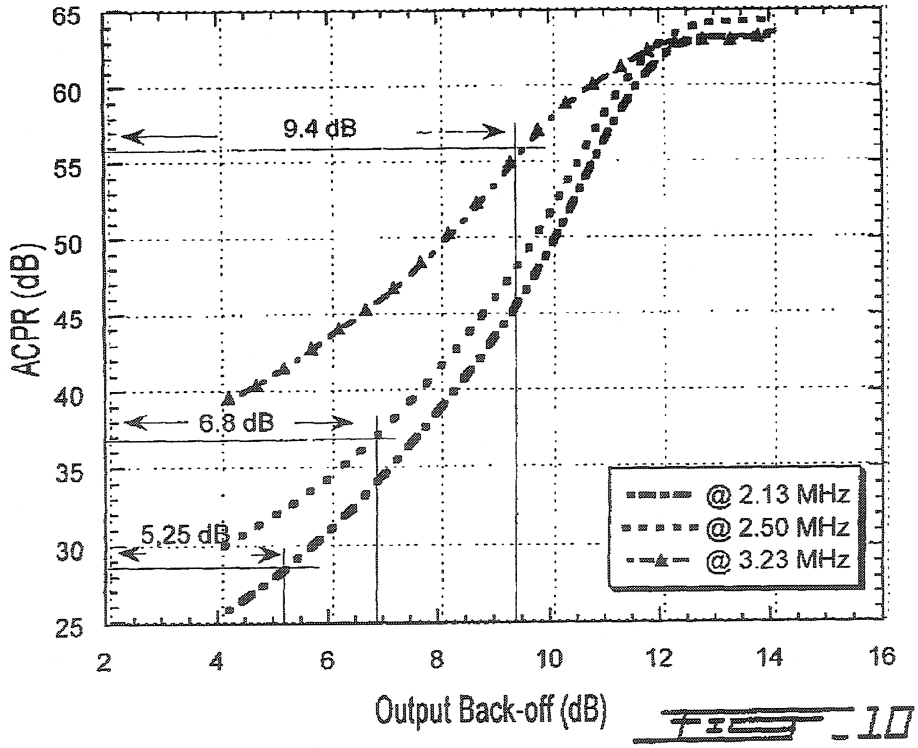

FIG. 10

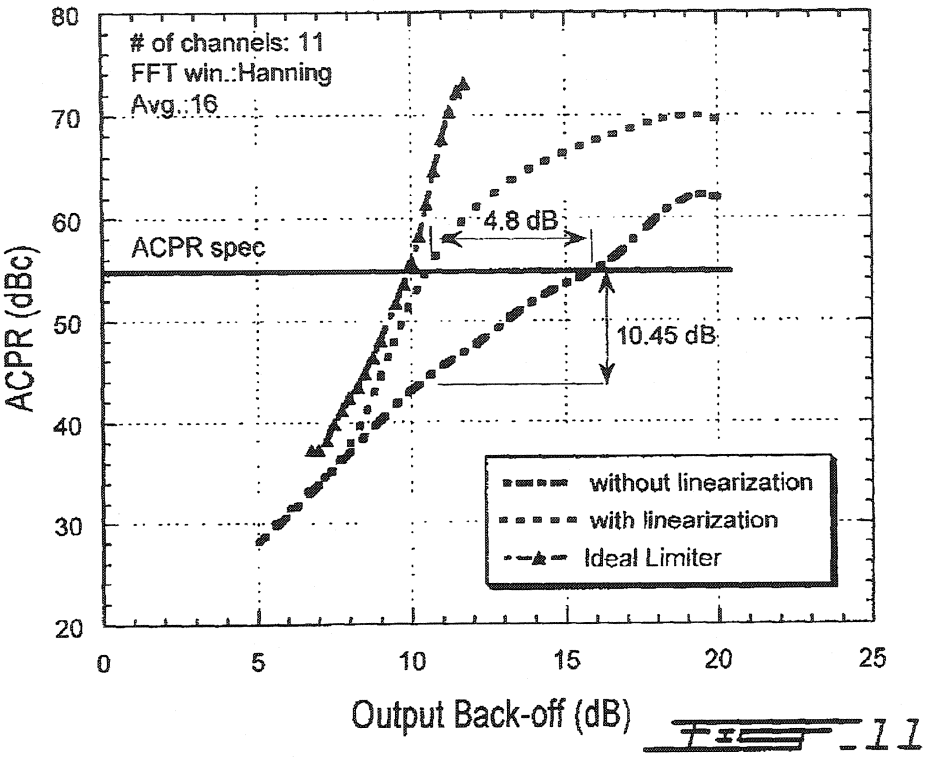

Fig. 11

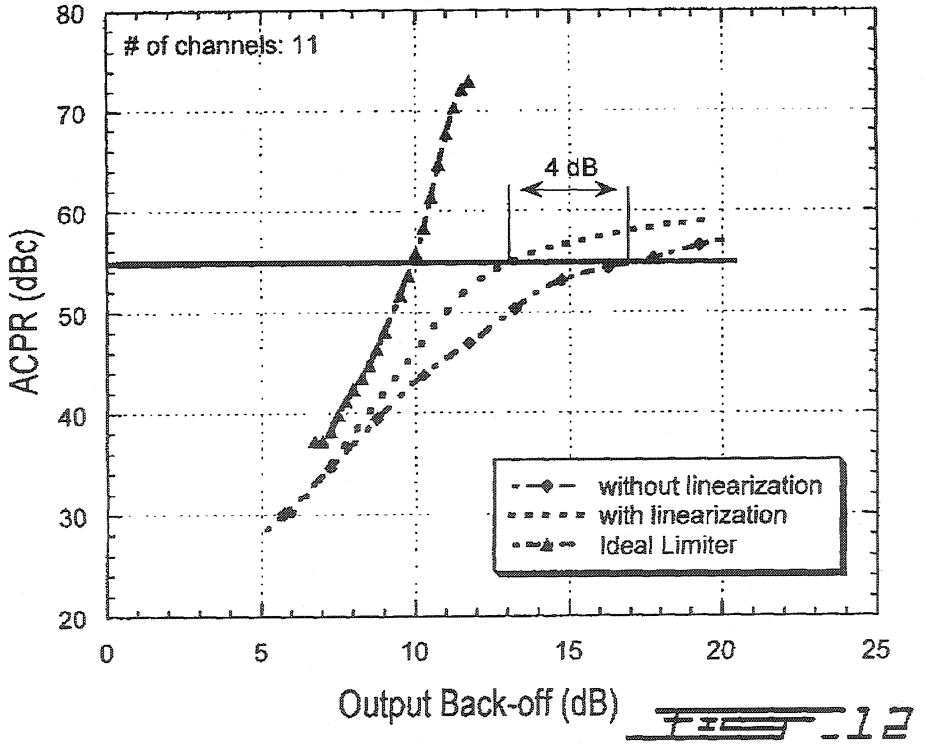

Fig. 12

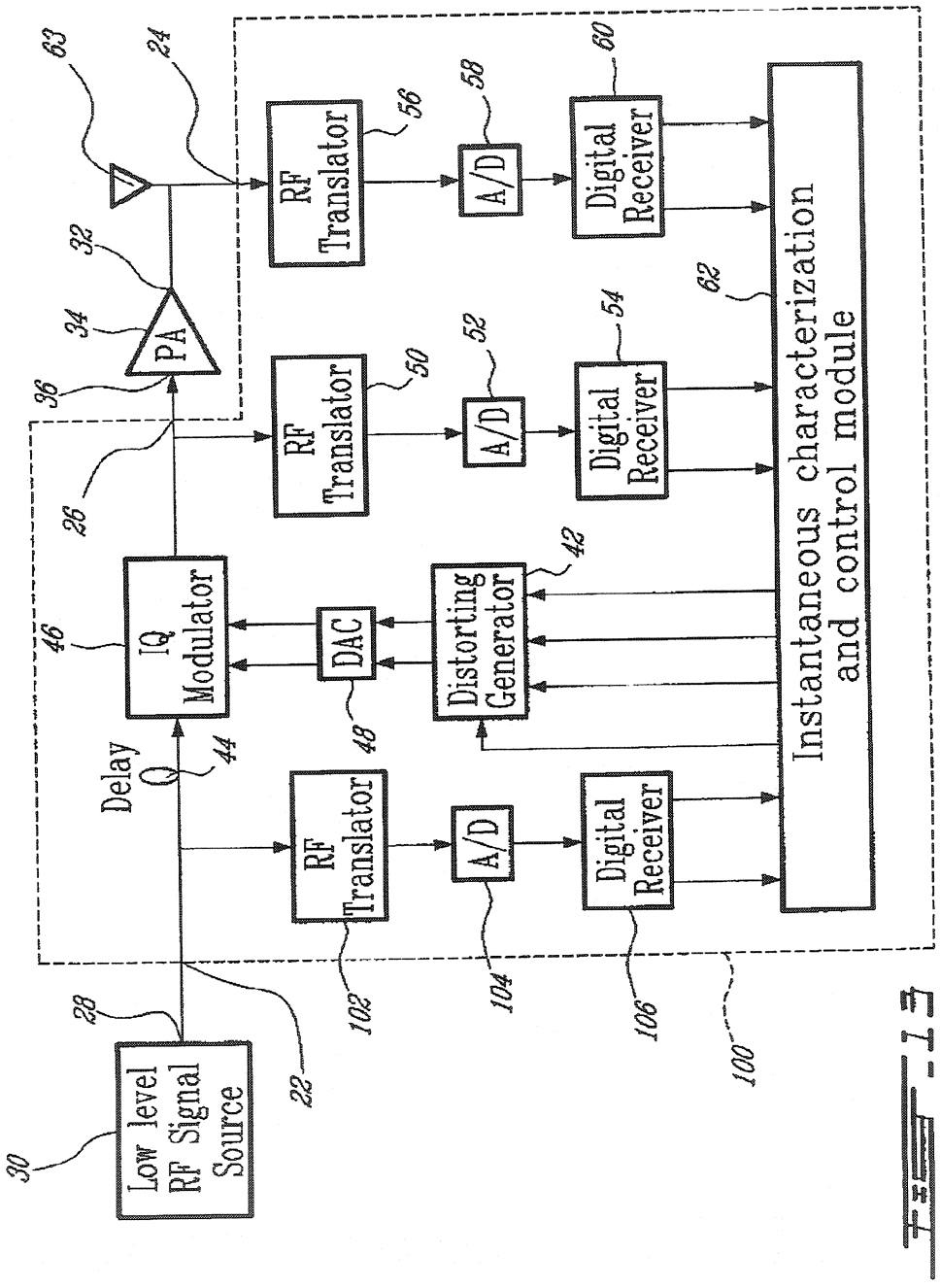

FIG. 13

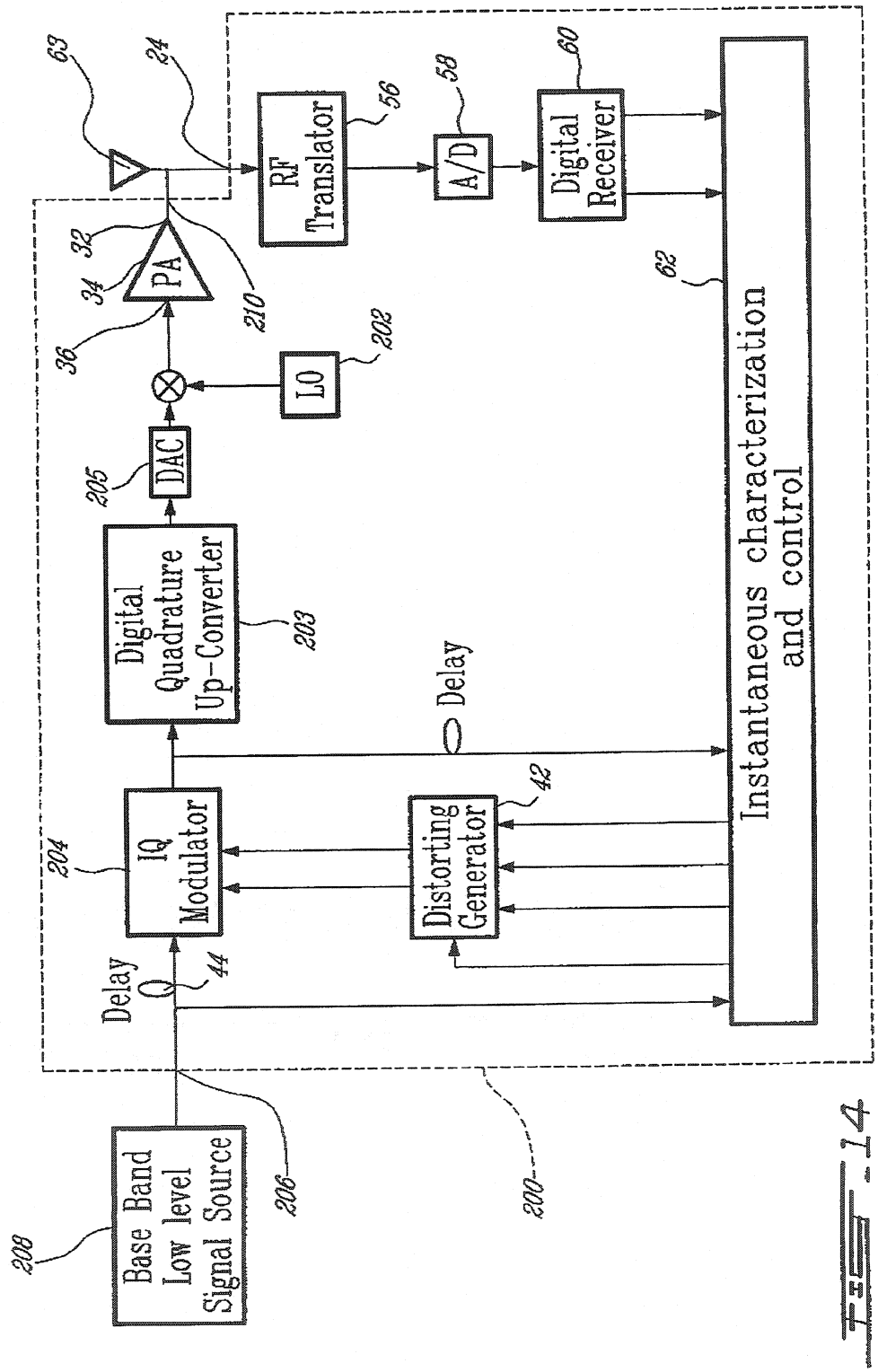

FIG. 14

ADAPTIVE PREDISTORTION DEVICE AND METHOD USING DIGITAL RECEIVER

FIELD OF THE INVENTION

[0001] The present invention relates to predistorting devices. More specifically, the present invention is concerned with a predistorting device and to a method of predistortion using digital receivers.

BACKGROUND OF THE INVENTION

[0002] The demand for developing ultra-linear microwave transmitter, supporting high crest factor signals, increases rapidly, for example by the definition of the third generation (hereinafter "3G") of mobile radio standards.

[0003] The demanding adjacent channel power ratio (hereinafter "ACPR") requirements of these systems, i.e., W-CDMA or cdma2000, present a critical issue for transmitter designers if both ultra-linearity and high power efficiency must be met. In fact, the degradation of linearity becomes significant as the power amplifier (hereinafter "PA") operates close to saturation where both high power efficiency and high output power emission are achieved. Therefore, for different stimulus levels driving the amplifiers and for a given ACPR specification, the trade-off between power efficiency and linearity impose an operating point with poor power efficiency. In this case, linearization techniques become the only possible way to recuperate the linearity and to allow optimal trade-off.

[0004] Various linearization methods have been reported and are derived, by any measure, from three main types named:

[0005] Feed-forward (R. Meyer, R. Eschenbach and W. Edgerley, Jr. "A wide-Band Feedforward Amplifier", IEEE J. of Solid-State Circuits, vol. sc-9, no. 6, pp. 442-428, December 1974), which includes an open loop configuration, can handle a multicarrier signal but can not easily be controlled against the effects of drift. Moreover, their low power efficiency make it suitable in base station only. A good analysis of adaptation behavior has been presented in J. Cavers, "Adaptation Behavior of a Feedforward Amplifier Linearizer", IEEE Transactions on Vehicular Technology, vol. 44, no. 1, pp. 31-40, February 1995;

[0006] Feedback (A. Bateman & D. Haines, "Direct Conversion Transceiver Design for Compact Low-Cost Portable Mobile Radio Terminals" IEEE Conf. pp. 57-58, 1989), which presents an excellent reduction of out-of-band emissions, is relatively easy to implement. However, stability requirement limits its bandwidth because of its critical dependence on the loop delay; and

[0007] Predistortion (N. Imai, T. Nojima and T. Murase, "Novel Linearizer Using Balanced Circulators and Its Application to Multilevel Digital Radio Systems", IEEE Transactions on Microwave Theory and Techniques, vol. 37, no. 8, pp. 1237-1243, August 1989), this technique has historically been the most common method in analog implementation. This method uses a nonlinear element which precedes the device to be compensated, its gain-expansion characteristic cancels the gain compression of the amplifier. Like feed-forward, it has an open loop configuration and therefore is very sensitive to drifts.

[0008] The predistortion technique has historically been the most common method in analog implementation. Now, this technique is well suited to digital implementation, for example by integrating a DSP chip to handle high-speed arithmetic. In this way, important experimental results have been presented in the following papers, demonstrating the capability in reducing the spectral spreading and how adaptive correction for drift, aging and temperature variation can be achieved using DSP circuits.

[0009] [1] Y. Nagata, "Linear Amplification Technique for Digital Mobil", in Proc. IEEE Veh. Technol. conf., San Francisco, Calif., 1989, pp. 159-164.

[0010] [2] M. Faulkner, T. Mattsson and W. Yates, "Adaptive Linearization Using Predistortion" in Proc. 40th IEEE Veh. Technol. Conf. 1990. pp. 35-40.

[0011] [3] A. S. Wright and Willem G. Durtled, "Experimental Performance of an Adaptive Digital Linearized Power Amplifiers", IEEE Transactions on Vehicular Technology, vol. 41, no 4, pp. 395-400, November 1992.

[0012] [4] J. Cavers, "Amplifier Linearization Using a Digital predistorter with Fast Adaptation and Low Memory Requirement", IEEE Transaction on Vehicular Technology, vol. 39, no 4, pp. 374-382, November 1990.

[0013] [5] E. G. Jeckeln, F. M. Ghannouchi and Mohamad Sawan, "Adaptive Digital Predistorter for Power Amplifiers with Real Time Modeling of Memoryless Complex Gains", IEEE MTT-S 1996 International Microwave Symposium, San Francisco, Calif., June 1996.

[0014] Although the above-mentioned technique is powerful due to its digital operating principles, it presents certain inflexibility in the sense that; it is suitable only when the baseboard signal is acceded directly before the up-conversion. In most cases, linearizer designers have no access to baseband signal; hence, they found themselves confined to use traditional Radio-frequency (hereinafter "RF") analog predistortion techniques. In this case, it is more difficult to meet severe ACPR for a high crest factor's signals specifications while operating not in far back-off regions.

[0015] The RF-based predistorter proposed by Stapelton et al. (S. P. Stapelton and F. C. Cotescu, "An Adaptative Predistorter for a Power Amplifier Based on Adjacent Channel Emissions", IEEE Transactions of Vehicular Technology, vol. 41, no 1, pp 49-56, February 1992) offers an interesting alternative. It includes a complex gain tuning circuit that controls the amplitude and phase of the RF signal. The baseband environment is confined to optimize two nonlinear work functions by monitoring the ACP-minimization (Adjacent Channel Power) measured by a power detector. Drawbacks of this method are its slow convergence toward the minimum and its sensitivity to the measurement noise.

OBJECTS OF THE INVENTION

[0016] An object of the present invention is therefore to provide an improved predistortion device and method.

SUMMARY OF THE INVENTION

[0017] More specifically, in accordance with the present invention, there is provided an adaptive method for predistorting a signal to be transmitted, supplied by a signal source to an input of a power amplifier having an output for delivering an amplified output signal, said method comprising the steps of:

[0018] predistorting the signal to be transmitted by means of predistortion amplitude and phase look-up tables interposed between the signal source and the input of the power amplifier;

[0019] producing, via a first digital receiver, a first feedback signal in response to the predistorted signal;

[0020] producing, via a second digital receiver, a second feedback signal in response to the amplified output signal from the power amplifier;

[0021] modeling the power amplifier in response to the first and second feedback signals; and

[0022] updating the predistortion amplitude and phase look-up table means in response to said modeling of the power amplifier.

[0023] According to a second aspect of the present invention, there is provided an adaptive device for predistorting a signal to be transmitted, supplied by a signal source to an input of a power amplifier having an output for delivering an amplified output signal, said adaptive device comprising:

[0024] a complex gain adjuster interposed between the signal source and the input of the power amplifier;

[0025] distorting generator including predistortion amplitude and phase look-up table; said distorting generator being so configured as to control said complex gain adjuster to predistort the signal to be transmitted in amplitude and in phase;

[0026] a first digital receiver producing a first feedback signal in response to the predistorted signal from said complex gain adjuster;

[0027] a second digital receiver producing a second feedback signal in response to the amplified output signal from the power amplifier;

[0028] a control module receiving said first and second feedback signals from said first and second digital receivers; said control module being so configured as to model the power amplifier in response to the first and second feedback signals and to update said amplitude and phase look-up table of said distortion generator in response to said modeling of the power amplifier.

[0029] According to a third aspect of the present invention, there is provided a transmitter system for amplifying and up-converting a baseband signal from a signal source; said transmitter system comprising:

[0030] a power amplifier having a signal input and an amplified signal output;

[0031] a complex gain adjuster interposed between the signal source and said signal input;

[0032] distorting generator including predistortion amplitude and phase look-up table; said distorting generator being so configured as to control said complex gain adjuster to predistort the baseband signal in amplitude and in phase;

[0033] an up-converter receiving said predistorted baseband signal; said up-converter being so configured as to supply an up-converted predistorted signal to said signal input of said power amplifier;

[0034] a first digital receiver producing a first feedback signal in response to the predistorted baseband signal;

[0035] a second digital receiver producing a second feedback signal in response to the up-converted amplified output signal from said amplified signal output;

[0036] a control module receiving said first and second feedback signals from said first and second digital receivers; said control module being so configured as to model said power amplifier in response to the first and second feedback signals and to update said amplitude and phase look-up table of said distorting generator in response to said modeling of said power amplifier.

[0037] According to a final aspect of the present invention, there is provided an adaptive device for predistorting a signal to be transmitted, supplied by a signal source to an input of a power amplifier having an output for delivering an amplified output signal, comprising:

[0038] predistorter means comprising predistortion amplitude and phase look-up table means interposed between the signal source and the input of the power amplifier for amplitude and phase predistorting the signal to be transmitted;

[0039] digital receiver means for producing a first feedback signal in response to the predistorted signal from the predistorter means;

[0040] digital receiver means for producing a second feedback signal in response to the amplified output signal from the power amplifier;

[0041] means for modeling the power amplifier in response to the first and second feedback signals; and

[0042] means for updating the predistortion amplitude and phase look-up table means in response to said modeling of the power amplifier.

[0043] Other objects, advantages and features of the present invention will become more apparent upon reading of the following non-restrictive description of preferred embodiments thereof, given by way of example only with reference to the accompanying drawings.

BRIEF DESCRIPTION OF THE DRAWINGS

[0044] In the appended drawings:

[0045] **FIG. 1** is a general block diagram of a predistortion device according to a first embodiment of the present inveniton;

[0046] **FIG. 2** is a block diagram illustrating the algorithm the PA characterization made via the digital receivers of the predistortion device of **FIG. 1**;

[0047] **FIG. 3** is a block diagram of the distorting generator of the predistortion device of **FIG. 1**;

[0048] **FIG. 4A** is a block diagram illustrating the algorithm to process the ACPR for the PA output signal;

[0049] **FIG. 4B** is a block diagram similar to **FIG. 4A** illustrating an alternate algorithm to process the distortion evaluation for the PA output signal, by using a complex envelope cross correlation function;

[0050] **FIG. 5** is a graphic illustrating CCDF plots of different CDMA signals;

[0051] **FIG. 6** is a graphic illustrating the 30 kHz normalized requirement for 44 dBm PA;

[0052] **FIG. 7** is a graphic illustrating a simulation of ACPR vs OBO of the ideal limiter under the stimulus of nine channels CDMA standard signal;

[0053] **FIG. 8** is a graphic illustrating a simulation of ACPR vs OBO of a 40 dBm PA under the stimulus of a W-CDMA standard signal;

[0054] **FIG. 9** is a graphic illustrating a simulation of ACPR vs OBO of a linearized 44 dBm PA under the stimulus of nine channels CDMA standard signal;

[0055] **FIG. 10** is a graphic illustrating a simulation of ACPR vs OBO of the ideal limiter under the stimulus of a cdma2000 DS signal;

[0056] **FIG. 11** is a graphic illustrating a simulation of ACPR vs OBO of both the ideal limiter and a 40 dBm PA under the stimulus of a W-CDMA standard signal;

[0057] **FIG. 12** is a graphic illustrating measurements of ACPR vs OBO of both the ideal limiter and a 40 dBm PA under the stimulus of a W-CDMA signal;

[0058] **FIG. 13** is a general block diagram of a predistortion device according to a second embodiment of the present invention; and

[0059] **FIG. 14** is a general block diagram of an amplification system integrating a predistorting device according to the present invention.

DESCRIPTION OF THE PREFERRED EMBODIMENT

[0060] Generally stated, the present invention relates to an adaptive baseband/RF predistorting device, which advantageously integrates the concept of digital receiver technology into the linearization techniques, and to a method therefor. By taking advantage of the digital receiver technology to digitally translate signal from RF to baseband with very high accuracy, the predistorting device of the present invention performs the instantaneous characterization of the memoryless nonlinearity in baseband to supply a correlated predistortion function. The distortion is generated in baseband by addressing the extracted predistortion function and then, the distortion is embedded into the RF signal by dynamically adjusting the amplitude and the phase of the carrier.

[0061] Turning now to **FIG. 1** of the appended drawings, a predistorting device **20** according to a first embodiment of the present invention will be described. The predistorting device **20** has two inputs **22** and **24** and an output **26**. The first input **22** is connected to the low level RF output **28** of a low level RF signal source **30** to thereby receive an input RF signal therefrom; and the second input **24** is connected to the RF output **32** of a PA **34**. The RF output **32** delivering an amplified output RF signal. The output **26**, on the other hand, is connected to the input **36** of the PA **34**.

[0062] The RF signal from the first input **22** goes through an envelope detector **38** to provide the envelope variation thereof. This envelope is digitized by an analog to digital converter (hereinafter "A/D") **40**. The digitized envelope is used to index a distorting generator **42** as will be described hereinbelow.

[0063] The RF signal from the first input **22** also goes through a delay line **44** and then in an Quadrature modulator **46** (hereinafter referred to as an "IQ modulator") that is used as a complex gain adjuster that controls the amplitude and the phase of the RF input signal. The complex gain levels applied to the RF input signal are determined by the distorting generator **42** via a digital to analog converter (hereinafter "DAC") **48**.

[0064] Basically, the distorting generator **42** includes a lookup table for both the amplitude and the phase that are indexed by the output of the A/D converter **40** to supply the correction factor both for the amplitude and for the phase of the RF input signal to simulate a linear amplification curve of the PA **34** when the distorted RF signal is supplied to the input **36** of the PA **34**.

[0065] To determine the distortion applied to the signal by the PA **34**, the amplitude and phase of the signal supplied to its input **36** and the corresponding amplitude and phase of the amplified signal from its output **32** are compared.

[0066] To achieve this, the PA input signal is supplied to a RF translator **50** that translates the signal down to within an alias-free sampling range from DC up to 35 MHz. After this translation stage, the signal is conditioned by an A/D converter **52** into digital samples at a high rate. For example, it has been found that a 12-bit A/D converter operating at the sampling rate of 70 MHz is adequate.

[0067] The digital samples from the A/D converter **52** are supplied to a digital receiver **54**. The entire subsequence complex down converting, filtering and decimating is performed digitally by the digital receivers **54**.

[0068] The signal of the output **32** of the PA **34** follows a similar route via a RF translator **56**, an A/D converter **58** and a digital receiver **60**.

[0069] It is understood that, the complex envelope from the output **32** of the PA **34** brings the information of non-linearity when it is driven further into nonlinear operation mode. This non-linearity information can be discriminated when this complex envelope is referenced to the complex envelope from the input **36** of the PA **34**. Therefore, the instantaneous characterization (i.e., AM-AM and AM-

PM curves) can be performed following both complex envelopes variation during a real work condition. It allows an instantaneous characterization and control module **62**, which is supplied with a first feedback signal in the form of both curves from the digital receiver **54** and a second feedback signal in the form of both curves from the digital receiver **60**; to correlate the predistortion function of the PA **34** in real time. As will be further described hereinbelow with reference to **FIGS. 4A and 4B**, when necessary, the instantaneous characterization and control module **62** updates the amplitude and phase lookup tables of the distorting generator **42** to ensure that the IQ modulator **46** correctly distort the RF signal so that the amplified signal supplied to the antenna **63** corresponds to the low level RF signal entering the input **22** of the predistorting device **20**. Of course, as will easily be understood by one skilled in the art, the instantaneous characterization and control module **62** applies an adequate delay between the curves supplied by the digital receiver **54** and the digital receiver **60** to compensate for the delay introduced by the PA **34**. This delay may be determined by a cross-correlation function.

[**0070**] Instantaneous Characterization Algorithms

[**0071**] In terms of algorithms, the translation and filtering process are the two major signals processing operations performed by the digital receivers **54** and **60**.

[**0072**] First, a single-sideband complex translation is accomplished by mixing the real signal with the complex output of a digital quadrature local oscillator **64** (hereinafter "LO"), as shown in **FIG. 2**. It is to be noted that even though a single LO **64** is shown in **FIG. 2**, a different local oscillator could be used for each digital receiver.

[**0073**] Then, decimators, under the form of decimation filters **66** and **68**, condition the complex baseband signal by fixing an appropriate value of the decimation parameter M. This parameter controls the reduction of the cutoff frequency f_{cutoff} and the sampling rate f_s, as follows:

$$f_{cutoff}=f_s/2M \tag{1}$$

$$f'=f_s/M \tag{2}$$

[**0074**] Where f' is the reduced sampling rate under the effect of the decimation parameter. In a multi rate system there are two or more sampling rate that are related by the parameters M1, M2 . . . Mn]

[**0075**] Therefore, by tuning the digital frequency of the LO **64** and the M value, any signal can be selected digitally from the RF domain and put it into the baseband domain for further processing by the instantaneous characterization and control module **62**.

[**0076**] In this way, the two digital receiver output data, that represent the stimulus and response of the PA **34**, are routed through the instantaneous characterization and control module **62** to carry out the nonlinearity behavioral analysis.

[**0077**] At this point, the required sample frequency to capture the n h order intermod products of both signals is advantageously taken into consideration. Following the Nyquist criterion, the required sample frequency for a signal of RF bandwidth BW is given by:

$$f'=n\cdot BW \tag{3}$$

[**0078**] Note that the sampling rate for the real signal is twice that of the complex signal. Using the equation (2) and fixing the sampling frequency f_s, the decimator parameter M can be calculated by:

$$M=\frac{f_s}{n\cdot BW}. \tag{4}$$

[**0079**] In order to characterize the PA **34** through its input and output signals, we can assume that the PA input bandpass signal is given by:

$$v_i(t)=Re\{\rho(t)e^{j\{\omega_c t+\theta(t)\}}\} \tag{5}$$

[**0080**] where ω_c is the midband angular frequency, $\rho(t)$ is the amplitude variation and $\theta(t)$ is the phase variation. Then, the PA output bandpass signal can be represented by

$$v_{out}(t)=Re\{g[\rho(t)]e^{j\{\omega_c t+\phi[\rho(t)]+\theta(t)\}}\} \tag{6}$$

[**0081**] where $g[\rho(t)]$ and $\phi[\rho(t)]$ are two memoryless nonlinear functions that represent the instantaneous AM-AM and AM-PM curves.

[**0082**] Note that these functions are characterized in terms of the input and output bandpass complex envelopes, without including all harmonics effect, Additionally, it is understood that both bandpass complex envelopes are oversampled at the rate of f'. Following the processing path, the optimal compensator is correlated straightforward as follows:

$$\rho_d(t)=g^{-1}[\rho(t)] \tag{7}$$

$$\alpha(t)=-\phi\{g^{-1}[\rho(t)]\} \tag{8}$$

[**0083**] where, the complex envelope gain function of the predistorting device can be written as:

$$G_{PD}[\rho(t)]=\frac{\rho_d(t)}{\rho(t)}e^{j\alpha(t)} \tag{9}$$

[**0084**] Basically, the time domain functions of equation 7 and 8, characterize the amplitude predistortion transfer g^{-1} and the phase predistortion conversion ϕ in function of the input amplitude variation and the distorted amplitude variation respectively.

[**0085**] These functions are implemented in the distorting generator **42** through a mapping process using look up table technique as shown in **FIG. 3**. The mapping process is performed from the input to the output using linear interpolation and according to the number of complex sampled pairs acquired from the instantaneous characterization and control module **62**.

[**0086**] It is to be noted that the tables **70** and **72** are configured in polar representation and they are accessed in cascade form at a sampling rate f' adequate to generate the highest order distortion of interest (see E. G. Jeckeln, F. M. Ghannouchi and M. Sawan, "Non Iterative Adaptative Digital Predistortion Technique for Power Amplifiers Linearization", U.S. Pat. No 6,072,364, Jun. 6, 2000). The complex converter block accomplishes the reconstruction of the complex distortion gain and converts it into the Cartesian I/Q waveform.

[0087] As can be seen in **FIG. 4A**, in order to control the adaptation step, the system uses Adjacent Channel Power Ratio (hereinafter "ACPR") as figure of merit. In this way, taking advantage of the decimation process to perform a dramatic reduction in the signal bandwidth, the ACPR is monitored in different range of frequency by processing simultaneous real time FFT spectra. This is accomplished, once the characterization process (**FIG. 2**) is finished, by dynamically tuning both the LO frequency and the M value of the digital receivers as shown in **FIG. 4**. More specifically, the digital receiver includes a first channel tuned to the mean frequency and a second channel that is tuned to a predetermined offset frequency, The ACPR measurement includes comparing the average power at the mean channel and at the predetermined offset channel via a comparator **70** that starts the adaptation step when the measured ACPR overflow the reference value R. Notice that the system needs so many digital receiver channels as offset channel to be simultaneously monitored.

[0088] In other words, the systems calculates the ACPR between the mean channel and the different offset channels specified by the standard and, when the power at the offset channel is too high, the characterization process of the PA is done again and the look-up tables of the distorting generator are updated. In order to control the adaptation step, the system therefore uses the distortion level at the output signal as a quantifier of the transmitter performance

[0089] Turning now briefly to **FIG. 4B** of the appended drawings, another way of determining if the tables have to be updated will be presented. A cross correlation between the corrected output signal and the reference signal from branch is done. This cross correlation accounts for all distortion mechanisms between the two signals and therefore, it gives a measure of the distortion compensation level. In other words, if some of the transmitted energy does not correlate between the two signals, the uncorrelated power appears as added distortion, which amount is compared with an acceptable distortion level. A comparator C starts the adaptation step when the distortion level overflows the reference value Rho. In this way, the whole computation load is reduced more than half in comparison to the FFT algorithm process.

[0090] In all cases, signals are captured in time domain and converted to the frequency domain by applying FFT algorithm. In this process, the control of trade-off between leakage and loss of frequency resolution is performed by windowing a finite number of signal samples x(n) by Hanning window function w(n) as follow:

$$x_w(n)=x(n)w(n).\ 0\leq n\leq L-1 \tag{10}$$

[0091] where L is the window length that represent the quantity of captured signal samples. The real time FFT spectra is governed by the required sample rate f' in each channel and the required frequency resolution Δf that are related by the number of sample points N as:

$$N=\frac{f'}{\Delta f} \tag{11}$$

[0092] In other words, N is the FFT length and it is used to control the density of equally spaced frequency-sampling points represented by:

$$f_k=\frac{k}{N},\ 0\leq k\leq N-1 \tag{12}$$

[0093] where k is an integer, thus, the frequency domain is determined via the following expression using FFT algorithms:

$$X(k)=\sum_{0}^{L-1}x_w(n)e^{-j\frac{2\pi}{N}kn}\quad 0\leq k\leq N-1 \tag{13}$$

[0094] and the total power in a specified channel is computed by:

$$P_{channel}(\text{dBm})=10\log\left[\left(\frac{NBW}{BW_{Noise}}\right)\left(\frac{C}{N}\right)\sum_{k=0}^{N-1}|X(k)|^2\right] \tag{14}$$

[0095] where c is a factor that considers the 1 mW reference power and the independance condition, NBW is the normalization bandwidth and BW_{noise} is the noise equivalent bandwidth. The ACPR is performed between in-band and out-of-band power spectral densities at specified offset channels as follow:

$$ACPR(dB)=P_{offset}(dB)-P_{mean}(dB) \tag{15}$$

Evaluation Condition

[0096] Stimulus Conditions

[0097] In order to evaluate the performance, the system is exposed under different stimulus conditions that allow it to be characterized in term of efficiency and distortion. In this way, CDMA, W-CDMA and cdma2000 standard signals are implemented under simulation to apply different stress level characterized by theirs complementary cumulative distribution function (hereinafter "CCDF").

[0098] As known, these standards signal exhibit different levels of the instantaneous signal amplitudes representing a widely varying envelope that drives the system following a random property. Usually, a set of these level values are referenced to the root-mean-square (hereinafter "RMS") value of the signal giving a set of peak voltage-to-RMS voltage ratio values that allows characterizing a time waveform into the statistical domain, This capability is represented by the CCDF function and it becomes a common tool to represent the stress degree that a stimulating signal can place on nonlinear system. In this function, the ratio values are also referred as peak power-to-average power ratio and the highest ratio value, called crest factor (hereinafter "CF"), give a measure of the dynamic range of the signal. In **FIG. 5** we can see the CCDF curves showing the statistical property of each standard signals built in simulation; in all cases, the simulator generates around 800,000 signal samples that allow attaining the 0.0001% probability value with high stability.

[0099] In the case of the CDMA signal, the statistical property reveals a peak-to-average ratio of 10.29 dB for a 0.1% of probability and the CF is 13.28 dB. This signal is simulated using a typical Walsh-code channels configuration, i.e., pilot, sync, paging, 8, 16, 24, 40, 48 and 56, and it is among the most stressful signal that satisfies the nine channel requirements of IS-97. For the W-CDMA signal, two different channel configurations including 11 and 15 code channels are simulated; the chip rate is 3.84 MHz and the shaping filter is a root cosine with a roll-off of 0.22 and using Hanning as window function. In the case of the cdma2000, the simulation is performed using a direct spread (hereinafter "DS") as air interface with a single 3.75 MHz-wide carrier and with a spreading rate of 3.6864 Mcps; the filter is three times wider than the CDMA case and the window function is Hanning. Under these simulation conditions, a comparison of the statistical properties represented by the CCDFs in **FIG. 5** reveals that for a given probability, i.e. 0.1%, each signal presents different peak factor. Therefore, each signal will drive the nonlinear system further into saturation having a different impact in terms of distortion and efficiency. It points out the effect that as the curves move further to the right, the peak-to-average value becomes higher, which makes the signals more stressful. Consequently, for an acceptable amount of distortion according to the spectrum emission mask, as the signal become more stressful the system will be conditioned to operate in higher back off with the corresponding worsening of the power efficiency. This kind of evaluation allows characterizing the system in term of efficiency and distortion and also predicting the system performance under different work conditions.

[0100] Clipping Effect and Soft Limiter

[0101] It is believed well known that a class AB power amplifier presents different types of distortion sources and not all of them can be compensated by predistortion. While distortion from the nonlinearity near both the crossover point and the saturation point can be compensated by fitting numerically a correlative predistortion function, distortion from clipping effect escapes from the cancellation capability of the predistortion technique. This limitation represents a drawback of this technique.

[0102] In order to estimate this kind of limitation and to predict the highest theoretical performance that can be reached by the predistorting device of the present invention, the performance of a soft limiter is analyzed for all stimulus condition. As known, in an ideal limiter, the phase conversion is constant over the range of the input signal and the output voltage follows exactly the input voltage up to a certain value. Above this value, the output voltage remains constant when the input voltage is further increased. Under this condition, it is evident that as the probability of instantaneous clipped peak values increases, distortion from clipping effect will increase. Consequently, this phenomenon places a rigorous limitation in the system operation point with a direct impact in the power efficiency. Again, we point out that signals having high crest factor will impose an operating point beyond a region of poor power efficiency. Backing-off the operating point will prevent that the distortion masked by the clipping effect overflow the standard requirement. Notice that the characteristic of an ideal limiter represents a perfect linearized class A power amplifier and therefore, its performance places an important reference to the degree of improvement given by a predistortion linearizer.

[0103] ACPR

[0104] For analysis purpose, the ACPR is evaluated for different operating point by computing the ratio between the in-band and the out-of-band power spectral densities at specified offset channels. In the case of the CDMA, the ACPR is evaluated in three pairs of offset channels that are normalized to the same bandwidths of 30 kHz at the offset frequencies of ±885 kHz, ±1.256 MHz, and ±2.75 MHz. The normalization factor (hereinafter "NF") is calculated by logging, the ratio between the normalization bandwidth NBW, i.e., 30 kHz, and the specified bandwidth BW, as follow:

$$NF(\text{dB}) = 10\log\left(\frac{NBW}{BW}\right) \tag{16}$$

[0105] By applying this equation to the J-STD-008 standard requirements that states that the power emissions limitation must be at least −45 dBc/30 kHz, −13 dBm/12.5 kHz and −13 dBm/1 MHz for the first second and third offset channels respectability, the NF values are: −16.2 dB=10 log(30 kHz/1.25 MHz), 3.8 dB=10 log(30 kHz/12.5 kHz) and −15.2 dB=10 log(30 kHz/1 MHz). The normalized limit values of the standard requirement become −28 dB/30 kHz, −9.2 dBm/30 kHz and −28.2 dBm/30 kHz, and the relative limit values of the power spectral densities for the three offsets are given by:

$$R_1(dB)=28.8\ dB \tag{17}$$

$$R_2(dB)=28.8\ dB+\Delta dB \tag{18}$$

$$R_3(db)=47.8\ dB+\Delta dB \tag{19}$$

[0106] where Δ is given by:

$$\Delta = \begin{cases} P_{PA}(\text{dBm}) - 35.8\ \text{dBm} & \text{for } P_{PA} \le 35.8\ \text{dBm} \\ 0 & \text{elsewhere} \end{cases}$$

[0107] In **FIG. 6** we can see a graphical representation of requirement for a typical 44 dBm PA; after normalization, the mean power become 27.8 dBm/30 kHz, A take the value 8.2 dB and the relative limit values are R_1=28.8 dB, R_2=37 dB and R_3=56 dB. Notice that the dBc unit is used when the total power contained in the mean channel is given as reference.

[0108] In the case of cdma2000 with DS as air interface, we assume the similar methodology that is applied in the CDMA case (see "performing cdma2000 measurements today", Application Note 1325, HEWLETT PACKARD). The frequency centers of the offset channel are 2.65 MHz, 3.75 MHz, and 5.94 MHz. For W-CDMA standard, the ACPR is evaluated over 3.84 MHz bandwidth at the offset frequency of 5 MHz and the limited emission power is considered at −55 dBc. For all cases, the spectrum analysis is accomplished by converting the time domain signal to frequency domain using Hanning window and with FFT length of 8192 points. The integration bandwidth (IBW)

method is used to calculate both mean channel power and offset channel powers and it is performed by applying equation (14). In addition, the simulator computes an average power for each specified integration channel bandwidth and over a specified number of data acquisitions avr=16.

Results and Discussions

[0109] The entire system is RF/DSP co-simulated using HP-ADS software for a typical 44-dBm class AB Power Amplifier. Temperature noise, quantization noise, and impairment from other components such as amplitude and phase imbalance of I/Q modulator have been taken into consideration to realistically model the system. The A/D and DAC converters are simulated having 12-bits and 14 bits resolution respectively at the high rate of 70 MHz. The digital receivers are considered as both narrowband and wideband where the M values are ranged from 2 to 2^{17}.

[0110] Simulations are performed applying the set of stimulus mentioned hereinabove in the section entitled "stimulus conditions" on the ideal limiter, on the PA and on the PA including the linearizer. Each simulation is repeated for different operating points to allow characterizing the performance in term of distortion and power efficiency. The Output Back-Off (hereinafter "OBO") referenced to Single Carrier (hereinafter "SC") saturation that represent in any measure the power efficiency, the peak power-to-average power characterized by the CCDF, the word-length of bits and the ACPR are chosen as important factors to analyze the performance for the three cases. FIGS. **7** to **10** detail the simulated results of ACPR versus OBO corresponding for the offset bands above the mean signal frequency. In all cases, the horizontal lines indicate the system specifications for ACPR where the minimum acceptable OBO are illustrated. At this point, it is important to mention that any change on the parameters values and conditions established hereinabove in the section entitled "stimulus conditions", such as roll-off, average number, window function, filters, etc., will have a direct effect on the results.

[0111] **FIG. 7** shows the effect of the CDMA signal on the ACPR of the ideal limiter; the simulation is based on 44-dBm-output power. In the three plots, corresponding to the three offset channels, we can see that the minimum acceptable OBO are 6 dB at 885 kHz, 7.4 dB at 1.25 MHz and 9.4 dB at 2.75 MHz; according to the specifications, the results reveal that the ideal limiter cannot be operated with an OBO smaller than 9.4 dB.

[0112] In **FIG. 8**, the ideal limiter is simulated under the stimulus of cdma2000 signal; in this case, the minimum acceptable OBO are 5.25 dB at 2.65 MHz, 6.8 dB at 3.75 MHz and 9.4 dB at 5.94 MHz. Like CDMA signal case, the third offset channel limits the operating point at least 9.4 dB of OBO. From a comparison, we can notice that although the CDMA signal is shown to be most stressful than the cdma2000 signal, what it is justified in the first and the second offset channels, both case show the same minimum acceptable OBO. From this analysis, the clipping effect seems to be dominant on both first and second channel and with a slight effect on the third channel. It is foreseeable because the AM-PM conversion factor, that has a significant effect in generating higher order of intermodulation, is considered constant over the range of the input signal. Additionally, in both cases, the third offset channel governs the minimum acceptable OBO.

[0113] Now, considering the situation of the PA under the stimulus of the CDMA standard signal in **FIG. 9**, it is clear that more OBO is necessary to pass the spectrum emission mask. This is because now the spectral leakage includes both the clipping effect and the continuous nonlinearity effect of the PA. In this case, the standard requirement limits the PA operating point at least 8.2 dB at 885 kHz, 9.9 dB at 1.25 MHz, and 14.15 dB at 2.75 MHz.

[0114] Again, we can see that the third offset channel governs the minimum acceptable OBO and therefore, the PA cannot be operated with an OBO smaller than 14.15 dB. As expected, we can see by comparing results from **FIGS. 7 and 9** that the PA needs 4.75 dB more in OBO than the minimum theoretical value given by the ideal limiter. On the other hand, it is the maximum amount in OBO reduction that can be theoretically achieved by predistortion for this PA.

[0115] Under linearization effect, the plots in **FIG. 10** show a minimum OBO of 7 dB at 885 kHz, 7.95 dB at 1.25 MHz and 10.5 dB at 2.75 MHz prevailing the value of 10.5 dB as the minimum acceptable OBO according to the spectrum emission mask. This result shows that the predistortion action from the linearizer diminish the OBO by 3.6 dB, it means 1 dB less than the maximum reduction in OBO that can be achieved theoretically. Notice that this difference is absorbed by the impairment from other components considered in the simulation.

[0116] The last set of simulation is performed for the same PA under W-CDMA standard signal including 11 channels as was described in section III-A.

[0117] **FIG. 11** shows the ACPR simulation of the PA with and without linearization and including the ACPR plot of the ideal limiter, The plots reveal a reduction of 4.8 dB resulting a minimum acceptable OBO of 10.6 dB.

[0118] To estimate the performance of the linearizer under realistic condition, experimental results have been carried out in open loop condition for a 20 W class AB power amplifier operating at 1.96 GHz. In this case, the AM-AM and AM-PM transfer characteristics of the PA were measured by instantaneous characterization using a peak power analyzer for the first one, and a conventional measurement by network analyzer for the second one. Data from these measurements were used into the simulator to generate a long string of predistorted samples for W-CDMA standards signal including 11 channels. Then, these predistorted signals were fed into an arbitrary waveform generator to generate and supply a realistic predistorted signal to the PA.

[0119] **FIG. 12** shows the ACPR measurements of the PA with and without linearization; in addition, the ACPR simulation of the ideal limiter is included by aims of comparison. We can observe that the PA must be operated at least 17 dB OBO to meet the standard requirement, 1 dB more than the simulation result. Under linearization effect, the minimum acceptable OBO becomes about 13 dB allowing moving the operating point 4 dB toward the saturation region and giving an ACPR improvement of 5 dB. Notice that the lowest theoretical OBO performed by the ideal limiter is reached at 10 dB and still an improvement of 3 dB more in OBO reduction can be theoretically achieved. It means that the dynamic action of the adaptation step of the predistortion function and the instantaneous characterization which are supported by the digital receivers and the DSP environment,

have an acceptable amount of room to improve the OBO reduction given under open loop condition. These results help us to predict the performance for the whole system with a minimum acceptable OBO of around 11 dB and with a predictable improvement of 6 dB in OBO reduction.

[0120] In summary, the improvement in OBO reduction is significant in the sense that in all cases the output power can be at least doubled with a resulting increase in power efficiency. It means that for the same linear output power, the OBO reduction allows the reduction of the absolute power rating of the PA. On the other hand, the improvement in OBO reduction is significant, i.e. around 5 dB.

[0121] Turning now to **FIG. 13** of the appended drawings, a predistorting device **100** according to a second embodiment of the present invention will be described. It is to be noted that the same reference numeral are used to refer to the same elements. It is also to be noted that the predistorting device **100** is very similar to the predistorting device **20** and therefore, for concision purposes, only the difference therebetween will be discussed hereinbelow.

[0122] Basically, the envelope detector **38** and the A/D converter **40** used to index the distorting generator **42** of the predistorting device **20** have been replaced by a third RF translator **102**, A/D converter **104** and third digital receiver **106** route. The output of the digital receiver **106** is supplied to the instantaneous characterization and control module **62** which is used to index the distorting generator **42** as previously discussed. The other elements and the operation of the predistorting device **100** are identical to the predistorting device **20**.

[0123] This predistorting device **100** is advantageous since the delay compensation between the delay line **44** an the digital path can be adjusted by software. In addition, this configuration gives the phase information of the input signal.

[0124] Finally, **FIG. 14** schematically illustrates a transmitter system **200** integrating a predistorting device similar to the predistorting device **100** of **FIG. 13**.

[0125] Since the signal is up-converted inside the transmitter system **200** by the combination of a local oscillator **202**, a digital Quadrature Up-converter **203** and a DAC **205**, only one RF translator **56** is required since it is the only path where a RF signal is picked up. Furthermore, since the predistortion is performed digitally in the baseband, a digital baseband **10** modulator **204** is used. The transmitter system **200** includes a baseband low level signal input **206** to which a baseband low level signal source **208** may be connected and a RF amplified signal output **210** to which an antenna **63** may be connected.

[0126] An adaptive basedband/RF predistorting device tracking the emerging technologies evolution of digital receivers was presented. The linearizer develops the algorithm of two digital receivers to execute an instantaneous characterization of the AM-AM and AM-PM non-linearities. The digital receivers allow a direct IQ demodulation in digital form from RF to baseband. Consequently, the disturbing effect of gain and phase imbalances of a RF analogue quadrature demodulator are completely avoided by directly processing the data with very high accuracy using analytical expressions. Additionally, the system can monitor the ACPR by processing simultaneous real time FFT spectra in different range of frequencies; it is accomplished by the advantage of the decimation process to perform a dramatic reduction in the signal bandwidth, RF/DSP co-simulation and experimental results have been carried out for evaluation purpose under different signals condition. Results reveal a significant reduction in effective output power back off (OBO) for the linearized power amplifier. Finally, the fact that the system can support different standard signals by tuning the values LO, M and R by software, this technique provides an attractive design suitable for mass production.

[0127] Although the present invention has been described hereinabove by way of preferred embodiments thereof, it can be modified, without departing from the spirit and nature of the subject invention as defined in the appended claims.

What is claimed is:

1. An adaptive method for predistorting a signal to be transmitted, supplied by a signal source to an input of a power amplifier having an output for delivering an amplified output signal, said method comprising the steps of:

predistorting the signal to be transmitted by means of predistortion amplitude and phase look-up tables interposed between the signal source and the input of the power amplifier;

producing, via a first digital receiver, a first feedback signal in response to the predistorted signal;

producing, via a second digital receiver, a second feedback signal in response to the amplified output signal from the power amplifier;

modeling the power amplifier in response to the first and second feedback signals; and

updating the predistortion amplitude and phase look-up table means in response to said modeling of the power amplifier.

2. An adaptative method as recited in claim 1, wherein said first feedback signal includes the complex envelope of the predistorting signal.

3. An adaptative method as recited in claim 2, wherein said second feedback signal includes the complex envelope of the amplified output signal.

4. An adaptative method as recited in claim 3, wherein said modeling step includes the discrimination of the complex envelope of the first feedback signal referenced to the complex envelope of the second feedback signal to yield a predistortion function correlated to the behaviour of the power amplifier.

5. An adaptative method as recited in claim 4, wherein said modeling step is done in real time.

6. An adaptative method as recited in claim 1, wherein said updating step is done when an adjacent channel power ratio (ACPR) measurement sub-step indicates that the predistorting step is not adequate to meet predetermined ACPR standards.

7. An adaptative method as recited in claim 6, wherein said ACPR measurement sub-step is done via a digital receiver that includes a first channel tuned to the mean frequency and a second channel that is tuned to a predetermined offset frequency, said ACPR measurement sub-step includes comparing the average power at the means frequency and at the predetermined offset frequency.

8. An adaptive device for predistorting a signal to be transmitted, supplied by a signal source to an input of a

power amplifier having an output for delivering an amplified output signal, said adaptive device comprising:

a complex gain adjuster interposed between the signal source and the input of the power amplifier;

distorting generator including predistortion amplitude and phase look-up table; said distorting generator being so configured as to control said complex gain adjuster to predistort the signal to be transmitted in amplitude and in phase;

a first digital receiver producing a first feedback signal in response to the predistorted signal from said complex gain adjuster;

a second digital receiver producing a second feedback signal in response to the amplified output signal from the power amplifier;

a control module receiving said first and second feedback signals from said first and second digital receivers; said control module being so configured as to model the power amplifier in response to the first and second feedback signals and to update said amplitude and phase look-up table of said distortion generator in response to said modeling of the power amplifier.

9. An adaptative device as recited in claim 8, wherein said look-up tables of said dirtorting generator are indexed by an envelope detector that detects the envelope of the signal to be transmitted before predistortion.

10. An adaptative device as recited in claim 9, wherein said envelope detector indexes the distorting generator via an analog to digital converter.

11. An adaptative device as recited in claim 8, wherein said look-up tables of said dirtorting generator are indexed by the data from a third digital receiver that down-converts the signal to be transmitted to baseband.

12. An adaptative device as recited in claim 11, wherein the data from said third digital receiver is supplied to said control module that indexes said distorting generator accordingly.

13. An adaptative device as recited in claim 8, wherein said control module is so configured as to update said amplitude and phase look-up tables when an adjacent channel power ratio (ACPR) measurement indicates that the predistortion made by said predistorting generator is not adequate to meet predetermined ACPR standards.

14. An adaptative device as recited in claim 13, wherein said ACPR measurement is done via said second digital receiver that includes a first channel tuned to a mean frequency and a second channel that is tuned to a predetermined offset frequency, said ACPR measurement including comparing the average power at the means frequency and at the predetermined offset frequency

15. An adaptative device as recited in claim 8, wherein said control module is also so configured as to insert an adequate delay between the first feedback signal and the second feedback signal.

16. A transmitter system for amplifying and up-converting a baseband signal from a signal source; said transmitter system comprising:

a power amplifier having a signal input and an amplified signal output;

a complex gain adjuster interposed between the signal source and said signal input;

distorting generator including predistortion amplitude and phase look-up table; said distorting generator being so configured as to control said complex gain adjuster to predistort the baseband signal in amplitude and in phase;

an up-converter receiving said predistorted baseband signal; said up-converter being so configured as to supply an up-converted predistorted signal to said signal input of said power amplifier;

a first digital receiver producing a first feedback signal in response to the predistorted baseband signal;

a second digital receiver producing a second feedback signal in response to the up-converted amplified output signal from said amplified signal output;

a control module receiving said first and second feedback signals from said first and second digital receivers; said control module being so configured as to model said power amplifier in response to the first and second feedback signals and to update said amplitude and phase look-up table of said distorting generator in response to said modeling of said power amplifier.

17. An adaptive device for predistorting a signal to be transmitted, supplied by a signal source to an input of a power amplifier having an output for delivering an amplified output signal, comprising:

predistorter means comprising predistortion amplitude and phase look-up table means interposed between the signal source and the input of the power amplifier for amplitude and phase predistorting the signal to be transmitted;

digital receiver means for producing a first feedback signal in response to the predistorted signal from the predistorter means;

digital receiver means for producing a second feedback signal in response to the amplified output signal from the power amplifier;

means for modeling the power amplifier in response to the first and second feedback signals; and

means for updating the predistortion amplitude and phase look-up table means in response to said modeling of the power amplifier.

* * * * *

ANNEXE II

ARTICLES DE CONFERENCES

ANNEXE II.1:

IEEE IMS1998 International Microwave Symposium, Baltimore

An L Band Adaptive Digital Predistorter for Power Amplifiers Using Direct I-Q Modem.

181

AN L BAND ADAPTIVE DIGITAL PREDISTORTER FOR POWER AMPLIFIERS USING DIRECT I-Q MODEM

Ernesto G. Jeckeln, Fadhel M. Ghannouchi and Mohamad A Sawan

Department of Electrical and Computer Engineering
Ecole Polytechnique de Montréal
C.P. 6079, Station Centre-Ville, Montréal, Canada H3C 3A7

Abstract

This paper presents an L band experimental implementation of an adaptive digital predistorter (ADP) using direct I-Q modem for power amplifiers suitable to spectrally efficient mobile communication equipments. The linearizer, which is implemented in digital signal processor (DSP) environment, performs the real time modeling (RTM) of the power amplifier to supply its AM-AM and AM-PM non-linearities characteristics. Experimental results demonstrate that the spectral spreading is reduced by of 20 dB. The ADP achieve both power and spectral efficiencies and without the need for complex convergence algorithms and complex circuit.

Introduction

Linearization techniques become a useful way to compensate the distortion effects and spectral spreading caused by the amplifier non-linearities on the linear modulation method. In other words, linearization techniques permits to achieve both power efficiency and spectral efficiency while signal degradation is compensated. These parameters are important in design consideration of modern wireless radio systems allowing to extend the portable's battery life, to maximize the output power emission and to satisfy the restriction on the available limited spectrum. Thus, linear modulation, which has a high envelop variation, is adopted to maximize the spectral efficiency. In addition, the power amplifier (PA) is operated close to saturation (non-linear region) to achieve both high power efficiency and high output power emission.

Various linearization methods have been reported and many different ways can be used to segment this topic. But in general, all these techniques are, by any measure, derived from three main types named: i) Feed-forward [1], ii) Feedback [2] and iii) Predistortion [3]. The last technique, that has historically been the most common method in analog implementation, now can be well suited to digital implementation using digital signal processor (DSP) environment. The benefits of fast computational engine from this technology in several applications motivate the designers to focus toward the DSP/RF-Microwave integration. In this way, predistortion became one of the most robust linearization techniques that can be suited within this segment and dedicated for narrow frequency band system.

Important experimental results of this technique have been reported [4], [5], [6] demonstrating the capability in reducing the spectral spreading and how adaptive correction for drift, aging and temperature variation can be achieved. All algorithms of these previous work are based on iterative procedure [7], where the adaptation is exposed to critical condition such as stability and convergence rate. In this sense, this paper presents an experimental implementation of an ADP for PA operating near to saturation and without the need for complex convergence algorithms in the adaptation update step. This work validate the theoretical analysis presented by authors in [8], where the Real Time Modeling (RTM) algorithm models the Memoryless Complex Gains (MCG) of the PA to supply the knowledge of the non-linearities. The prototype is implemented with a DSP where both the RTM algorithm and the ADP are performed.

0-7803-4471-5/98/$10.00 (c) 1998 IEEE

182

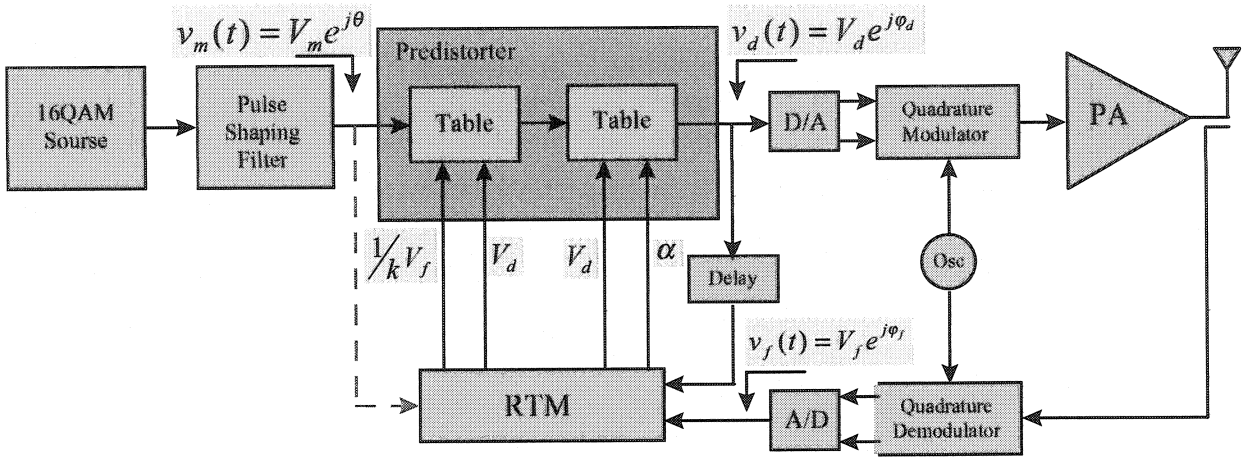

Fig. 1. Adaptive predistorter diagram.

The adaptive digital predistorter

General description

A simplified block diagram is shown in Fig.1. The signal source is the 16-QAM modulation schema, which is passed through a pulse shaping filter. In the RTM algorithm, the input $V_d e^{j\varphi_d}$ and output $V_f e^{j\varphi_f}$ equivalent lowpass complex envelope signals of the amplifier are oversampled and scaled to model the MCG. Then, a number q of complex data are sampled and sorted in order following an ascending list of values of the input signal's amplitude V_d. The sequences of complex samples can be written as following:

$$\sum_{i=1}^{q} V_{di} e^{j\varphi_{di}} \gamma(n - iT), \quad \sum_{i=1}^{q} 1/k\, V_{fi} e^{j\varphi_{fi}} \gamma(n - iT) \tag{1}$$

where $\gamma(n\text{-}iT)$ represents the impulse sampling at the signaling intervals iT (i = 1,2,3,...), T is the sampling period, k is the gain of the feedback loop of the equivalent baseband system and V_{di}, φ_{di} and V_{fi}, φ_{fi} are the discrete amplitudes and phases of both signal trajectories in the signal-space diagram. Now, letting the power amplifier be considered as a zero memory system and exploiting the rotational invariance of the amplifier nolinearity [7]. Then, the input-output relationship of such system can be written as follows :

$$v_f(t) = T\{v_d(t)\}, \tag{2}$$

where the complex transfer function is given by :

$$T\{v_d(t)\} = \left|T\{V_d(t)\}\right| e^{j\phi\{V_d(t)\}}. \tag{3}$$

Note that $\left|T\{V_d(t)\}\right|$ and $\phi\{V_d(t)\}$ determine the amplitude and phase nonlinearity respectively. Based on equations (2) and (3) and using equation (1), the modeling of the MCG can be performed straightforward where $\phi = \varphi_f - \varphi_d$. From this model, the inverse function of the AM-AM characteristic is performed and the AM-PM conversion factor is complemented according to obtain gain expansion and phase advance.

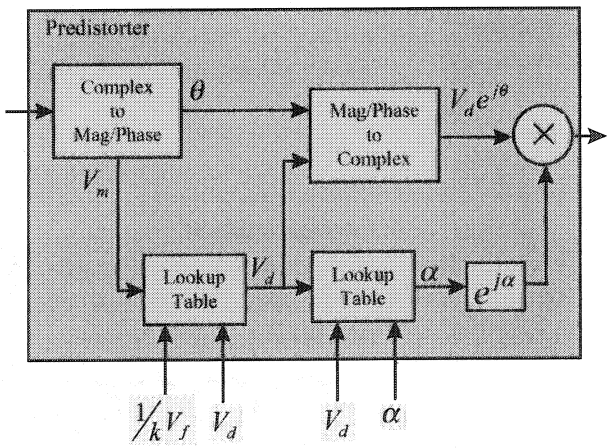

Fig. 2. Lookup tables using polar representation of processed signal.

0-7803-4471-5/98/$10.00 (c) 1998 IEEE

183

Then, The set of data from the RTM is loaded into the predistorter where the predistorted signal is provided using one-dimensional lookup table technique (LUT). Note that pipeline structure is employed in the LUT technique to generate amplitude predistortion V_d and phase predistortion α (Fig. 2). An important feature to be considerate is the adaptability dedicated to drift correction. Adapting the predistorter requires a feedback path through which the linearizer can be notified of this change. In this case, mean error criterion between the desired and the distorted feedback signals is used to shoot adaptability. After each adaptation and during normal data transmission, the feedback loop is opened until new significant drifts have occurred and new data has to be entered in the LUT.

Prototype

The entire system has been built as shown in Fig.3. The system boards is a LSI card, running on a PC, including a TMS320C40/50 MHz device and a module with 16 bit/60-200 KHz dual DA/AD converters. The power amplifier was a 1 W class AB driven at 1,780 GHz. The 16QAM modulation method is used as the signal source with a baud rate of 6 kHz. The pulse shaping filter is a raised cosine having a roll off (α) of 0.35, and the oversampled rate was 10 samples/symbol. Careful attention has been paid to reduce the local oscillator carrier feedthrough from the QM, [6]. It was reduced by using a cancellation loop which include an attenuator and phase shifter in parallel with the QM.

Experimental results and discussion

Results

To evaluate the predistorter performance, the PA was driven near saturation with 1 dB peak back-off (the radio of the saturation output power and peak output power) [7]. From the experimental results, as shown in Fig. 4, it is demonstrated that the spectral spreading may be reduced in excess of 20 dB. A further reduction can be achieved by improving the compensation of the feedback loop impairments (carrier leak, gain and phase imbalance, etc.,). Note that the degradation on spectral magnitude from these impairment limits the out of band spectral reduction obtained from the linearizer (Fig. 4).

Advantage

This technique uses the benefits that any mathematics function is easy to be performed by software and therefore, significant improvements can be obtained using inverse nonlinearities from the RTM algorithm. Due to its operating principle, the proposed linearizer performs adaptation without the need of complex convergence algorithms and can supply correction for any order of nonlinearity and any modulation format.

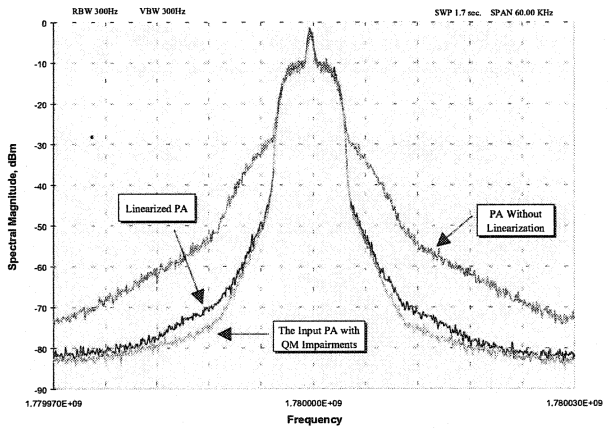

Fig. 4. Power spectrum showing the effect of the linearization and the QM impairment.

Limitation

A quite examination revealed that the precision of the RTM in modeling the non-linearities have a critical dependence of the feedback loop impairments. The distortion, due to imperfection from other components are added to the signal limiting the accuracy when the non-linearities are sounded. Also, a limitation in bandwidth is imposed to the system. In fact, the processor performs its task in real time where data are presented to the system by the external environment and whether the processor is ready or not. Therefore, if the algorithm cannot process data adequately because of time consuming, it may lose input data resulting a failure in the system.

0-7803-4471-5/98/$10.00 (c) 1998 IEEE

184

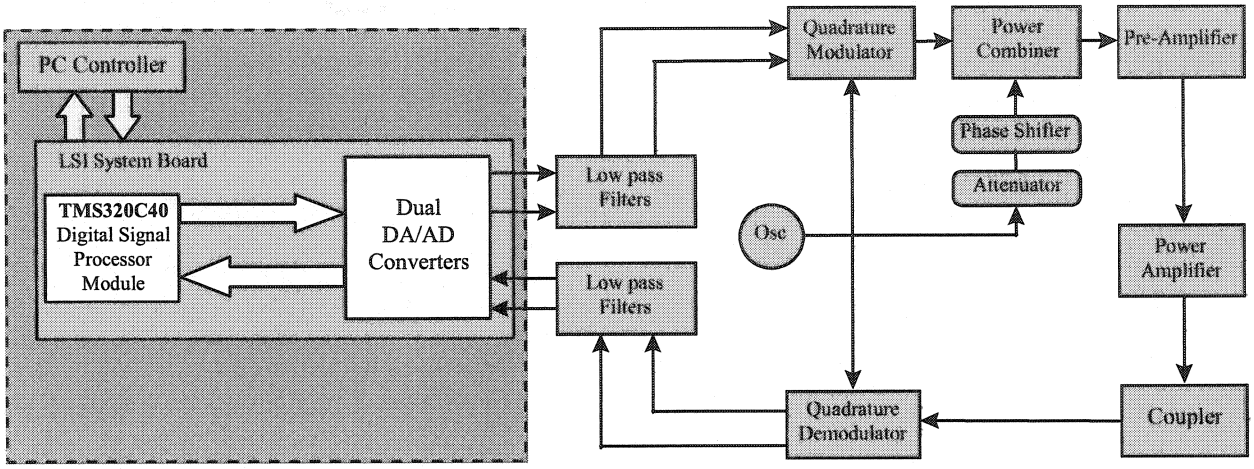

Fig. 3 Simplified block diagram of the hardware.

Conclusion

In this paper, an experimental validation of new method dedicated to ADP with real time modeling of AM-AM and AM-PM characteristics is presented. The RTM algorithm has demonstrated to be a powerful tool for sounding and modeling the memoryless complex gains during normal data transmission. Its ability is in eliminating the need for complex convergence algorithms in the adaptation update step. The predistorter can be self corrected for any drift in the operating points and also, any order of nonlinearity and any modulation format can be supported. Finally, although the technique is limited in bandwidth, the evolution of DSP technology, that improves the speed of digital processing, will allow researchers to handle higher bandwidth signal.

Acknowledgments

This work is supported by the "Programme Synergie" of the Quebec government through the AMPLI project in collaboration with Advantech Inc. and NSI Communications.

References

[1] R. Meyer, R. Eschenbach and W. Edgerley, Jr." A Wide-Band Feedforward Amplifier", IEEE J of Solid-State Circuits, vol.sc-9, no. 6, pp. 442-428, December 1974.

[2] C. C. Hsieh and E. Strid. "A S-band high power feedback amplifier", IEEE MTT-S International Microwave Symposium, San Diego, CA, June 21-23, 1977, pp. 182-184.

[3] N. Imai, T. Nojima and T. Murase, "Novel Linearizer Using Balanced Circulators and Its Application to Multilevel Digital Radio Systems", IEEE Transactions on Microwave Theory and Techniques, vol. 37, no 8, pp. 1237-1243, August 1989.

[4] Y. Nagata, "Linear Amplification Technique for Digital Mobil Communications", in Proc. IEEE Veh. Technol. Conf., San Francisco, CA, 1989, pp. 159-164.

[5] M. Faulkner, T. Mattsson and W. Yates, "Adaptive Linearization Using Predistortion" in Proc. 40th IEEE Veh. Technol. Conf. 1990. pp. 35-40.

[6] A. S. Wright and Willem G. Durtled, "Experimental Performance of an Adaptive Digital Linearized Power Amplifiers", IEEE Transactions on Vehicular Technology, vol. 41, no 4, pp 395-400, November 1992.

[7] J. Cavers, "Amplifier Linearization Using a Digital Predistorter with Fast Adaptation and Low Memory Requirement", IEEE Transactions on Vehicular Technology, vol. 39, no 4, pp 374-382, November 1990.

[8] E.G. Jeckeln, F.M. Ghannouchi and Mohamad Sawan, "Adaptive Digital Predistorter for Power Amplifiers with Real Time Modeling of Memoryless Complex Gains", IEEE MTT-S 1996 International Microwave Symposium, San Francisco, CA, June 1996.

ANNEXE II.2:

IEEE IMS2000 International Microwave Symposium, Boston

Adaptive Baseband/RF Predistorter for Power Amplifiers through Instantaneous AM-AM and AM-PM Characterization Using Digital Receivers

ADAPTIVE BASEBAND/RF PREDISTORTER FOR POWER AMPLIFIERS THROUGH INSTANTANEOUS AM-AM AND AM-PM CHARACTERIZATION USING DIGITAL RECEIVERS

E. G. Jeckeln, F.Beauregard*, M. A. Sawan and F. M. Ghannouchi

Department of Electrical and Computer Engineering
Ecole Polytechnique de Montréal
P.O. Box 6079, Station. Centre-Ville, Montreal, QC,Canada, H3C 3A7

* AmpliX, Wireless & Satcom
3333 Queen Mary, R-320
Montreal, QC, Canada, H3V 1A2

Abstract

This paper presents a powerful adaptive basedband/RF predistorter, which uses advantageously the concept of digital receiver technology into power amplifier (PA) linearization area. The linearizer performs an instantaneous characterization of the PA using two digital receivers to supply its AM-AM and AM-PM transfer functions. W-CDMA signals applying different stress level on PA are used to evaluate the performance of the predistorter. The entire system is validated using DSP/RF co-simulation for a typical class AB power amplifier. Results from different cases of standards signals reveal a significant reduction in effective output power back off (OBO).

Introduction

While the third generation (3G) of mobile radio standards is being defined, the demand for developing ultra-linear microwave transmitter, supporting high crest factor signals is greater than ever. The demanding adjacent channel power ratio (ACPR) requirements of these new systems, i.e., W-CDMA or CDMA2000, present a critical issue for transmitter designers if both ultra-linearity and high power efficiency must be met. In fact, the degradation of linearity becomes significant as the PA operates close to saturation where both high power efficiency and high output power emission are achieved. Therefore, for different stimulus levels driving the amplifiers and for a given ACPR specification, the trade-offs between power efficiency and linearity impose an operating point with poor power efficiency. In this case, linearization techniques become the only possible way to recuperate the non-linearity and to allow optimal trade-offs.

Various linearization methods have been reported and are derived, by any measure, from three main types named: i) Feed-forward, ii) Feedback and iii) Predistortion. Referring to the last one, the predistortion technique has historically been the most common method in analog implementation. Now, this technique is well suited to digital implementation, by integrating a DSP chip to handle high-speed arithmetic. In this way, important experimental results have been presented [1-5] demonstrating the capability in reducing the spectral spreading and how adaptive correction for drift, aging and temperature variation can be achieved using DSP circuits.

Although the above-mentioned technique is powerful due to its digital operating principles, it presents certain inflexibility in the sense that; it is suitable only when the baseband signal is acceded directly before the up-conversion. In most cases, linearizer designers has no access to baseband signal, hence, they found themselves confined to use traditional RF analog predistortion techniques. In this case, it is more difficult to meet severe ACPR for a high crest factor's signals specifications while operating not in far back-off regions.

The RF-based predistorter proposed in [6] offer an interesting alternative. It includes a complex gain tuning circuit that controls the amplitude an phase of the RF signal. The baseband environment is confined to optimize two nonlinear work functions by monitoring the ACP-minimization measured by a power detector. Drawbacks of this method are its slow convergence toward the minimum and its sensitivity to the measurement noise.

0-7803-5687-X/00/$10.00 (c) 2000 IEEE

We present in this paper an advanced adaptive baseband/RF predistorter, which integrate advantageously the concept of digital receiver technology into the linearization techniques. By taking advantage of this technology to digitally translate signal from RF to baseband with very high accuracy, the linearizer performs the instantaneous characterization of the memoryless nonlinearity in baseband to supply a correlated predistortion function. Results from different cases of standards signals reveal a significant reduction in effective OBO.

Description of the Predistorter

The proposed technique is based on a new concept supported by the emergent digital receiver technology. This technique uses an envelope detector to provide the envelope variation that is digitized to index a distorting generator, as shown in Fig.1.

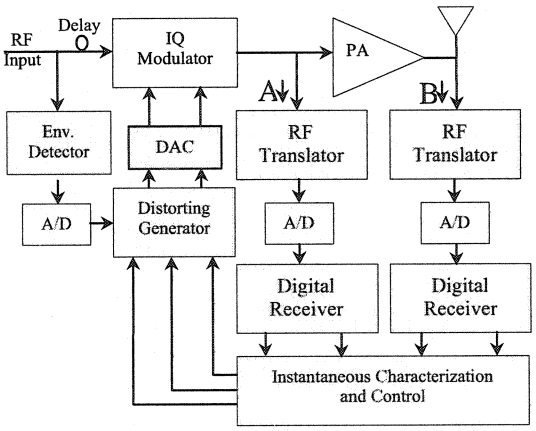

Fig. 1 General block diagram of the linearizer

Following the RF signal path, an IQ modulator is used as complex gain adjuster, that controls the amplitude and phase of the RF input signal. Then, the RF signal is picked up from the input and the output of the PA and translated down to within an alias-free sampling range from DC up to 35 MHz. Right after the translator stages, one for each branch, the signals are conditioned by 12-bit A/D converters into digital samples at the high rate of 70 MHz. All of the subsequence complex down converting, filtering and decimating is performed digitally by two digital receivers. It is understood that, the complex envelop from the output of the PA in branch "B" bring the information of non-linearity when it is driven further into nonlinear operation mode. This non-linearity information can be discriminated when this complex envelop is referenced to the complex envelop from the input of the PA in branch "A". It means that the instantaneous characterization (i.e., AM-AM and AM-PM curves) can be performed following both complex envelopes variation during a real work condition [7]. It allows to correlate the predistortion function in real time and to control the adaptation update step whenever it is necessary to be update into the distorting generator.

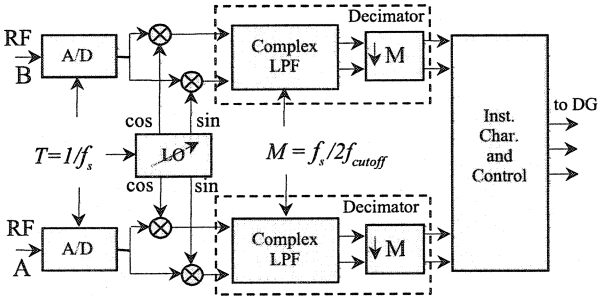

Fig.2 Block diagram of the digital receiver algorithms showing the translation and decimation process.

In terms of algorithms, the translation and filtering process are the two majors signals processing operations performed by the digital receiver blocks. First, a single-sideband complex translation is accomplished by mixing the real signal with the complex output of a digital quadrature local oscillator (LO), as shown in Fig.2. Then, a decimation filter conditions the complex baseband signal by fixing an appropriate value of the decimation parameter M. It controls the reduction of the cutoff frequency f_{cutoff} and the sampling rate f_s as follows:

$$f_{cutoff} = f_s/2M\,, \qquad (1)$$

$$f^{\cdot\cdot} = f_s/M\,. \qquad (2)$$

It means that, by tuning the LO frequency and the M value, any signal can be selected digitally from the RF domain and put it into the baseband domain for further processing. In this way, the two receiver output data, that represent the stimulus and response of the PA, are routed through the instantaneous

characterization block to carry out the nonlinearity behavioral. Assuming that the input bandpass signal is given by

$$v_i(t) = \mathrm{Re}\{\rho(t)e^{j[\omega_c t + \theta(t)]}\}, \quad (3)$$

where ω_c is the midband angular frequency, $\rho(t)$ is the amplitude variation and $\theta(t)$ is the phase variation. Then, the bandpass output signal can be represented by

$$v_i(t) = \mathrm{Re}\{g[\rho(t)]e^{j\{\omega t + \phi[\rho(t)]+\theta(t)\}}\}, \quad (4)$$

where $g[\rho(t)]$ and $\phi[\rho(t)]$ are two memoryless nonlinear functions that represent the instantaneous AM-AM and AM-PM curves. Notice that these functions are characterized in terms of the input and output bandpass complex envelopes, without including all harmonics effect. The optimal compensator is correlated straightforward by

$$\rho_d(t) = g^{-1}[\rho(t)], \quad (5)$$

$$\alpha(t) = -\phi\{g^{-1}[\rho(t)]\}. \quad (6)$$

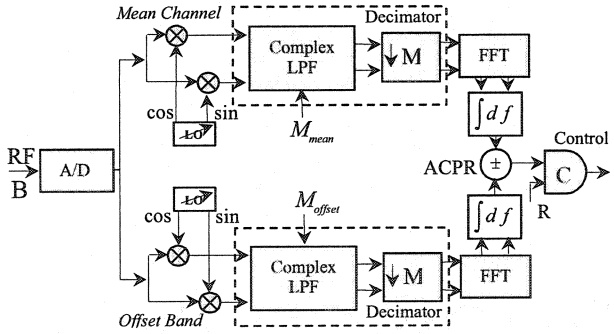

Fig.3 ACPR processing of the output signal.

Taking advantage of the decimation process to perform a dramatic reduction in the signal bandwidth, the ACPR can be monitored in different range of frequency by processing simultaneous real time FFT spectra, as show in fig.3. This is accomplished, once the characterization process is finished, by dynamically tuning both the LO frequency and the M value of each digital receiver. A comparator C shoots the adaptation step when the measured ACPR overflow the reference value R.

Results and Discussions

The entire system is RF/DSP co-simulated using HP-ADS software for a typical class AB Power Amplifier [7]. Temperature noise, quantization noise and impairment from other components have been taken into consideration to realistically model the system. The digital receivers are considered as both narrowband and wideband where the M values are ranged from 2 to 2^{17}. To evaluate the performance of the linearization system, CDMA and W-CDMA standard signals are used to apply different stress level characterized by its complementary cumulative distribution function (CCDF). To estimate the performance of the whole system under realistic condition, experimental results have been carried out in open loop condition for a 20 W class AB power amplifier operating at 1.96 GHz. In this case, the AM-AM and AM-PM transfer characteristics of the PA were measured by instantaneous characterization using a peak power analyzer for the first one, and a conventional measurement by network analyzer for the second one. Data from this measurement was used into the simulator to generate a long string of predistorted samples for different CDMA and W-CDMA standards signals. Then, these predistorted signals were fed into an arbitrary waveform generator to generate and supply a realistic predistorted signal to the PA.

Several important results have been obtained, the main of them are presented here. The OBO referenced to Single Carrier (SC) saturation, the Crest Factor (peak power-to-average power (CF)) defined at 0.1% of the CCDF, the word-length of bits and the ACPR are chosen as important factors to analyze the performance of the whole system. Figures 4-5 show the ACPR vs. OBO corresponding for the offset bands above the mean signal frequency. The horizontal line indicates the system specification where the minimum acceptable OBO are illustrated. Fig.3 and 4 reveal a reduction in the OBO of 4.8 dB in simulation and 4 dB under realistic condition respectively. Also the plots reveal an ACPR improvement of 10 dB and 5 dB respectively. The stimulus is a W-CDMA standard signal with a CF=11.5 dB.

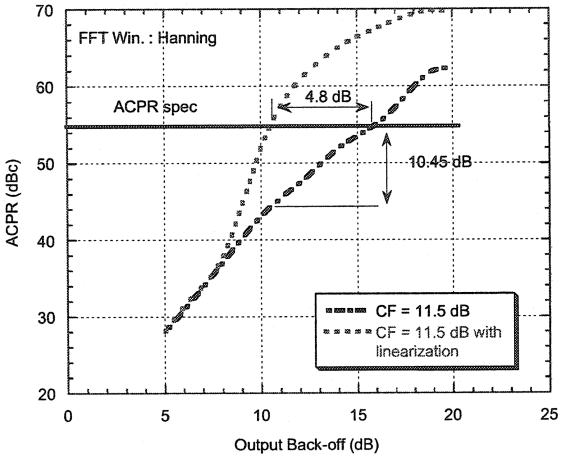

Fig.4 ACPR simulation of W-CDMA standard signal and the linearization effect.

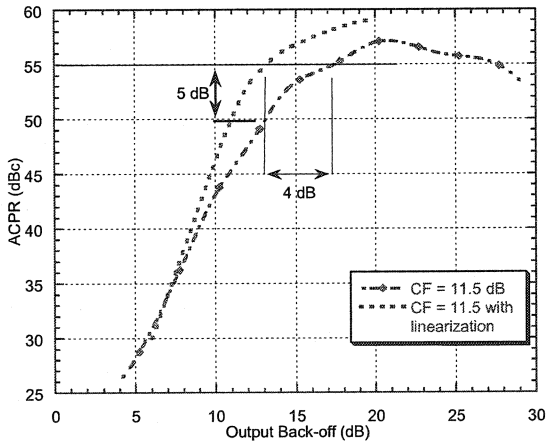

Fig.5 ACPR Measurements of W-CDMA signal with different crest factor (dB) and the linearization effect for the worse case.

Conclusion

An adaptive basedband/ RF predistorter, which develops the algorithm of two digital receivers to perform an instantaneous characterization of the AM-AM and AM-PM non-linearities, was presented. The digital receivers allow a direct I/Q demodulation from RF to baseband straightforward without any need to use IF frequency conversion. The disturbing effect of gain and phase imbalances of a RF analogue quadrature demodulator are completely avoided by directly processing the data with very high accuracy using analytical expressions. In addition, the system can monitor the ACPR by processing simultaneous real time FFT spectra in different range of frequency. CDMA and W-CDMA standard signals applying different stress levels on power amplifiers are used to evaluate the performance of the new adaptive predistorter. RF/DSP co-simulation and experimental results have been carried out for evaluation purpose. Results reveal a significant reduction in effective output power back off (OBO) for the linearized power amplifier. Finally, the fact that the system can support different modulation format by tuning the values LO, M and R by software, this technique provide an attractive design suitable for mass production.

References

[1] Y. Nagata, "Linear Amplification Technique for Digital Mobil Communications", in Proc. IEEE Veh. Technol. Conf., San Francisco, CA, 1989, pp. 159-164.

[2] M. Faulkner, T. Mattsson and W. Yates, "Adaptive Linearization Using Predistortion" in Proc. 40th IEEE Veh. Technol. Conf. 1990. pp. 35-40.

[3] A. S. Wright and Willem G. Durtled, "Experimental Performance of an Adaptive Digital Linearized Power Amplifiers", IEEE Transactions on Vehicular Technology, vol. 41, no 4, pp 395-400, November 1992.

[4] J. Cavers, "Amplifier Linearization Using a Digital Predistorter with Fast Adaptation and Low Memory Requirement", IEEE Transactions on Vehicular Technology, vol. 39, no 4, pp 374-382, November 1990.

[5] E.G. Jeckeln, F.M. Ghannouchi and Mohamad Sawan, "Adaptive Digital Predistorter for Power Amplifiers with Real Time Modeling of Memoryless Complex Gains", IEEE MTT-S 1996 International Microwave Symposium, San Francisco, CA, June 1996.

[6] S. P. Stapleton and F. C. Costescu, "An Adaptive Predistorter for a Power Amplifier Bsaed on Adjacent Channel Emissions", IEEE Transactions on Vehicular Technology, vol. 41, no 1, pp 49-56, February 1992.

[7] E.G. Jeckeln, F.M. Ghannouchi and Mohamad Sawan, " An L Band Adaptive Digital Predistorter for Power Amplifiers Using Direct I-Q Modem ", IEEE MTT-S 1998 International Microwave Symposium, Baltimore, MA, June 1998.

[8] HP Advance Design System, HEWLETT PACKARD.

ANNEXE II.3:

ICECS'2K

Amplifier's Predistortion -based Linearizers for Forward-channel Link Broadband Applications

Amplifier's Predistortion -based Linearizers for Forward-channel Link Broadband Applications

E. G. Jeckeln, F. M. Ghannouchi, M. A. Sawan and F.Beauregard*

Department of Electrical and Computer Engineering
Ecole Polytechnique de Montréal
P.O. Box 6079, Station. Centre-Ville, Montreal, QC, Canada, H3C 3A7

* AmpliX, Wireless & Satcom
3333 Queen Mary, R-320
Montreal, QC, Canada, H3V 1A2

Abstract

In this paper, an adaptive basedband/ RF predistorter tracking the emerging technologies evolution of digital receivers is presented. The linearizer performs the extraction of the nonlinear time-variant behaviour of the PA to correlate the predistortion transfer functions and develop an adaptation algorithm performing a distortion level computation in time domain. CDMA standard signals applying different stress level on PA are used to evaluate the performance of the predistorter. The entire system is validated using DSP/RF co-simulation for a typical 44-dBm-class AB power amplifier. Results from different cases of standards signals reveal a significant reduction in effective output power back off (OBO).

Introduction

While the third generation (3G) of mobile radio standards is being defined, the demand for developing ultra-linear microwave transmitter, supporting high crest factor signals is greater than ever. The demanding adjacent channel power ratio (ACPR) requirements of these new systems, i.e., W-CDMA or CDMA2000, present a critical issue for transmitter designers if both ultra-linearity and high power efficiency must be met. In fact, the degradation of linearity becomes significant as the PA operates close to saturation where both high power efficiency and high output power emission are achieved. Therefore, for different stimulus levels driving the amplifiers and for a given ACPR specification, the trade-offs between power efficiency and linearity impose an operating point with poor power efficiency. In this case, linearization techniques become the only possible way to recuperate the non-linearity and to allow optimal trade-offs.

Various linearization methods have been reported and are derived, by any measure, from three main types named: i) Feed-forward, ii) Feedback and iii) Predistortion. Referring to the last one, the predistortion technique has historically been the most common method in analog implementation. Now, this technique is well suited to digital implementation, by integrating a DSP chip to handle high-speed arithmetic. In this way, important experimental results have been presented [1-5] demonstrating the capability in reducing the spectral spreading and how adaptive correction for drift, aging and temperature variation can be achieved using DSP circuits.

Recently, a variant of the above-mentioned technique was presented by the authors [8]. It uses two digital receivers for nonlinear characterization purpose and a complex gain adjuster to dynamically embed the predistortion into the RF signal. The robustness of this technique is the optimal instantaneous characterization algorithm under real time constrains, and the real time analysis of the distortion level to make decision on the adaptation step. A drawback of this technique is the time consuming of the FFT algorithm in monitoring the distortion level.

We present in this paper an advanced adaptive baseband/RF predistorter including three digital receivers. The linearizer performs the extraction of the nonlinear time-variant behavior of the PA to correlate the predistortion transfer functions and develop an adaptation algorithm performing a distortion level computation in time domain. The distortion is generated in baseband by addressing the extracted predistortion function

and then, it is embedded into the RF signal by dynamically adjusting the amplitude and the phase the RF signal. The linearization system is evaluated by applying different stress level of CDMA standard signals and computing the ACPR between in-band and out-of-channel power spectral densities at specified offset channels and for different operating point. The entire system is RF/DSP co-simulated using HP-ADS software for a typical 44-dBm class AB Power Amplifier [9]. Results from different cases of standards signals reveal a significant reduction in effective OBO.

Description of the Predistorter

The proposed technique is based on a new concept supported by the emergent digital receiver technology. Fig.1 shows the block diagram of the linearizer using three digital receivers for down converting purpose. In branch "C", a digital receiver is used to provide the envelope variation that allows indexing a distorting generator.

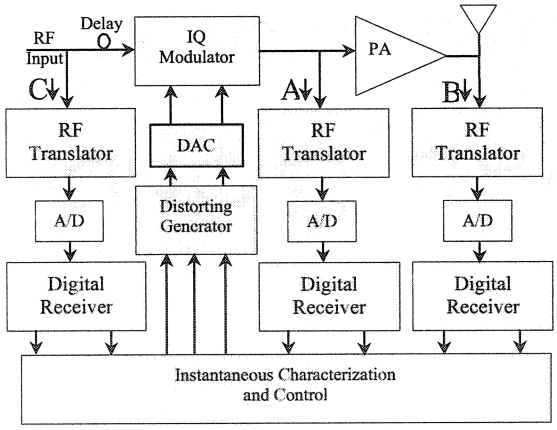

Fig. 1 General block diagram of the linearizer

Following the RF signal path, after the delay line, an IQ modulator is used as complex gain adjuster, that controls the amplitude and phase of the RF input signal. Then, the RF signal is picked up from the input and the output of the PA and translated down to within an alias-free sampling range from DC up to 35 MHz. Right after the translator stages, one for each branch, the signals are conditioned by 12-bit A/D converters into digital samples at the high rate of 70 MHz. The entire subsequence complex down converting, filtering, and decimating is performed digitally by two digital receivers. It is understood that, the complex envelop from the output of the PA in branch "B" bring the information of non-linearity when it is driven further into nonlinear operation mode. This non-linearity information can be discriminated when this complex envelop is referenced to the complex envelop from the input of the PA in branch "A". It means that the instantaneous characterization (i.e., AM-AM and AM-PM curves) can be performed following both complex envelopes variation during a real work condition [7]. It allows to correlate the predistortion function in real time and to control the adaptation update step whenever it is necessary to be update into the distorting generator.

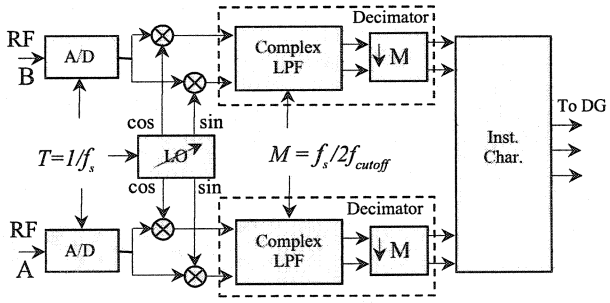

Fig.2 Block diagram of the digital receiver algorithms showing the translation and decimation process.

In terms of algorithms, the translation and filtering process are the two majors signals processing operations performed by the digital receiver blocks. First, a single-sideband complex translation is accomplished by mixing the real signal with the complex output of a digital quadrature local oscillator (LO), as shown in Fig.2. Then, a decimation filter conditions the complex baseband signal by fixing an appropriate value of the decimation parameter M. It controls the reduction of the cutoff frequency f_{cutoff} and the sampling rate f_s as follows:

$$f_{cutoff} = f_s/2M\,, \tag{1}$$

$$f^{\cdot\cdot} = f_s/M\,. \tag{2}$$

It means that, by tuning the LO frequency and the M value, any signal can be selected digitally from the RF domain and put it into the baseband domain for

further processing. In this way, the two receiver output data, that represent the stimulus and response of the PA, are routed through the instantaneous characterization block to carry out the nonlinearity behavioral. Assuming that the input bandpass signal is given by

$$v_i(t) = \mathrm{Re}\{\rho(t)e^{j[\omega_c t + \theta(t)]}\}, \qquad (3)$$

where ω_c is the midband angular frequency, $\rho(t)$ is the amplitude variation and $\theta(t)$ is the phase variation. Then, the bandpass output signal can be represented by

$$v_i(t) = \mathrm{Re}\{g[\rho(t)]e^{j\{\omega t + \phi[\rho(t)]+\theta(t)\}}\}, \qquad (4)$$

where $g[\rho(t)]$ and $\phi[\rho(t)]$ are two memoryless nonlinear functions that represent the instantaneous AM-AM and AM-PM curves. Notice that these functions are characterized in terms of the input and output bandpass complex envelopes, without including all harmonics effect. The optimal compensator is correlated straightforward by

$$\rho_d(t) = g^{-1}[\rho(t)], \qquad (5)$$

$$\alpha(t) = -\phi\{g^{-1}[\rho(t)]\}. \qquad (6)$$

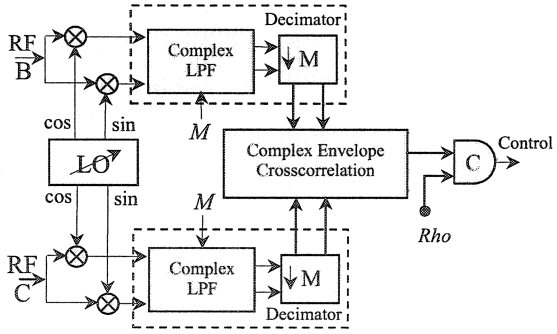

Fig.3 ACPR processing of the output signal.

In order to control the adaptation step, the system uses the distortion level at the output signal as a quantifier of the transmitter performance. As shown in Fig.3, it is accomplished by performing a crosscorrelation between the corrected output signal and the reference signal from branch "c". It accounts for all distortion mechanisms between the two signals and therefore, it gives a measure of the distortion compensation level. In other words, if some of the transmitted energy does not correlate between the two signals, the uncorrelated power appears as added distortion, which amount is compared with an acceptable distortion level. A comparator C shoots the adaptation step when the distortion level overflows the reference value *Rho*. In this way, the whole computation load is reduced more than half in comparison to the FFT algorithm process.

Results and Discussions

The entire system is RF/DSP co-simulated using HP-ADS software for a typical class AB Power Amplifier [9]. Temperature noise, quantization noise and impairment from other components have been taken into consideration to realistically model the system. The digital receivers are considered as both narrowband and wideband where the M values are ranged from 2 to 2^{17}.

Several important results have been obtained, the main of them are presented here. Simulations are performed applying the stimulus on the PA and on the PA including the linearizer. Each simulation is repeated for different operating points to allow characterizing the performance in term of distortion and power efficiency. The OBO referenced to Single Carrier (SC) saturation that represent in any measure the power efficiency, the peak power-to-average power characterized by the CCDF, the word-length of bits and the ACPR are chosen as important factors to analyze the performance for the two cases. Figures 4-5 detail the simulated results of ACPR versus OBO corresponding for the offset bands above the mean signal frequency. In all cases, the horizontal lines indicate the system specifications for ACPR where the minimum acceptable OBO are illustrated. At this point, it is important to mention that any change on the parameters values of the simulation conditions such as roll-off, average number, window function, filters, etc., will have a direct effect on the results. In Fig.4 we can see that the standard requirement limits the PA operating point at least 8.2 dB at 885 kHz, 9.9 dB at 1.25 MHz,

and 14.15 dB at 2.75 MHz. Notice that the third offset channel governs the minimum acceptable OBO and therefore, the PA cannot be operated with an OBO smaller than 14.15 dB. Under linearization effect, the plots in Fig.5 show a minimum OBO of 7 dB at 885 kHz, 7.95 dB at 1.25 MHz and 10.5 dB at 2.75 MHz prevailing the value of 10.5 dB as the minimum acceptable OBO according to the spectrum emission mask. This result shows that the predistortion action from the linearizer diminish the OBO by 3.6 dB.

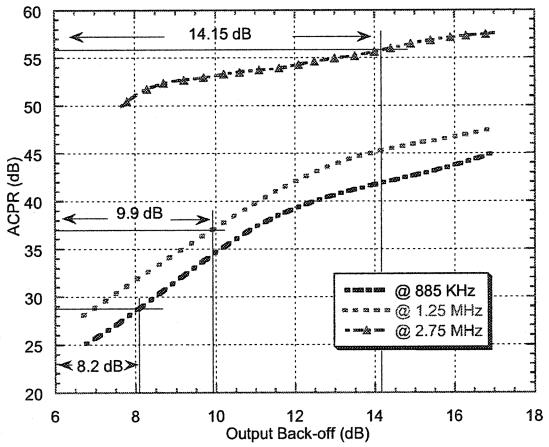

Fig.4 ACPR simulation of CDMA standard signal.

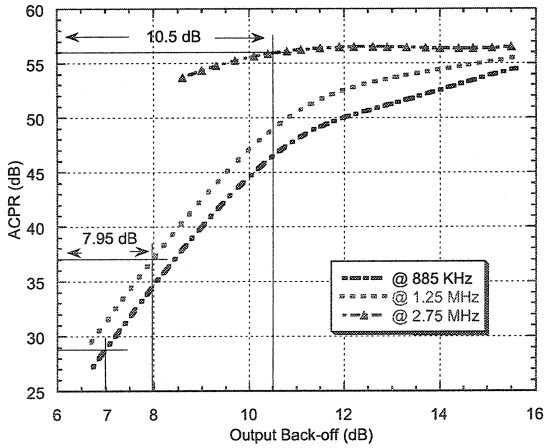

Fig.5 ACPR simulation of CDMA standard signal under linearization effect.

Conclusion

An adaptive basedband/ RF predistorter tracking the emerging technologies evolution of digital receivers was presented. The linearizer develops the algorithms of three digital receivers to execute a direct I/Q demodulation in digital form from RF to baseband. The disturbing effect of gain and phase imbalances of a RF analogue quadrature demodulator are completely avoided by directly processing waveform with very high accuracy using analytical expressions. This advantage allows DSP algorithms to characterize the AM-AM and AM-PM non-linearities following both input and output complex envelopes variation of the PA during a real work condition, and control the adaptation step by quantifying the distortion level through crosscorrelation process. Results reveal a significant reduction in effective output power back off (OBO) for the linearized power amplifier.

References

[1] Y. Nagata, "Linear Amplification Technique for Digital Mobil Communications", in Proc. IEEE Veh. Technol. Conf., San Francisco, CA, 1989, pp. 159-164.

[2] M. Faulkner, T. Mattsson and W. Yates, "Adaptive Linearization Using Predistortion" in Proc. 40th IEEE Veh. Technol. Conf. 1990. pp. 35-40.

[3] A. S. Wright and Willem G. Durtled, "Experimental Performance of an Adaptive Digital Linearized Power Amplifiers", IEEE Transactions on Vehicular Technology, vol. 41, no 4, pp 395-400, November 1992.

[4] J. Cavers, "Amplifier Linearization Using a Digital Predistorter with Fast Adaptation and Low Memory Requirement", IEEE Transactions on Vehicular Technology, vol. 39, no 4, pp 374-382, November 1990.

[5] E.G. Jeckeln, F.M. Ghannouchi and Mohamad Sawan, "Adaptive Digital Predistorter for Power Amplifiers with Real Time Modeling of Memoryless Complex Gains", IEEE MTT-S 1996 International Microwave Symposium, San Francisco, CA, June 1996.

[6] S. P. Stapleton and F. C. Costescu, "An Adaptive Predistorter for a Power Amplifier Bsaed on Adjacent Channel Emissions", IEEE Transactions on Vehicular Technology, vol. 41, no 1, pp 49-56, February 1992.

[7] E.G. Jeckeln, F.M. Ghannouchi and Mohamad Sawan, " An L Band Adaptive Digital Predistorter for Power Amplifiers Using Direct I-Q Modem ", IEEE MTT-S 1998 International Microwave Symposium, Baltimore, MA, June 1998.

[8] E. G. Jeckeln, F. M. Ghannouchi, M. A. Sawan and F.Beauregard, IEEE MTT-S 2000 International Microwave Symposium, Boston, M, June 2000.

[9] HP Advance Design System, HEWLETT PACKARD.

ANNEXE II.4:

IEEE IMS2001 International Microwave Symposium, Phoenix

Efficient Baseband/RF Feedforward Linearizer through a Mirror Power Amplifier Using Software-Defined Radio and Quadrature Digital Up-Conversion

Efficient Baseband/RF Feedforward Linearizer through a Mirror Power Amplifier Using Software-Defined Radio and Quadrature Digital Up-Conversion

E. G. Jeckeln, F. M. Ghannouchi, M. Sawan and F. Beauregard*

Department of Electrical and Computer Engineering
Ecole Polytechnique de Montréal
P.O. Box 6079, Station. Centre-Ville, Montreal, QC, Canada, H3C 3A7

*AmpliX Wireless & Satcom
3333 Queen Mary Rd., R-320
Montreal, Quebec, Canada

Abstract — **This paper describes an efficient feedforward linearizer suitable for base station 3G power amplifiers based on and using both software-defined radio and quadrature digital up-conversion technologies. The linearizer accomplishes the extraction of the PA complex nonlinear behavior in real time and performs a numerical quasi-perfect carrier's cancellation that allows the reduction of the power rating of the error amplifier (EA) and eliminates the requirement for any output delay line. This enhances the overall power efficiency of the feedforward amplifier. The entire system is validated using DSP/RF co-simulation for the LDMOS model of a typical 44 dBm class AB power amplifier (PA_{AB}) as the main amplifier.**

I. INTRODUCTION

While the third generation (3G) of mobile radio standards is being defined, the demand for developing ultra-linear microwave transmitter, supporting high crest factor signals is greater than ever. The demanding adjacent channel power ratio (ACPR) requirements of these new systems, i.e., W-CDMA or cdma2000, present a critical issue for transmitter designers if both ultra-linearity and high power efficiency must be met. In fact, the degradation of linearity becomes significant as the PA operates close to saturation where both high power efficiency and high output power emission are achieved. Therefore, for different stimulus levels driving the amplifiers and for a given ACPR specification, the trade-offs between power efficiency and linearity impose an operating condition with poor power efficiency. In this case, linearization techniques become the only possible way to recuperate the non-linearity and to allow optimal trade-offs.

Various linearization methods have been reported and are derived, by any measure, from three main types named: i) Feed-forward, ii) Feedback and iii) Predistortion. Referring to the first one, the feed-forward technique is characterized for its broadband performance [1-2]. It has a high level intermodulation reduction that is achieved with an unconditionally stable condition. A drawback of this technique is its low power efficiency due to the high average power requirement needed in the error amplifier and the insertion loss from couplers and the delay line at the output of PA. The error signal needs to be amplified up to the necessary power level with high linearity and therefore, it constrains the error amplifier to work in Class A (EA_A) with high output back off. One way to minimize the power requirement of the error amplifier is to reduce the residual carrier power from the carrier cancellation loop, but it is limited to the typical value of –30 dBc depending upon the performance of the phase and gain tracking of the cancellation loop.

Today, the high clock speeds in DSPs, which are entering the microwave frequency bands, offer the possibilities to migrate most of the analog signal processing to the digital domain [3-6]. Hence, we propose in this paper an efficient baseband/RF feedforward linearizer that incorporates advanced software defined radio and quadrature digital up converter [7]. By taking advantage of these technologies to digitally translate signal from IF to baseband and vice versa, the linearizer performs the instantaneous characterization of the memoryless transfer function of the PA, which is used to develop the first cancellation loop in digital domain. The added benefits of this technique are that the power requirement of the error amplifier is reduced and the output delay line is removed enhancing the overall power efficiency of the feedforward amplifier.

0-7803-6540-2/01/$10.00 (C) 2001 IEEE

II. DESCRIPTION OF THE PREDISTORTER

Fig. 1 shows the block diagram of the linearizer. Following the RF signal path, the RF signal is picked up from the input and the output of the PA and translated down to within an alias-free sampling range from DC up to 35 MHz.

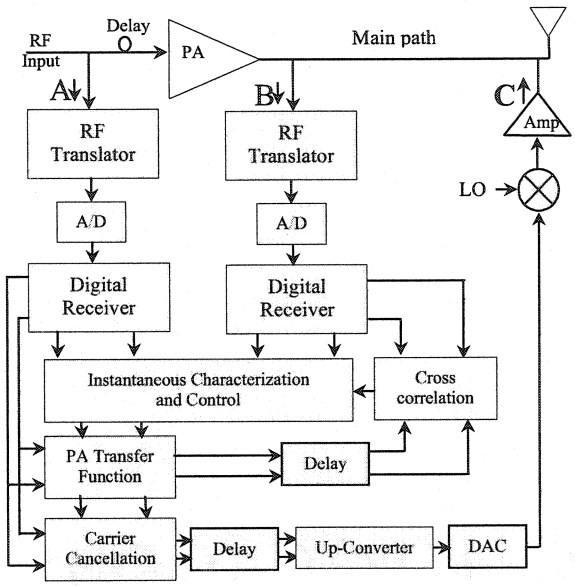

Fig. 1 General block diagram of the linearizer

Right after the translator stages, one for each branch, the signals are conditioned by 12-bit A/D converters into digital samples at the high rate of 70 MHz. The entire subsequence complex down converting, filtering, and decimating is performed digitally by two digital receivers [7]. It is understood that, the complex envelop from the output of the PA in branch "B" bring the information of non-linearity when it is driven further into nonlinear operation mode. This non-linearity information can be discriminated when this complex envelop is referenced to the complex envelop from the input of the PA in branch "A". It means that the instantaneous characterization (i.e., AM-AM and AM-PM curves) can be performed following both complex envelopes variation during a real work condition [8]. It allows correlating the PA transfer function in real time and to control the adaptation update step, through the cross correlation block, whenever it is necessary to be update into the PA transfer function block. Notice that, the cross correlation block compares the distorted signal from the main PA with the distorted signal from the PA transfer function allowing to truck any change due to temperature variation, aging, etc. In order to perform the carrier cancellation loop, the complex envelop from the branch "A" is split into the two paths at the input of the PA transfer function and then, the carrier cancellation block process the suppression given a free carrier error signal. The resulting error signal containing only distortion components is processed through the branch "C" and then added to the main path for distortion cancellation purpose. Notice that, the delay line is placed at the input of the PA, and it is compensated by software.

In terms of algorithms, the translation and filtering process are the two majors signals processing operations performed by the digital receiver blocks. First, a single-sideband complex translation is accomplished by mixing the real signal with the complex output of a digital quadrature local oscillator. Then, a decimation filter conditions the complex baseband signal by fixing an appropriate value of the decimation parameter M [7]. It controls the reduction of the cutoff frequency f_{cutoff} and the sampling rate f_s as follows:

$$f_{cutoff} = f_s / 2M , \qquad (1)$$

$$f' = f_s / M . \qquad (2)$$

It means that, any signal can be selected digitally from the IF domain and put it into the baseband domain for further processing. In this way, the two receiver output data, that represent the stimulus and response of the PA, are routed through the instantaneous characterization block to carry out the nonlinearity behavioral. Assuming that the input bandpass signal is given by

$$v_i(t) = \mathrm{Re}\{\rho(t) e^{j[\omega_c t + \theta(t)]}\}, \qquad (3)$$

where ω_c is the midband angular frequency, $\rho(t)$ is the amplitude variation and $\theta(t)$ is the phase variation. Then, the bandpass output signal can be represented by

$$v_o(t) = \mathrm{Re}\{g[\rho(t)] e^{j\{\omega_c t + \phi[\rho(t)] + \theta(t)\}}\}, \qquad (4)$$

where $g[\rho(t)]$ and $\phi[\rho(t)]$ are two memoryless nonlinear functions that represent the instantaneous AM-AM and AM-PM curves. Notice that these functions are characterized in terms of the input and output bandpass complex envelopes, without including all harmonics effect.

III. RESULTS AND DISCUSSIONS

The entire system is validated using DSP/RF co-simulation for the LDMOS model of a typical 44 dBm class AB power amplifier. Temperature noise,

quantization noise, and impairment from other components have been taken into consideration to realistically model the system. The digital receivers are considered as both narrowband and wideband where the decimation values are ranged from 2 to 2^{17}. The performance of the feedforward system is evaluated by applying CDMA standard signal which stress level is characterized by its complementary cumulative distribution function (CCDF) as shown in Fig 2.

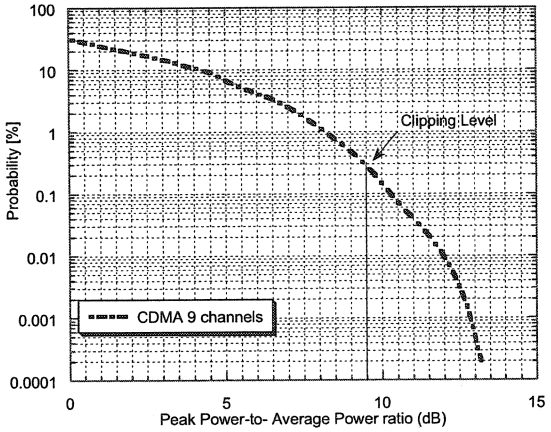

Fig.2 The CCDF plots of CDMA standard signals

The CCDF curves illustrate the statistical property of the nine channel standard signal built in simulation; the simulator generates around 800,000 signal samples that allow attaining the 0.0001% probability value with high stability.

For analysis purpose, the ACPR is evaluated by computing the ratio between the in-band and the out-of-band power spectral densities for three pairs of offset channels. The channels are normalized to the same bandwidths of *30 kHz* at the offset frequencies of *±885 kHz, ±1.256 MHz,* and *±2.75 MHz*. The normalization factor (NF) is calculated by logging the ratio between the normalization bandwidth NBW, i.e., 30 kHz, and the specified bandwidth BW, as follow:

$$NF(dB) = 10\log(\frac{NBW}{BW}) \qquad (5)$$

By applying this equation to the J-STD-008 standard requirements, the relative limit values of the power spectral densities for the three offsets are given by:

$$R_1(dB) = 28.8\ dB \qquad (6)$$

$$R_2(dB) = 28.8\,dB + \Delta\ dB \qquad (7)$$

$$R_3(dB) = 47.8\,dB + \Delta\ dB \qquad (8)$$

where Δ is given by:

$$\Delta = \begin{cases} P_{PA}\,(dBm) - 35.8dBm & for\ P_{PA} \geq 35.8\,dBm \\ 0 & elsewhere \end{cases} \qquad (9)$$

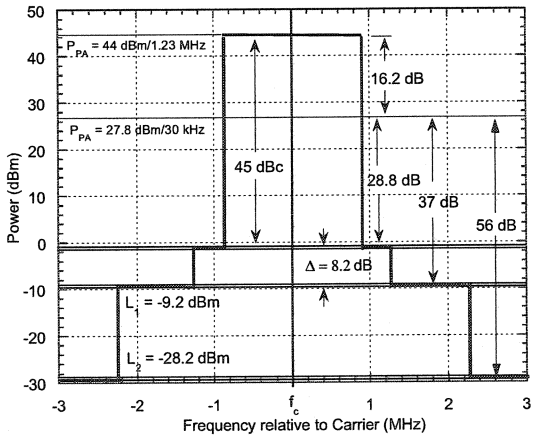

Fig.3 Graphical representation of 30 kHz normalized CDMA standard requirement for *44 dBm* PA

In Fig 3 we can see a graphical representation of requirement for a typical *44 dBm* PA; after normalization the mean power become *27.8 dBm/30 kHz,* Δ take the value *8.2 dB* and the relative limit values are R_1= *28.8 dB,* R_2=*37 dB* and R_3=*56 dB*.

The power calculation for each channel is accomplished by converting the time domain signal to frequency domain using Hanning window and with FFT length of 8192 points. The integration bandwidth (IBW) method is used to calculate both mean channel power and offset channel powers. In addition, the simulator computes an average power for each specified integration channel bandwidth and over a specified number of data acquisitions, *avg.*= 16.

Several important results have been obtained, the main of them are summarized in table 1. The OBO referenced to Single Carrier (SC) saturation, the Crest Factor (peak power-to-average power (CF)), the word-length of bits, the ACPR (R_1, R_2, R_3) and the power efficiency η% are

chosen as important factors to analyze the performance of the whole system.

The numbers in the Table 1 indicate the operating condition of the feedforward amplifier (PA_{FF}) under the standard requirement. The PA_{FF} achieves 44 dBm with an overall power efficiency of 10%. The result revels about 5% greater than a conventional feedforward. Notice that the PA_{AB} operate at 9.5 dB OBO to achieve 45 dBm with an efficiency of 16%. Under this operating condition, the clipping level becomes 3.5 dB from the CF as shown in Fig. 2. The total insertion losses of the couplers are considerate to be 0.55 dB. To achieve an acceptable distortion cancellation, the P_{1dB} of the EA_A was optimized given an average power capability of 28.8 dBm operating at 18 dB of OBO. This is a critical operation condition showing a poor efficiency of 1.5%.

TABLE 1
OPERATING CONDITION OF THE PA_{FF} UNDER THE STANDARD REQUIREMENT

	OBO [dB]	P_{out} [dBm]	η [%]	R_1 [dB]	R_2 [dB]	R_3 [dB]
PA_{AB}	9.5	45	16	33	36	52.8
EA_A	18	28.8	1.5	-	-	-
PA_{FF}	-	44	10	43	45	56.2

IV. CONCLUSION

An efficient baseband/RF feedforward linearizer has been presented. This new design improves the overall power efficiency by about 5% in comparison with conventional feedforward systems. The improvement is achieved by eliminating the delay line at the output of the power amplifier and by reducing the average power rating of the error amplifier. Progress in this technique should be a control loop for up-converter's LO in branch C to perform good matching frequency between mean path and error path. Finally, the fact that the system can be controlled and tuned by software, this design provides an attractive solution for feedforward amplifiers mass production with almost no need for unit's test bench adjustment.

REFERENCES

[1] R. Meyer, R. Eschenbach and W. Edgerley, Jr." A Wide-Band Feedforward Amplifier", IEEE J of Solid-State Circuits, vol.sc-9, no. 6, pp. 442-428, December 1974.

[2] J. Cavers, "Adaptation Behavior of a Feedforward Amplifier Linearizer", IEEE Transactions on Vehicular Technology, vol. 44, no 1, pp. 31-40, February 1995.

[3] Y. Nagata, "Linear Amplification Technique for Digital Mobil Communications", in Proc. IEEE Veh. Technol. Conf., San Francisco, CA, 1989, pp. 159-164.

[4] J. Cavers, "Amplifier Linearization Using a Digital Predistorter with Fast Adaptation and Low Memory Requirement", IEEE Transactions on Vehicular Technology, vol. 39, no 4, pp 374-382, November 1990.

[5] E.G. Jeckeln, F.M. Ghannouchi and Mohamad Sawan, "Adaptive Digital Predistorter for Power Amplifiers with Real Time Modeling of Memoryless Complex Gains", IEEE MTT-S 1996 International Microwave Symposium, San Francisco, CA, June 1996.

[6] E.G. Jeckeln, F.M. Ghannouchi and Mohamad Sawan, " An L Band Adaptive Digital Predistorter for Power Amplifiers Using Direct I-Q Modem ", IEEE MTT-S 1998 International Microwave Symposium, Baltimore, MA, June 1998.

[7]E. G. Jeckeln, F. M. Ghannouchi and F. Beauregard "Adaptive Baseband/RF Predistorter for Power Amplifiers through Instantaneous AM-AM and AM-PM Characterization Using Digital Receivers" IEEE MTT-S International Microwave Symposium, Boston, June 11-16, 2000, pp. 489-492.

[8] E. G. Jeckeln, F. M. Ghannouchi and M. Sawan, " Non Iterative Adaptive Digital Predistortion Technique for Power Amplifiers linearization ", U.S. Patent 6,072,364, June 6, 2000.

ANNEXE II.5:

27TH EUROPEN MICROWAVE-97

Linearization of Microwave Emitters using an Adaptive Digital Predistorter

Linearization of Microwave Emitters using an Adaptive Digital Predistorter

Ernesto G. Jeckeln, Fadhel M. Ghannouchi and Mohamad Sawan

Department of Electrical and Computer Engineering
Ecole Polytechnique de Montréal
C.P. 6079, Succ. Centre Ville, Montréal, Canada H3C 3A7

Abstract

Adaptive digital predistortion for nonlinear power amplifier (PA) became one of the most robust linearization techniques that can be implemented in digital signal processors (DSP) environment. However, its precision compensation for AM-AM and AM-PM distortion is wasted when the quadrature modulator (QM) impairments are not to be considered. This paper presents a new digital predistorter for microwave emitters with real time modeling of both, PA and QM distortions, that can compensate for nonlinearity, gain imbalance, phase imbalance and DC offset. An improvement of 35 dB of out-of-band power is obtained in simulating with 10^5 complex input look-up table using 2D interpolation.

Introduction

Spectral efficiency and high power added efficiency became the importants factors in Cellular and Personal Communication Services (PCS). To maximize these parameters, linear modulation methods and saturated power amplifiers have to be used. However, the fluctuating envelope of the resulted signal from linear modulation methods causes distortion and spectral spreading in the output of microwave emitters. A generic microwave emitter is constituted by a quadrate vector modulator and power amplifier (see Fig.1). In order to reduce these undesired effects and meeting both, power efficiency and spectral efficiency, linearization techniques must be introduced. In addition, quadrature modulator suffers from severe deficiencies [1], such as gain imbalance, phase imbalance and DC offset. As a result, the residual intermodulation products in the output signal of the microwave emitter cause the BER degradation. Therefore, a compensation technique for these impairments must be included.

A variety of linearization methods have been reported and predistortion linearization [2] and [3] is one of the techniques that can be chosen for an analog or digital implementation. This method uses a nonlinear element preceding the device to be compensated and its gain expansion characteristic cancels the gain compression of the amplifier. In the case of the digital implementation, one of the most important feature is that any function is easy to be performed by software and therefore, significant improvements can be obtained using inverse nonlinearities. The first successful work were presented by Nagata [4], using a two-dimensional look-up table technique with

adaptive digital feedback at baseband and pulse shaping filter prior to predistortion. This technique has the advantage that any order of nonlinearity and any modulation format can be performed. Moreover, the use of two-dimensional look-up table permits also correction of PM-PM and PM-AM distortion generated in the QM of analog part. The disadvantage of this technique is that for an acceptable accuracy, the size of the look-up tables must be kept higher (two millions complex words). Therefore, the memory requirement becomes large and results in the slowly convergence each time when the tables are updated.

Several drawbacks of this technique have been improved, by Caver [5] and Faulkner [6], using one-dimensional table. It has made possible that less memory is needed and therefore, the convergence time is reduced. In this way, another successful approach has been presented by [7], using real time nonlinearity modeling, where the iterative algorithm and the convergence time have been eliminated. It is to be noted that the improvement in the last three techniques [5], [6]and[7] comparing to the one proposed by [4] is at the expense of the QM impairments.

Because of the DSP is expanding at high rate, the benefits of this technology have become available to RF and microwave community. The contribution in the last few years had permitted that the processing power required, which are not available on a single processor, is recently available by multiprocessing architecture. This technology can handle higher bandwidth signal and can perform more intensive processing.

Taking into account this potentiality, we propose in this paper a new adaptive digital predistorter with Real Time Modeling (RTM) of both, PA and QM distortions, that can supply correction for any order of non linearity, gain imbalance, phase imbalance and DC offset. This technique have been developed to be implemented with a digital signal multiprocessors, where the RTM of the all distortions generated in the forward path signal is performed to provide, using a two-dimensional lookup table technique, the predistorted signal.

The adaptive digital predistorter

Fig.1 shows a simplified block diagram of the proposed adaptive digital predistorter where, in addition to the digital domain, a dual DA/AD converters, a quadrature modulator and demodulator, a microwave coupler and a microwave power amplifier form the analog domain to complete the entire system. The spectrally efficient 16-QAM modulation method is used as a transmitted signal source, which is passed through a pulse shaping filter to ensure free Inter-Symbol-Interference (ISI). In the RTM algorithm, the input digital baseband signal and output lowpass equivalent complex envelopes of the amplifier are sampled, scaled and updated into the lookup tables to provide the predistorted signal. These tables are configured to implement a mapping from the input (I,Q) to the output (I_d,Q_d) using 2D interpolation and according to the number of sampled pairs measured. Because of the random nature of the data measurement, unequal spacing between tables entries are used. An important feature to

be considerate is the adaptability dedicated to drift correction. The predistorted signal over time-varying characteristics (AM-AM and AM-PM) requires that the predistorter adapt to this change. Adapting the predistorter to compensate this variation requires a feedback path through which the linearizer can be notified of this change. In this case, mean error criterion between the desired and the distorted feedback signals is used to perform adaptability. The feedback loop is used only to update the LUT. After each adaptation and during normal data transmission, the feedback loop is opened until new significant drifts have occurred and new data has to be entered in the LUT. In order to estimate the delay in the feedback loop, correlation between input amplifier and feedback signals is performed, and the delay is compensated by the same amount in the input signal.

Let the Emitter be considered as a zero memory system. Then, the input-output relationship of such system can be written as follows :

$$w(t) = T[z(t)], \tag{1}$$

where $z(t)$ and $w(t)$ represent the input digital baseband signal and the output lowpass equivalent complex envelopes of the emitter respectively. The complex transfer function is given by :

$$T[z(t)] = |T[z(t)]| e^{j\Phi[z(t)]}. \tag{2}$$

Since $z(t)$ is complex-valued, $z(t) = I_d(t) + jQ_d(t)$, where $I_d(t)$ and $Q_d(t)$ are real values. Hence, $w(t)$ can be written as a complex-valued function of the real values $I_d(t)$ and $Q_d(t)$ as follows :

$$w(t) = I(I_d, Q_d) + jQ(I_d, Q_d), \tag{3}$$

where $I(I_d, Q_d)$ and $Q(I_d, Q_d)$ are real functions of the variables I_d and Q_d. Now, let the complex transfer function $T[z(t)]$ be analytic on a set S. Then, it is always possible to find a complex function $z(t) = P[w(t)]$ that satisfies $w(t) = T\{P[w(t)]\}$ and which is unique in that no other function has this properties. Then, $P[w(t)]$ become the inverse function of the $T[z(t)]$ and can be used as a complex predistortion transfer function. Thus,

$$z(t) = I_d(I, Q) + jQ_d(I, Q), \tag{4}$$

and the complex predistortion transfer function is given by :

$$P[w(t)] = |P[w(t)]| e^{j\Phi[w(t)]}. \tag{5}$$

Simulations results

The global system has been built with SPW environment and several important analysis results are presented here. The spectrally efficient 16QAM modulation method with a baud rate of 24.3 kHz is used as signal source. Hence, 16 different possible symbols form the signal-space diagrams where we have assumed equally likely signal set. The pulse shaping filter was a raised cosine having a roll off α= 0.35, and the oversampled rate was 16 samples/symbol. In addition to estimate the spectral magnitude, the signals have been multiplied by a blackman window function to smooth the signals frequency spectrum, then, Discrete Fourier Transform (DFT) have been obtained for each signal with N=1024 points. The P_{in}-P_{out} characteristics of a class AB power amplifier were modeled using cubic spline interpolation and stored in two look-up tables for simulation purpose. QM impairments were 5^{o} of phase error, 2% of gain error and 5% of DC offset. From the time domain analysis, shown in fig.2, four constellation diagram is used to evaluate the distortion and the compensation. In fig.2(b), we can see a compression and an expansion in the real and imaginary part, respectively, where the vector signal will follow an offset elliptical trajectory. In real system, the PA nonlinearity and the QM impairments can be lumped together and modeled using 2D interpolation. Fig. 2(c) shows the distorted constellation diagram at the output of the emitter and Fig.2(d) shows that the distorted symbols are mapped back to the desired positions when the compensation is performed. In Fig.3, a comparison of the spectral magnitude shows clearly a degradation in out of band emissions, Fig.3(c), and that the spectral magnitude floor is limited by the QM impairments, Fig.3(b). Note, in Fig.3(d), that an improvement of 35 dB of out-of-band power can be reached using 10^5 complex words in each table (real and imaginary part). A further reduction in spectral distortion can be achieved if the table sizes is increased.

Conclusion

In this paper, a new method dedicated to Adaptive Digital Predistorter that can compensate for non linearity, gain imbalance, phase imbalance and DC offset of a microwave emitters is proposed and simulation results using SPW software are presented. The real time modeling of both PA and QM distortions was implemented to calculate the predistortion function using 2D interpolation. Two dimensional look-up tables were used with unequal spacing between table entries. The RTM algorithm has demonstrated to be a powerful tool for sounding the distortion during normal data transmission and supplying the knowledge of the nonlinearity to the predistorter. The major advantages of this technique in comparison with the predistorter presented by [6] is the reduced memory requirements, from 2 millions complex words to 200K complex words. In addition, the proposed adaptive linearization technique can be self corrected for any drift in the operating points and without any iterative procedure. It is noted that the ability of the RTM algorithm is in eliminating the need for complex convergence algorithms in the adaptation update step.

Acknowledgment

This work was supported by the "Programme Synergie" of the Quebec government through the AMPLI project in collaboration with Advantech Inc. and NSI Communications.

References

[1] N. Imai, T. Nojima and T. Murase, "Novel Linearizer Using Balanced Circulators and Its Application to Multilevel Digital Radio Systems", IEEE Transactions on Microwave Theory and Techniques, vol. 37, no 8, pp. 1237-1243, August 1989.

[2] N. Imai, T. Nojima and T. Murase, "Novel Linearizer Using Balanced Circulators and Its Aplication to Multilevel Digital Radio Systems" IEEE Transactions on Microwive Theory and Techniques, vol. 37, No 8, august 1989

[3] Stapleton S.; Costescu, C. "An Adative Predistorter for et Power Amplifier Based on Adjacent Channel Emissions", IEEE T.V.T. vol. 41 No 1 Februery 1992

[4] Y. Nagata, "Linear Amplification Technique for Digital Mobil Communications", in Proc. IEEE Veh. Technol. Conf., San Francisco, CA, 1989, pp. 159-164.

[5] J. Cavers, "Amplifier Linearization Using a Digital Predistorter with Fast Adaptation and Low Memory Requirement", IEEE Transactions on Vehicular Technology, vol. 39, no 4, pp 374-382, November 1990.

[6] M. Faulkner, T. Mattsson and W. Yates, "Adaptive Linearization Using Predistortion" in Proc. 40th IEEE Veh. Technol. Conf. 1990. pp. 35-40.

[7] E.G. Jeckeln, F.M. Ghannouchi and Mohamad Sawan, "Adaptive Digital Predistorter for Power Amplifiers with Real Time Modeling of Memoryless Complex Gains", IEEE MTT-S 1996 International Microwave Symposium, San Francisco, CA, June 1996.

[10] Signal Processing WorkSystem (SPW), Alta Groupe of Cadence Design System, Inc., 1996.

ANNEXE II.6:

Asia Pacific Microwave Conference **APMA'96**, December 17-20, 1996

(Invited Paper)

Linearization Techniques of SSPAs : State of the Art and Prospective for Future Communication Transceivers

ANNEXE III

LIST DES PRINCIPALES DEFINITIONS

Function

A *function* maps a scalar or vector into a scalar or vector.

Operator

An *operator* maps a function into a function.

System

In the most general case, a system particularly one with memory, is represented by an operator. Occasionally, however, a system may be simple enough to be represented by a functional, or a function.

Linear System

A system H is a *linear system* if, for any inputs $x_1(t)$ and $x_2(t)$, and for any constant c, the additive property and the homogeneity property are satisfied.

Nonlinear System

A system H is *nonlinear* if the additive and/or the homogeneity properties are *not* satisfied.

Memoryless Linear Systems

A linear system H, is *memoryless*, if the output at time *t* depends on the input at only time t. That is, as well as satisfying the additive and homogeneous properties, it also satisfies the property given by:

Thus, the only memoryless linear system is an ideal amplifier, with infinite bandwidth.

Linear System with Memory

A linear system *H has memory* if the output at time *t* depends on the input at time t, as well as the input over a previous time interval.

Memoryless Nonlinear Systems

A nonlinear system *H* is *memoryless*, if the output at time t depends only on the input at time t. In some of these cases, we may use simple, infinite bandwidth, power series representations.

Nonlinear System with Memory

A nonlinear system *H* has memory if the output at time t, depends on the input at time t, as well as the inputs over a previous time interval. More complex models (such as a Volterra model) are required to represent such a system.

Finite Nth Order Nonlinear System

A finite Nth order nonlinear system H is one that has nonlinear behaviour that is limited to Nth order, thereby producing up to Nth order distortion products at its output.

System Identification

The process of obtaining the parameters of a suitable system model is referred to as *system identificatio*n.